UNIVERSITÄT DUISBURG ESSEN

Open-Minded

Protein-based Assessment of Activated Sludge

Dissertation

Zur Erlangung des akademischen Grades

Doktor der Ingenieurwissenschaften (Dr.-Ing.)

Fakultät für Ingenieurwissenschaften Abteilung Bauwissenschaften der

Universität Duisburg-Essen

Vorgelegt von: Asma Sumayyah Azizan, M. Sc.

1. Gutachter: Prof. Dr. rer. nat. Martin Denecke (Universität Duisburg-Essen)

2. Gutachter: Univ.-Prof. Dr.-Ing. Jörg Londong (Bauhaus Universität Weimar)

Mündliche Prüfung: 27.07.2020

Essen, 2020

Acknowledgements

I wish to thank Prof Dr. Martin Denecke for the opportunity to be a part of AGDE working group and for his supervision and guidance throughout my work. I would also like to thank Prof. Dr.-Ing. Jörg Londong for being the second examiner and for his valuable feedback.

My sincere thanks go to all my colleagues especially Erika de Leon, Leon Steuernagel, Lukas Moesgen, Jan Möller, Tobias Gehrke and Mohammad Azari for their care, support and encouragement throughout this work. I am very grateful for the invaluable discussions that helped me move forward with this work.

I am especially thankful to Dr. Farnush Kaschani for the collaboration which allowed me to do proteomics analyses on my samples. My appreciation also goes to all the students who were involved in this research for their assistance and great work, especially to Hellen Barinas for her competence in the lab.

Lastly, I would like to thank my family, without whom I would not be here in the first place.

Abstract

This present study involves the assessment of activated sludge based on the roles of proteins and extracellular polymeric substances (EPS) in continuous flow activated sludge treatment systems. The first objective of the study is to investigate the applicability of total protein quantification to estimate the quantity of active biomass. Activated sludge samples from three industrial wastewater treatment plants (WWTPs) and a lab-scale plant were analysed for this purpose. The total protein concentration of the sludge was compared to the conventional biomass parameters, i.e. suspended solids (SS) and volatile suspended solids (VSS), and correlated to the respirometric activity measured by the oxygen uptake rate (OUR). In both industrial and lab-scale plant samples, VSS showed the strongest correlation to the OUR, followed by SS, while total protein concentration showed weak or no correlation. Therefore, it is concluded that there was no direct relationship between protein content in activated sludge to the activity thus total protein concentration is not suitable to be used to measure active biomass.

Most problems related to activated sludge systems involve sludge separation problems. The second objective of this study was to determine the roles of the EPS components in sludge settleability and dewaterability. For this purpose, the protein, humic acid and carbohydrate contents of bound EPS were correlated to the sludge volume index (SVI) and capillary suction time (CST), which represented sludge settleability and dewaterability respectively. The results were contradictory between the industrial and lab-scale plant samples and the correlations, if any, were weak. As the EPS properties seemed to differ from plant to plant, defining the roles of the EPS from their 'bulk' contents was found to be inconclusive and speculative at best.

The third aim was to investigate the total protein and EPS at a molecular level to obtain more conclusive information on how they affect sludge properties and nutrient removal efficiency. For this purpose, activated sludge samples were subjected to nitrogen and phosphorous limiting conditions, two common problems in activated sludge process. Label-free quantification (LFQ)-proteomics analyses were performed to determine the qualitative and quantitative changes in the protein expressions of total protein and EPS under these conditions. Differential protein expression illustrated that the system adopted different strategies towards mitigating the effects of nutrient deficiency. N-limiting period caused the upregulation of various antioxidant enzymes and DNA-binding protein from starved cells (Dps), signifying the system reacted to protect the cells from oxidative stress and DNA-damage. The system also reacted by increasing nitrogen uptake through GS/GO-GAT system and the expressions of urease and nitrogenases. Phosphorous limitation also caused the upregulation of various antioxidant enzymes but it was not clear how the system regulated phosphorous uptake in this condition. With the help of proteomics, there is now more appreciation for the roles of the EPS in activated sludge process. EPS was found to contain

chaperones, transport proteins, antioxidant enzymes, and other proteins that are essential for cell integrity under normal conditions as well as under environmental stress. This study proved that the application of quantitative proteomics using LFQ-MS is beneficial in retrieving various information about the state of sludge and gaining further understanding of the activated sludge process.

Abstrakt

Im Rahmen der vorliegenden Arbeit wurden Proteine und extrazelluläre polymere Substanzen (EPS) in kontinuierlichen Belebtschlamm-Abwasserbehandlungsanlagen analysiert. Das erste Ziel der Arbeit bestand darin, zu überprüfen, ob die Quantifizierung der Gesamtproteinkonzentration eine bessere Abschätzung der Menge an aktiver Biomasse in Belebtschlamm liefert, als die herkömmlichen Biomassen-Parameter Trockensubstanz (TS) und organische Trockensubstanz (oTS). Zu diesem Zweck wurden Belebtschlammproben aus drei industriellen Kläranlagen und einer Laboranlage bewertet. Die TS-, oTS- und Gesamtproteinkonzentrationen wurden mit der respirometrischen Aktivität korreliert. Sowohl in Proben der industriellen als auch der Laboranlage erwies die oTS die stärkste Korrelation mit der Aktivität. Als Nächstes zeigte TS die zweitbeste Korrelation. Das Gesamtprotein zeigte nur schwache oder gar keine Korrelation mit der respirometrischen Aktivität. Es konnte daher keine direkte Beziehung zwischen der Proteinkonzentration und der Aktivität festgestellt werden und die Ergebnisse deuteten darauf hin, dass die Bestimmung der Gesamtproteinkonzentration keine bessere Alternative zu oTS für die Quantifizierung der aktiven Biomasse ist.

Eine der Herausforderungen im Betrieb der Belebtschlammanlage betrifft das Problem der Schlammabscheidung. Als zweites Ziel der Arbeit sollte die Rolle der EPS bei der Schlammabsetzbarkeit und -entwässerbarkeit untersucht werden. Der Protein-, Huminsäure- und Kohlenhydratgehalt von gebundener EPS wurde mit dem Schlammvolumenindex (SVI) und der Kapillarsaugzeit (capillary suction time, CST), die die Absetzbarkeit bzw. Entwässerbarkeit des Schlamms charakterisieren, korreliert. Es ergaben sich widersprüchliche Ergebnisse und die Korrelationen waren schwach. Die EPS-Eigenschaften unterscheiden sich offenbar von Anlage zu Anlage. Die Rolle der EPS alleine anhand der Konzentrationen ihrer Hauptkomponenten zu definieren ist daher unschlüssig und bestenfalls spekulativ.

Das dritte Ziel bestand darin, das Gesamtprotein und die EPS auf molekularer Ebene zu untersuchen, um konkretere Informationen zu erhalten, wie diese sich auf die Schlammeigenschaften und die Reinigungseffizienz auswirken. Zu diesem Zweck wurde die Entwicklung des Schlamms unter dem Einfluss von Stickstoff- und Phosphormangel untersucht und eine Proteomanalyse mithilfe von Label-Free Quantification (LFQ) angewendet, um Änderungen der Proteinexpressionen in Gesamtprotein- und EPS-Proben qualitativ und quantitativ zu bestimmen. Anhand der differentiellen Proteinexpressionen konnte gezeigt werden, dass das System mit unterschiedlichen Strategien zur Abschwächung der Auswirkung des Nährstoffmangels reagierte. Der Stickstoffmangel verursachte die Hochregulation verschiedener antioxidativer Enzyme und DNA-bindender Proteine (DNA-binding protein from starved cells, Dps), die die Zellen vor oxidativem Stress und DNA-Schäden schützten. Das System reagierte auch mit

einer Erhöhung der Stickstoffaufnahme durch das GS/GO-GAT-System und der Expression von Urease und Nitrogenasen. Phosphorlimitierung verursachte ebenfalls die Hochregulierung verschiedener antioxidativer Enzyme. Es blieb aber unklar, wie das System die Phosphoraufnahme in diesem Zustand regulierte. Außerdem wurde mithilfe der Proteomik die wichtige Rolle der EPS im Belebtschlammprozess belegt. Es wurde festgestellt, dass EPS Chaperone, Transportproteine, antioxidative Enzyme und andere Proteine enthält, die für die Zellintegrität unter normalen Bedingungen sowie unter Umweltstress wesentlich sind. Im Rahmen dieser Studie konnte bewiesen werden, dass die Anwendung der LFQ-Proteomik sehr nützlich ist, um zahlreiche Informationen über den Zustand von Belebtschlamm zu erfassen, wodurch ein besseres Verständnis des Belebtschlammprozesses ermöglicht wird.

Table of Contents

List of Figures

APPENDICES

List of Tables

APPENDICES

Abbreviations, Acronyms and Symbols

A	Absorbance
2DGE	Two-dimensional gel electrophoresis
ADP	Adenosine diphosphate
ATP	Adenosine triphosphate
BOD	Biochemical oxygen demand
BOD_5	Biochemical oxygen demand in 5 days
BSA	Bovine serum albumin
CBBG	Coomasie Brilliant Blue G-250
CER	Cationic exchange resin
COD	Chemical oxygen demand
CST	Capillary suction time
CSTR	Continuously stirred tank reactor
df	Degree of freedom
DNA	Deoxyribonucleic acid
DO	Dissolved oxygen concentration (g/L)
E.C.	Enzyme commission number
EBPR	Enhanced biological phosphorous removal
EPS	Extracellular polymeric substance
FISH	Fluorescence in situ Hybridization
HA	Humic acid
HSP	Heat-shock protein
KEGG	Kyoto Encyclopedia of Genes and Genomes
LB-EPS	Loosely-bound EPS
LC	Liquid chromatography
LC-MS	Liquid chromatography in combination with mass spectrometry

LC-MS/MS	Liquid chromatography in combination with tandem mass spectrometry
LFQ	Label-free quantification
MLSS	Mixed liquor suspended solids (g/L), synonym to SS
MLVSS	Mixed liquor volatile suspended solids (g/L), synonym to VSS
MS	Mass spectrometry
N	Sample size
OUR	Oxygen uptake rate (mg O_2/L·s)
PAO	Phosphorous accumulating organism
PBS	Phosphate buffered saline
PCR	Polymerase chain reaction
PHB	Poly- β-hydroxybutyrate
P_i	Inorganic phosphate
Q	Flow rate (m^3/h)
r	Pearson's correlation coefficient
RNA	Ribonucleic acid
ROI	Reactive oxygen intermediates
SBR	Sequencing batch reactor
SD	Standard deviation
SDS-PAGE	Sodium dodecyl sulfate polyacrylamide gel electrophoresis
SI	Sludge Index (mL/L)
SOUR	Specific oxygen uptake rate (mg O_2/g SS·h)
SS	Suspended solids (g/L), synonym to MLSS
TB-EPS	Tightly-bound EPS
TP	Total protein
VFA	Volatile fatty acid
VSS	Volatile suspended solids (g/L), synonym to MLVSS
WWTP	Wastewater treatment plant

1 Introduction

Around 50% of the activated sludge dry weight is made up of proteins [2]. The functions of proteins in activated sludge systems are manifold. As enzymes, they catalyse a variety of biochemical processes that contribute to bacterial activity and cell growth. Proteins are also found to be the main polymer in the extracellular polymeric substance (EPS) matrix [3], a component of activated sludge which is known to greatly influence the sludge properties such as sludge settleability and dewaterability [4,5]. Most problems in activated sludge process are associated with poor sludge settleability and failure to meet the effluent requirement as a result of low bacterial activity and nutrient deficiency. Hence, to tackle these problems, the measurement of proteins in activated sludge, both of the cells and the EPS matrix, is indispensable in order to understand how their functions affect the purification process.

Previous research by Yücesoy et al. [6] proposed the use of total protein concentration in place of conventional parameters of suspended solids (SS) and volatile suspended solids (VSS) for estimation of active biomass in activated sludge. They demonstrated in a sequencing batch reactor (SBR) that the SS and VSS could only be reliably used as biomass parameters under stable operation. By correlating the different biomass parameters to the respirometric activity, they concluded that under nutrient (carbon, nitrogen, phosphorous, and potassium) limiting conditions, only total protein content showed significant correlations to the activity. Most wastewater treatment plants (WWTPs), however, are operated in continuous flow configuration. The operation of an SBR differs from a continuous flow system in terms of hydrodynamics as well as the kinetics of substrate removal and bacterial growth, which will likely affect the protein expression of the microorganisms. Therefore, this raises the question if the findings of Yücesoy et al. [6] are transferable to continuous flow systems as well.

The protein and carbohydrate contents of the EPS, either analysed separately or combined as the total EPS content, have been commonly related to sludge settleability and dewaterability. The numerous investigations, however, could not come to a common ground as to how exactly the EPS affected the sludge properties [7]. Proteins as enzymes are specific in their functions and their expression is highly regulated [8]. The measurement of total protein and EPS concentrations alone is hypothesized to provide limited information on the roles of proteins in the purification process and this calls for a more accurate investigation at the molecular level using proteomics.

Proteomics is the study of the whole proteomes expressed in a sample [9]. The characterization of proteins in an environmental sample is called metaproteomics [10]. As microbial protein expression is stimulated by their environment, proteomics has a great potential to be used as a

bioindicator of the present state of activated sludge [11]. Quantitative proteomics allows the quantification of each protein in the samples separately. The identification and quantification of protein expressions using metaproteomics could be the missing piece in understanding sludge behaviour and properties under various conditions.

1.1 Motivation and Aims

Hence the aims of this research were as the followings:

1. To investigate if total protein quantification could also provide a better estimation of the amount of active biomass compared to the conventional biomass parameters SS and VSS in a continuous flow activated sludge system.
2. To determine the roles of EPS components in sludge settleability and dewaterability by measurement of protein and carbohydrate contents of the EPS.
3. To investigate the use of metaproteomics analysis to retrieve information about sludge conditions by studying the protein expression changes during nitrogen and phosphorous limiting conditions in total protein and EPS samples.

For these purposes, activated sludge samples from three different WWTPs were analysed for 7−9 weeks and a continuous flow lab-scale WWTP was operated for a total of 474 days.

1.2 Outline

This work is divided into 6 chapters. **Chapter 1** is the introductory chapter which explains the research topic, the motivation and the aims of the research.

Chapter 2 provides a review of the fundamental of activated sludge treatment. It includes the description of the conventional treatment process and the different bacterial metabolisms that are responsible for nutrient removal.

Chapter 3 includes a literature review regarding the topics of protein, EPS and proteomics, together with their significance in the activated sludge process.

Chapter 4 explains the material and methods used in this research. The first part provides the methods for the study of activated sludge from industrial WWTPs and the second part includes the methods for the study of activated sludge from the lab-scale WWTP.

Chapter 5 presents and discusses the results of both parts of the study.

Finally, **Chapter 6** concludes the work with a summary of the results and provides an outlook on the research topic by summarizing the limitations and providing suggestions for future research improvements.

2 Activated Sludge Process

Activated sludge process is a biological wastewater treatment process that depends on microbial metabolisms to purify the wastewater [12]. Microbial populations oxidise biodegradable compounds in the wastewater resulting in stable end products such as CO_2, H_2O, NO_3^-, and SO_4^{2-} and the synthesis of new cell mass [2,12].

Activated sludge consists of biological and non-biological components. The biological components of activated sludge include bacteria and other organisms such as fungi, protozoans and metazoans [13], which are bound together by organic and inorganic particulates such as extracellular polymeric substances (EPS) and humic substances to form a sludge floc (Figure 2-1). The suspension containing the sludge flocs and the wastewater is called mixed liquor and the concentration of solids in the mixture is named mixed liquor suspended solids (MLSS or SS). MLSS and its volatile fraction, mixed liquor volatile suspended solids (MLVSS or VSS), are normally used to estimate the concentration of biomass in the system [12]. Normally, the microstructures of the flocs are held together by filamentous bacteria, which due to their structure, form the backbone of the floc. Both the floc and the sludge properties are highly influenced by the microbial composition of the floc [14]. The abundance of filamentous bacteria in the floc, for example, could cause sludge bulking and settling problems [13].

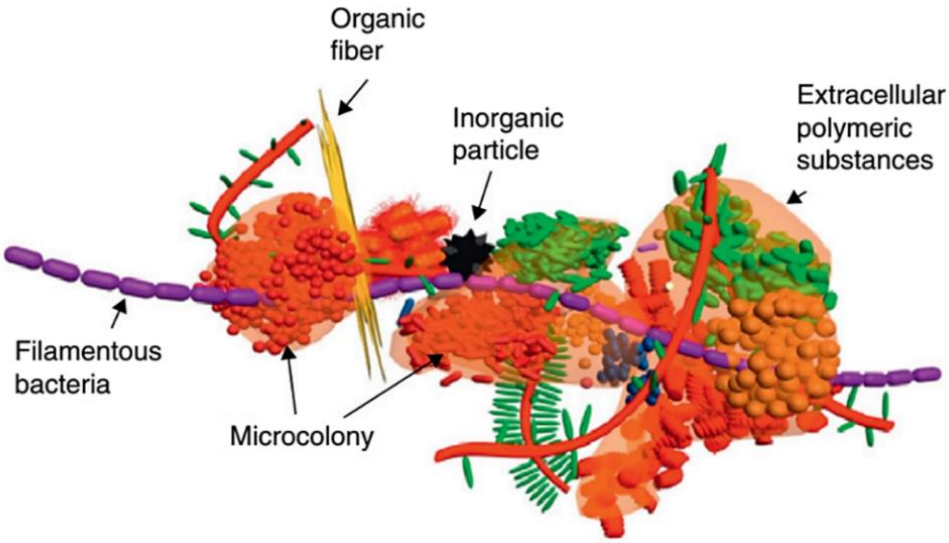

Figure 2-1: Components of activated sludge floc [14]

The aim of a conventional activated sludge process is the removal of carbonaceous organic matter, nitrogenous compounds and phosphorous compounds in the wastewater to ensure that the treated water can be released into the water bodies without polluting the environment. The main components of a conventional activated sludge system are the aeration tank and the

clarifier (Figure 2-2). In the aeration tank, microorganisms and the influent wastewater are thoroughly mixed and aerated. The effective contact between the biomass and the biodegradable substances contained in the wastewater is the basis of the purification process. The mixture then flows to the clarifier where sludge settles at the bottom and the treated water can be discharged as the effluent. A part of the sludge is returned to the aeration tank to keep a certain concentration of biomass for efficient treatment and the rest will be discarded as excess sludge [15].

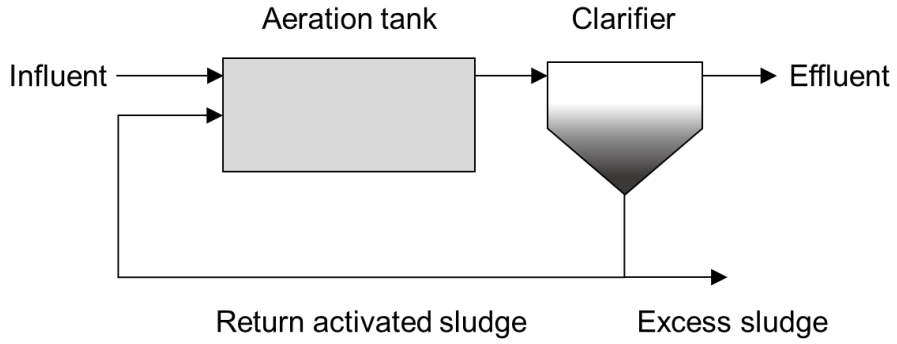

Figure 2-2: Typical arrangement of conventional activated sludge system

To successfully treat the wastewater, four basic requirements must be met: (1) suitable organisms must be present for the purification process to take place. (2) These organisms must be provided with the required nutrients and trace elements for cell growth. (3) The growth rate must be controlled by varying the sludge age to allow selection and to maintain the concentration of the needed organisms. (4) Optimal environmental conditions such as the right pH, temperature, and oxygen concentration must be assured for optimal degradation [16].

2.1 Bacterial Cell

Bacteria are prokaryotes. A prokaryotic cell can be divided into three regions: (1) the cytoplasm and its contents, (2) the cytoplasmic membrane, cell wall and outer membrane, and (3) the external surface structures (Figure 2-3) [17]. Prokaryotes exist as Gram-positive and Gram-negative bacteria. The cell structure differs slightly between the two groups.

The cell wall is a rigid multi-layered structure made of peptidoglycan (also known as murein), a polymer consisting of amino acids and sugars [16,18]. Through the support of the peptidoglycan, the cell is able to maintain its shape [18]. Due to the thicker cell wall of Gram-positive bacteria, they retain the crystal violet stain when Gram-stained, while Gram-negative bacteria with a thinner cell wall do not. Gram-negative bacteria also differ from Gram-positive bacteria through the presence of a lipopolysaccharide-rich outer membrane.

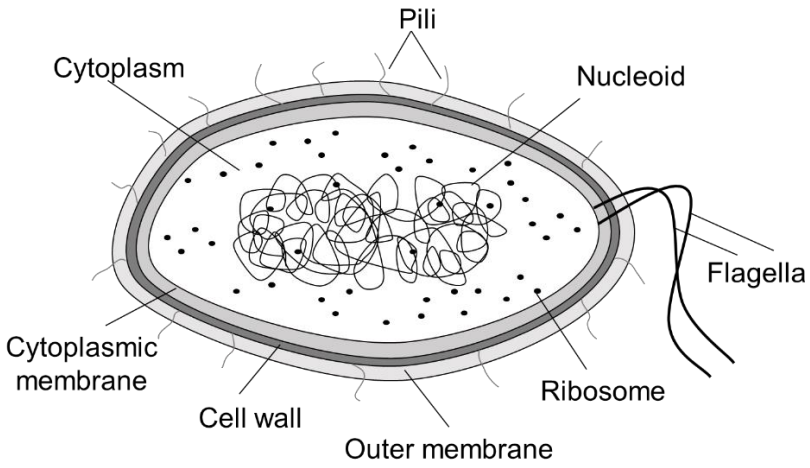

Figure 2-3: Prokaryotic cell, adapted from [19]

Internal to the cell wall is the cytoplasmic membrane that envelopes the cytoplasm. This semi-permeable membrane regulates substance transport into and out of the cell. The cytoplasm consists mostly of water and contains suspensions of proteins, carbohydrates, lipids, and ions [17]. The cytoplasm region is rich in ribosomes, where protein synthesis takes place, and nucleoid containing DNA [18]. Some bacteria possess external cell structures like flagella or pili whose function is to provide motility [17,20].

The ratio of protein, nucleic acid, carbohydrate, and lipid in the cell varies with the growth stage [21]**.** The composition of a bacterial cell as an example of *Escherichia coli* (*E. coli*) is shown Table 2-1.

Table 2-1: Composition of bacteria (*E. coli*) [22] cited in [23]

Substance	Mass percentage of dry matter (%)
Proteins	55
Nucleic acids RNA	16-17
DNA	3-4
Lipids	10
Cell wall	20

2.2 Nutrient Requirements

Carbon (C), nitrogen (N), phosphorous (P), hydrogen (H), oxygen (O), and sulphur (S) are the main nutrients required by bacteria to grow and sustain metabolic activity. The ratio of the main macronutrients C, N and P for activated sludge treatment is suggested to be in the BOD_5 (five-day

biochemical oxygen demand):N:P ratio of 100:5:1 [15,16]. This hypothetical value is based on the assumption of a net sludge yield of 0.5 g VSS/g BOD_5 being removed and that the sludge VSS is composed of 10% N and 2% P [13].

Nitrogen and phosphorous are crucial macronutrients for cell growth [13]. Nitrogen is essential for the synthesis of amino acids and nucleic acids for the production of proteins, ribonucleic acid (RNA) and deoxyribonucleic acid (DNA) [24]. Phosphorous is required for the production of adenosine triphosphate (ATP) for the transmission of chemical energy [23]. It is also a major constituent of the phospholipid of the cell membrane and the sugar phosphates which form the backbone of the RNA and the DNA [25]. Nitrogen and phosphorous compounds in wastewater need to be in the forms that can be assimilated by the microorganisms, such as ammonium (NH_4^+) and nitrate (NO_3^-), and orthophosphates ($H_2PO_4^-$,HPO_4^{2-} ,PO_4^{3-}) respectively, for them to be available to the biomass [15]. In industrial wastewaters, where the concentration of the nutrients vary, the deficiency of the macronutrients N and P is common [17]. In such a case, it is necessary to supplement nitrogen and phosphorous sources to the treatment system to ensure optimal degradation [15]. Failure to provide sufficient nutrients may lead to sludge problems such as filamentous and slime bulking [26].

The microelements calcium (Ca), iron (Fe), potassium (K), magnesium (Mg), and sodium (Na) [17], and trace amounts of micronutrients such as zinc (Zn), manganese (Mn), Selenium (Se), cobalt (Co), copper (Cu), and nickel (Ni) are also required in small quantities for microbial growth [27]. Most of the microelements and trace elements function as co-factors for enzymes or as enzyme activators [28].

2.3 Bacterial Metabolism and Nutritional Types

Bacterial metabolism can be divided into anabolism and catabolism. Catabolism is the degradation of complex molecules such as proteins and lipids into simpler end products, such as CO_2 and H_2O (Figure 2-4). This type of metabolism generates chemical energy in the form of ATP. The energy generation involves three stages (Figure 2-5). In the first stage, complex molecules are hydrolysed into their simple molecules building blocks such as amino acids, monosaccharides and fatty acids. These building blocks are then broken down into acetyl coenzyme A (acetyl CoA) in the second stage. The last stage is the citric cycle where acetyl CoA is oxidised, producing CO_2 and generating ATP. Anabolism is the synthesis of the building blocks into new complex molecules. Anabolism requires energy, which is provided by catabolic reactions when ATP is broken down to adenosine triphosphate (ADP) and inorganic phosphate (P_i) [16,25].

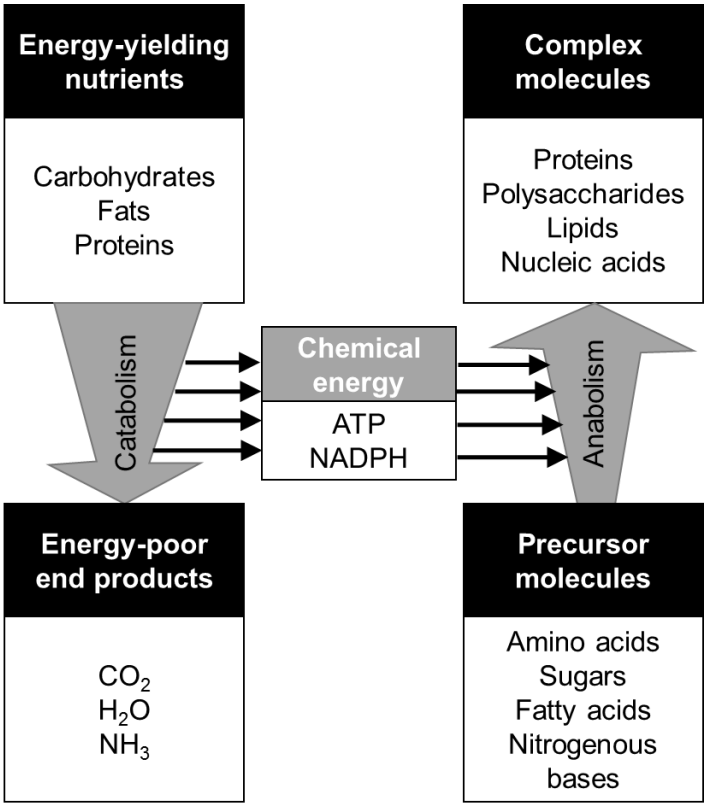

Figure 2-4: Comparison between catabolic and anabolic pathways [25]

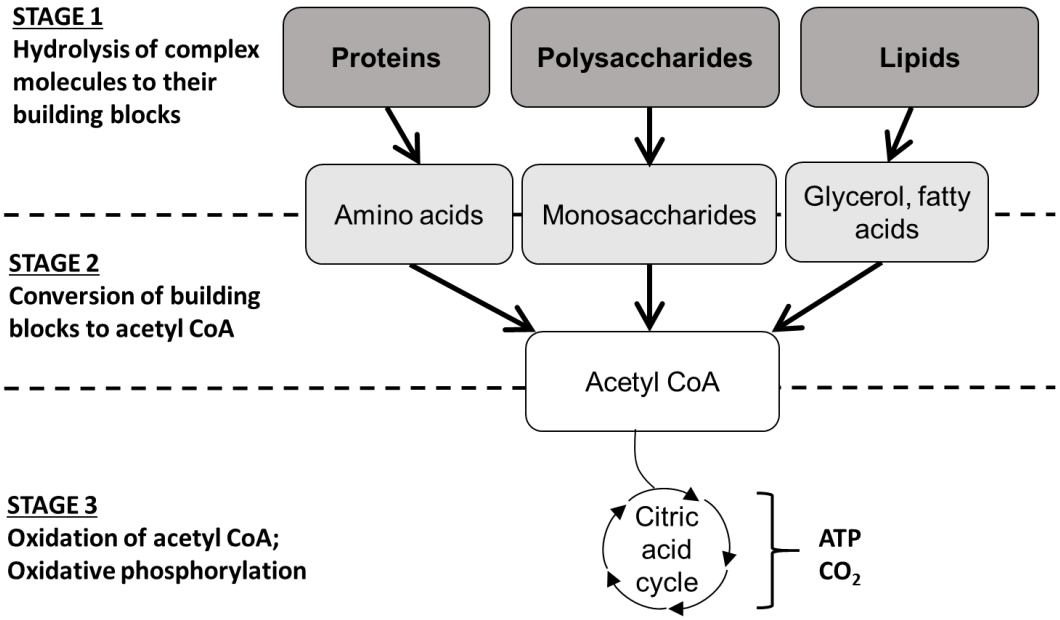

Figure 2-5: Stages of catabolism [25]

Bacterial nutritional type can be categorised according to their carbon and electron sources, which are obtained from either organic or inorganic compounds, and their energy source, which can be obtained either from chemical compounds (organic or inorganic) or light, as shown in Table 2-2. The four main nutritional types of bacteria are [28]:

1. Photolithotrophic autotrophy
2. Photo-organotrophic heterotrophy
3. Chemolithotrophic autotrophy
4. Chemo-organotrophic heterotrophy

Table 2-2: Classification of bacteria according to their nutritional type [28]

	Inorganic compound	**Organic compound**	**Light**
Carbon source	autotroph	heterotroph	
Energy source	chemotroph		phototroph
Electron or hydrogen source	lithotroph	organotroph	

2.4 Substrate Removal

Conventional wastewater treatment aims at the removal of BOD, nitrogen and phosphorous before the wastewater is released into the environment. This is realised in different processes with the help of a variety of bacteria that use the components to be removed either as electron donour or electron acceptor (Table 2-3).

Table 2-3: Nutrient removal processes with their corresponding electron donours and acceptors [28]

Reaction	**Electron donour**	**Electron acceptor**
BOD removal	Organic material	Oxygen
Nitrification	Ammonia	Oxygen
Denitrification	Organic material	Nitrate
Phosphorous release	Polyphosphate	Poly- β-hydroxybutyrate (PHB)
Phosphorous uptake	Acetate	Phosphate

2.4.1 BOD Removal

The removal of organic matter is undertaken by the heterotrophic organisms in activated sludge. Heterotrophic bacteria are suggested to make up the major population of activated sludge organisms [20]. Eq. (2-1) describes the organic matter removal by the metabolism of aerobic heterotrophs [27]:

$$C_6H_{12}O_6 + O_2 + NH_3 + other\ nutrients \rightarrow C_5H_7O_2N + CO_2 + H_2O \quad (2\text{-}1)$$

To guarantee a high BOD removal efficiency, biomass needs to be provided with enough time to metabolise the organic matter in the wastewater. This is achieved by having a sludge retention time (SRT) higher than the hydraulic retention time (HRT) [27].

2.4.2 Nitrogen Removal

Nitrogen in wastewater occurs mostly in the form of ammonium (NH_4^+) or bound in organic compounds such as urea and amino acids. Nitrification and denitrification are the two main processes of nitrogen removal in a conventional activated sludge system [20]. The nitrogen cycle of the nitrification and denitrification processes is illustrated in Figure 2-6.

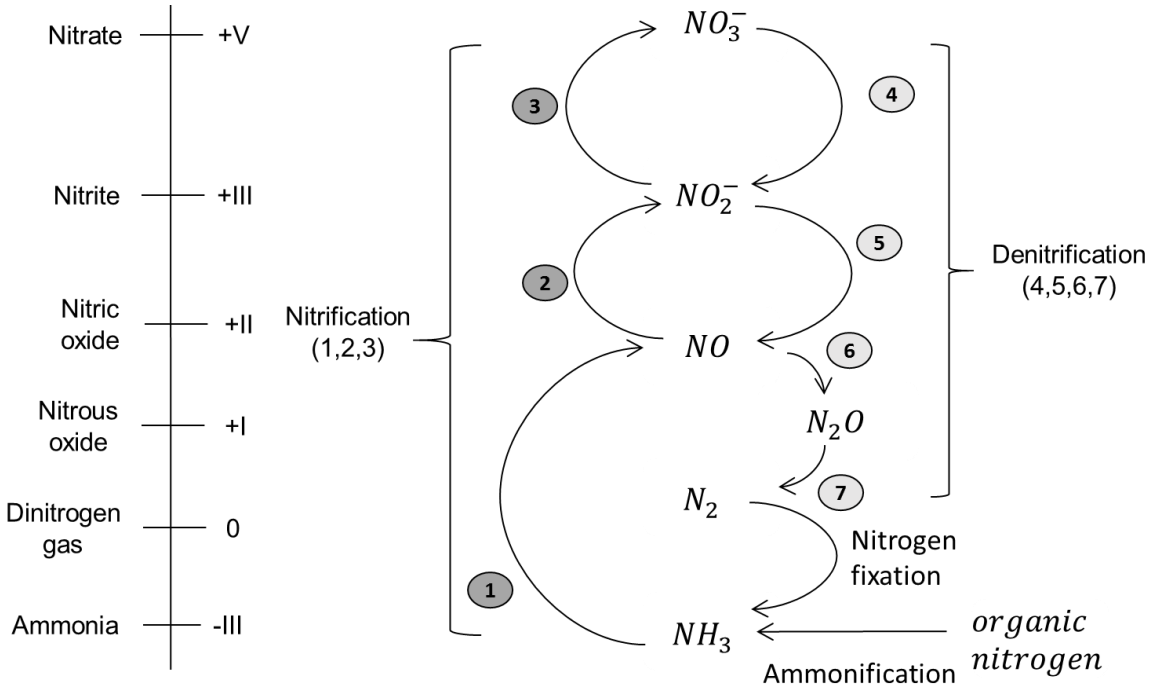

Figure 2-6: Nitrogen cycle of nitrification and denitrification, adapted from [24]

Nitrification involves the oxidation of ammonia into nitrate via nitric oxide and nitrite. Ammonium oxidising bacteria (AOB) are chemolithoautotrophs. They utilise inorganic substrates as carbon source, mainly in the form of carbon dioxide CO_2 [20]. Ammonia oxidation is catalysed by the enzyme ammonia monooxygenase (AMO), which oxidises ammonia into intermediate hydroxylamine (NH_2OH; Eq. (2-2)) [29]. Previously it was thought that the subsequent reaction involved the direct oxidation of hydroxylamine into nitrite by the enzyme hydroxylamine oxidase (HAO) [30]. A recent finding from Caranto and Lancaster [31] however suggests that the enzyme converts hydroxylamine to nitric oxide (NO) instead (Eq. (2-3)), before NO is further oxidised to nitrite by a yet unknown enzyme. Nitrite oxidation to nitrate by nitrite oxidizing bacteria (NOB) is catalysed by nitrite oxidoreductase (NXR; [24]). The overall nitrification reaction is described by Eq. (2-4) [15]. Recently, a new metabolic pathway involving complete ammonium oxidation (commamox) to nitrate was discovered in members of the genus *Nitrospira* [32], gaining the interest of many researchers worldwide.

$$NH_3 + O_2 + 2H^+ + 2e^- \xrightarrow{AMO} NH_2OH + H_2O \quad (2\text{-}2)$$

$$NH_2OH + H_2O \xrightarrow{HAO} NO + 3H^+ + 3e^- \quad (2\text{-}3)$$

$$NH_4^+ + 2O_2 \rightarrow 2H^+ + NO_3^- + H_2O + Energy \quad (2\text{-}4)$$

To remove the nitrogen from wastewater, the product of nitrification needs to be reduced to nitrogen gas through the denitrification process. Denitrification occurs under anoxic environment, using nitrate as the electron acceptor. Nitrate is reduced to nitrite and subsequently to gaseous nitrogen [15], with nitric oxide and nitrous oxide being the intermediate molecules (Figure 2-6). Nitrate reduction to nitrite is initiated by the membrane-bound nitrate reductase (NAR) or periplasmic nitrate reductase (NAP). Nitrite reduction to nitric oxide is catalysed by the enzyme nitrite reductase (NIR). Nitric oxide is then further oxidised to nitrous oxide and nitrogen gas by the enzyme nitric oxide reductase (NOR) [24]. As easily biodegradable carbon sources are required for heterotrophic denitrification, this process simultaneously removes a significant amount of BOD from the wastewater. [12,16]. To ensure enough BOD for denitrification, the nitrified wastewater needs to be recycled back to the anoxic tank (Figure 2-7 (a)) or the wastewater needs to be added with an external carbon source such as methanol (Figure 2-7 (b)) [16]. The overall denitrification is described by Eq. (2-5) [15].

$$2NO_3^- + 2H^+ \rightarrow N_2 + 2.5\ O_2 + H_2O \quad (2\text{-}5)$$

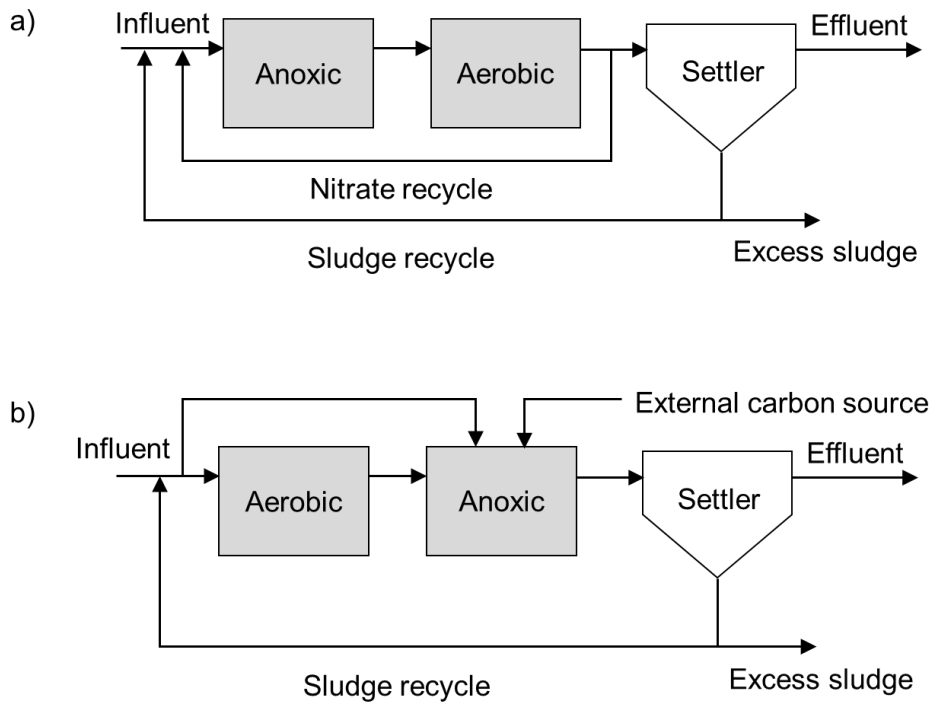

Figure 2-7: Plant configuration for optimised denitrification. (a) Upstream denitrification and (b) addition of carbon source [23]

2.4.3 Phosphorous Removal

Phosphorous in wastewater can mostly be found in the form of orthophosphates PO_4-P [33]. Conventional activated sludge treatment normally does not include a specific treatment step for removing phosphorous. As a result, only about 25% of the phosphorous contained in the wastewater is removed [16]. If necessary, phosphorus may be removed through chemical precipitation with metal ions such as aluminium chloride or ferric salts. The insoluble salt formed is separated through excess sludge removal [23].

Enhanced biological phosphorous removal (EBPR) can be applied to wastewater with high phosphorous content. The principle of EBPR involves phosphorous accumulating organisms (PAO), which are capable of storing phosphorous intracellularly in forms of polyphosphates and Poly- β-hydroxybutyrate (PHB) in excess of their normal metabolic requirement [15]. The treatment process prerequisites alternating aerobic (feed) and anaerobic (famine) phases and the addition/formation of volatile fatty acid (VFA) such as acetate in the anaerobic phase to stimulate the growth of the PAOs (Figure 2-8) [27]. As PAOs assimilate VFA better than other organisms, there is a positive selection for PAO in the anaerobic zone [15].

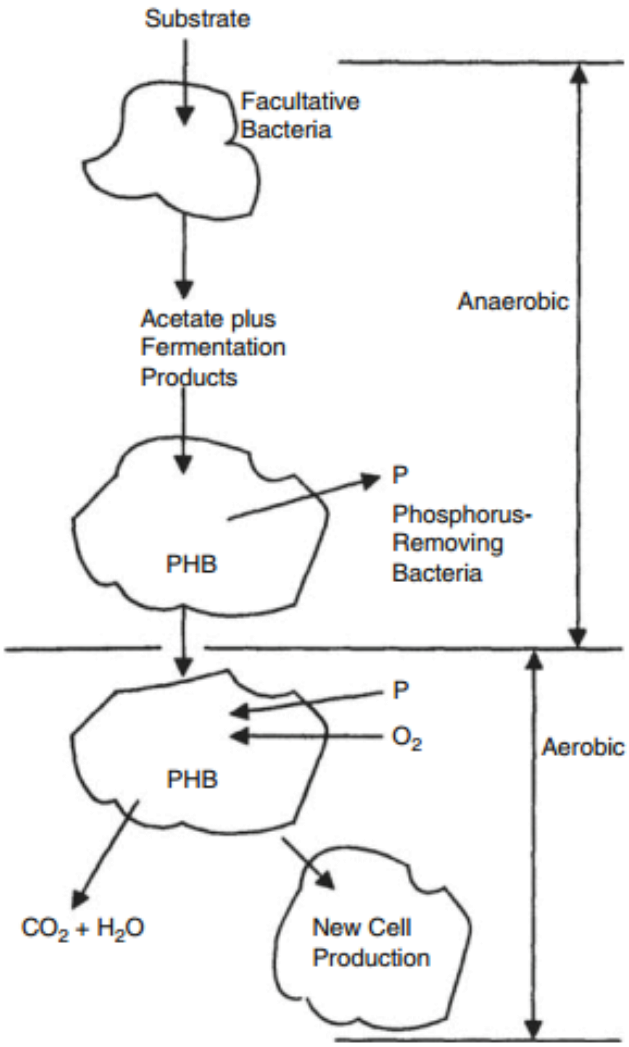

Figure 2-8: Mechanism of biological phosphorous removal, U.S. EPS cited in [34]

Under anaerobic conditions, VFA is assimilated by the PAOs and there is an increase of soluble phosphate in the bulk liquid as a result of the release of intracellular polyphosphate (phosphate redissolution) [16], which has been previously accumulated in the aerobic stage [15,20]. During the subsequent aerobic stage, phosphate in the wastewater is taken up to form polyphosphate in the cells [15,16]. The higher the rate of phosphate redissolution, the higher is also the rate of the aerobic phosphate uptake. As the aerobic phosphate uptake is greater than phosphate redissolution, this results in the nett elimination of phosphate from the wastewater [16]. The phosphorous accumulated in the bacterial cells is subsequently removed as excess sludge [20].

2.5 Kinetics of Growth and Substrate Utilisation

The kinetics of cell growth and substrate utilisation are a combination of cell metabolism and cell replication [35]. The simplest kinetic model to describe the specific bacterial growth rate μ is the Monod kinetic model [36] (Eq. (2-6)).

$$\mu = \mu_{max} \cdot \left(\frac{S}{K_s + S}\right) \tag{2-6}$$

$\boldsymbol{\mu_{max}}$	maximum specific growth rate (d^{-1})
$\boldsymbol{S}$	concentration of limiting substrate (mg/L)
$\boldsymbol{K_s}$	half-saturation constant, the concentration of substrate at which $\mu = 0.5\ \mu_{max}$ (mg/L)

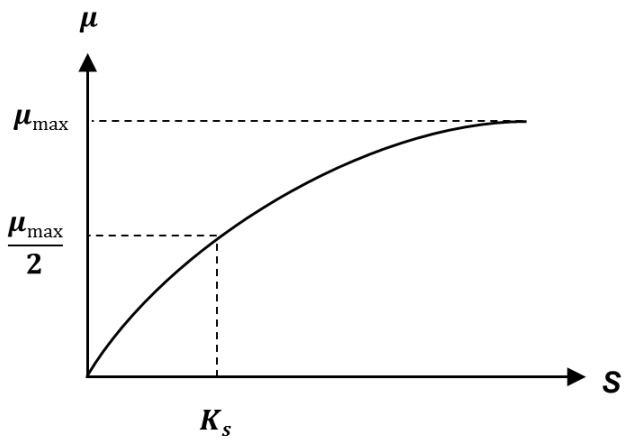

Figure 2-9: Relationship between growth rate and substrate concentration according to Monod kinetics

In an ideal continuous flow reactor (continuously stirred tank reactor (CSTR)), the substrate concentration is directly diluted to the effluent concentration once it enters the reactor. Thus, the reaction rate is determined by this reduced concentration [38]. According to the Monod kinetics (Figure 2-9), the growth rate is a first-order reaction under substrate limiting condition, which is also the case for conventional wastewater treatment plants that apply continuous flow configuration. This means that the growth rate of microorganisms is directly proportional to the substrate concentration. As opposed to the CSTR, the substrate concentration does not drop to the effluent concentration in a batch reactor. Instead, the concentration varies with time. The growth rate is a zero-order reaction in a batch reactor at high substrate concentration ($S \approx K_s + S$). Thus, the growth rate and substrate utilisation rate of a continuous flow reactor are lower than those of a batch reactor [35]. A sequencing batch reactor (SBR) applies fed-batch mode, in which both the substrate concentration and reactor volume varies with time as the substrates are added intermittently [39]**.** Its kinetics is similar to that of a batch reactor [40]**.**

2.6 Quantification of Active Biomass

The biomass of activated sludge can be divided into active biomass, the viable part that is responsible for the biodegradation of wastewater content, and the inert residue, which is formed through the decay process [33]. It is estimated that only a small fraction of the activated sludge is viable and actively growing [12].

The conventional method to estimate the concentration of biomass in activated sludge is by the measurement of mixed liquor suspended solids (MLSS or SS) and mixed liquor volatile suspended solids (MLVSS or VSS). The SS is measured by drying a known volume of the mixed liquor filtrate at 105°C. The dry mass is then incinerated at 550°C to remove the volatile fraction of the solids. The weight after incineration is the inorganic fraction of the SS and the weight loss upon combustion is the VSS, the organic fraction of the SS [17]. Between both parameters, VSS provides a better estimate of the biomass concentration. Unfortunately, even VSS does not differentiate between active biomass and the inert residue, which poses the limitation to the design and operation of an activated sludge process [12,33]. Furthermore, volatile solids may vary significantly when the wastewater contains organics substances such as grease and humic acid, and this parameter is not able to provide information on the activity, toxicity or inhibition of the bacterial population [17].

Different alternative methods based on ATP [41], nucleic acid content [42], protein content [6], and respirometry [43] have been applied to measure the amount of viable biomass in water and wastewater samples. ATP was found to reflect the biomass concentration only at the maximum activity, as the correlation between the biomass and activity was only observed at the exponential growth phase [41]. The nucleic acid content of individual cells was suggested as a better alternative to the total cell count to measure actively growing cells in aquatic systems but was still insufficient to differentiate between cell-specific activity [42]. Yücesoy et al. [6] proposed the use of total protein concentration to estimate the active biomass of activated sludge in a sequencing batch reactor. They compared the protein concentration with conventional parameters of SS and VSS, and found that the latter parameters correlated well to the respirometric activity only during stable operation. Under nutrient deficient conditions, only protein concentration showed a significant correlation to activity. Among the alternative parameters to SS and VSS, respirometry is probably the most widely used parameters and the most accurate to measure the activity of an aerobic system [44]. It allows the determination of cell-specific activity and the differentiation between active and inhibited systems, as well as systems affected by toxicity [45,46]. Hence it is normally used as a reference parameter for the activity [6,41].

Except for respirometry, most of the above mentioned parameters were used to measure either environmental sample, samples from batch experiments or plants operated in a fed-batch mode in

SBR configuration. Only a few of them measured samples from a continuous flow reactor, which is the arrangement of choice in most WWTPs. The operation of an SBR or a batch reactor is different from a continuous flow system in terms of hydrodynamics and kinetics of substrate utilisation and bacterial growth. Therefore, it is likely that the results of these systems cannot be directly used to represent that of continuous flow reactors.

3 Protein

Proteins are polymers made of polypeptide chains. A polypeptide chain is a combination of 20 α-amino acid monomers, which differ in the nature of their side chains R (Table 3-1). Except for the simplest amino acid glycine, α-amino acids can be either L or D-isomers. Protein contains only L-α-amino acids [8]. Each amino acid consists of a hydrogen atom (H), an amino group (NH_2), a carboxyl group (COOH), and a side chain (R) group [47]. The general structure of L- α-amino acid is shown in Figure 3-1.

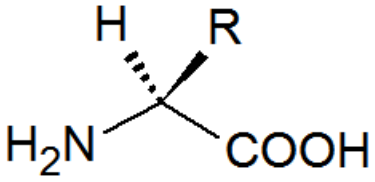

Figure 3-1 General structure of L- α-amino acid

The amino acids in a polypeptide chain are linked by the peptide (amide) bonds that are formed by condensation reactions when the amino group of an amino acid reacts with the carboxyl group of the adjacent amino acid (Figure 3-2). Protein structure can be differentiated into 4 organisational levels in increasing complexity (Figure 3-3) [47]:

1. **Primary structure** is a linear sequence of 100–1,000 amino acids. The amino acid sequence contains information that determines the 3D-configuration of a protein molecule [8].
2. **Secondary structure** describes the arrangement of a polypeptide backbone of 10–20 amino acids [8,47]. A polypeptide backbone is a stable 3D-structure formed by hydrogen bonds. The major forms of secondary structures are the α-helix and the β-sheet [8].
3. **Tertiary structure** is the full 3D-structure of a polypeptide chain formed from the folding of elements of secondary structures to a stable global confirmation [47].
4. **Quaternary structure** is the arrangement of the polypeptide subunits within proteins consisting of two or more polypeptide chains [47].

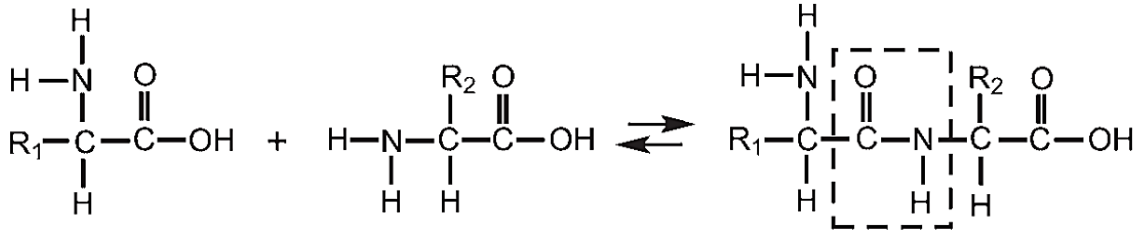

Figure 3-2: Formation of a peptide bond [23]

Table 3-1: The 20 commonly occurring amino acids [47,48]

R group classification	R group or whole amino acid	Amino acid	Abbreviated name		Occurrence in 'average' protein (%)
			3 letter	1 letter	
Non-polar, aliphatic	-H	Glycine	Gly	G	7.2
	$-CH_3$	Alanine	Ala	A	8.3
	$-CH(CH_3)_2$	Valine	Val	V	6.6
	$-CH_2CH(CH_3)_2$	Leucine	Leu	L	9.0
	$-CH(CH_3)CH_2CH_3$	Isoleucine	Ile	I	5.2
	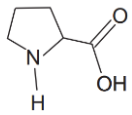	Proline	Pro	P	5.1
Aromatic	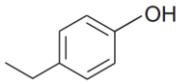	Tyrosine	Tyr	Y	3.2
	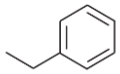	Phenylalanine	Phe	F	3.9
	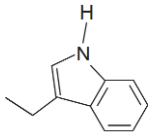	Tryptophan	Trp	W	1.3
Polar uncharged	$-CH_2SH$	Cysteine	Cys	C	1.7
	$-CH_2OH$	Serine	Ser	S	6.0
	$-CH_2CH_2SCH_3$	Methionine	Met	M	2.4
	$-CH(OH)CH_3$	Threonine	Thr	T	5.8
	$-CH_2CONH_2$	Asparagine	Asn	N	4.4
	$-CH_2CH_2CONH_2$	Glutamine	Gln	Q	4.0
Positively charged (basic)	$-CH_2CH_2CH_2NHCNHNH_2$	Arginine	Arg	R	5.7
	$-CH_2CH_2CH_2CH_2NH_2$	Lysine	Lys	K	5.7
	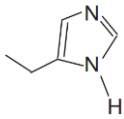	Histidine	His	H	2.2
Negatively charged (acidic)	$-CH_2COOH$	Aspartic acid	Asp	D	5.3
	$-CH_2CH_2COOH$	Glutamic acid	Glu	E	6.2

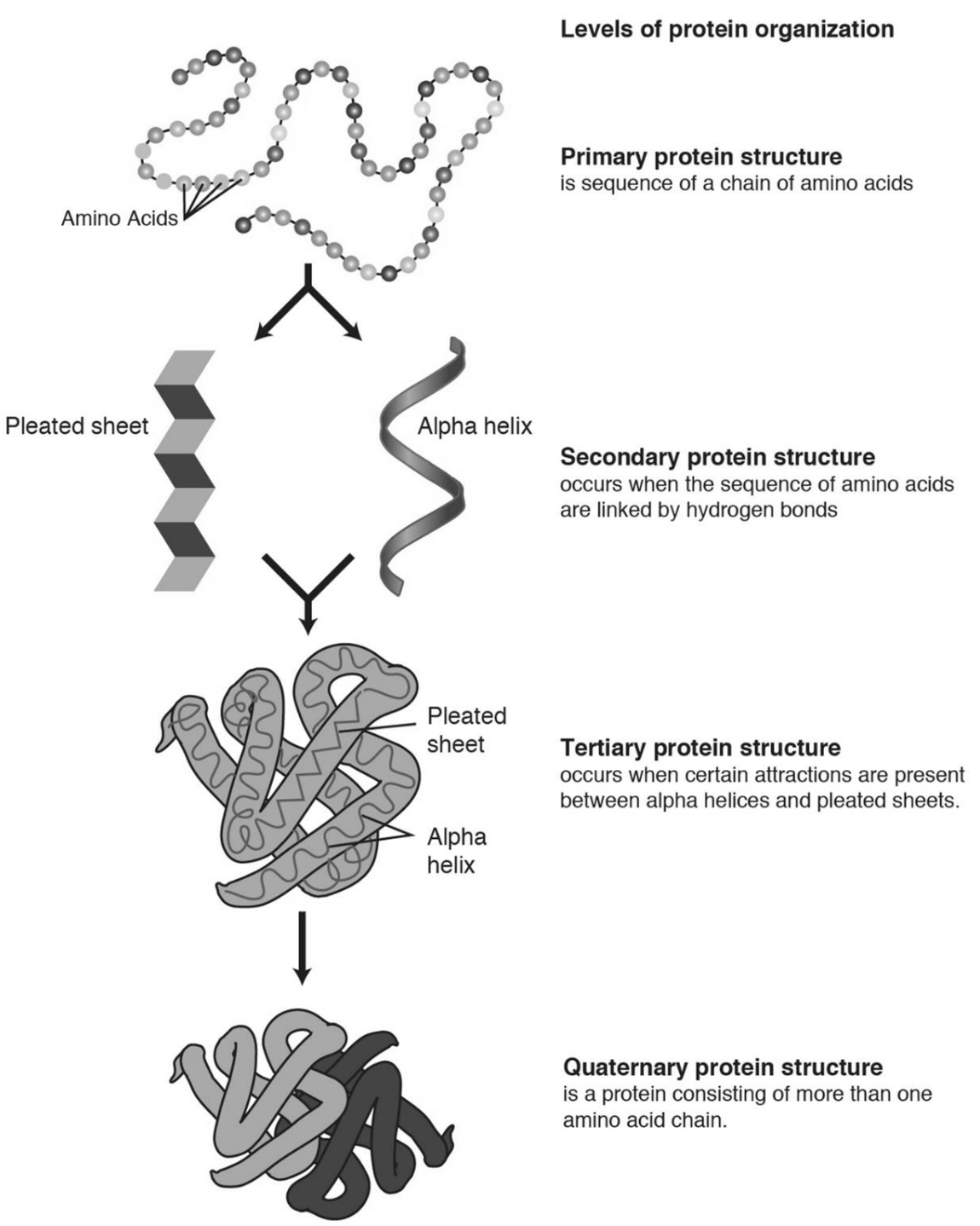

Figure 3-3: Four levels of protein organisation [49]

3.1 Protein Synthesis

Protein is the final product of the genetic expression in the flow called the central dogma. Protein synthesis starts with self-replication of DNA, where the double-stranded DNA unwinds to form a complementary strand. This is followed by the transcription process, where the genetic information in the DNA is copied to the RNA. The messenger RNA (mRNA) acts as a template of information transfer from the DNA to the ribosomes. In the subsequent translation process, transfer RNAs (tRNAs) bring the specific amino acids to the ribosomes, where proteins are synthesized (Figure 3-4) [2].

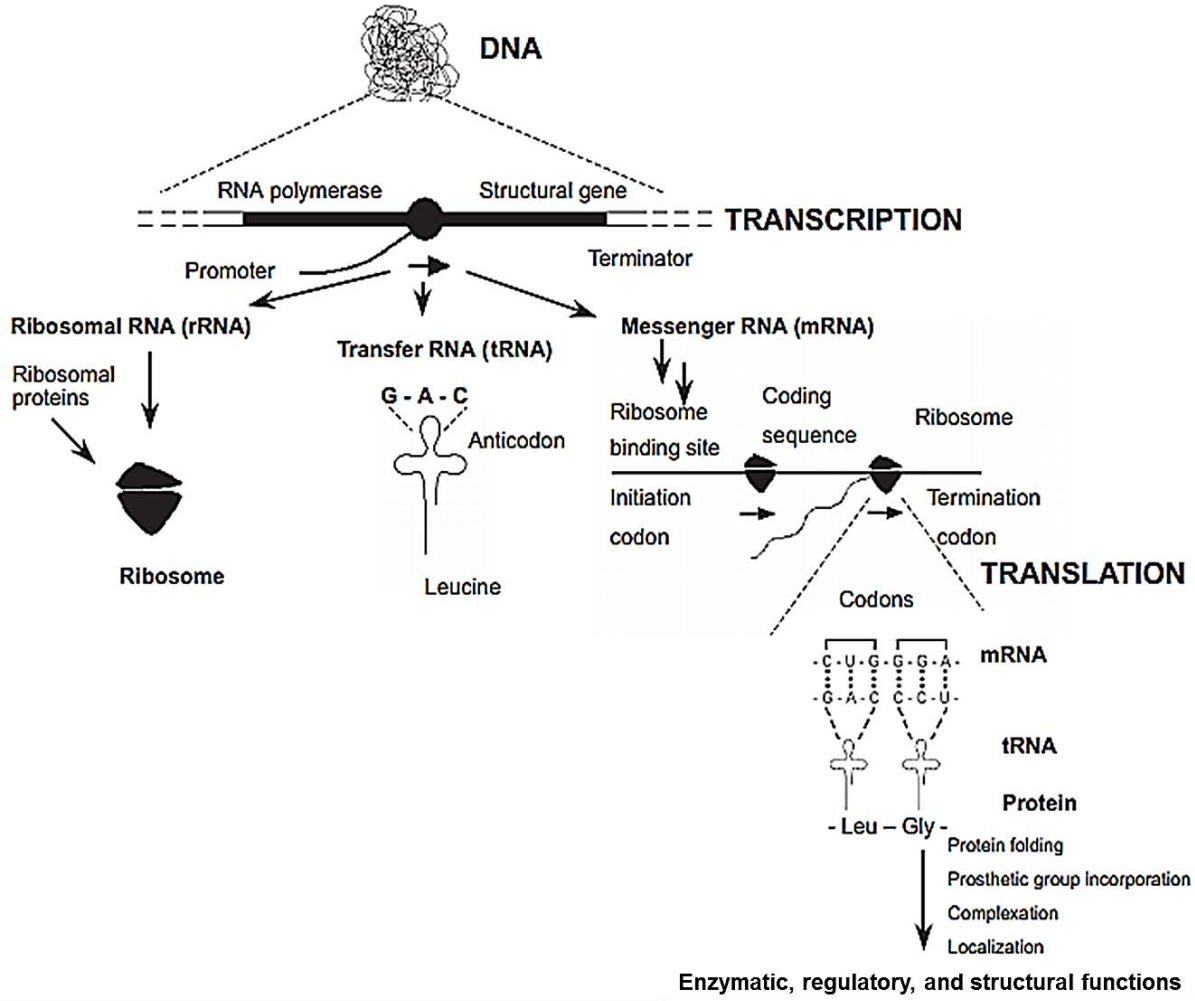

Figure 3-4: The sequence of protein synthesis [51]

3.2 Significance of Proteins

Proteins serve different roles in living organisms [52]. They function as enzymes, transport and storage proteins, provide structural and mechanical support to the cell, and are responsible for cell communication and regulation [9,23]. Enzymes refer to the proteins that possess catalytic activity. As enzymes, protein catalyses a variety of biochemical reactions including metabolism, synthesis, detoxification, and processing of DNA. Enzyme production is regulated by the cell's DNA. Various enzymes are produced in variable quantities by the different cells of an organism. Since most biochemical mechanisms of living organisms are common, certain enzymes are found in many, if not in all organisms. Oftentimes, the structure of the enzymes that catalyse the same reaction is similar even in different organisms.

Despite the majority of the enzymes are located in the aqueous cytoplasm of the cell, a significant amount of enzymes are associated with the cell membrane. This is because most biochemical processes involve the transport of molecules across membranes and are often facilitated by membrane proteins. These membrane proteins are normally enzymes since they display catalytic activity [52]. Enzymes can be grouped into different classes based on the type of chemical reactions they catalysed (Table 3-2):

Table 3-2: Classes of enzymes [23]

Class	Chemical reaction catalysed
Isomerase	Reversible rearrangement of isomeric compounds
Oxidoreductase	Oxidation/reduction reaction by transfer of electron or hydrogen ions
Transferase	Transfer of functional groups
Hydrolase	Hydrolysis (addition of water)
Lyase	Removal of groups of molecules without hydrolysis
Ligase	Combination of two molecules during the splitting of an energy-rich bond

3.3 Protein and EPS in Activated Sludge

Protein in activated sludge can be divided into the total protein and the protein contained in the extracellular polymeric substances (EPS). The total protein is the fraction of protein inside the cell. It makes up about half of the activated sludge dry composition. Sridhar and Pillai [53] reported that protein makes up 43% of the activated sludge dry mass. When the activated sludge bacteria were isolated, a composition of about 73% protein was measured, showing that the activated sludge was not composed entirely of bacteria. Frølund et al. [3] found that the VSS of activated sludge

consisted of only 46−52% of protein. A significant amount of activated sludge was made of humic acid (18-23% of VSS) and carbohydrate (17% of VSS). Total protein is extracted through cell lysis. This can be achieved by various mechanical methods such as mills, homogenizer and ultrasonic treatment, as well as non-mechanical methods that disrupt the cells through chemical (e.g. EDTA), mechanical (e.g. osmotic pressure) and enzymatic permeabilisation to release the intracellular proteins [54].

EPS are a combination of macromolecules including proteins, humic substances, polysaccharides, nucleic acids, lipids, and other polymeric compounds [55]. The total EPS represents the extracellular polymers produced by the cells during metabolism and cell lysis, as well as a fraction that is contributed by the wastewater [5]. It makes up half of the organic fraction of activated sludge. Protein makes the biggest fraction of the EPS, followed by humic substances, polysaccharides, and nucleic acids (Figure 3-5) [56].

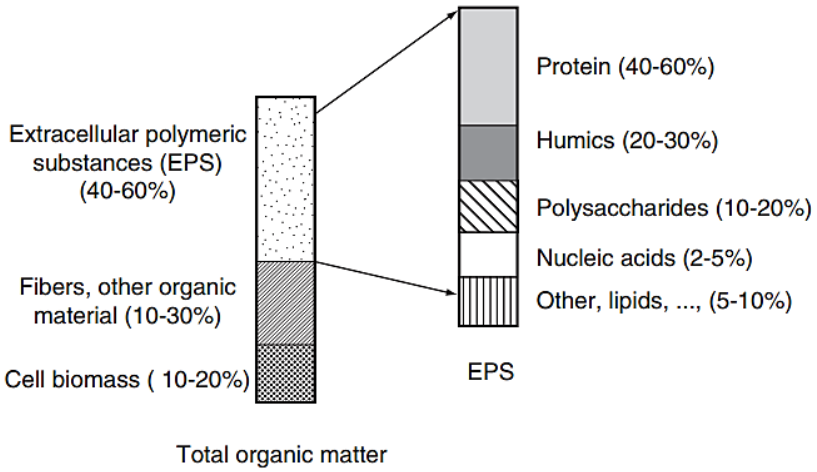

Figure 3-5: Composition of the VSS of activated sludge [56]

The EPS can be divided into bound and soluble EPS (Figure 3-6). Bound EPS, either loosely bound or tightly bound, is associated with the cell, while soluble EPS is the gel matrix weakly bounded to the cell or fully soluble in the solution [55,57]. The two EPS types can be separated through centrifugation, with the EPS remaining with the pellet being the bound EPS and the EPS in the supernatant being the soluble EPS [57]. The matrices in the EPS are bridged by divalent cations, mainly Ca^{2+} and Mg^{2+}. Exchanging these cations by monovalent cations will cause the EPS structure to fall apart. In fact, cationic exchange using cationic exchange resin (CER) is one of the most used methods to extract EPS from activated sludge [3,58].

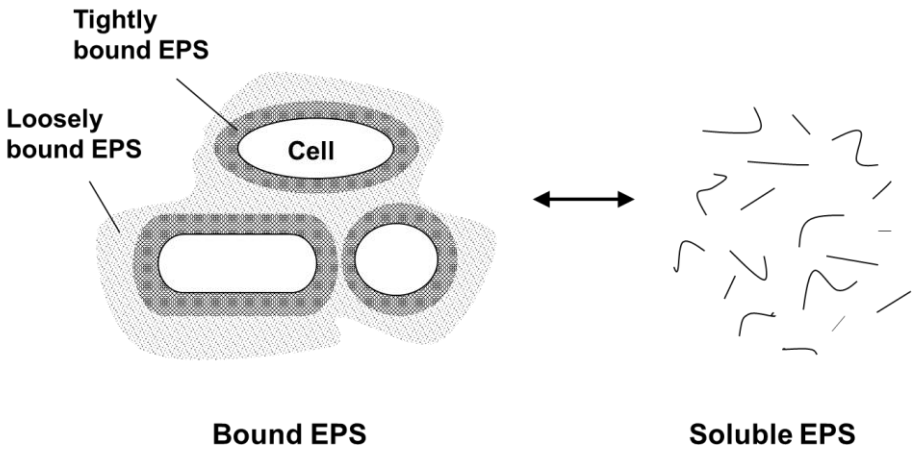

Figure 3-6: EPS structure adapted from [55]

The functions of the EPS are manifold. One of its most important functions is in the floc formation by filling the intercellular space between cells, thus facilitating the cohesion of the cells. Through its protein content, EPS also displays various functions associated with proteins [55]. Table 3-3 summarizes the main functions of the EPS.

Table 3-3: Functions of EPS [55]

Function	**Relevance**
Adhesion	Initial step in colonisation and accumulation on surfaces
Cell aggregation, floc and biofilm formation	Filling the gaps between cells to allow aggregation and immobilisation of bacterial community
Cell-to-cell recognition	Interaction between cells with surrounding flora and fauna
Structural component of the biofilm	Providing mechanical stability to biofilm, determining the shape of the EPS structure
Protective barrier	Providing resistance to biocides and harsh environment
Water retention	Preventing cell from dehydration
Sorption of exogenous organic compounds	Accumulation of substrate from the environment, detoxification through sorption of xenobiotics
Sorption of inorganic ions	Detoxification through sorption of toxic metal ions, promotion of polysaccharide gel formation, mineral formation
Enzymatic activities	Digestion of extracellular macromolecules to provide nutrients to the cell, degradation of structural EPS thereby releasing the cells from the biofilm

3.4 Protein Measurement

A robust protein measurement should include minimum possible sample pre-treatment steps, as each step increases cost and measurement time and reduces analytical precision by introducing errors. Furthermore, the measurement method should ideally have the following properties [1]:

- simple procedure
- rapid measurement
- sensitive to small amount of proteins
- compatible with a diverse range of proteins

A variety of protein measurement methods based on different mechanisms was developed, several of which will be discussed in the following sections.

3.4.1 Lowry Assay

The Lowry assay is a photometric assay based on two consecutive steps. The first step of the colour development is the Biuret reaction, where the peptide bond of the protein reacts with the cupric ion (Cu^{2+}) in the alkaline Lowry reagent to produce a blue protein-copper-complex. The second step is the reduction of tungstate–molybdate (W^{6+}/Mo^{6+}) in Folin-Ciocalteau phenol reagent. Upon reaction, the amino acid side chains of the copper-treated protein form a complex with tungstate–molybdate, whose maximum absorption can be measured at 750 nm [1,59,60]. The colour development is primarily attributed to the amino acids of tyrosine and tryptophan, and to a lesser extent, cysteine and histidine [61]. The Lowry method is relatively simple but the standard curve is linear only for a low concentration range of protein [59]. Furthermore, it is subjected to a variety of interfering substances such as carbohydrate, surfactant sodium dodecyl sulphate (SDS) and metal chelate such as EDTA [61]. In activated sludge sample, the presence of humic acid also interferes with the measurement by contributing to an increase in absorbance of Lowry assay.

Several modifications to the Lowry method were introduced to correct the interference due to humic acid in activated sludge samples, for example the corrected Lowry assay by Frølund et al. [58]. This assay is based on two separate measurements. The first measurement is the classic Lowry method whose total absorbance is contributed by both protein and humic acid. In the second measurement, the copper reagent is omitted, resulting in the absorbance of protein to decrease to about 20% of its initial value whilst the absorbance of humic acid remains constant. This enables the differentiation between the absorbance due to the humic acid and protein, hence allowing the elimination of the interference by humic acid [62]. The details of the calculation for the correction are given in Section 4.1.3.8.

3.4.2 Bradford Assay

The Bradford Assay is based on the binding of Coomasie Brilliant Blue G-250 (CBBG) dye to the basic and aromatic residues of a protein [63]. The protein binds to the CBBG dye by electrostatic and van der Waals' forces. The production of protein-dye-complex leads to a change in colour from red to blue, which shifts the absorption maximum from 465 nm to 595 nm [63]. The absorption can be measured at 595 nm and is strongly correlated to the sum of arginine, lysine and histidine residues in the protein sample. The main advantage of Bradford assay is that it is compatible with substances that interfere with other colorimetric protein measurement methods such as EDTA and carbohydrates. This method is also rapid, allowing measurement after only 5 minutes of incubation time. The drawback of this method is that the binding only occurs with large polypeptides of >3 kDa [1], hence the protein concentration measured using this method is normally lower than other methods such as Lowry [64] or ninhydrin-based assay [65]. Bradford assay was reported to be less reliable compared to Lowry assay for the measurement of protein in activated sludge [3].

3.4.3 Ninhydrin-based Assay

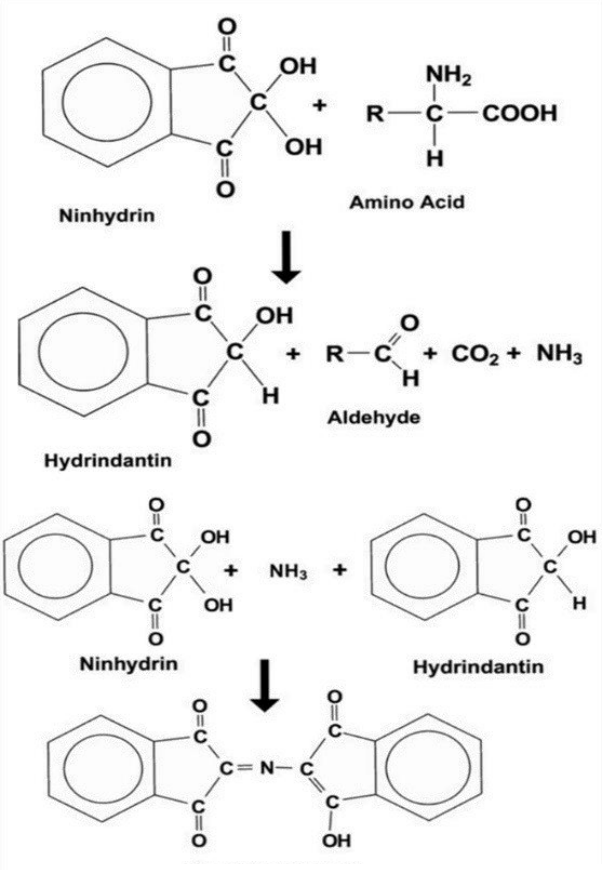

Figure 3-7: Reaction between amino acid and ninhydrin [1]

The first step in the quantification of total protein using ninhydrin-based assay involves the hydrolysis of proteins into amino acids [66]. This is followed by the addition of ninhydrin reagent. Upon reaction with the amino acids, ninhydrin is reduced to hydrindantin. The reaction also oxidises amino acids into ammonia and aldehyde. Hydrindantin and ninhydrin then react with the ammonia, producing a purple-coloured product called Ruhemann's purple (Figure 3-7) that can be measured at 570 nm [1].

Ninhydrin assay was found to be more sensitive to small amount of proteins and to have a wider linear range compared to Bradford assay. This assay also showed low protein-to-protein variability, as similar colour development was seen for different types of proteins. Another advantage of this method is that solid samples and proteins with low solubility can be easily measured through prior hydrolysis.

Furthermore, this method is more reproducible than other methods that require proteins to be soluble thus requiring, for example, prior extraction procedure. The drawbacks of this method are the relatively long hydrolysis time and a more complicated measurement step, such as involving heating of reagent at 100°C [65]. As ninhydrin reacts with all primary amines such as amines, amino acids and ammonia, interference from non-protein primary amine is possible.

Table 3-4 summarised the advantages and disadvantages of the different protein assays.

Table 3-4: Summary of protein assays, adapted from [60]

Method	Advantages	Disadvantages
Copper Binding (Biuret, Lowry, BCA)	• Inexpensive	• A variety of interfering substances • Extraction step necessary
Bradford	• Rapid and simple • High selectivity for protein	• Poor solubility of some proteins under reaction condition • Extraction step necessary
Ninhydrin	• Applicable for many sample states	• Hydrolysis time • Interference from non-protein primary amines

3.5 Proteomics and Metaproteomics

As discussed in Section 3.1, protein is expressed in a flow called the central dogma (DNA→RNA→Protein). Traditional molecular biology has been focussing on the analysis of specific genes and their products. In contemporary molecular biology, the focus has shifted to a global analysis of all genes belonging to an organism (genome). This gives rise to the transcriptome (the entire mRNA of a cell) and the proteome, the entirety of proteins expressed by a cell, tissue or organism [9]. Proteomics is thus an analysis of the proteomes, the product of the final stage of the genetic information [9,47,67].

The term ‘meta’ describes an analysis of a mixed community [10]. Figure 3-8 shows the schematic flow of meta-analysis from metagenomics to metabolomics [68], the analysis of chemical compounds or metabolites of the processes regulated by proteins [9]. Wilmes and Bond [10] introduced the term metaproteomics to define ‘the large-scale characterisation of the entire protein complement of environmental microbiota at a given point in time’. Hence metaproteomics is the

snapshot of the entire proteins expressed in an environmental sample. Generally, the aims of (meta-)proteomics are to determine [67]:

- the structure and function of the proteome.
- protein-protein interaction.
- protein response to environmental changes/stimuli.

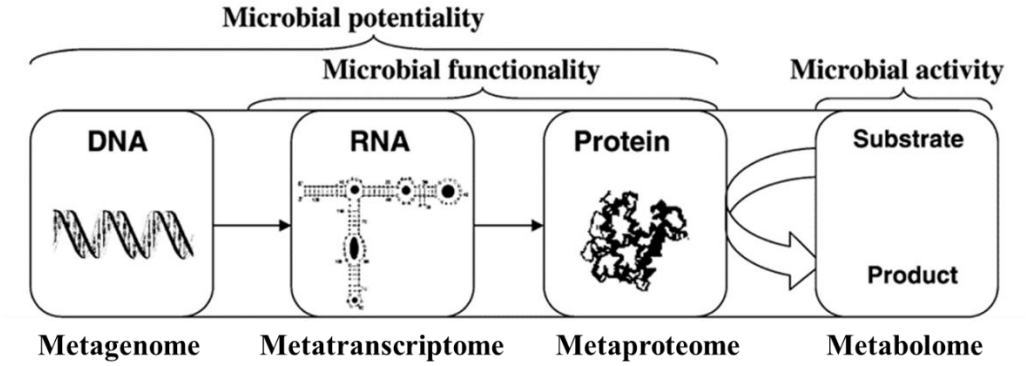

Figure 3-8: Schematic flow from metagenomics to metabolomics [68]

3.5.1 Significance of Metaproteomics in Activated Sludge

The main characteristic that differentiates the genome from transcriptome and proteome is that the information contained in the gene is constant throughout the whole organism, irrespective of the cell type and the environmental conditions. Genome is able to describe at best the potential functions of an organism, but not the functionality itself (Figure 3-8). Transcriptome and proteome, on the other hand, undergo dynamic qualitative and quantitative changes based on their environments and stimuli due to the regulation of transcription and translation, the stability of RNA and protein, alternative splicing, and protein modification. As the gene's end product, proteins are essentially the most important molecules as they control the majority of the cell's biochemical activities through their various roles as enzymes, receptors, transporters, etc. The relevance of proteomics over genomics and transcriptomics is as follows [9]:

- Protein functions are associated with their structure, distribution and protein-protein interaction. This information cannot be obtained solely from the nucleic acid (DNA/RNA) sequence.
- The abundance of gene expressions does not necessarily correlate to the abundance of proteins and vice versa.
- Many proteins undergo post-translational modifications, hence are more diverse than their transcripts.
- Some biological samples do not contain nucleic acid.

The significance of the assessment of the metaproteome of the whole microbial community is that it will help reveal the polypeptides that are expressed as a result of the cell's response to environmental changes [52]. In biological wastewater treatment, particularly activated sludge treatment, the identification of different proteomes could enable the discovery of the different roles of the microorganisms in the treatment process. Wilmes and Bond [10] and Albertsen et al. [69], for example, identified the main proteins in the activated sludge system of enhanced biological phosphorus removal (EBPR) system and investigated their functions in the purification process. Proteomes can also serve as biomarkers for the recognition of the actual state of the activated sludge and the identification of the substances that are responsible for the different behaviours of the sludge, especially those that contribute to its function or malfunctions [11]. This was demonstrated by Steiner et al. [70], who used proteomics methods to gather information on the malfunctions of activated sludge treating landfill leachate.

3.5.2 Proteomics Workflow

The adaptation of mass spectrometry (MS) for the identification of proteins and the development of algorithms for protein identification based on mass spectra data in the early 1990s have contributed to the breakthrough of proteomics [9]. Figure 3-9 shows the typical workflow of proteomics.

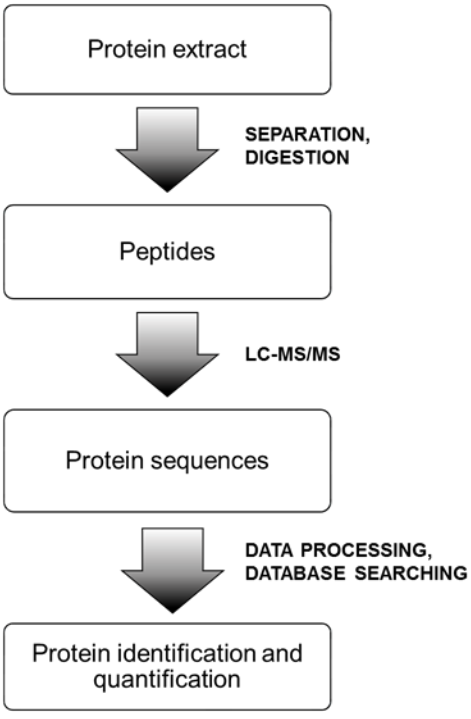

Figure 3-9: Workflow of proteomics

The first step of proteomic analysis involves the separation of proteins and/or peptides. The method typically applied for the separation of the proteins is either the two-dimensional gel electrophoresis (2DGE) followed by the digestion of the protein spots or using an approach called shotgun proteomics, where the proteins are directly digested into peptides [71]. 2DGE is a combination of isoelectric focusing and sodium dodecyl sulphate polyacrylamide gel electrophoresis (SDS-PAGE), which separates the proteins in the first dimension by charge and in the second dimension by mass. The digestion step is normally done with the help of a chemical or a proteolytic enzyme such as trypsin. Trypsin cleaves the protein specifically at the carboxyl terminal (c-terminal) end of lysine and arginine residues, except when the next residue is proline. The specificity of the cleavage allows the backtracking of the peptides to their parent proteins. The peptide mixture is normally separated using liquid

chromatography (LC) before the subsequent step of mass detection using mass spectrometry (MS). The data from the mass spectra enables the generation of amino acid sequences. With the help of specialized algorithms and a suitable database, these sequences will be assigned to the probable proteins. MS also enables the quantification of proteins in a sample [9].

3.5.3 Quantitative Proteomics

Quantitative proteomics can be done either as absolute quantification or relative quantification between samples. Relative quantification is used to obtain information regarding changes in protein expression between two sample states. The proteins of interest need to be detected in both samples to allow the relative abundance of the proteins to be quantified. Absolute quantification requires a protein or peptide sample to be spiked with a known quantity of standard, normally a stable isotope-labeled peptide. Absolute quantification enables not only the comparison of a protein between samples but also between different proteins within a sample [72].

Label-free quantification (LFQ) is a relative quantification method based on either the comparison of the spectral count or peptide ion signal intensity [71,73]. The spectral count approach is based on the observation that the number of mass spectra detected correlates to the protein abundance. Comparing the number of spectra of a given peptide between samples allows the determination of the relative abundance. The relative quantification by ion signal intensity, on the other hand, is calculated by comparing the integrals of the peak area of the ion chromatograms from LC-MS/MS. Label-free quantification has the advantage of relatively simple procedure in comparison to absolute quantification using isotope-labelled peptide. Furthermore, it allows whole proteome analysis, unlike isotope labelling which is limited to just a few selected peptides, as the relative quantification is not limited by costly and time-consuming labelling procedure. LFQ is also reported to provide higher dynamic quantification range compared to isotope labelling. However, this method is less accurate as all the variations in the procedure prior to the measurement will be reflected in the mass spectral data [73]. Table 3-5 provides the comparison of the characteristics and application between the different quantification methods.

To compare protein abundance using LFQ, the intensitz values are normally log2-transformed to reduce data variance, assuming that the data are log-normal distributed [73]. Log ratios are calculated based on the difference in log2_LFQ intensity (log2-fold change) [74].

Table 3-5: Comparison of characteristics and application of quantitative mass spectrometry methods [75]

Method	Application	Accuracy (process)	Quantitative coverage	Linear dynamic range
Spiked peptide	Medium complexity biochemical workflows Targeted analysis of few proteins	++	+	2 logs
Label-free (ion intensity)	Simple biochemical workflows Whole proteome analysis Comparison of multiple states	+	+++	2−3 logs
Label-free (spectrum counting)	Simple biochemical workflows Whole proteome analysis Comparison of multiple states	+	+++	2−3 logs

3.5.4 Limitations of Proteomic Analysis

Unlike nucleic acids that can be amplified by polymerase chain reaction (PCR), the same is not possible for protein. Due to this reason, the identification and quantification of low abundance proteins are still among the main challenges of proteomics studies [76]. The proteomics procedure comprises sample preparation step, separation with LC−MS and algorithm-based protein identification and quantification step (bioinformatics), all of which come with their own limitations [9]. Table 3-6 provides the limitations in the different stages of proteomic analysis.

Despite the limitations, proteomics has undoubtedly many advantages as a lot of specific information regarding the cell cannot be provided by other omics approaches, as discussed in Section 3.5.1. Hence, this technology is expected to continue to expand and will become the norm in cell biology studies [9].

Table 3-6: Limitations in the different stages of proteomics [9, 77]

Stage of analysis	Limitations and bottlenecks
Sample preparation	• Functional inactivation • Protein degradation • Sample contamination
Separation and identification	• Quantification of small protein • Detection of low abundance protein • Quantification of small fold change • Reproducibility
Bioinformatics	• Diverse data types and sources • Identification of proteins not present in the database • Large data volume

4 Material and Methods

4.1 Industrial WWTP

The first part of the work involved the investigation of total protein and EPS in activated sludge from three industrial wastewater treatment plants in Germany. The activated sludge samples were taken from the following plants, with the sampling points named plant A−D:

WWTP Leverkusen, Germany. This WWTP treats industrial wastewater using a conventional activated sludge process in two treatment steps. The first treatment step is the tower biology **(Plant A)** which consists of an aeration tank with upstream denitrification. The second step is the cascade biology **(Plant B)** which consists of four basins arranged in a cascade of alternating aerobic and anoxic zones. Plant A only treats industrial process wastewater while plant B treats effluent from plant A and domestic wastewater in equal ratio. Plant B experienced frequent foaming and sludge bulking problems. Due to this reason, the scum/foam layer sample from this treatment unit was also investigated.

WWTP Cologne, Germany (Plant C). This plant treats effluent from an upstream nitrification tank of petrochemical industry. The activated sludge treatment process consists of carbon removal with simultaneous denitrification.

WWTP Elberfeld, Germany (Plant D). This plant treats process wastewater from pharmaceutical industry using conventional activated sludge process of nitrification and denitrification.

4.1.1 Sampling

5 different samples were investigated from the sampling points as listed in Table 4-1. The samples were taken weekly over a period of 7−9 weeks. All samples were stored at 4 °C and measured within 7 days of sampling.

Table 4-1: Sludge source and types of samples

Treatment plant	Sample
Plant A	Activated sludge
Plant B	Activated sludge and foam/scum
Plant C	Activated sludge
Plant D	Activated sludge

4.1.2 Instruments

Table 4-2 shows the commonly used instruments for the experiments and their usage.

Table 4-2: List of instruments

Instrument	Usage
Centrifuge (Eppendorf Centrifuge 5810R)	Centrifugation of sample between 5 and 50 mL Maximum speed 4,000 rpm (3,100 x g)
Microcentrifuge (Hettich Zentrifuge Mikro 22 R)	Centrifugation of sample up to 2 mL Maximum speed 18,000 rpm (31,514 x g)
Sonicator (Branson Sonifier S-450D)	Macrotip (13 mm diameter): total protein extraction of industrial plant samples Microtip (3.2 mm diameter): total protein extraction of lab-scale plant samples
Spectrophotometer (CADAS 50 S, Dr. Lange)	Protein and carbohydrate measurement

4.1.3 Analytical methods

This section describes the analytical methods applied in this part of the work. All chemicals used were of analytical grade unless otherwise stated.

4.1.3.1 Mixed Liquor Suspended Solids

10 mL activated sludge sample was thoroughly mixed and filtered through a weighed cellulose acetate filter (Sartorius Stedim Biotech GmbH, Germany) with a pore size of 0.45 µm by pressure filtration. The filter with filtrate was then dried for about 2 h at 105 °C until a constant weight was achieved. The suspended solids concentration of the sample was calculated from the increase in weight of the filter per unit sample volume [78] (Eq. (4-1)).

$$\text{MLSS (g/L)} = \frac{\text{weight of filter containing dried residue (mg) - weight of filter (mg)}}{\text{sample volume (mL)}} \quad (4\text{-}1)$$

4.1.3.2 Mixed Liquor Volatile Suspended Solids

To measure the volatile suspended solids, the filter containing the dried residue from MLSS measurement was transferred to a ceramic dish and ignited at 550 °C for at least 4 h until a constant weight was obtained. Volatile suspended solids concentration was calculated from the weight loss upon ignition per unit sample volume [79] (Eq. (4-2)).

$$\text{MLVSS (g/L)} = \frac{\text{weight loss of dried residue after ignition (mg)}}{\text{sample volume (mL)}} \quad (4\text{-}2)$$

4.1.3.3 Sludge Volume Index

Activated sludge sample was poured into a 1 L graduated cylinder and allowed to settle for 30 min. After that, the volume occupied by the settled sludge was recorded. This volume is named sludge index (SI). Sludge volume index (SVI) was determined by dividing the settled sludge volume by the MLSS [80] (Eq. (4-3)). A sludge is said to have a good settleability when the SVI value is below 100−120 mL/g. An SVI value above 150 mL/g indicates poor settling property and possible sludge bulking problems [12].

$$\text{SVI (mL/g)} = \frac{\text{settled sludge volume after 30 min, SI (mL/L)}}{\text{MLSS (g/L)}} \quad (4\text{-}3)$$

4.1.3.4 Sludge Washing Step

A washing step is necessary to remove the supernatant containing ions and nutrients in the mixed liquor that could interfere with sludge analysis. For this purpose, sludge sample was centrifuged for 15 min at 4,000 rpm and 4 °C (Eppendorf centrifuge 5810R). The supernatant was discarded, and the pellet was resuspended to the original volume with deionized water. The procedure was repeated for 3 times.

4.1.3.5 Oxygen Uptake Rate

The total oxygen uptake rate (OUR) was used to measure the respirometric activity of viable biomass in a sample. Table 4-3 lists the chemicals used for the OUR measurement. Ammonium chloride and sodium acetate were used as ammonium and carbon substrate respectively.

Procedure: 300 mL activated sludge sample was washed according to the procedure described in Section 4.1.3.4. The sample was then aerated using compressed air for about 5 min to obtain a dissolved oxygen (DO) concentration of about 7−8 mg/L. The aerated sludge was transferred into a BOD bottle and then placed in a water bath to keep the temperature constant at 30 °C throughout the measurement. The sludge was stirred with a magnetic stirrer to ensure complete mixing and to prevent sedimentation. The schematic diagram of the respirometer is shown in Figure 4-1.

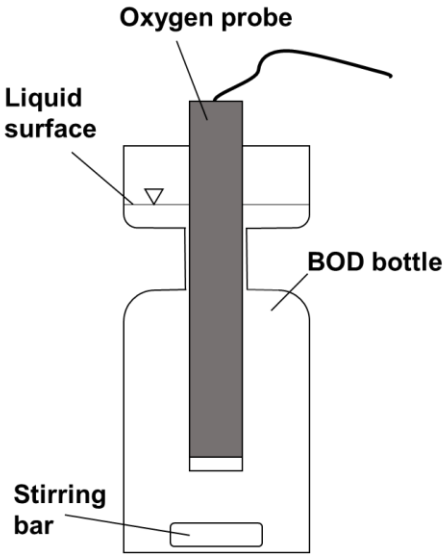

Figure 4-1: Schematic diagram of OUR measurement

Substrates ammonium chloride and sodium acetate were added to the sludge sample for total OUR measurement. Oxygen probe (IntelliCat LDO 101, Dr. Hach Lange GmbH, Germany) was inserted into the BOD bottle and the measurement of DO concentration was started immediately. DO concentration was measured using a DO meter (HQ440d from HACH, Germany) and the data were recorded automatically every 10 s (software HQ44 multi V.1.1.8.1). The measurement was stopped after about 5 min or when the DO concentration dropped below 1 mg/L.

Table 4-3: Chemicals used in OUR measurement. The concentrations in the table are the final concentration in the BOD bottle

Component	**Formula**	**Concentration**
Ammonium chloride	NH_4Cl	50 mg/L NH_4-N
Sodium acetate	CH_3COONa	100 mg/L

For the evaluation of the result, the graph of oxygen concentration over time was plotted using Microsoft Excel. OUR value was determined from the slope of the graph. DO concentrations below 1 mg/L were not used for OUR calculation. An example of the graph for OUR determination is shown in Figure 4-2. Based on the slope of the graph, the total OUR is 0.00407 mg/L· s. A steeper slope indicates a higher oxygen consumption rate.

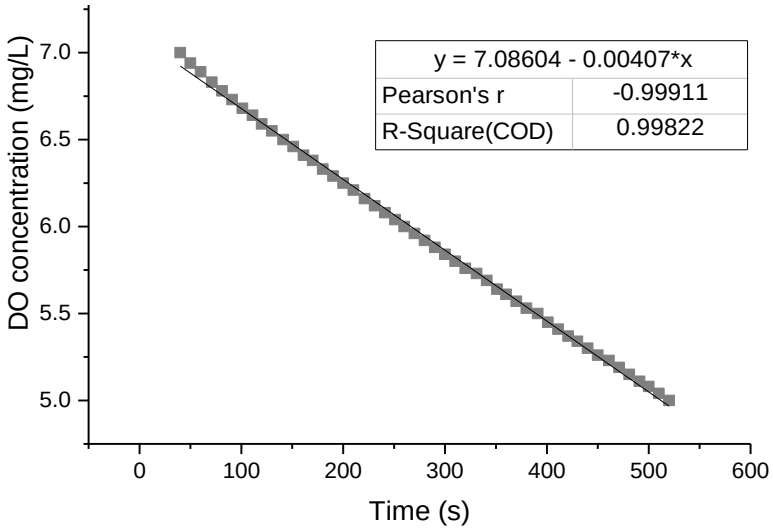

Figure 4-2: Example of OUR measurement

The specific oxygen uptake rate (SOUR) is calculated by dividing OUR value with MLVSS concentration, as shown in Eq. (4-4).

$$\text{SOUR}\ (\text{mg}\,O_2/\text{g}\,\text{VSS}\cdot\text{h}) = \frac{\text{OUR}\ (\text{mg}\,O_2/\text{L}\cdot\text{s})}{\text{MLVSS}\ (\text{g}\ \text{VSS/L})} \cdot 3{,}600\ \text{s/h} \qquad (4\text{-}4)$$

4.1.3.6 Total Protein Extraction

The extraction of total protein was achieved by cell lysis through ultrasonication. The composition of the extraction buffer is given in Table 4-4. For this purpose, 30 mL of washed sludge sample was centrifuged, and the pellet resuspended with cold extraction buffer (4°C). The sample was filled into a stainless steel cylinder and the macrotip (13 mm) of the sonicator was inserted about 2 cm into the sample. The sample was sonicated for 15 min at 50 % amplitude on pulse (on/off cycles of 0.5 s). The sonicated sample was then centrifuged for 15 min at 18,000 rpm and 4 °C. The supernatant containing the protein extract was stored at −20 °C if not measured directly. All steps of protein extraction were done on ice.

Table 4-4: Composition of extraction buffer

Component	Formula	Concentration	
		mM	g/L
Tris (pH 7.5)	$C_4H_{11}NO_3$	50	6.057
Sodium Chloride	NaCl	150	8.766
Ethylenediaminetetraacetic acid (EDTA)	$C_{10}H_{16}N_2O_8$	2	0.585
Sodium dodecyl sulphate (SDS)	$C_{12}H_{25}NaO_4S$	1%	

4.1.3.7 EPS Extraction

EPS extraction was done according to Frølund et al. [58] using cationic exchange resin (CER) Dowex® Marathon C sodium form (Sigma Aldrich, 91973). The ratio of biomass to the CER was 0.5 g MLVSS/ 35 g Dowex®. Phosphate buffered saline (PBS) was used as the extraction buffer (Table 4-5). PBS stock solution of 10x concentration was prepared beforehand and autoclaved. The solution was diluted to 1x concentration with deionized water right before use.

Procedure: 35 g of Dowex® was rinsed by stirring with 100 ml PBS in the dark for 1 h and then drained thoroughly. A volume of sludge corresponding to 0.5 g MLVSS was washed and the pellet transferred into a 50 mL Eppendorf tube. The pellet was resuspended with 25 mL PBS and the tube was placed on ice. Sample was homogenized using ultra-turrax (Polytron PT 60000, Kinematica AG) for 4 min at 8,000 rpm. PBS was added to the homogenized biomass to a final volume of 100 mL. Sample was poured into the conical flask containing the drained Dowex®. A magnetic stirrer bar was inserted into the conical flask and the sample was stirred for 3 h in the dark at 750 rpm on ice. EPS extract was collected in 50 mL tubes and centrifuged for 10 min (4,000 rpm, 4 °C) to separate the supernatant from the Dowex®. The supernatant was transferred

into 2 mL Eppendorf caps and centrifuged for 10 min (18,000 rpm, 4 °C). The sample was kept at −20 °C if not measured directly.

Table 4-5: PBS composition [58]

Component	Formula	Concentration	
		mM	g/L
Sodium phosphate dodecahydrate	$Na_3PO_4 \cdot 12H_2O$	2	0.328
Sodium dihydrogen phosphate monohydrate	$NaH_2PO_4 \cdot H_2O$	4	0.552
Sodium chloride	NaCl	9	0.256
Potassium chloride	KCl	1	0.0746

4.1.3.8 Protein Measurement

Protein measurement was done according to the modified Lowry assay by Yücesoy [81], which was originally based on the corrected Lowry method described by Frølund et al. [58]. The following solutions were prepared separately (Table 4-6). This assay differentiated the absorbance due to protein from the absorbance due to humic acid by the use blind Lowry reagent, whose composition differed from the normal (total) Lowry reagent by the omission of copper sulphate (Table 4-7).

Procedure: Protein sample was diluted 1:10 with extraction buffer (Table 4-4 for total protein and Table 4-5 for EPS sample). 800 µL of the diluted sample was mixed with 800 µL of Lowry reagent and incubated for 10 min in the dark. 400 µL of 0.2 N Folin reagent was added to the mixture and the mixture was vortexed immediately. The sample was subsequently incubated for 30 min in the dark. After incubation, the absorbance was measured at 750 nm. Blank measurement for both types of Lowry reagent was measured by substituting the sample with deionized water.

Bovine serum albumin (BSA; Sigma Aldrich, 53680) and humic acid (Sigma Aldrich, A3059) were used as standards. The standard curves for the measurement of total protein and EPS are shown in Appendix 1 (Figure A1−Figure A4).

Table 4-6: Chemicals needed for modified Lowry assay

Chemical	Formula	Concentration
Copper sulphate pentahydrate	$CuSO_4.5H_2O$	20 g/L
Sodium tartrate	$C_4H_4Na_2O_6$	175.2 g/L
Sodium carbonate	Na_2CO_3	76.92 g/L
Sodium dodecyl sulphate (SDS)	$C_{12}H_{25}NaO_4S$	1 %
Sodium hydroxide	NaOH	1 M
Folin reagent (Applichem, A5084)	$C_{10}H_5NaO_5S$	0.2 N*
Bovine Serum Albumin (BSA) (≥ 98 %; Sigma Aldrich, 53680)	-	1.5 g/L
Humic acid (technical grade; Sigma Aldrich, A3059).	-	1.5 g/L

*Folin reagent: (prepared fresh from 1:10 dilution of 2 N Folin reagent on the measurement day, protected from light by covering with aluminium foil)

Table 4-7: Preparation of Lowry reagent

Copper reagent, 6 mL (prepared fresh, max. 1-week storage)

Total	Blind
• 0.4 mL copper sulphate solution • 0.4 mL sodium tartrate solution • 5.2 mL sodium carbonate solution	• 0.4 mL deionized water • 0.4 mL sodium tartrate solution • 5.2 mL sodium carbonate solution

Lowry reagent, 10 mL (prepared fresh, max. 1-week storage)

- 6 mL copper reagent
- 2 mL 1 % SDS
- 2 mL 1 M NaOH

The absorbance of the protein $A_{protein}$ and humic acid $A_{humic\ acid}$ in the sample was determined according to Frølund et al [58]. A_{total} (Eq. (4-5)) represents the total absorbance by both protein and humic acid while A_{blind} (Eq. (4-6)) represents the absorbance value in the absence of the copper sulphate solution. ΔBSA and ΔHA are the difference in gradients of BSA and humic acid respectively in the presence and absence of copper sulphate solution.

$$A_{total} = A_{protein} + A_{humic\ acid} \quad (4\text{-}5)$$

$$A_{blind} = (1 - \Delta BSA) \cdot A_{protein} + (1 - \Delta HA) \cdot A_{humic\ acid} \quad (4\text{-}6)$$

Hence Eq. (4-7) describes the difference between A_{total} and A_{blind}

$$A_{total} - A_{blind} = \Delta BSA \cdot A_{protein} - \Delta HA \cdot A_{humic\ acid} \quad (4\text{-}7)$$

Replacing the ΔBSA and ΔHA (≈ 0) with the difference in gradients calculated from the standard curves gives the absorbance for protein and humic acid according to Eqs. (4-8) and (4-9).

$$A_{protein} = \frac{A_{total} - A_{blind}}{\Delta BSA} \quad (4\text{-}8)$$

$$A_{humic\ acid} = A_{total} - A_{protein} \quad (4\text{-}9)$$

The protein concentration was differentiated between modified and unmodified Lowry protein. The protein of unmodified Lowry was calculated by referring the total absorbance A_{total} directly to the standard curve of protein (Appendix 1 Figure A1 or Figure A3). The protein of modified Lowry was determined by considering the absorbance caused by humic acid using the calculation described above. Based on the absorbance from Eqs. (4-8) and (4-9), the standard curves of protein and humic acid were referred (Figure A1−Figure A4). The concentration was multiplied by the dilution factor to get the concentration of the undiluted sample. All the measurements were done in triplicates.

4.1.3.9 Carbohydrate Measurement

Total carbohydrate concentration was measured according to Dreywood's anthrone method using glucose as standard [82,83]. Table 4-8 shows the chemicals needed for the preparation of anthrone solution (Table 4-9).

Procedure: 500 µL cold of 75 % H_2SO_4 was combined with 250 µl sample and vortexed. 1 mL of cold anthrone solution was added to the solution and the mixture was vortexed. The sample was then heated for 15 min at 105 °C in a heating block. After heating, the sample was cooled to room temperature before absorbance was measured at 625 nm.

The standard curve was prepared in the concentration range between 0−100 mg/L (Appendix 1, Figure A5). All measurements were done in triplicates.

Table 4-8: Chemicals for anthrone method

Chemical	Formula	Concentration
Anthrone (97%; Sigma-Aldrich, 319899)	$C_{14}H_{10}O$	-
Sulphuric acid*	H_2SO_4	75 %
Ethanol absolute	C_2H_5OH	100 %
D-Glucose (≥ 99 %; Applichem, A3666)	$C_6H_{12}O_6$	100 mg/L

*cooled to 4 °C

Table 4-9: Preparation of anthrone solution

Anthrone solution, 50 mL (prepare fresh on measurement day)
• Dissolve 0.1 g anthrone in 2 mL absolute ethanol • Add cold 75 % H_2SO_4 to 50 mL

4.1.3.10 Capillary Suction Time

Capillary suction time (CST) was measured using a filtration unit (Hengstler 400, TRITON Germany) equipped with an automatic timer. CST procedure was carried out according to DIN EN 14701-1 [84].

Procedure: A filter paper (Whatman No.17) was placed between the base plate and the electrode holder as shown in Figure 4-3. 1a, 1b and 2 are the positions of electrodes on the reference rings that rest on the filter paper. 5 mL of a well-mixed sample was pipetted into the reservoir (18 mm diameter). The time for the water to spread through the filter paper from the first ring (1a and 1b) to the second ring (2) was recorded. The procedure was repeated in triplicates.

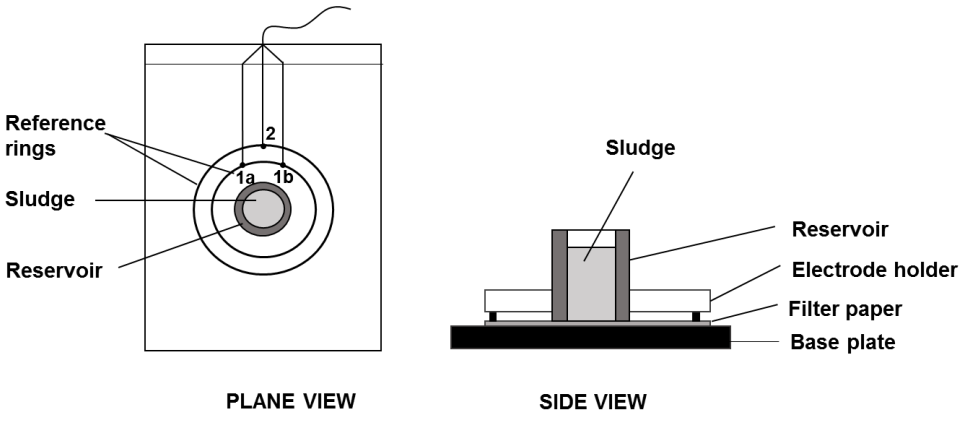

Figure 4-3: Schematic diagram of the CST measuring device, adapted from [85]

4.1.4 Statistical Analysis

The strength of the relationship between two variables was predicted by Pearson's correlation. A two-tailed test of Pearson's correlation coefficient r was conducted at 95% confidence level (α=0.05). Both variables were assumed to be normally distributed.

The following hypotheses were made:

1. Null hypothesis H_0 : there is no correlation between the two variables ($\rho^* = 0$)
2. Alternative hypothesis H_1 : there is a correlation between the two variables ($\rho^* \neq 0$)

The table of the critical values (p) for Pearson's r is shown in Appendix 4 (Table A3). The correlation is statistically significant if r > p, thus the H_0 is rejected. The statistical analysis was done using the software OriginPro 2016. The interpretation of Pearson's correlation coefficient is as follows (Table 4-10):

Table 4-10: Interpretation of correlation coefficient r

r value	Interpretation
> 0	positive correlation
+ 1	perfect positive correlation
< 0	negative correlation
− 1	perfect negative correlation
0	no correlation

*ρ refers to the population correlation coefficient. If every unit in the reference population could be measured, then r = ρ [86]

4.2 Lab-scale WWTP

The second part of the work involved the investigation of total protein and EPS of activated sludge from a lab-scale WWTP. The plant was operated for a sum of 474 days at the lab of the Department of Urban Water and Waste Management, University of Duisburg-Essen, Germany.

4.2.1 Experimental Setups

The lab-scale plant consisted of three plexiglass reactors: an anoxic tank (7 L), an aerobic tank (14 L) and a clarifier (7 L). The anoxic and aerobic reactors were double-walled reactors connected to a water bath for temperature regulation. The treatment system was conventional nitrification-denitrification whereby the denitrification (in anoxic tank) is upstream of the nitrification (Figure 4-4).

The influent of synthetic wastewater was provided by a peristaltic pump at the flow rate of 40 L/d. The synthetic wastewater was stored in a 120 L storage tank and refilled every 3 days. The settled sludge from the clarifier was recirculated at a return ratio of 90 %. Nitrate recirculation was set at 4–5 times the influent flow rate. In the case of sludge bulking, the clarifier was stirred for 5 s every 30 min to prevent sludge loss to the effluent.

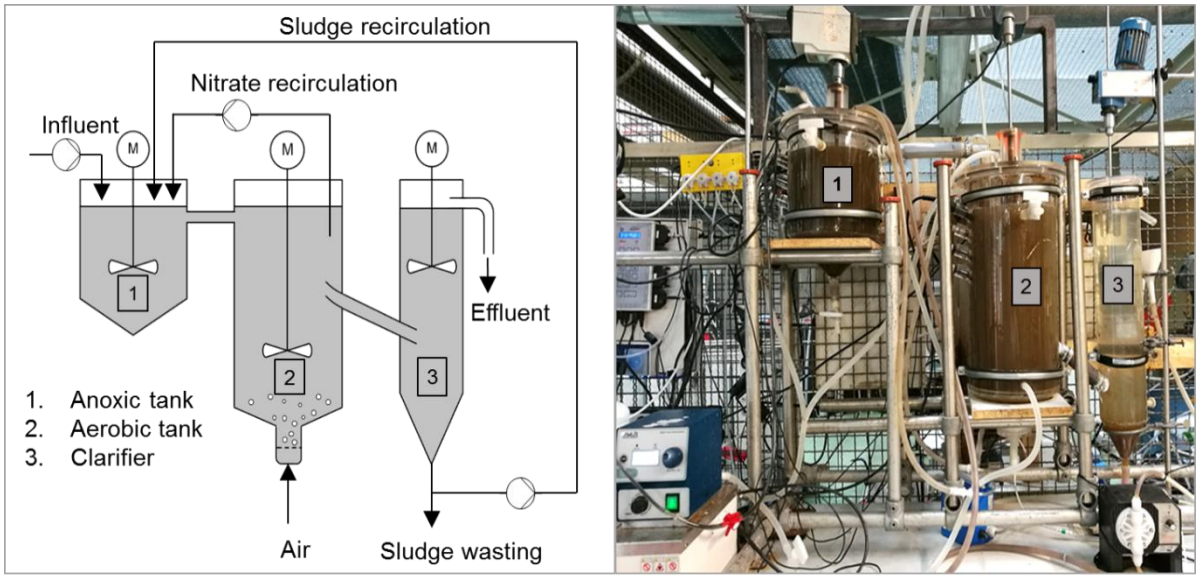

Figure 4-4: Schematic diagram (left) and picture of the actual lab-scale plant (right)

4.2.2 Sludge Source

The seed sludge was taken from the aeration tank of the municipal WWTP Kaßlerfeld, Germany. The plant treats domestic wastewater at a capacity of 450,000 population equivalent. The treatment processes are the conventional treatment of nitrification, denitrification and phosphorous removal by chemical precipitation.

4.2.3 Phases of Operation

The operation of the lab-scale plant was divided into 5 phases. The plant was inoculated with new sludge from WWTP Kaßlerfeld at the beginning of each phase. Table 4-11 shows the different operational phases of the lab-scale plant. Nutrient limitation was introduced in phases 3−5 after the sludge had acclimatized to the synthetic wastewater and a stable operation was achieved. A stable operation was assumed when the COD and ammonium removal, as well as the SS concentration of the plant, no longer fluctuated.

Table 4-11: Operational phases of the lab-scale plant

Phase	Days of operation (d)	Purpose
1	95	Start-up phase I, data collection to obtain the settings for optimal operational conditions
2	72	Start-up phase 2, simulation of a stable operation
3	161	Simulation of activated sludge treatment under phosphorous limiting condition
4	50	
5	96	Simulation of activated sludge treatment under nitrogen limiting condition

4.2.4 Operational Parameters

The operational parameters of the plant are summarized in Table 4-12. Any variations of the operational parameters from Table 4-12 will be discussed in the results (Section 5.2). Due to changes in operational conditions, the MLSS and MLVSS values varied from phase to phase and also within a phase. The sludge age was controlled at 30−35 days through sludge wastage to allow full nitrification and denitrification [3]. However, the sludge age varied unavoidably during unstable operations e.g. during nutrient limiting conditions as the growth rate decreased and settling problem occurred. In such a case, sludge wastage had to be reduced to avoid further sludge loss.

No excess sludge was removed when the SS value dropped below 1.5 g/L although around 300 mL sludge was taken as usual twice a week for sampling.

The pH of the anoxic and the aerobic reactors was controlled between 7.5 and 7.8 by the addition of 0.25 M HCl and 50 mg/L $NaHCO_3$. pH and DO control was automated using IKS Aquastar control system (IKS Computersysteme GmbH, Germany). The pH and temperature of both reactors, the redox potential of the anoxic reactor and the DO concentration of the aerobic reactor were continuously monitored using the same system.

Table 4-12: Operational parameters of the lab-scale plant

Parameter	Value
Temperature	25 °C
pH	7.5 – 7.8
DO concentration	2−3 mg/L
Hydraulic retention time (HRT)	12.6 h
Sludge age	30−35 d
Organic loading (F/M ratio)	0.5 g COD/g SS.d
VSS/SS (mean)	81 %

4.2.5 Influent Composition

The influent was a combination of synthetic wastewater and trace metal solution modified from Zhang et al. [87]. Both solutions were prepared as stock solutions of 1,000x the concentration described in the literature and stored at 4 °C until use. The composition of the stock solution of the synthetic wastewater is given in Table 4-13 and the composition of the trace metal stock solution is shown in Table 4-14. The 1x concentration of the synthetic wastewater gave approximately the following concentrations [87]:

- COD 400 mg/L
- Total nitrogen (TN) 80 mg/L
- Total phosphorous (TP) 4 mg/L
- Ammonia nitrogen (NH_3-N) 48 mg/L

The synthetic wastewater stock solution was diluted to a sludge loading of 0.5 g COD/g SS·d. The same dilution was applied to the trace metal stock solution. Nutrient limitation was simulated by

changing the content of the synthetic wastewater. Nitrogen limiting wastewater was prepared as previously described without ammonium chloride and peptone in the synthetic wastewater, and without EDTA in the trace metal solution. Phosphorous limiting wastewater was prepared by the omission of potassium dihydrogen phosphate.

Table 4-13: Composition of the synthetic wastewater stock solution (pH 7.5). (x) Included in the wastewater, (-) not included

Component	Formula	Concentration [g/L]	N-limiting wastewater	P-limiting wastewater
Glucose	$C_6H_{12}O_6$	150	x	x
Sodium acetate	$C_2H_3NaO_2$	80	x	x
*Peptone from meat (Sigma-Aldrich, 82962)	-	150	-	x
**Ammonium chloride	NH_4Cl	160	-	x
Potassium dihydrogen phosphate	KH_2PO_4	260	x	-

* At the beginning of phase 3, peptone from casein (for microbiology; Applichem, 403898.1210) was used. This was later changed to the one in the table from day 89.

**The concentration of NH_4Cl was doubled from [87] to ensure the required COD:N ratio for complete nitrification activity.

Table 4-14: Composition of the trace metal stock solution (pH 7.5)

Component	Formula	Concentration [g/L]
Calcium chloride	$CaCl_2$	10.6
Magnesium sulfate heptahydrate	$MgSO_4 \cdot 7H_2O$	20
Ethylenediaminetetraacetic acid (EDTA) disodium salt	$C_{10}H_{14}N_2Na_2O_8$	3
Iron (III) chloride hexahydrate	$FeCl_3 \cdot 6H_2O$	0.45
Manganese (II) chloride tetrahydrate	$MnCl_2 \cdot 4H_2O$	0.036
Boric acid	H_3BO_3	0.045
Zinc sulfate heptahydrate	$ZnSO_4 \cdot 7H_2O$	0.036
Copper (II) sulfate pentahydrate	$CuSO_4 \cdot 5H_2O$	0.009
Potassium iodide	KI	0.054

4.2.6 Sampling and Sample Storage

The influent and effluent samples, as well as the sludge sample from the aeration tank, were taken twice weekly. All samples were stored at 4 °C. If not measured within 7 days, the influent and effluent samples were stored at −20° C. Sludge samples were washed and the pellets after centrifugation were stored at −20° C if not measured within a week.

4.2.7 Sludge Loading

Sludge loading or food to microorganism ratio (F/M) was calculated by the ratio of the COD entering the reactor to the amount of microorganisms (suspended solids) in the reactor. Phosphorous and nitrogen loadings were calculated similarly by exchanging the COD concentration to the PO_4-P and NH_4-N concentration respectively.

$$\text{Sludge loading (g COD/(g SS·d))} = \frac{Q\ (\text{L/d}) \cdot \text{COD (g/L)}}{V_R(\text{L}) \cdot \text{SS (g/L)}} \qquad (4\text{-}10)$$

Q	Influent flow rate
COD	COD concentration of the influent
V_R	Volume of anoxic and aerobic reactors (21 L)

4.2.8 Sludge Age

Sludge age was determined by the ratio of the sludge in the reactor to the wastage rate of the excess sludge. The SS of the effluent was not measured hence sludge loss through effluent was not included in the calculation of sludge age.

$$\text{Sludge age (d)} = \frac{V_R(\text{L}) \cdot \text{SS (g/L)}}{Q_{excess}\ (\text{L/d}) \cdot SS_{excess}\ (\text{g/L})} \qquad (4\text{-}11)$$

Q_{excess}	Rate of excess sludge removal
SS_{excess}	Excess sludge suspended solids concentration

4.2.9 Total Protein Extraction

Modifications were done to the protein extraction method of Section 4.1.3.6 to adjust to a smaller sample volume. PBS was used as the extraction buffer with the addition of EDTA and AEBSF as the protease inhibitors (Table 4-15). The sludge sample was lysed using a sonicator (microtip 3.2 mm diameter).

Table 4-15: Extraction buffer (final concentration)

Component	Formula	Value
PBS (Table 4-5)	-	1 x
Ethylenediaminetetraacetic acid (EDTA)	$C_{10}H_{16}N_2O_8$	1 mM
4-(2-aminoethyl) benzenesulfonyl fluoride hydrochloride (AEBSF; Applichem, A1421)	$C_8H_{10}FNO_2S.HCl$	1 mM

Procedure: Washed activated sludge sample was centrifuged and the pellet resuspended in extraction buffer. The sample was sonicated in 5 mL Eppendorf tube for 15 min at 25 % amplitude on pulse (on/off cycles of 30 s). After sonication, the sample was centrifuged for 15 min at 18,000 rpm and 4 ˚C. The supernatant was kept at −20 °C until measurement.

4.2.10 EPS Extraction

The extraction procedure was similar to the method described in section 4.1.3.7 but modified to adjust to a smaller sample volume. As the amount of biomass used was one-tenth of previously described, the biomass and Dowex® amount were adjusted to 0.05 g MLVSS/3.5 g Dowex®.

Procedure: 3.5 g Dowex® was rinsed by stirring with 10 mL PBS to in the dark for 1 h and then drained. A volume of sludge corresponding to 0.05 g MLVSS was washed and the supernatant discarded. The pellet was transferred into a 50 mL Eppendorf tube and resuspended with PBS to 10 mL. The sample was poured into a conical flask containing the washed Dowex® and stirred for 4h in the dark at 750 rpm on ice.

The extract was collected in 15 mL tubes then centrifuged for 10 min at 4,000 rpm and 4 °C to separate the extract from the Dowex®. The supernatant was then transferred into 2 mL Eppendorf caps and centrifuged for 15 min (18,000 rpm and 4 °C). The supernatant from the second centrifugation was kept at −20 °C until measurement.

4.2.11 Oxygen Uptake Rate

The OUR measurement from 4.1.3.5 was modified to adjust to 20 mL sample volume. The total OUR of lab-scale plant sample was differentiated between autotrophic and heterotrophic OUR by addition of allylthiourea (ATU) to inhibit the conversion of ammonium into nitrite thus inhibiting the nitrification process. The OUR measured after the addition of ATU was of heterotrophic OUR. The OUR due to nitrification (autotrophic OUR) was calculated from the difference between the total and heterotrophic OUR (Eq. (4-12)). The total and heterotrophic OUR were determined from the gradient of dissolved oxygen concentration as explained in Section 4.1.3.5:

$$OUR_{auto} = OUR_{total} - OUR_{hetero} \quad (4\text{-}12)$$

OUR_{auto} Autotrophic OUR (g/L·h)

OUR_{total} Total OUR (mg/L·h)

OUR_{hetero} Heterotrophic OUR (mg/L·h)

Procedure: 20 mL of washed sludge sample was shaken in a 50 mL Eppendorf tube under a headspace of air to achieve oxygen saturation concentration of around 7−8 mg/L. The aerated sludge was transferred into a BOD bottle and then placed in a water bath of 25 °C, the same temperature as the lab-scale plant.

Substrates ammonium chloride and sodium acetate were added to the sludge sample for total OUR measurement (Table 4-16). Oxygen probe was inserted into the BOD bottle and measurement of DO concentration was started immediately. DO concentration was measured and after about 5 min, the measurement was paused and the ATU was added to the mixture. The measurement was continued for another 5 min or until the DO concentration dropped to 1 mg/L.

Table 4-16: Reagents for OUR measurement (final concentration)

Component	Formula	Concentration
Ammonium chloride	NH_4Cl	50 mg/L NH_4-N
Sodium acetate	CH_3COONa	100 mg/L
Allylthiourea (ATU)	$C_4H_8N_2S$	11.6 mg/L (0.1 mM)

4.2.12 Protein Measurement

Protein samples in this part of the work were not measured directly after extraction. Instead, they were frozen at −20 °C before quantification. Frozen samples were then thawed and centrifuged for a second time for 15 min (18,000 rpm, 4 °C) to precipitate humic acid [88]. The clear supernatant was taken for further analysis.

4.2.12.1 Lowry Assay

The Lowry assay was carried out using the DC Protein Assay kit (Bio-RAD, 500-0116) which contained an alkaline copper tartrate solution (reagent A) and a dilute Folin reagent (reagent B).

Procedure: 150 µl reagent A was added to 30 µL protein sample and vortexed to mix. 1.2 mL reagent B was added to the mixture and vortexed immediately. The sample was incubated at room temperature for 15 min. The absorbance was measured at 750 nm. The standard curve was done using BSA (Sigma Aldrich, 53680) as standard (Appendix 2 Figure A6).

4.2.12.2 Bradford Assay

The Bradford assay was carried out using the Bio-RAD Protein Assay containing Coomassie dye reagent concentrate (Bio-RAD, 500-0006). The dye reagent concentrate was diluted 1:10 dilution and filtered with a cellulose filter paper (12-15 µm pore size, Ratilabo 11A, Carl-Roth). The reagent was store at room temperature and used within 2 weeks.

Procedure: 1 mL of diluted dye reagent was added to 20 µL sample and vortexed. The solution was incubated at room temperature for 5 min. The standard curve was done using BSA (Sigma Aldrich, 53680) as standard (Appendix 2 Figure A7 and Figure A8).

4.2.12.3 Ninhydrin Assay

Protein quantification with the ninhydrin-based assay was done according to the reduced Free Amino Nitrogen (rFAN**)** assay by Abernathy et al. [89]. The chemicals needed for the assay are listed in Table 4-17. Ninhydrin reagent was prepared according to Table 4-18.

Table 4-17: Chemicals for ninhydrin-based assay

Component	Formula
Hydrochloric acid (6 N and 12 N)	HCl
Stannous chloride	$SnCl_2$
Sodium acetate trihydrate	$CH_3COONa \cdot 3H_2O$
Ethylene glycol	$C_2H_6O_2$
Glacial acetic acid	CH_3COOH
Ninhydrin (Applichem, A0902)	$C_9H_6O_4$

Table 4-18: Preparation of ninhydrin reagent

Sodium acetate Buffer (4 N)

- 544 g sodium acetate trihydrate
- Addition of 400 mL glacial acetic acid
- Addition water to 1 L
- The buffer should be around pH 5.5 without adjustment

Ninhydrin Stock Solution (stable for 6 months at room temperature)

- 8 g of ninhydrin dissolved in 300 mL of ethylene glycol
- Addition of 100 mL sodium acetate buffer

Stannous Chloride Solution (stable for 6 months at room temperature)

- 500 mg $SnCl_2$ dissolved in 5 mL ethylene glycol

Ninhydrin Reagent/Working Solution (prepare fresh)

- 1 mL of ninhydrin stock solution
- Addition of 25 µL $SnCl_2$ solution, mix well

Procedure:

Acid Hydrolysis

The hydrolysis can be done for liquid sludge and sludge pellet samples. In a fume hood, 250 µL of 12 N HCl was added to an equal amount of liquid sample (or 500 µL of 6 N HCl to solid pellet sample). The mixture was heated for 1.5 h at 148 °C in 2 mL Eppendorf microfuge tube with a hole

punched in the lid. This reduced heating time was optimised from 24 h heating time at 100 °C based on preliminary studies referring to Mok et al. [90].

After heating, the sample was cooled to room temperature. As some water could be lost during the heating, sample volume was adjusted back 500 µL with distilled water when necessary. Hydrolysed sample was then centrifuged at 18,000 rpm and the supernatant was taken for analysis.

Quantification

100 µL working solution was added to 15 µL of hydrolysed sample and vortexed. The mixture was heated in a heating block at 100 °C for 10 min. Afterwards, 1.4 mL cold distilled water was added and the mixture vortexed. The absorbance was read at 575 nm.

4.2.13 Nutrient Measurement

The nutrient composition in the influent and the effluent of the plant was measured by UV spectrometry using Hach Lange cuvette test kits (Hach Lange GmbH, Germany). The samples were filtered using 0.45 µm cellulose acetate filter (Sartorius Stedim Biotech GmbH, Germany) prior to measurement. The test kits used and their corresponding standards are listed in Table 4-19. The supplier's manual was followed without modifications.

Table 4-19: Hach-Lange cuvette test kits

Kit	Measurement	Range [mg/L]	Standard
LCK 314	COD	15 – 150 O_2	ISO 6060-1989 DIN 38406-H411-A44
LCK 514	COD	100 – 2,000 O_2	ISO 6060-1989 DIN 38406-H411-A44
LCK 338	Total nitrogen	20 – 100 TN_b	EN ISO 11905-1
LCK 138	Total nitrogen	1 – 16 TN_b	EN ISO 11905-1
LCK 303	Ammonium	2 – 47 NH_4-N (2.5 – 60 NH_4)	ISO 7150-1 DIN 38406 E5-1
LCK 304	Ammonium	0.015 – 2.0 NH_4-N (0.02 – 2.5 NH_4)	ISO 7150-1 DIN 38406 E5-1
LCK 339	Nitrate	0.23 – 13.5 NO_3-N (1 – 60 NO_3)	ISO 7890-1-2-1986 DIN 38405 D9-2

-Table 4-19 continued-

LCK 340	Nitrate	5 – 35 NO_3-N (22 – 155 NO_3)	ISO 7890-1-2-1986 DIN 38405 D9-2
LCK 342	Nitrite	0.6 – 6.0 NO_2-N (2 – 20 NO_2)	EN ISO 26777 DIN 38405 D10
LCK 341	Nitrite	0.015 – 0.6 NO_2-N (0.05 – 2 NO_2)	EN ISO 26777 DIN 38405 D10
LCK 049	Ortho-phosphate	1.6 – 30 PO_4-P (5 – 90 PO_4)	-
LCK 349	Total phosphorous/ ortho-phosphate	0.05 – 1.5 PO_4-P (0.15 – 4.5 PO_4)	ISO 6878-1-1986 DIN 38405 D11-4
LCK 350	Total phosphorous/ ortho-phosphate	2 – 20 PO_4-P (6 – 60 PO_4)	ISO 6878-1-1986 DIN 38405 D11-4

4.2.14 Proteomic analysis

Shotgun proteomic analyses were done for the selected total protein samples of the sludge from phase 1, 4 and 5, as well as the EPS and foam/scum samples from phase 4 and 5. The procedure of proteomics involved protein extraction and digestion followed by LC-MS/MS prior to protein identification and quantification.

4.2.14.1 Protein extraction

Extraction of Total Protein

1 g of washed sludge pellet was resuspended with 3 mL of extraction buffer (Table 4-20). The suspension was sonicated for 5 min on pulse (30 s on /off cycles) at 25 % amplitude using the microtip. The lysate was cleared by centrifugation at 18,000 rpm (15 min, 4 ºC) and the supernatant was stored at −20°C until measurement. Before analysis, the frozen sample was thawed and centrifuged at 18,000 rpm for 15 min and 4 ºC to precipitate humic acid and the protein concentration in the supernatant was measured using the Bradford method ([63]; see Section 4.1.3.8). The same procedure was applied to extract protein from foam/scum samples.

EPS Extraction

EPS sample for proteomics was extracted as described in Section 4.2.10 using the extraction buffer as shown in Table 4-20. The extract was treated with the same procedure as the total protein lysate.

Table 4-20: Composition of extraction buffer for proteomic analysis

Component	Formula	Value
PBS (Table 4-5)	-	1x concentration
Ethylenediaminetetraacetic acid (EDTA)	$C_{10}H_{16}N_2O_8$	1 mM
Protease inhibitor cocktail (cOmplete™ Mini EDTA-free; Roche, 4693159001)	-	1 tablet/10 mL PBS

4.2.14.2 Concentration Step

For proteomic analysis, the protein concentration of the sample should be higher than 0.2 g/L. Samples of lower concentrations were concentrated before proteomic analysis. The chemicals required for the concentration step are shown in Table 4-21.

Table 4-21: Chemicals for concentration of protein

Component	Formula	Concentration
Trichloroacetic acid (TCA)	$C_2HCl_3O_2$	100 %
Acetone	C_3H_6O	100 %
Sodium carbonate	Na_2CO_3	100 mM

Procedure: 100% TCA solution was added to protein sample to a final concentration of 10 %. The sample was incubated overnight at −20 ºC to precipitate the proteins. After thawing, the sample was centrifuged for 15 min at 18,000 rpm and 4 ºC. The supernatant was removed and the pellet was washed with 500 µL ice-cold acetone (−20 ºC) and centrifuged for 30 min at 18,000 rpm and 4 ºC. The acetone washing procedure was repeated 2−3 times to completely remove traces of TCA from the sample. After the washing procedure, the acetone was carefully removed with a pipette and the rest of acetone was evaporated at 35 ºC, being careful not to overdry the pellet. Sodium carbonate solution was added to soften the pellet (ca. 50 µL, just enough to cover the pellet). Extraction buffer (Table 4-20) was added to the pellet and the sample was sonicated for a few seconds to solubilize the protein. Bradford assay was repeated to quantify protein concentration.

4.2.14.3 LC-MS/MS

The protein samples were sent to an external lab for LC-MS/MS procedure. In brief, the procedure was as follows:

Sample Preparation and Clean-up for LC-MS

A volume corresponding to 15 µg of protein was precipitated using the methanol/chloroform extraction method [91]. The protein pellet was resuspended in 8 M urea and proteins were then reduced with dithiothreitol. This was followed by alkylation with iodoacetamide, digestion with LysC (Wako, 37 °C, 3 h) and after dilution of the urea to a concentration below 1 M, digestion with trypsin (Promega, 37 °C, 16 h). Finally, the acidified tryptic digests were desalted on home-made 2-disc C18 StageTips as described in [92]**.** After elution from the StageTips, samples were dried using a vacuum concentrator (Eppendorf) and the peptides were taken up in 10 µL of 0.1 % formic acid solution.

LC-MS/MS settings

Experiments were performed on an Orbitrap Elite instrument (Thermo) coupled to an EASY-nLC 1000 liquid chromatography (LC) system (Thermo), operated in the one-column mode. The settings were as described in [93].

Peptide and Protein Identification and Quantification using MaxQuant

RAW spectra were submitted to an Andromeda [94] search in MaxQuant (1.5.3.30) using the default settings [95]. The search settings were as described in [93] except that the MS/MS spectra data were searched against the clustered amino acid sequence of metagenome 4463936.3 from WWTP Aalborg, Denmark [96], downloaded from the MG-RAST server [97] (initial file name: mgm4463936.3.550.cluster.aa90.faa; 297317 entries).

Some of the important settings were as follows: Enzyme specificity was set to “Trypsin/P (semispecific)” with two missed cleavages allowed. Minimum peptide length was 7 amino acids. For protein quantification, unique, razor and modified peptides were allowed. The minimum score for modified peptides was 40. Label-free quantification (LFQ) was switched on, and unique and razor peptides were considered for quantification with a minimum ratio count of 2. At least two quantitation events were required for a quantifiable protein. Relative quantification between different MS runs was solely based on the LFQ’s as calculated by MaxQuant (MaxLFQ algorithm; [74]).

4.2.14.4 Protein Annotation

The amino acid sequences identified from LC-MS/MS were annotated for functions using KEGG automatic annotation tool for metagenome, GhostKOALA [98] and searched against KEGG GENES prokaryotes database at the genus level.

4.2.15 Microscopic Evaluation

To assess the physical changes of the flocs, activated sludge samples were examined using Zeiss Axio Imager.M2 digital microscope at 100x, 400x and 1,000x magnifications. The digital images were analysed using Axiovision V4.8 software.

4.2.16 FISH analysis

Fluorescence in situ Hybridisation (FISH) using 16S rRNA-targeted oligonucleotide probes was done to validate the presence of the class or genus of bacteria whose proteins were identified in large amount by proteomics. The procedure was as described in Nielsen et al. [99] with minor modifications. In brief, activated sludge sample was fixed with an equal volume of 96 % ethanol and stored at −20 °C until use. The sample was immobilized on microscope slides before being dried in the oven at 46 °C. This was followed by sample dehydration by dipping the slides in increasing ethanol concentrations (50 %, 80 % and 96 %) for 5 min in each step and then dried. For preparation of the gene probes (Table 4-22; Biomers, Germany), 90 µL of hybridisation buffer (Table 4-23) was mixed together with 10 µL of gene probe that had been resuspended according to manufacturer's instructions. 10 µL of the resulting mixture was applied to each well. For identification of the phylum *Chloroflexi*, the probes CFX 1223 and GNSB941 were combined before application. The hybridisation took place overnight at 46 °C followed by washing procedures by dipping the slides first in washing buffer (Table 4-23) for 15 min at 48 °C and then in deionized water for 5 min at room temperature. After drying, the sample was counterstained with DNA probe DAPI (4′,6-diamidino-2-phenylindol) for 10 min in the dark. After staining, the slide was dipped in distilled water for 5 min to rinse out the DAPI solution and then dried in the oven before being treated with anti-bleaching agent Citifluor (Citifluor ltd., UK). The digital images were captured using fluorescence microscope Zeiss Axio Imager.M2 and analysed using Axiovision V4.8 software.

Table 4-22: 16S rRNA-targeted oligonucleotide probes with their corresponding specificity, sequence and formamide concentration. Fluorochrome Cy3 was used for all target probes.

Probe	Specificity	Sequence	FA* (%)	Reference
Nmo254	*Nitrosomonas*	5'- GTA GGC CST TAC CCY ACC -3'	30	[100]
PAO651	Most members of the *Candidatus* Accumulibacter cluster	5'- CCC TCT GCC AAA CTC CAG -3'	35	[101]
CFX1223	Phylum *Chloroflexi*	5'- CCA TTG TAG CGT GTG TGT MG -3'	35	[102]
GNSB941	Phylum *Chloroflexi*	5'- AAA CCA CAC GCT CCG CT -3'	35	[103]

*FA = formamide concentration

Table 4-23: Composition of hybridisation and washing buffer [99]

	Hybridisation buffer		**Washing buffer**	
Formamide concentration	**30 %**	**35 %**	**30 %**	**35 %**
	(µL)	(µL)	(µL)	(µL)
NaCl 5 M	360	360	1,020	700
Tris/HCl 1 M	40	40	1,000	1,000
Formamide	600	700	-	-
Deionized water	1,000	900	-	-
SDS 10 %	2	2	50	50
EDTA 0.5 M	-	-	500	500

5 Results and Discussion

5.1 Industrial WWTP

The first part of the study involved the investigation of activated sludge from three industrial WWTPs in Germany (see Section 4.1). Sludge samples were taken weekly for a period of 7−9 weeks. The conventional biomass parameters SS and VSS were analysed to determine their accuracy as parameters for quantification of active biomass. As these parameters also contain other compounds that do not contribute to the activity e.g. humic acid and carbohydrate [3,15], they were compared to the total protein to assess the potential use of total protein concentration as an alternative parameter to SS and VSS for estimation of the amount of active biomass. Furthermore, the EPS constituents in terms of the protein, humic acid and carbohydrate contents of the sludge were analysed to assess their influence on settleability and dewatering property.

5.1.1 Comparison of Biomass Parameters

Figure 5-1 (left) shows the comparison of the mean concentrations of the SS, VSS, total protein and humic acid between sampling points A−D. The total protein concentration is shown both in terms of unmodified Lowry, which does not differentiate between the absorbance caused by the protein and humic acid, and modified Lowry, which subtracts the interference by humic acid from the total absorbance for a more accurate determination of protein concentration. It can be seen that protein content measured by modified Lowry did not differ much from plant to plant despite high differences in SS and VSS values. They were in the range of 0.5 and 0.7 g/L, which made up between 11 and 18% of the VSS (Figure 5-1 (right) and Table 5-1). The protein and humic acid values were the average values of only 4 to 5 samples as the extraction process of the first three weeks were carried out using a bead beater, which was later found fail to give reproducible results. More importantly, the protein concentration of the extract was too low when compared to the protein extracted through sonication, believed to be due to incomplete lysis. Hence from week four, the extraction was carried out by sonication.

The protein and humic acid fraction in the VSS from this study were found to be lower than the values described in the literature e.g. Sridhar and Pillai [53] and Yücesoy [81] of around 40%. Yücesoy [81] employed a similar extraction procedure of ultrasonication while Sridhar and Pillai [53] extracted the protein by acetone drying followed by freeze and thaw cycles. In this work, the protein concentrations of unmodified Lowry were about twice as high as the modified Lowry with values between 27−30% of VSS (Table 5-1), confirming literature reports that unmodified Lowry method overestimates protein concentration in samples containing humic acid [58].

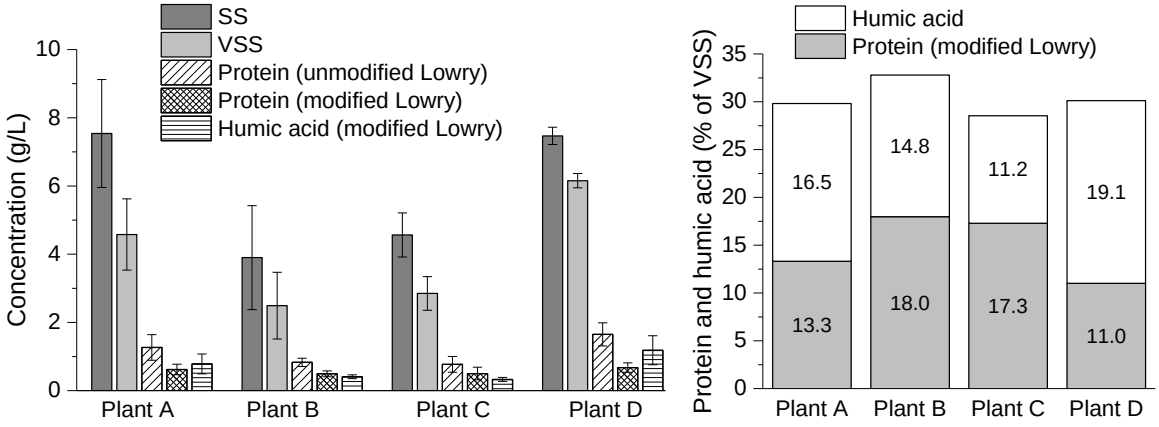

Figure 5-1: Comparison of the SS, VSS, protein and humic acid concentrations (left) and percentage of protein and humic acid in the VSS between the plants A-D (right)

Table 5-1: Protein and humic acid as percentages of VSS in different plants. N: sample size

% of VSS		Plant A (N=5)	Plant B (N=4)	Plant C (N=4)	Plant D (N=5)	All samples (N=18)
Protein (unmodified Lowry)	mean	26.9	30.2	26.6	26.6	27.5
	SD	5.8	7.5	10.4	5.0	6.7
Protein (modified Lowry)	mean	13.3	18.0	17.3	11.0	14.6
	SD	2.7	5.7	7.8	2.5	5.3
Humic acid (modified Lowry)	mean	16.5	14.8	11.2	19.1	15.7
	SD	4.7	2.5	3.3	6.3	5.1

Figure 5-2 shows the changes of SS, VSS, unmodified Lowry protein and humic acid with increasing concentration of modified Lowry protein. It reveals that the concentration of the other four parameters did not progress with a similar trend as the modified Lowry protein. Instead, SS, VSS and unmodified Lowry protein show similar development to that of humic acid. This illustrates the significant influence of humic acid in the total concentration of unmodified Lowry, SS and VSS. Failure to consider humic acid concentration will lead to erroneous estimation of biomass concentration.

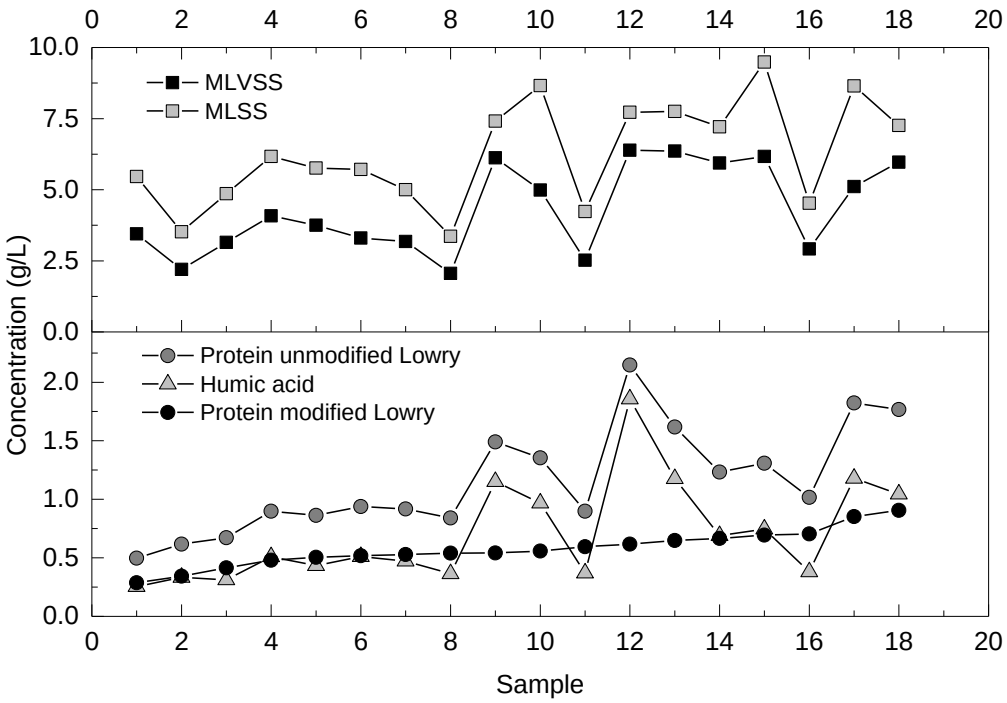

Figure 5-2: SS, VSS, protein (unmodified Lowry) and humic acid concentration with increasing concentration of protein (modified Lowry)

In general, the concentration of modified Lowry protein increased with increasing concentration of VSS (Figure 5-3 (left)) but its percentage in the VSS decreased with higher VSS concentration, as shown in Figure 5-3 (right). If total protein was to provide a better estimation of active biomass, then the error made if the biomass was measured by VSS would be bigger at high biomass concentrations.

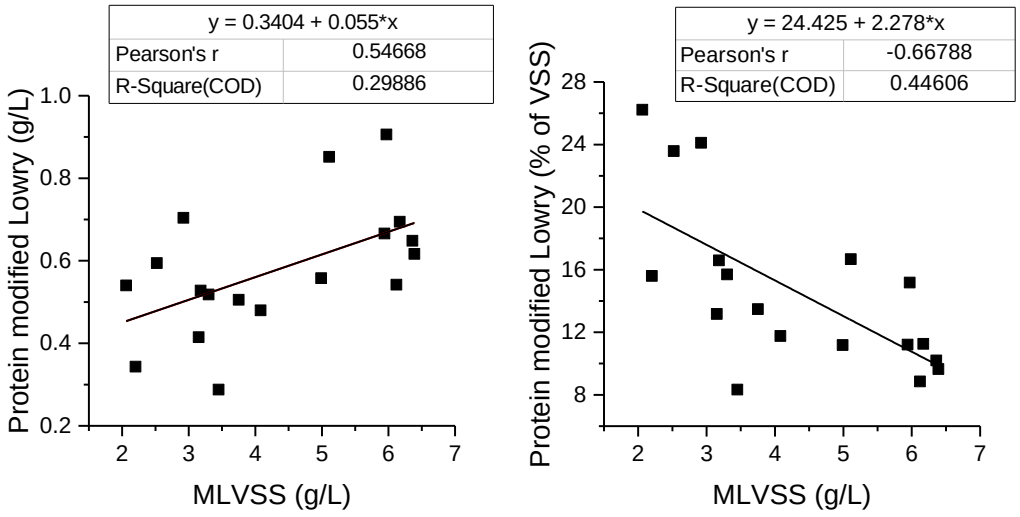

Figure 5-3: The concentration (left) and percentage in VSS (right) of modified Lowry protein with increasing concentration of VSS

5.1.2 Investigation of Total Protein as Alternative Parameter for Measuring Active Biomass

To determine the relationship between SS, VSS and protein with active biomass, these values were compared to the oxygen uptake rate (OUR), which is a measure of respirometric activity. As the different biomass parameters cannot differentiate between groups of bacteria, the correlations were determined only with the total OUR. The correlations were determined for the collective data of all plants. They were not separated for each plant as the values became insignificant due to small sample sizes. The results of the correlations are illustrated in Figure 5-4.The circled values indicate the data from Plant D. It can be seen that the OUR values of this plant were notably higher than the values of the other three plants for same range of the different biomass parameters, thus was not suitable to be used for describing generalised results. To avoid erroneous correlations, the data from plant D were not considered for the correlations.

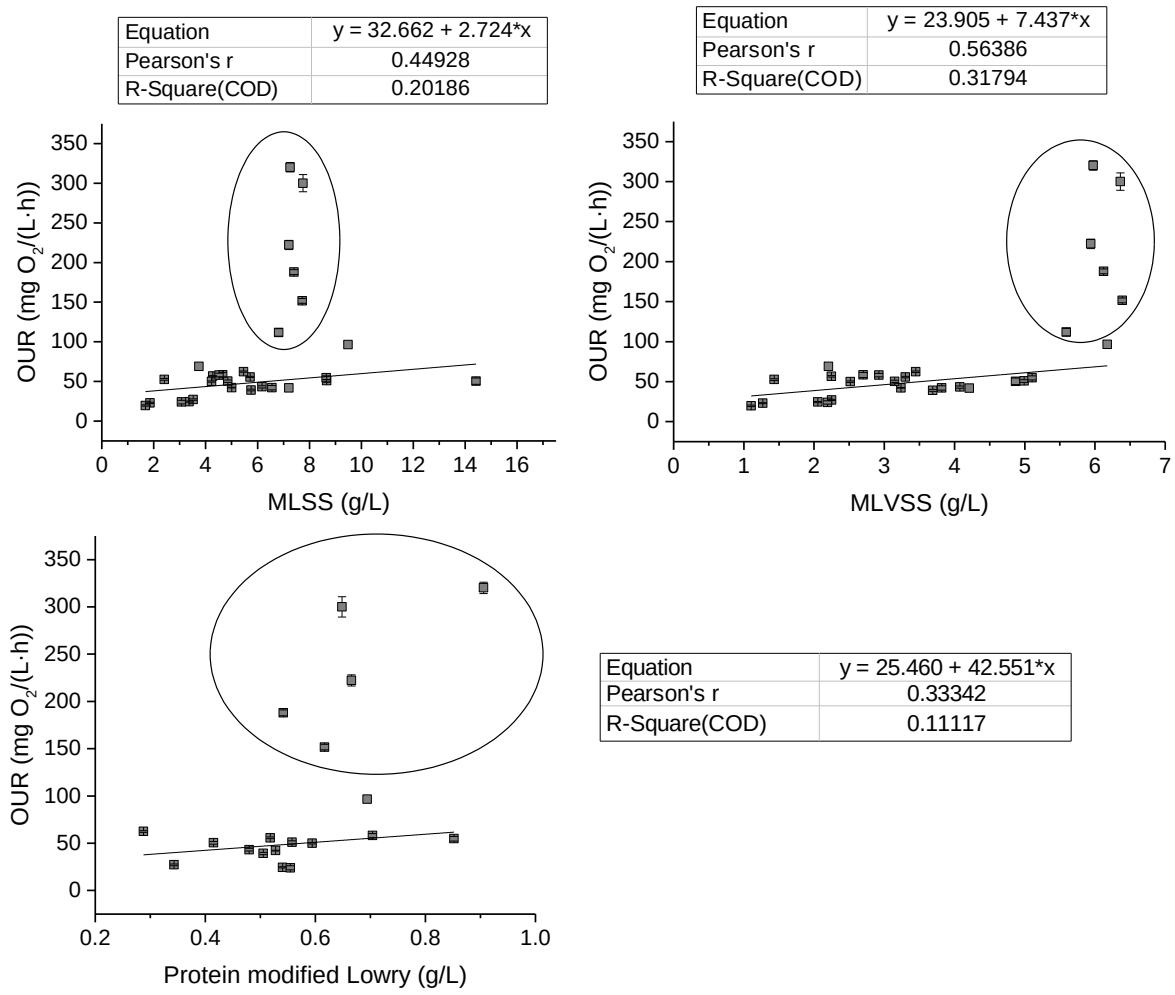

Figure 5-4: Comparison between the correlation of MLSS, MLVSS and total protein (modified Lowry) with OUR. The linear fits were calculated without considering the data from plant D (circled)

The highest correlation to the OUR was shown by the VSS followed by SS. Both biomass parameters showed a statistically significant correlation with the Pearson's r values exceeding the critical values p (Table 5-2). Protein concentration, however, did not show a significant correlation to the respirometric activity. These results raised a question on the applicability of total protein as an alternative parameter to the conventional biomass parameters of SS and VS. Furthermore, plant D had the highest respirometric activity although it had the lowest protein fraction in the VSS, which further questions the relationship between total protein and activity. The discussion on this matter is provided in Section 5.3.

Table 5-2: Results of the correlation between OUR and biomass parameters. Significant correlations are highlighted in grey. N: sample size, df: degree of freedom

Biomass parameter	N (df)	Pearson's r	Critical value p
SS	23 (21)	0.449	0.413
VSS	23 (21)	0.564	0.413
Protein	14 (12)	0.333	0.553

5.1.3 Roles of EPS on Settleability and Dewaterability

Bound EPS was extracted from sludge samples of plants A−D as well as from the scum sample of plant B. The EPS extracts were analysed for their protein, humic acid and carbohydrate contents. Figure 5-5 and Table 5-3 shows the average values of the EPS components as fractions of the VSS. It can be seen that the EPS constituents highly varied from plant to plant. EPS protein made in all plants the largest fraction of the VSS with values between 2.2 and 8.3 %, followed by humic acid (1.7−2.3%) and carbohydrate (0.9−1.4%).

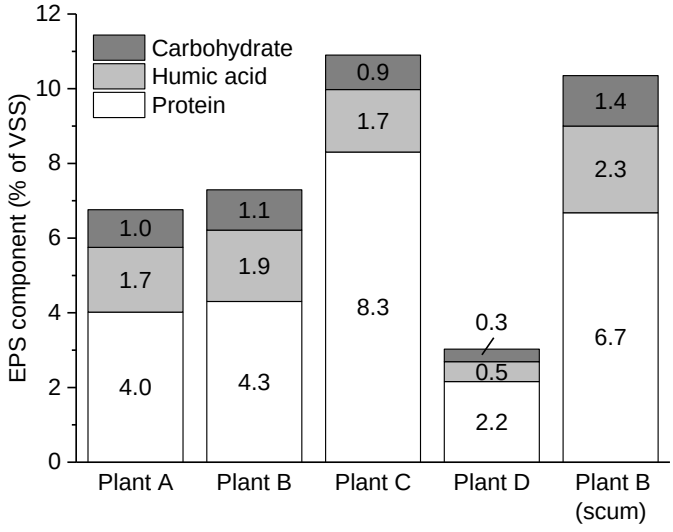

Figure 5-5: EPS constituents as percentage of VSS

Table 5-3: Fraction of EPS constituents in VSS shown as mean ± SD. N: sample size, SD: standard deviation

Sample	Protein (% of VSS)	Humic acid (%of VSS)	Carbohydrate (%of VSS)
Plant A (N = 8)	4.02 ± 1.57	1.73 ± 0.77	1.01 ± 0.43
Plant B (N = 7)	4.30 ± 1.46	1.91 ± 0.62	1.08 ± 0.41
Plant C (N = 7)	8.30 ± 1.75	1.67 ± 2.01	0.92 ± 0.28
Plant D (N = 7)	2.16 ± 1.31	0.53 ± 0.29	0.34 ± 0.19
Plant B (scum) (N = 7)	6.68 ± 3.40	2.32 ± 1.11	1.35 ± 0.61

The results of this study were in accordance with those published by Frølund et al. [3], who also found protein as the most abundant component in the EPS by using the same extraction method of cationic exchange resin (CER). The fractions of all the EPS constituents were however higher than the values measured in this study. They reported protein content of about 24.3% of the VSS and 12.6 and 4.8% for humic acid and carbohydrate, respectively. These differences in values were most probably attributed to the longer extraction time of 17 h in their study, as opposed to 3 h chosen for this study. EPS extraction using CER is a combination of chemical (exchange of divalent cations) and mechanical (shear caused by stirring) effects. Frølund et al. [3] also reported that cell lysis occurred for extraction time above 1−2 h. A mild extraction with low extraction time and low stirring speed reduced the risk of cell lysis, although an effective extraction was only given by longer extraction time of >12 h and high stirring speed. The choice of 3 h extraction time in this study was a compromise between the two conditions as a result of a preliminary study done which aimed at extracting the highest possible EPS concentration while keeping minimal cell lysis. Microscopic analysis showed minimum cell rupture at the chosen extraction time of 3 h.

The EPS components were analysed for their potential influence on sludge settleability and dewaterability by comparing these values to the sludge volume index (SVI) and capillary suction time (CST), respectively. As was the case with total protein, the low sample size for each plant did not allow meaningful individual analyses. Hence, the correlations were only done for the collective data of all plants. Figure 5-6 illustrates the correlation between SVI and the different EPS components. The SVI of plant D (circled) showed high values exceeding 200 mL/g, which highly differed from the results of the other three plants, thus were not included for the calculation of the linear fit.

Among the three EPS components, only humic acid showed a positive correlation with the SVI (Table 5-4), suggesting its negative influence on the sludge settling property. As opposed to humic acid, protein and carbohydrate contents of the EPS did not show a significant correlation to the SVI. Li and Yang [104] differentiated bound EPS between loosely-bound EPS (LB-EPS) and tightly-bound EPS (TB-EPS) and found that the amount of LB-EPS (measured in mg TOC/g SS) had a more significant effect on the settling property of the sludge than the TB-EPS. They reported that LB-EPS linearly correlated to the SVI, indicating poorer settleability with increasing amount of LB-EPS. They, however, did not specify further which EPS component contributed to the lower settleability. Their results indicated no correlation between TB-EPS and sludge settlement. This study did not differentiate between the two EPS types. As the LB-EPS accounts for only a small fraction of the total bound EPS [104,105], it can be assumed that the EPS values of this study represented those of the TB-EPS. That is probably the reason why protein and carbohydrate contents failed to show correlations to the SVI, although there were also reports of correlations between protein or carbohydrate contents of the EPS or total EPS to the settleability while also not differentiating between TB-EPS and LB-EPS [4,7].

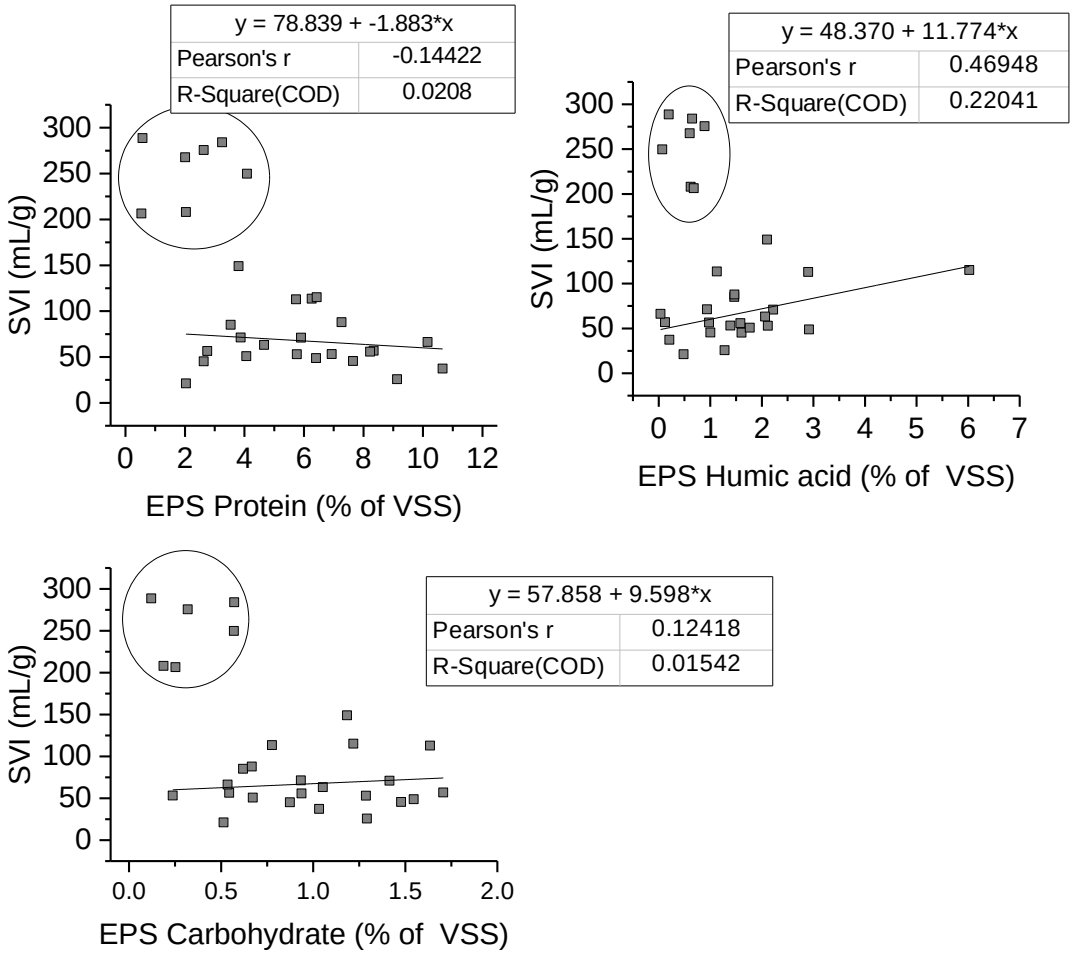

Figure 5-6: Correlation between SVI and EPS constituents. Values in the circle represent the data from plant D which were not included in the calculation of the linear fit

Table 5-4: Results of the correlation between SVI and EPS components. Significant correlation is highlighted in grey. N: sample size, df: degree of freedom

EPS component	N (df)	Pearson's r	Critical value p
Protein	22 (20)	-0.144	0.404
Humic acid	22 (20)	0.469	0.404
Carbohydrate	22 (20)	0.124	0.404

It is also well known that EPS is important for bacterial adhesion and aggregation [106], which will directly affect the flocculation thus probably also sludge settleability. It is possible that in the case of plant D, too low amount of EPS contributed to high SVI values > 200 mL/g measured in that plant, which indicated poor settleability and possible bulking problems [12]. The floating sludge (scum layer) of plant B, however, did not show similar EPS compositions as plant D (Figure 5-5).

Figure 5-7 shows the correlation of CST (measured per unit SS) with protein, humic acid and carbohydrate contents of the EPS. EPS protein exhibited a significant linear relationship with the CST, indicating the probability of a higher amount of protein leading to poorer dewaterability and filterability of the sludge. Humic acid and carbohydrate contents did not show a significant correlation to the CST, suggesting that these components of the EPS probably had less effect on the ease of water removal (Table 5-5).

Table 5-5: Results of the correlation between CST and EPS components. Significant correlation is highlighted in grey. N: sample size, df: degree of freedom

EPS component	N (df)	Pearson's r	Critical value p
Protein	29 (27)	0.589	0.367
Humic acid	29 (27)	-0.054	0.367
Carbohydrate	28 (26)	0.267	0.374

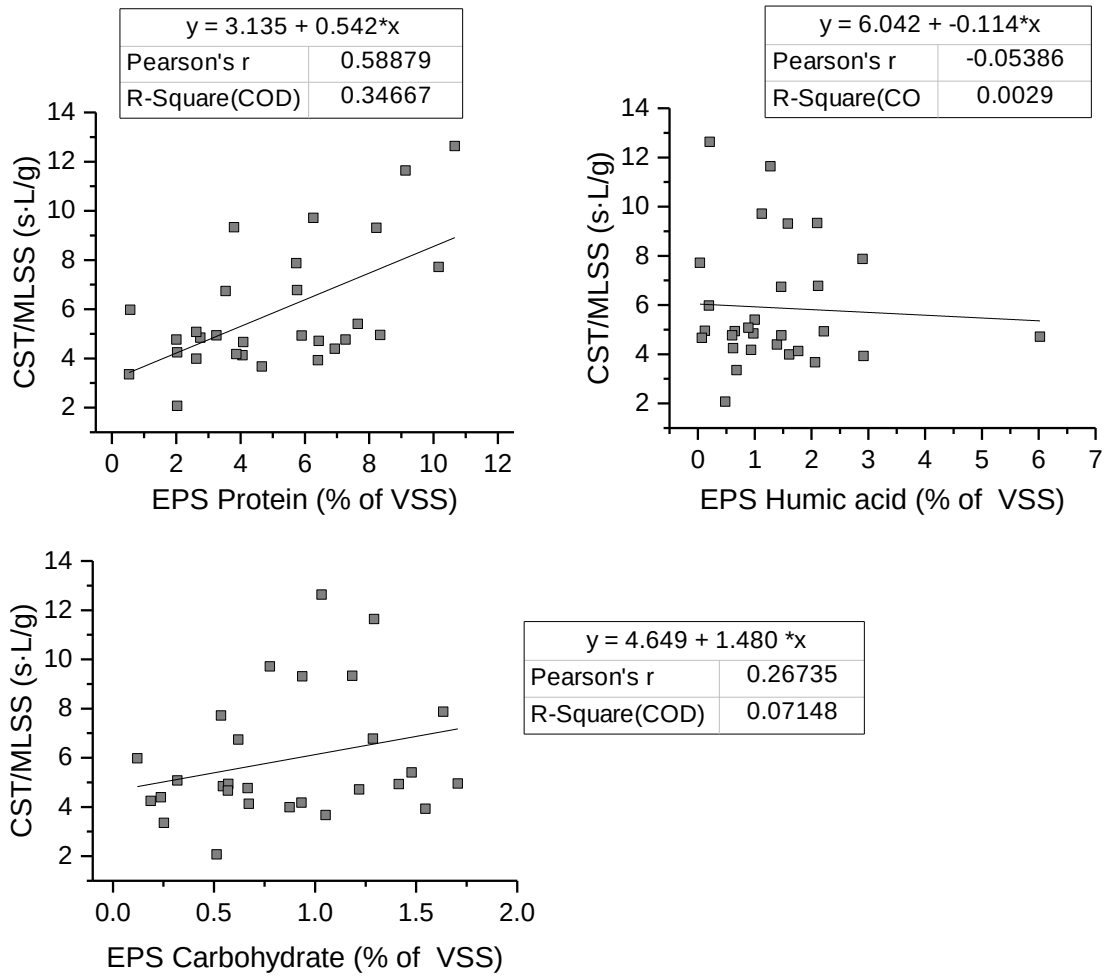

Figure 5-7: Correlation between CST and EPS constituents

5.2 Lab Scale WWTP

The second part of the study investigated activated sludge under different nutrient conditions. This conditions were simulated in a lab-scale WWTP. The plant was operated for a sum of 474 days in 5 different phases. At the beginning of each phase, the plant was inoculated with a fresh sludge from WWTP Kaßlerfeld, Germany. The aim of this part of the study was to investigate the use of different protein measurement methods to assess the state of activated sludge under various conditions. For this purpose, the operation was started with a start-up phase, followed by a phase of stable operation, before introducing phases of nitrogen and phosphorous limitation.

5.2.1 Optimising Protein Measurement

Several issues regarding protein measurement in the previous study of industrial sludges were addressed at the beginning of this part of the study:

- The modified Lowry method was laborious and time consuming due to the reagents needed to be prepared weekly and long incubation time. However, it was the only protein measurement method known which were able to eliminate the influence of humic acid in the protein measurement.
- The fraction of total protein and humic acid in the VSS was lower than the values stated in the literature. This raised a question if it was due to incomplete lysis.

5.2.1.1 Removal of Humic Compounds

Giesy and Briese [88] reported about the formation of brown particulates after freezing water sample containing humic substances which had been pre-treated to remove particles of >15 µm. The brown particulates, believed to be humic substances, could then be separated by centrifugation. No particulate formation was observed in the sample that had been left at room temperature. To investigate if this could be applied to protein sample of activated sludge as well, a protein extract was centrifuged at 18,000 rpm then filtered through a 0.2 µm cellulose acetate membrane using a syringe filter to remove particulates. The sample was subsequently divided into several aliquots of 2.0 mL, half of which were stored at 4 °C and the other half were frozen at −20 °C. After the samples at −20 °C were completely frozen (ca. 1 hour), they were thawed at room temperature. Brown particulate can be seen near the liquid surface, which can be separated by centrifugation at 18,000 rpm. No phase separation was observed for the samples stored at 4 °C, both before and after centrifugation (Figure 5-8). The protein concentrations were then measured using the Lowry method (DC Protein Assay kit, Bio-RAD) and a 37 % decrease in concentration was seen in the frozen sample.

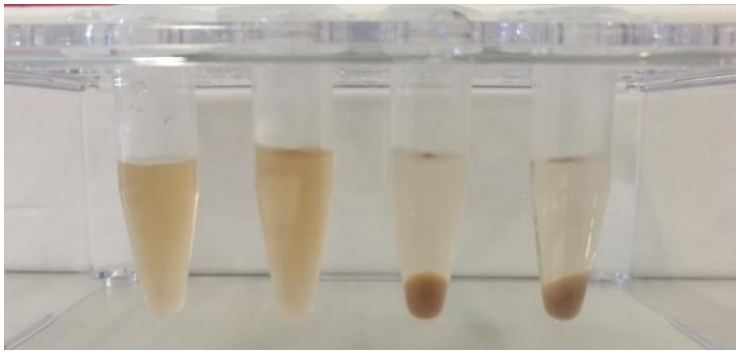

Figure 5-8: Comparison of protein samples stored at 4 °C (two on the left) and at −20 °C (two on the right) after centrifugation at 18,000 rpm

Denecke [11] reported smeared protein bands when performing sodium dodecyl sulfate-polyacrylamide gel electrophoresis (SDS-PAGE) of protein crude extract from activated sludge, hypothesized to be caused by polymeric substances, including humic compounds, which were masking the bands. A similar case was also observed in the PAGE profile of activated sludge sample by Duncan et al. [107], although they did not specify the cause. To further investigate the freeze-and-thaw method, three different activated sludge samples were treated as described above to remove humic substances and the samples before and after freezing were loaded in acrylamide gels (10 µg/well). SDS-PAGE was performed according to Laemmli [108] and the gels were stained with Coomassie Brilliant Blue. The comparison of the PAGE-gels illustrates clearer protein bands in all three samples after freezing (Figure 5-9). Therefore, it is believed that the majority of humic compounds were successfully removed by this method.

The advantage of the freeze-and-thaw method is that it allows protein extract to be measured using commercial kits which do not include correction procedure for the interference caused by humic compounds. Furthermore, humic compounds can be removed relatively easily through centrifugation without addition of chemicals which could further interfere with the protein measurement e.g. phenol extraction method [109]. Hence, measurements of protein extract in this part of the study employed the freezing method prior to measurement. Protein concentration was measured using commercial kit of Lowry and Bradford (see Section 4.2.12.1 and 4.2.12.2).

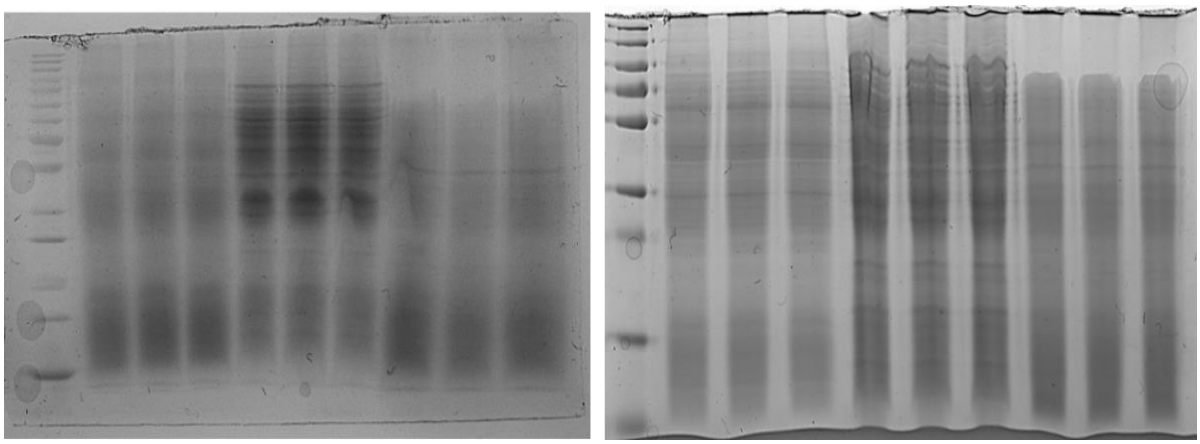

Figure 5-9: SDS-PAGE analysis of 3 different activated sludge samples showing the comparison of protein profiles before (left) and after (right) precipitation of humic substances. For both gels lane 1: protein marker, lane 2-4: sample 1, Lane 5-7: sample 2, Lane 8-10: sample 3

5.2.1.2 Investigation of Lysis Procedure

Preliminary studies were done to find the optimal setting for the lysis procedure through sonication by adjusting the amplitude and the extraction time until the maximum protein concentration was obtained (data not shown). This led to the sonication settings described in Section 4.1.3.6 and 4.2.9. To ensure that the lysis procedure was comparable to complete lysis, the protein samples of phase 1 and 2 were also measured using ninhydrin-based method (see section 4.2.12.3). In this method, the activated sludge sample was treated with concentrated sulphuric acid, thereby hydrolysing the proteins into amino acids. The hydrolysate can then be directly quantified. It was assumed that if both mechanical and chemical lysis procedure correlated, then the sonication procedure had successfully lysed substantial amounts of cells, comparable to acid hydrolysis. This was proven by the strong correlation between protein concentrations measured by the ninhydrin-based method and Lowry method (n=44, r=0.819 > p= 0.248; Figure 5-10).

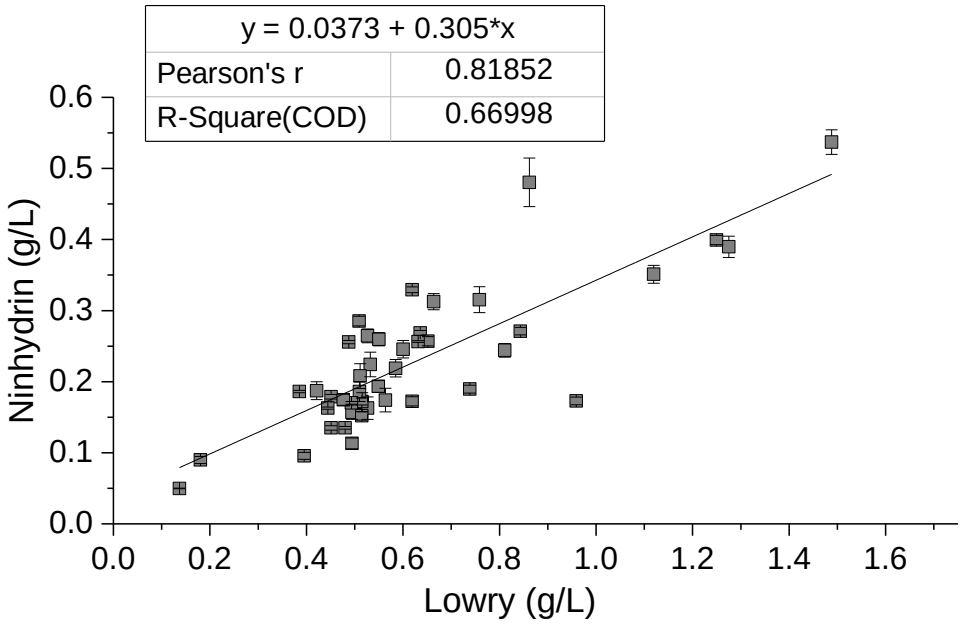

Figure 5-10: Correlation between protein quantification methods ninhydrin and Lowry

5.2.2 Phase 1 and Phase 2

The first and the second phase of the lab-scale plant operation were the start-up phases, which aimed at collecting data to find the optimal settings for stable operation. The settings determined from in the first phase e.g. pH control and nitrate recirculation rate were implemented in the second phase to ensure a stable operation could be achieved before introducing the phases of nitrogen and phosphorous limiting conditions so that interferences other than the nutrient limitation could be ruled out during the later phases. Phase 1 (P1) was operated for 95 days while phase 2 (P2) was operated for 72 days.

Figure 5-11 (A-C) shows the variations of SS concentration as well as COD and ammonium nitrogen (NH_4-N) loadings of both phases. During P1, pH fluctuations resulted in an unstable operation accompanied by sludge loss. This increased COD and ammonium loadings, which contributed to increased SVI values (Figure 5-12 (C)), resulting in further sludge loss. The autotrophic activity was severely affected by the pH fluctuations, which can be seen from the decrease in the ammonium removal performance (Figure 5-12 (B)) as well as the autotrophic SOUR seen in Figure 5-12 (D). This is discussed further in Section 5.2.3. At the end of P1, further sludge washout occurred although ammonium removal recovered after pH control was optimised. P1 was stopped at day 95.

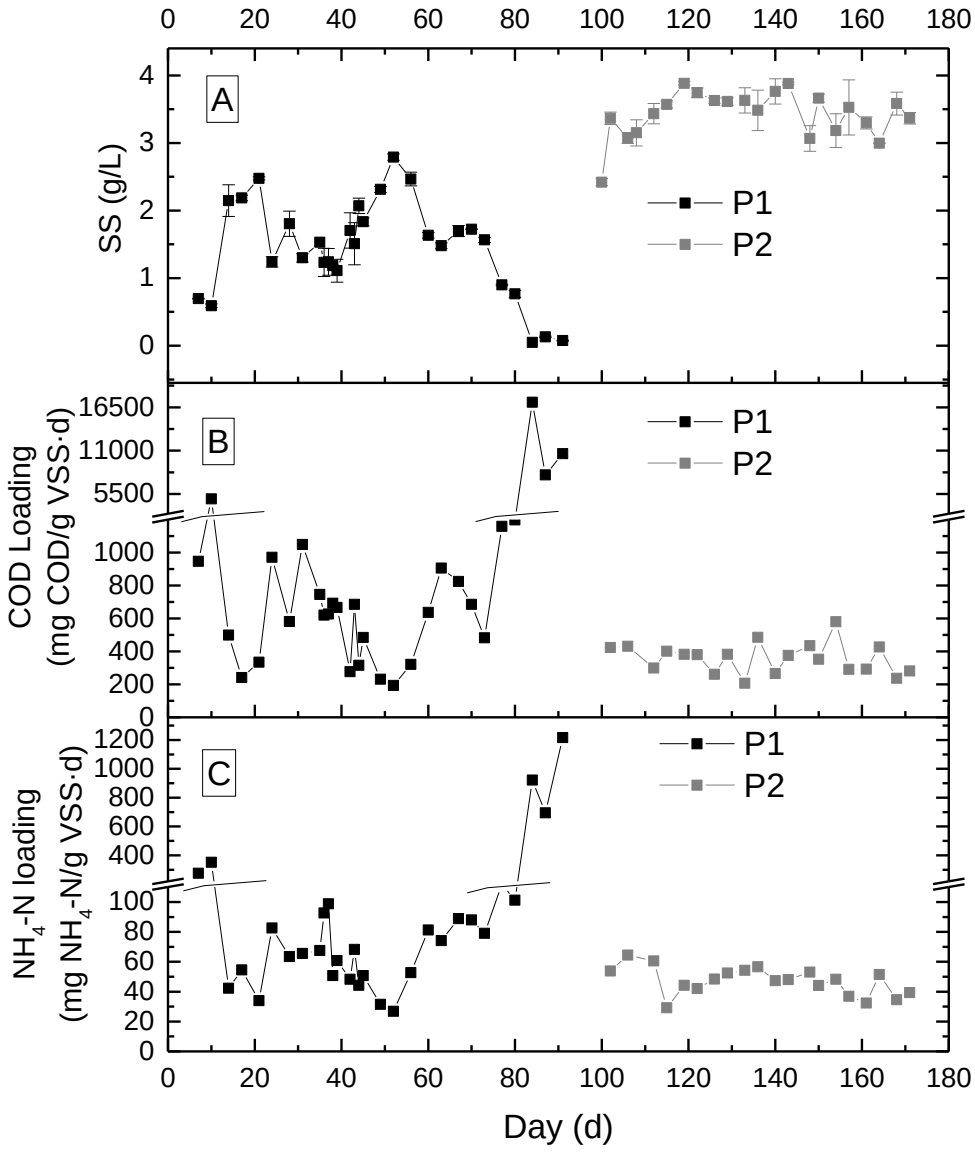

Figure 5-11: Suspended solids concentration (A), COD loading (B)and ammonium loading (C) of P1 and P2

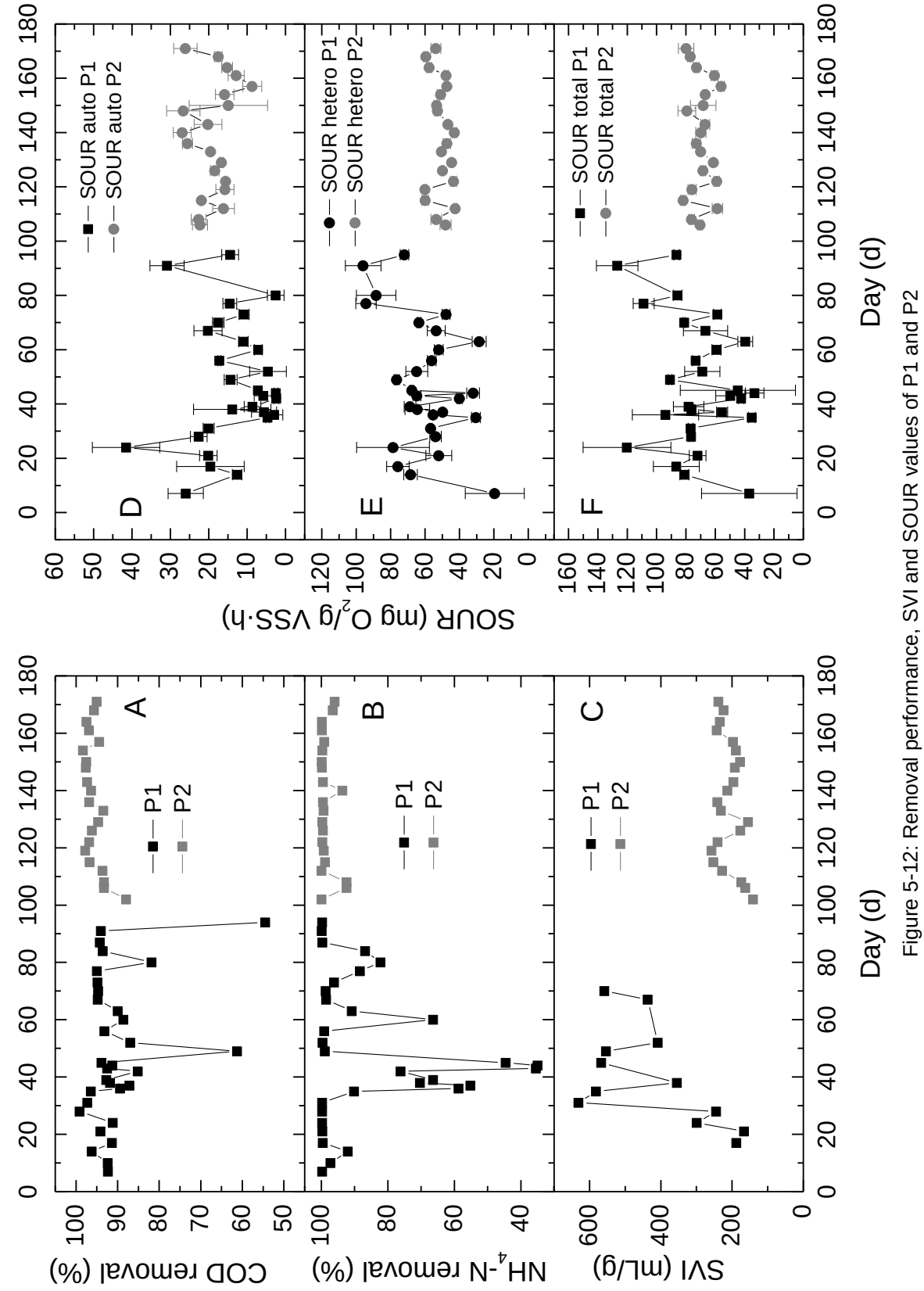

Figure 5-12: Removal performance, SVI and SOUR values of P1 and P2

P2 was started with a new sludge on day 100. The concentration of SS was started higher at around 2.5 g/L and no excess sludge was removed until the plant had stabilised. The concentration of the influent was not fixed. Instead, it was adjusted according to a COD loading of about 0.5 kg COD/kg SS·d. That means the influent concentration was adjusted according to the SS concentration, thus avoiding overloading. pH control was optimised and the concentrations of both acid and base were reduced to avoid pH fluctuations. The result was a stable operation with low fluctuations in all measured values as shown in Figure 5-11 and Figure 5-12. P2 was stopped on day 171.

5.2.2.1 Comparison of Biomass Parameters

In P1 and P2, protein concentration was measured using three different methods which were Lowry, Bradford and ninhydrin-based methods. Figure 5-13 illustrates the variations of conventional biomass parameters SS and VSS as well as protein concentrations in the course of P1 and P2.

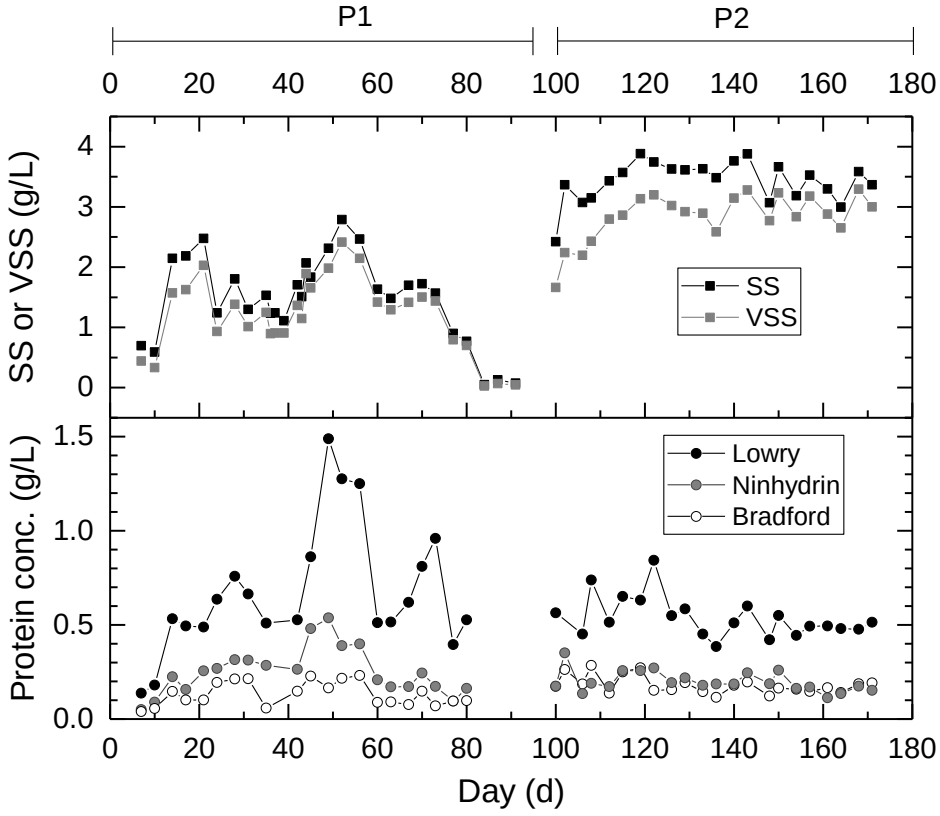

Figure 5-13: Variations of biomass parameters during P1 and P2.

Comparing the different protein assays, it can be seen that Lowry protein showed the highest concentrations for all measurements. On average, the concentration of Lowry protein was 2.8 and 5.5 times higher than ninhydrin and Bradford proteins respectively in P1. The difference in the

concentration of Lowry to ninhydrin stayed almost unchanged all the time but its difference to Bradford protein decreased to only 3.1 times higher in P2. The concentration difference between ninhydrin and Bradford valued also decreased from P1 to P2. Ninhydrin protein concentration was on average double that of Bradford in P1 but showed comparable values to Bradford in P2. It is possible that during P1, at lower VSS concentrations, there were more small-sized proteins that cannot be measured by Bradford method, as this method can only measure proteins larger than 3 kDa [1], thus resulting in the higher difference with Lowry and ninhydrin in values.

With exceptions of the few peaks shown by Lowry protein, protein concentrations did not vary significantly between P1 and P2, despite the increase of SS and VSS (Table 6-7). For proteins measured by Lowry and ninhydrin-based methods, their average concentrations were even higher in P1 than in P2. The reason for this and the low variations in concentrations between the two phases was that protein fraction decreased with increasing VSS concentrations, consistent with the observation of the first part of the study (Figure 5-14).

Table 5-6: Concentration of proteins and their percentage of VSS measured according to Lowry, ninhydrin and Bradford shown as mean ± SD. N: sample size, SD: standard deviation

Method	P1			P2		
	N	Conc. (g/L)	% of VSS	N	Conc. (g/L)	% of VSS
Lowry	22	0.67 ± 0.33	50.5 ± 14.9	21	0.54 ± 0.11	19.3 ± 5.1
Ninhydrin	22	0.25 ± 0.12	19.5 ± 7.5	22	0.20 ± 0.06	7.2 ± 2.4
Bradford	22	0.13 ± 0.06	10.5 ± 4.9	22	0.18 ± 0.05	6.6 ± 2.3

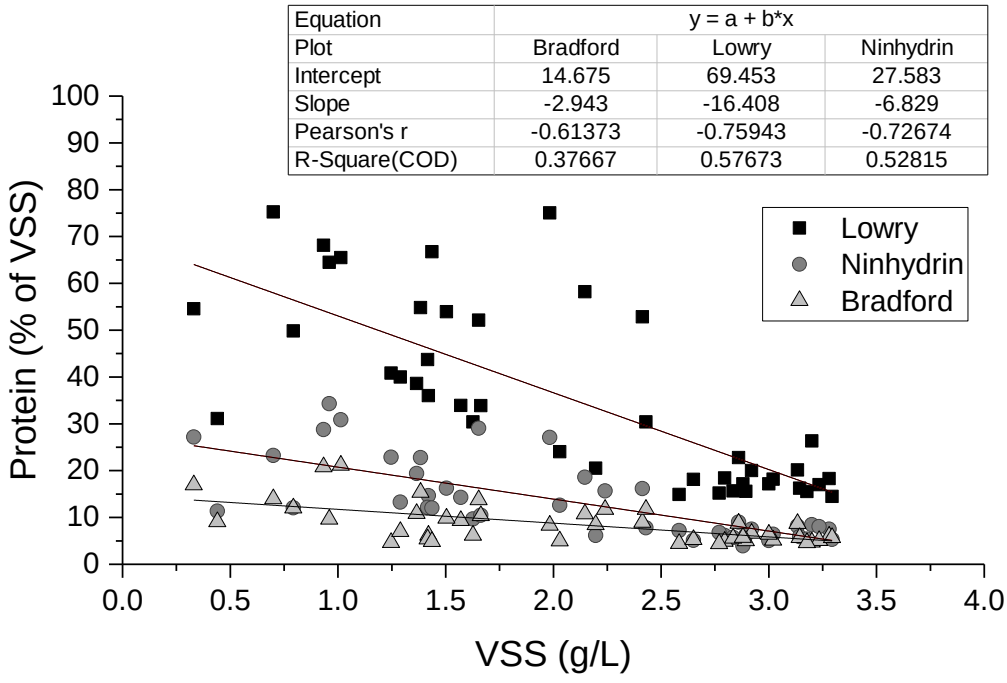

Figure 5-14: Relationship between protein fraction and VSS concentration

5.2.2.2 Investigation of Total Protein as Alternative Parameter for Measuring Active Biomass

The highly varying operational conditions of P1 and the difference in stability between P1 and P2 offered a good opportunity for comparing the applicability of the different biomass parameters (SS, VSS and protein) as parameters to measure active biomass. A good biomass parameter should be able to show a strong correlation with the activity regardless of the state of sludge. Figure 5-15 shows the correlations between the total OUR and the biomass parameters of both P1 and P2. The correlation of each separate phase can be taken from Appendix 3. The results of the correlations are summarized in Table 5-7.

Table 5-7: Results of the correlations between total OUR and biomass parameters. Significant correlations are highlighted in grey. N: sample size, df: degree of freedom

Biomass parameter	N (df)	Pearson's r	Critical value p
SS	51 (49)	0.918	0.236
VSS	51 (49)	0.917	0.236
Protein (Lowry)	42 (40)	0.0752	0.257
Protein (Bradford)	42 (40)	0.561	0.257
Protein (ninhydrin)	42 (40)	0.0140	0.257

SS and VSS showed strongest correlations with the OUR with $r = 0.92$. This was followed by Bradford protein. Lowry and ninhydrin protein did not show a significant correlation with the OUR. These results confirmed the findings of the previous study of industrial sludges. The data of each separate phase also showed a similar result for P1 (Appendix 3, Figure A10 and Figure A11). The correlations of P1 according to from strongest to weakest were SS > VSS > Lowry > ninhydrin > Bradford. For P2, only VSS and ninhydrin showed significant correlations to the OUR. The correlations from strongest to weakest were VSS > ninhydrin > SS > Bradford > Lowry. In general, all correlations were weaker in P2. This is mainly due to the smaller range of biomass parameters. SS values, for example, were between 3−4 g/L in P2 while its values in P1 were in the range of 0.05−3 g/L. If we consider the data of P1 to represent that of an unstable plant and P2 of a stable plant, it can be concluded that the only parameter which can be used to quantify active biomass in both systems is the VSS. Although VSS is known to include other non-active substances like humic compounds, lipids, carbohydrates, etc., the result of this and the previous part of the study point to the conclusion that VSS is more reliable than protein in estimating active biomass. The contradicting results between the different protein values show that protein evaluation is highly dependent on the quantification method used.

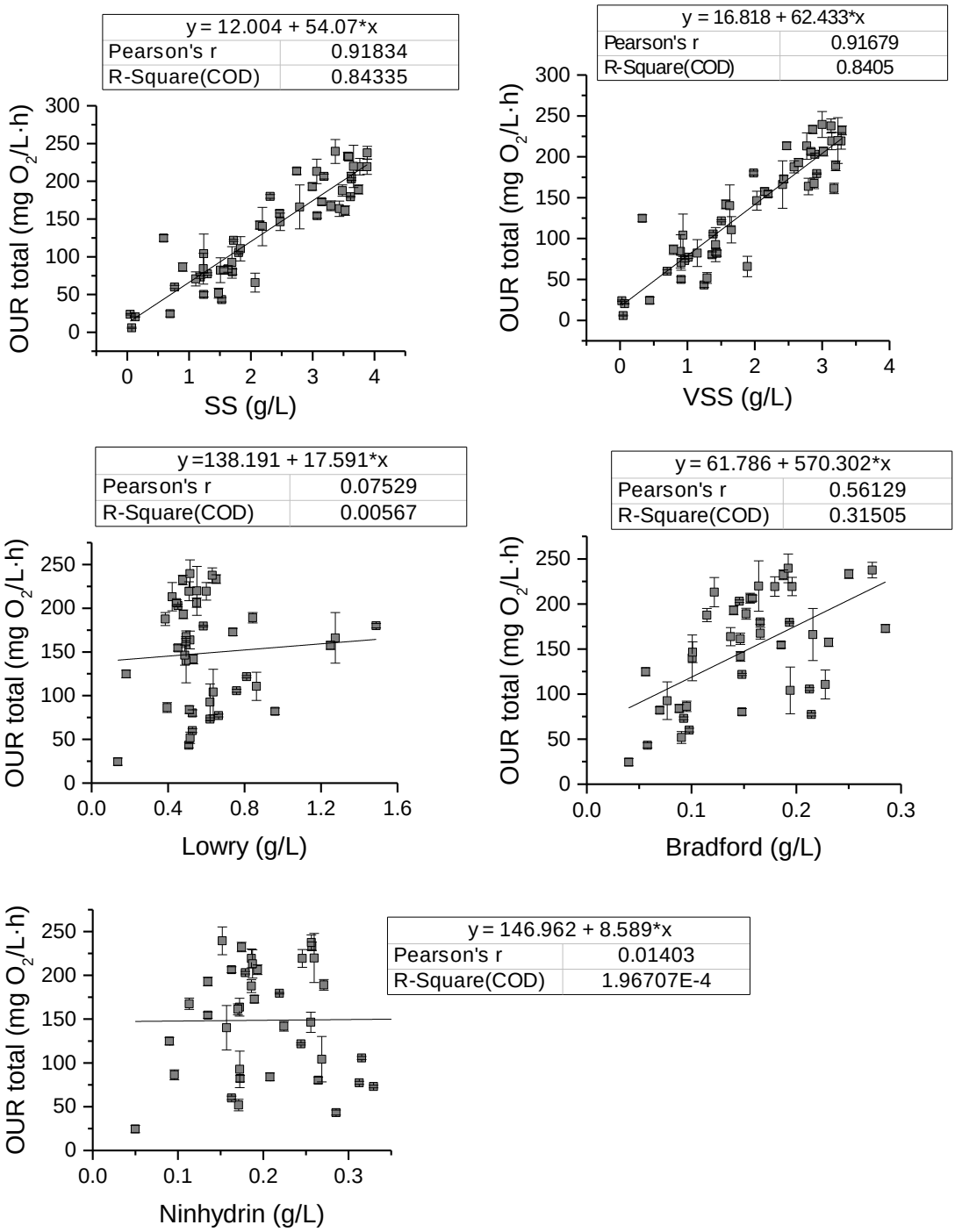

Figure 5-15: Correlation between total OUR and SS, VSS and protein concentration according to the Lowry, Bradford and ninhydrin methods of P1 and P2

5.2.2.3 Roles of EPS on Settleability and Dewaterability

Figure 5-16 shows the variations of Lowry and Bradford protein as well as the carbohydrate content of the EPS in the course of P1 and P2. It can be seen that the EPS contents of P1 were generally higher than those of P2. Under conditions that are non-optimal for growth, EPS can serve as a protective layer for bacteria against harsh environment [55]. It is likely that the pH fluctuations during P1 induced higher production of EPS to protect the microorganisms from the adverse effects of extreme pH.

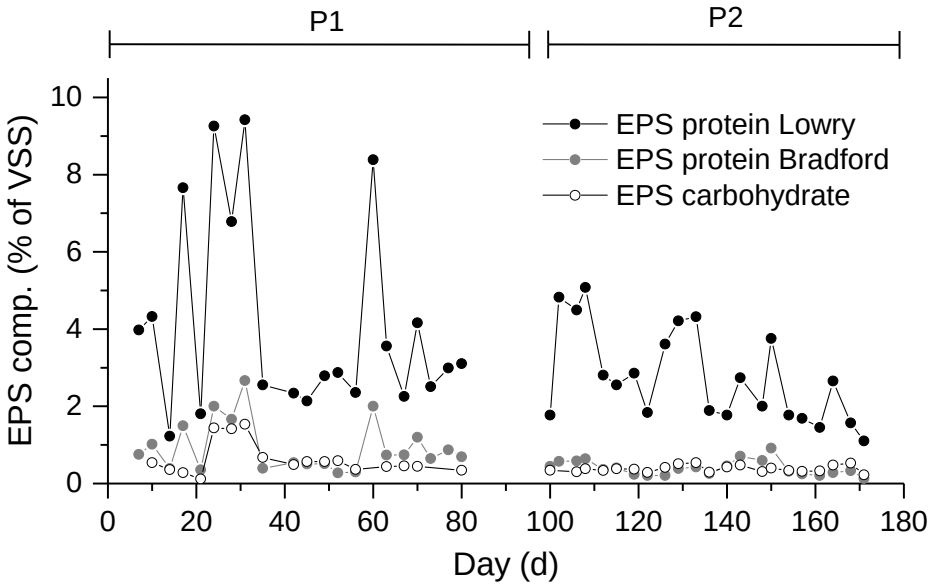

Figure 5-16: Variations of EPS protein and carbohydrate content in P1 and P2

The results on the influence of EPS on the settleability in this part of the study are in accordance with the investigation of industrial sludges in the first part of the study that there was no relationship between Lowry protein of the EPS and SVI. Bradford protein content showed a moderate correlation with the SVI (Figure 5-17 and Table 5-8). The results of carbohydrate contradicted the previous part of the study as in this study, the carbohydrate showed, albeit moderate, a significant correlation with the SVI.

Table 5-8: Results of the correlation between SVI and EPS components. Significant correlations are highlighted in grey. N: sample size, df: degree of freedom

EPS component	N (df)	Pearson's r	Critical value p
Protein (Lowry)	33 (31)	0.138	0.345
Protein (Bradford)	33 (31)	0.352	0.345
Carbohydrate	32 (30)	0.434	0.349

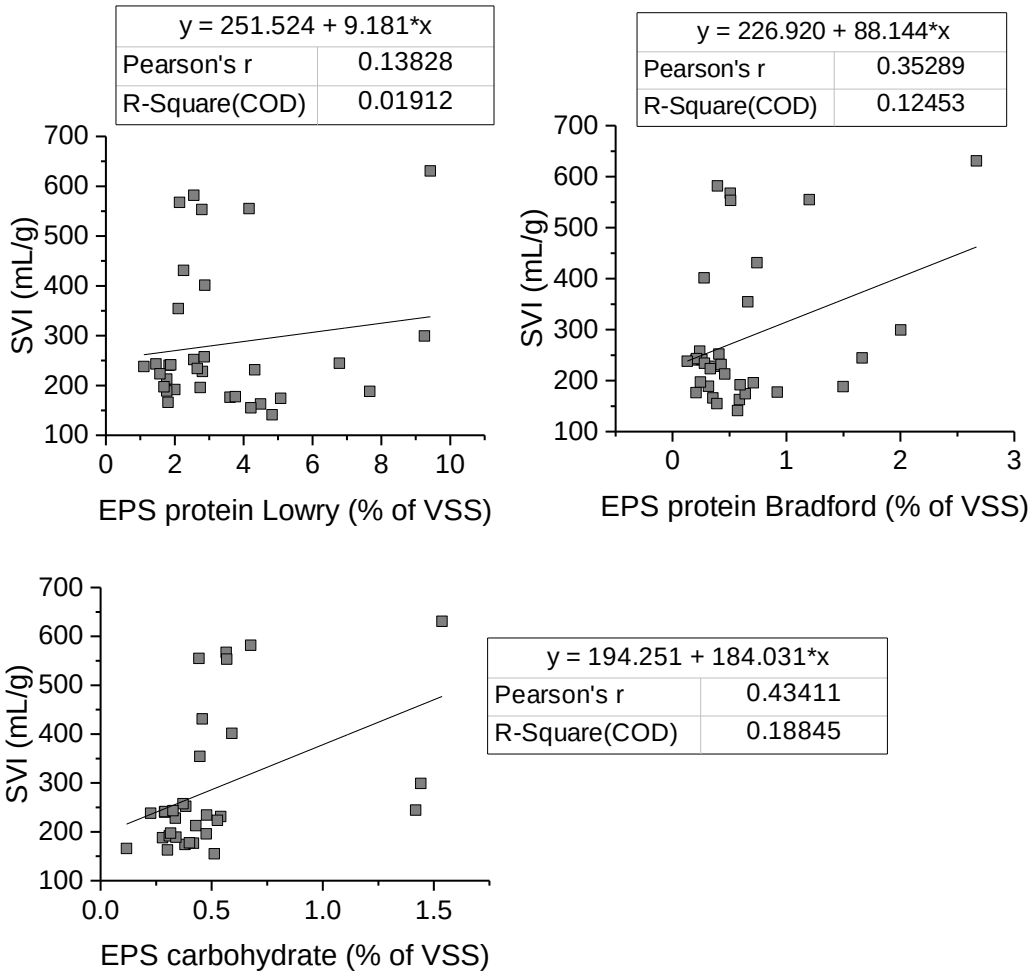

Figure 5-17: Correlation between SVI and EPS constituents

The data of CST were also contradictory to previous observations made on industrial sludge samples. In the previous case, there was a significant correlation that inferred the increase of Lowry protein affected sludge dewaterability. In this case, the only significant correlation with the CST was that of Bradford protein (Figure 5-18; Table 5-9).

The conflicting results on the influence of the EPS components on the settleability and dewaterability between this and the previous study only reinforced the literature report that the EPS components vary from plant to plant thus their roles cannot be generalised [7]. Defining the roles of EPS on settleability and dewaterability solely based on the concentration of its components is a popular simplification attempt for an insight into the factors affecting the sludge properties but at least in this present study, this method did not provide a satisfactory result.

Table 5-9: Results of the correlation between CST and EPS components. Significant correlation is highlighted in grey. N: sample size, df: degree of freedom

EPS component	N (df)	Pearson's r	Critical value p
Protein (Lowry)	32 (30)	0.275	0.349
Protein (Bradford)	32 (30)	0.503	0.349
Carbohydrate	28 (26)	-0.021	0.361

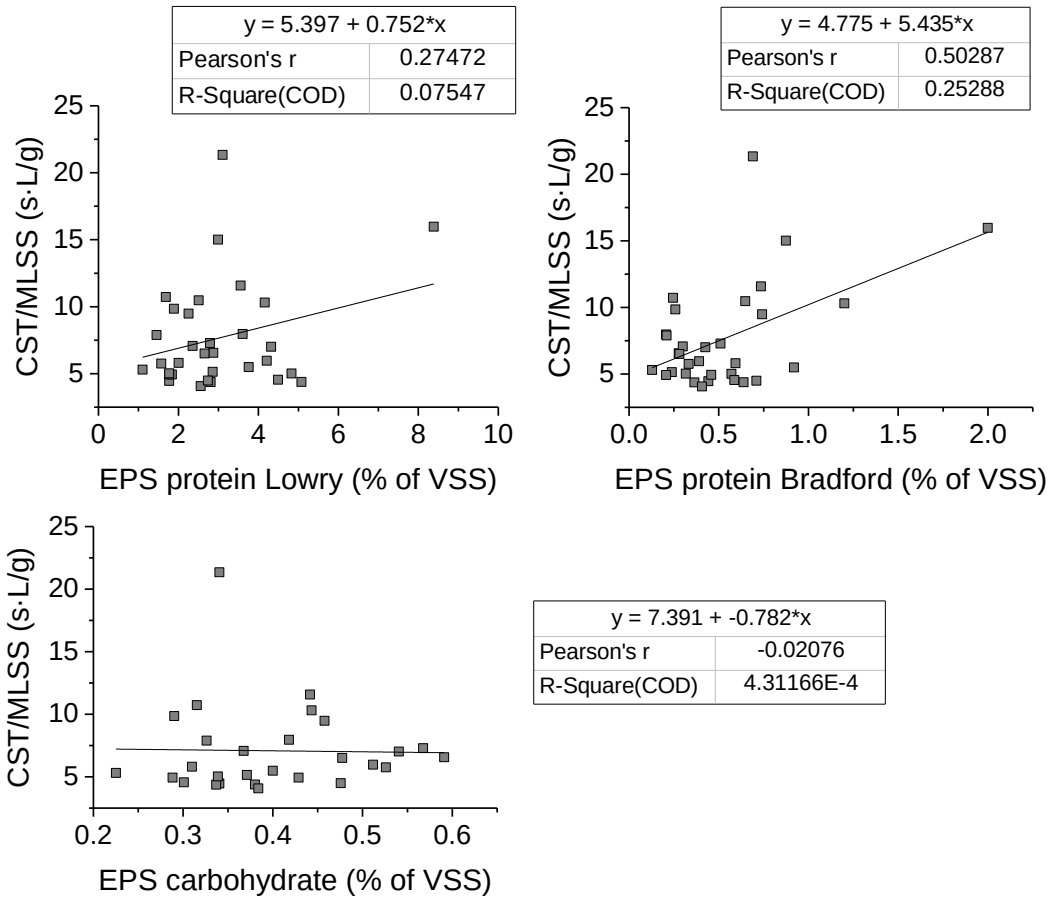

Figure 5-18: Correlation between CST and EPS constituents

5.2.3 Proteomics of Phase 1

The aim of proteomics of P1 was to assess the applicability of quantitative proteomics of label-free quantification (LFQ) in obtaining reliable and meaningful information on the state of activated sludge. For this purpose, the effect of pH fluctuations during this phase on the system was investigated. pH fluctuations between day 27 and day 50 (highlighted in grey in Figure 5-19) caused instability in the plant performance. The ammonium removal was particularly affected by this condition. During this period, ammonia nitrogen removal dropped drastically from 90−100 % to values below 80% removal, with the lowest at 35 %. Comparing the ammonium removal performance to the activity of ammonium oxidizing bacteria (AOB), measured by specific oxygen uptake rate (SOUR), it can be seen that the decrease in ammonia removal performance was preceded by a decrease in AOB activity. This shows that the AOB were adversely affected by the fluctuation in pH, thus resulted in a lower nitrification efficiency. After the pH problem was eliminated, the ammonium removal recovered, although not to the same extent as before (Figure 5-19). To understand what was happening during this period at a molecular level, 10 frozen sludge samples (day 1, 31, 38, 49, 52, 56, 73, 80, 90 and 95) were extracted for total protein and subjected to proteomics analysis using LC-MS/MS in duplicates. The procedure was as described in Section 4.2.14.

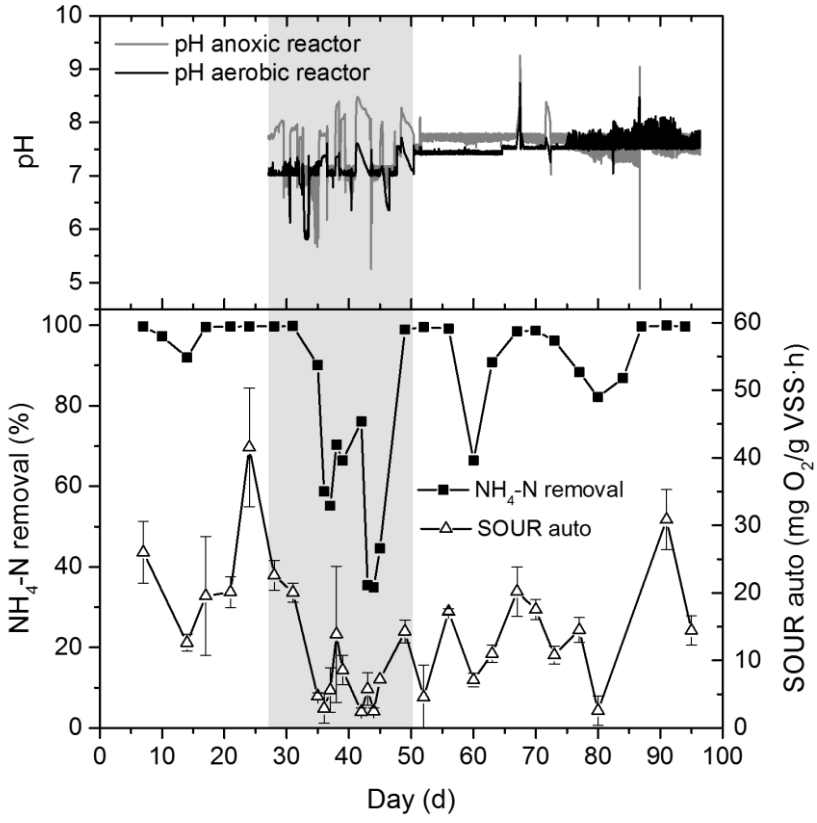

Figure 5-19: Top diagram: pH profiles of anoxic and aerobic reactors showing fluctuating pH measured between day 27 and day 50. Bottom diagram: profiles of autotrophic SOUR and ammonium removal. Period of pH fluctuations is marked in grey.

5.2.3.1 Choice of Database

In order to retrieve valuable information from proteomics, the MS/MS spectra data need to be searched against an appropriate database [69]. To identify the suitable database, preliminary searches were performed on the MS/MS spectra of one of the samples (sample of day 1). The first search was performed with Mascot [110] against the entire NCBI nucleotide database (www.ncbi.nlm.nih.gov/nucleotide; [111]). The search managed to identify only 80 protein groups, despite a long execution time of over 24 hours. The second search was performed against the amino acid sequence of the metagenomics database from WWTP Aalborg, Denmark [96]. At the time of the study, this was the only publicly available database whose treatment system was closest to the treatment of the lab-scale plant. Despite WWTP Aalborg specializes in enhanced biological phosphorus removal (EBPR), 122 protein groups were identified, which shows the advantage of using a specific database for wastewater bacteria over a general database like NCBI.

5.2.3.2 Protein Identification

Encouraged by the better identification, Aalborg database was used to identify the entire mass spectra data. Using this database, a total of 450 protein groups were identified across the 20 measurements. To get qualitative information about the proteins identified, the amino acid sequences were annotated for their gene function and taxonomic group using KEGG database. The annotation was automated through GhostKOALA [98]. Taxonomic evaluation revealed that the majority of proteins identified belonged to the class of Betaproteobacteria (36.7%), followed by Bacteroidetes (16.7%) and Chloroflexi (13.8%) (Figure 5-20 (A)). Proteins produced by bacteria related to the genus *Candidatus* Accumulibacter were found in the highest amount (7.1%) followed by the genus *Anaerolinea*, *Azospira*, *Candidatus* Promineofilum, *Nitrosospira, Dechloromonas*, and *Nitrosomonas* (Figure 5-20 (B)). Out of the 450 proteins groups identified, 337 (75%) were able to be automatically annotated for their functions. Proteins for genetic information processing and carbohydrate metabolism were found in the highest numbers, accounting to 24% and 21.7% respectively. These were followed by proteins for environmental information processing, energy metabolism and cellular processes (Figure 5-20 (C)). Among the proteins for genetic information processing, a large number of proteins required for translation (elongation factor Tu, large and small subunit ribosomal proteins) and degradation of bacterial RNA were identified. Proteins responsible for glycolysis and citrate cycle made up the highest number among carbohydrate metabolism proteins while membrane transport proteins, the ABC transporters, made up the majority of the environmental information processing proteins.

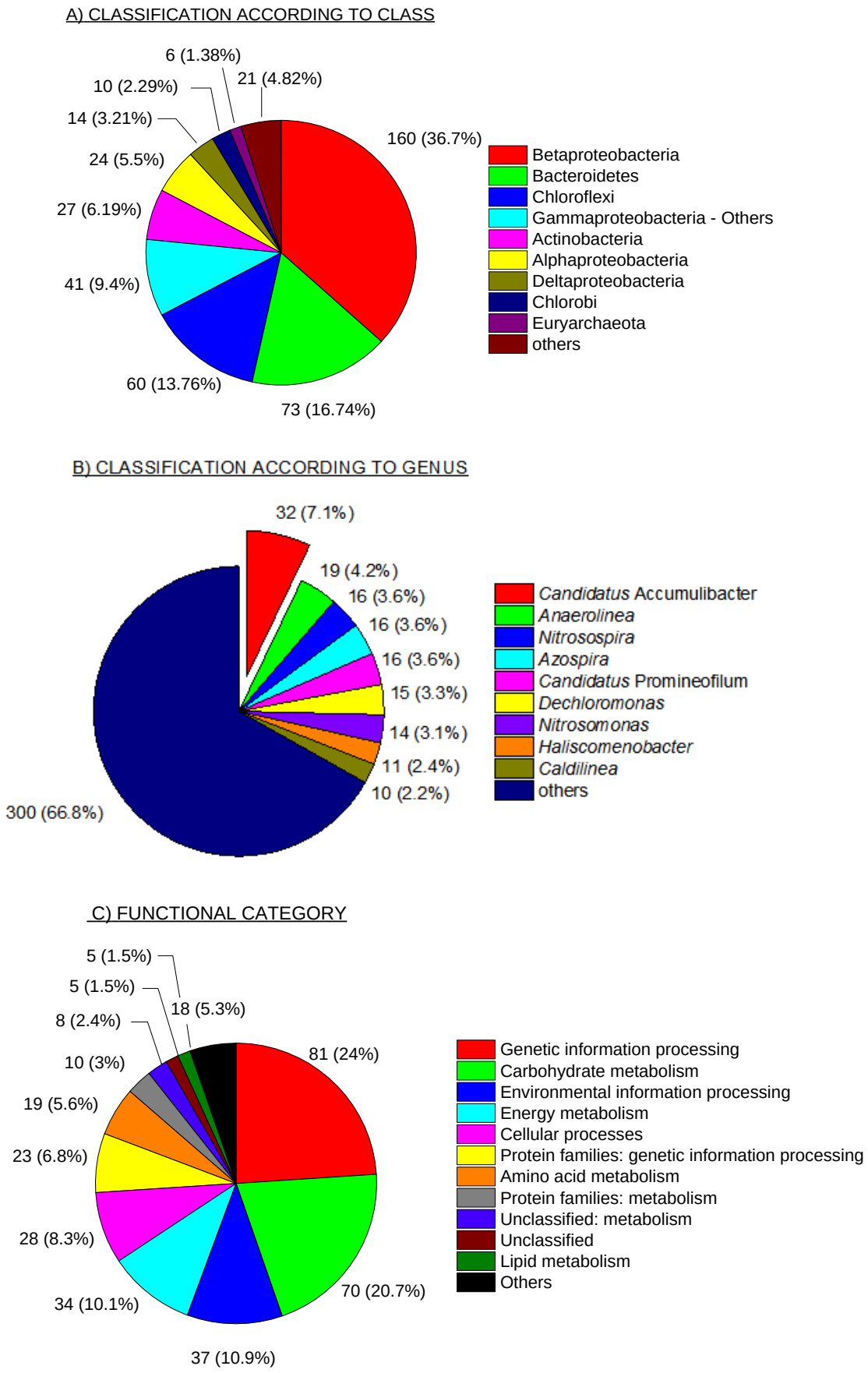

Figure 5-20: GhostKOALA annotation results, categorized according to class (A), genus (B) and functional category (C). In (B), only the genus with more than 10 identified proteins are differentiated

In regard to nitrogen metabolism, several enzymes responsible for nitrification and denitrification/anammox processes were identified (Table 5-10). Specific for nitrification process, the enzymes hydroxylamine oxidoreductase (HAO), ammonia monooxygenase AMO subunit A (AmoA) and AMO subunit B (AmoB) were identified.

Table 5-10: Proteins identified to be involved in nitrogen metabolism

Gene	Enzyme	Process
gdhA	Glutamate dehydrogenase (NAD(P)+) [EC:1.4.1.3]	
glnA	Glutamine synthetase [EC:6.3.1.2]	
pmoA-amoA	Methane/ammonia monooxygenase subunit A [EC:1.14.18.3 1.14.99.39]	Nitrification
pmoB-amoB	Methane/ammonia monooxygenase subunit B	Nitrification
hao	Hydroxylamine dehydrogenase [EC:1.7.2.6]	Nitrification
nirK	Nitrite reductase (NO-forming) [EC:1.7.2.1]	Denitrification/Anammox
nirS	Nitrite reductase (NO-forming)/ hydroxylamine reductase [EC:1.7.2.1 1.7.99.1]	Denitrification/Anammox
narG, narZ, nxrA	Nitrate reductase / nitrite oxidoreductase, alpha subunit [EC:1.7.5.11.7.99.-]	Denitrification
narH, narY, nxrB	Nitrate reductase / nitrite oxidoreductase, beta subunit [EC:1.7.5.1 1.7.99.-]	Denitrification
nosZ	Nitrous-oxide reductase [EC:1.7.2.4]	Denitrification

5.2.3.3 Database validation using FISH Microscopy

FISH microscopy was used to validate the presence of *candidatus* Accumulibacter, whose proteins were found in the largest number using the Aalborg database. The presence of *Nitrosomonas*, which was predicted to be the main bacteria responsible for nitrification activity, and the phylum *Chloroflexi*, which made the third largest amount of proteins based on class and the second based on genus (*Anaerolinea*), were also investigated by FISH. FISH microscopy from samples of day 70 and day 77 confirmed the presence of the investigated organisms, as seen by the clear fluorescence signal shown in Figure 5-21. *Candidatus* Accumulibacter (Figure 5-21 (A−B)) and *Nitrosomonas* (Figure 5-21 (C−D)) were seen in microcolonies of 30−40 µm and aggregates of 5−10 µm respectively, fitting to their description in the literature [99]. Phylum *Chloroflexi* was also

positively detected as shown by the filament-shaped signals in Figure 5-21 (E−F). FISH microscopy thus confirmed the presence of these organisms in the sample and validated the proteomics identification.

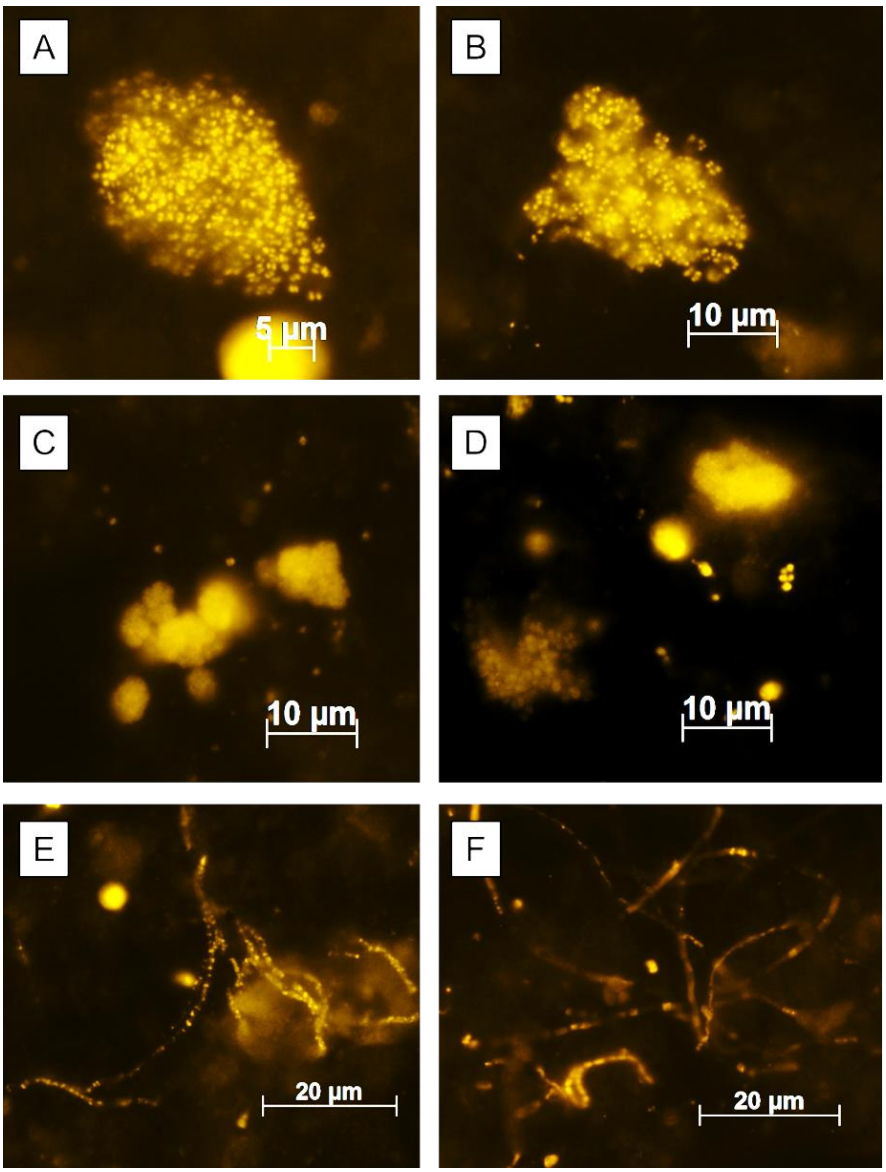

Figure 5-21: Cell aggregates of *Accumulibacter* PAO detected with probe PAO651 (Cy3) from samples of day 70 (A) and day 77 (B). Cell aggregates of *Nitrosomonas* detected with probe Nmo254 (Cy3) from samples of day 70 (C) and day 77 (D). Bacteria of phylum *Chloroflexi* detected with a mixture of probes CFX1223 + GNSB941 (Cy3) from samples of day 70 (E) and day 77 (F)

5.2.3.4 Investigation of Nitrification Activity

To specifically investigate the changes in the nitrification activity of the AOB, the amino acid sequences were then searched against protein database UniProtKB [112] to identify the proteins at the species level. The results were then filtered for the enzymes AMO and HAO. AmoA and AmoB (both from *Nitrosomonas* sp. Is79A3) were in each case only identified in only 2 samples.

HAO (*Nitrosomonas* sp. Is79A3) was found in all 10 samples, allowing the LFQ-intensity to be compared to the autotrophic activity. Comparing both data (Figure 5-22), it can be seen that the enzyme HAO was underexpressed during the period of lowest autotrophic activity. The lowest intensity of HAO was 3-fold change lower compared to initial intensity (day 1). Although a direct correlation between HAO-intensity and the specific autotrophic activity is not possible, HAO underexpression could very well be the reason why the activity of ammonia oxidation dropped, as hydroxylamine oxidation is the energy-yielding step in the growth of AOB [114].

Looking at other relevant enzymes, the chaperonin GroEL (*Nitrosomonas* sp. Is79A3) was also quantified in all samples (Figure 5-22). GroEL is a molecular chaperone belonging to the group of heat shock proteins (HSPs). It is a general stress protein which is responsible for protein folding, repair and degradation [115]. Its expression was found to be induced in activated sludge samples upon exposure to high temperature [107] and chemical stress [116]. Unexpectedly, its intensity was highest during the period of normal autotrophic activity and not when the activity was severely affected by the pH fluctuations. Bott et al. [116] previously reported that the use of GroEL as a stress indicator is limited due to the unspecific nature of this enzyme as it is inducible by a variety of stressors including starvation, which is a prerequisite condition in activated sludge treatment. This result is in agreement with their statement.

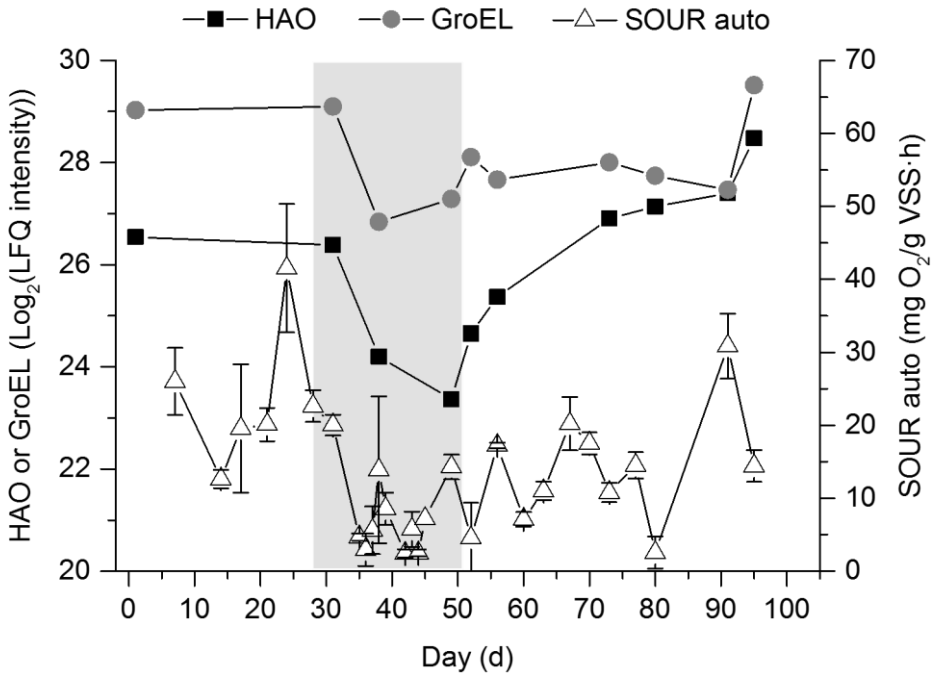

Figure 5-22: Comparison between specific autotrophic activity and log2-LFQ intensity of hydroxylamine oxidase enzyme and chaperonin GroEL

Despite better identification by using the database from WWTP Aalborg, protein scores were on average relatively low and only a few proteins were identified consistently in all samples. Furthermore, some proteins were not found in their duplicates. AmoA and AmoB, for example, were found only in 2 out of 20 measurements and not in their duplicates. Although according to Bock and Wagner [114] there is no direct correlation between the amount of AMO and the activity of ammonia oxidation, it is highly unlikely that these enzymes were not expressed at all in the samples in which they were not detected, as some samples corresponded to the days of complete ammonia removal. It shows that low protein abundance could have restricted the identification.

Proteins related to *Candidatus* Accumulibacter were found in the highest abundance in the investigated samples. *Candidatus* Accumulibacter is a genus of phosphate accumulating organism that also functions as a denitrifier in wastewater treatment [99]. It is commonly found in high amount in wastewater treatment plant performing EBPR [117]. Previous 16S rRNA sequencing result of sludge from WWTP Kaßlerfeld, where the seed sludge was taken, revealed that *Candidatus* Accumulibacter made up only 0.4% of the total abundance of the plant (Appendix 5, Table A4). Although the community composition in the lab-scale plant might have shifted from the seed sludge and there must not necessarily be any correlation between the abundance of organisms and the amount of proteins they produce, it is possible that the identification was biased towards proteins from the EBPR microbial community as a result of the database used. As the wastewater composition and the treatment system vary, the bacterial community also varies from plant to plant. This shows the importance of having a tailored database specific for each system for better identification.

The proteomic analysis of P1 shows that a lot of valuable information can be retrieved based on the identification of the types of proteins in the sample, their relative intensity and the organism they belong to. Due to this reason, proteomic measurements were continued and done in a more detailed manner for the samples from phases of phosphorous and nitrogen limitation, with the aim to understand the changes in the system during such conditions from a molecular point of view. For these phases, EPS samples were also analysed in addition to the total protein samples.

5.2.4 Phase 3: Phosphorous Limiting Condition I

Phosphorous limitation was introduced in the third and the fourth phase of plant operation by omitting potassium dihydrogen phosphate KH_2PO_4 from the synthetic wastewater. Phase 3 (P3) was operated for 161 d, of which 38 d was phosphorous limited. Figure 5-23 (A) shows the variation of the phosphate concentration and phosphate loading of P3 influent. At the beginning of the operation, the plant received synthetic wastewater of complete compositions until the sludge acclimatised to the wastewater and a stable operation was achieved. Due to two occurrences that resulted in sludge loss on day 26 and day 46 (marked 1 and 2 in Figure 5-23 (C)), the removal of KH_2PO_4 was only done after day 53. The influent was changed back to normal wastewater after day 127 until the end of P3.

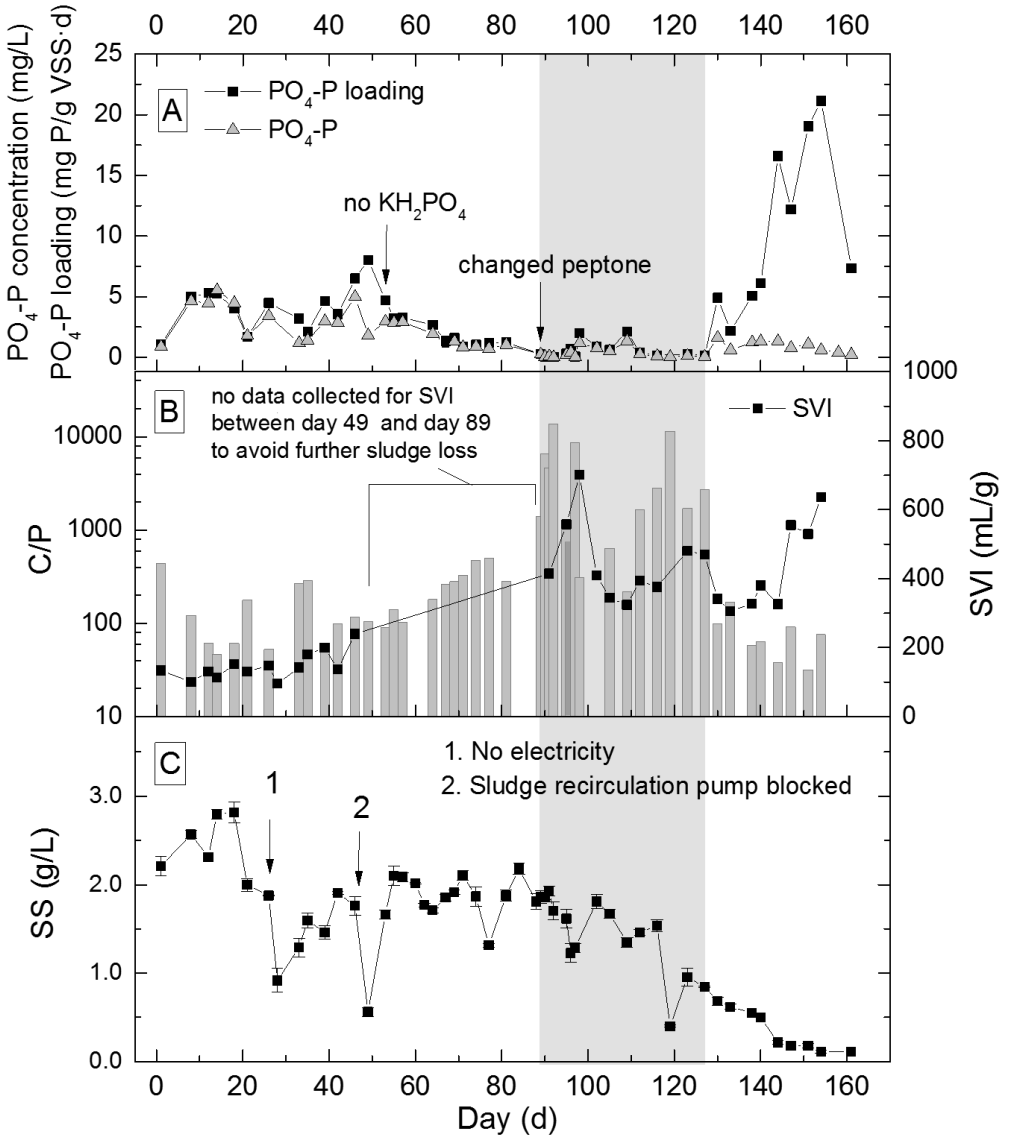

Figure 5-23: (A) Profiles of influent phosphate loading and concentration, (B) C/P ratio and SVI and (C) SS concentration of P3. Grey area marks the period of phosphorous limitation, after which synthetic wastewater with complete composition was provided

The suggested ratio of macronutrients C, N and P in wastewater for activated sludge treatment is a BOD_5:N: P ratio of 100:5:1. The actual macronutrient requirement depends on several conditions such as the temperature and sludge age. Systems of high sludge age require less N and P for a given BOD_5 since a significant amount of nutrients are recycled from lysed cells following cell death [13]. Liu and Liss [118] reported no signs of deficiency when activated sludge of 26-30 days sludge age was subjected to P-limitation at a BOD_5:N: P ratio of 100:5:0.1. From the results of phase 1 and phase 2, it was safe to assume that the COD of the synthetic wastewater was almost entirely biodegradable (COD≈BOD), as during stable operation the COD removal was mostly >90%. Hence, to introduce phosphorous limitation, the sludge was subjected to a COD:PO_4-P ratio of > 100:0.1 (C/P >1,000). This ratio, however, could not be achieved solely by removal of KH_2PO_4 from the wastewater (Figure 5-23 (B)). This was found to be caused by peptone from casein in the synthetic wastewater, which had a high concentration of phosphorous. Thus, from day 89, the peptone was changed to the one from meat with lower phosphorous concentration (see influent composition in Section 4.2.5). As soon as the peptone was changed, phosphorous concentration dropped nearing zero and the C/P increased to values >1,000. Hence, the real P-limitation is considered only after the change of peptone and the limitation period is marked in grey in all diagrams in this phase. As a result of P-scarcity, the SVI increased and the plant started to lose sludge, causing a decrease in SS concentration (Figure 5-23 (B) and (C)).

COD and ammonium removal were at the beginning unaffected by the phosphorous limitation as their values stayed beyond 90% removal (Figure 5-24 (A and B)). Phosphorous removal however dropped already a day after the limitation was started by showing a decrease from 77% to 32% removal. On the third day of phosphorous limitation, the concentration of phosphorous in the effluent was higher than in the influent, shown by the negative removal value (Figure 5-24 (C)). This was an indication that cell lysis may have occurred. It must be noted however that although the negative values were large by percentage, the absolute difference between the effluent and the influent were not that high (<0.5 mg/L). The phosphorous removal recovered on day 9 of the limitation (day 98 of operation), when the phosphorous loading increased slightly for an unclear reason and the C/P reduced to <1,000. The removal dropped again but stayed at positive values when the C/P value increased again to >1,000 from day 112. The ammonium COD and ammonium removal were this time affected by the limitation and showed a decrease in efficiency.

During P-limiting period, the plant experienced a continuous drop of respiration activity, as shown by the total SOUR values (Figure 5-24 (F)). This was as a result of the decrease in both autotrophic and heterotrophic activity (Figure 5-24 (D and E)). Both parameters continued to decrease until the P was resupplied, after which the heterotrophic SOUR slightly improved. Autotrophic SOUR was almost completely inhibited on day 112, 13 days after the P-limitation and did not recover even after the limitation was lifted. It was however peculiar that this time, the loss of autotrophic activity was not reflected in the ammonium removal, as was the case in P1.

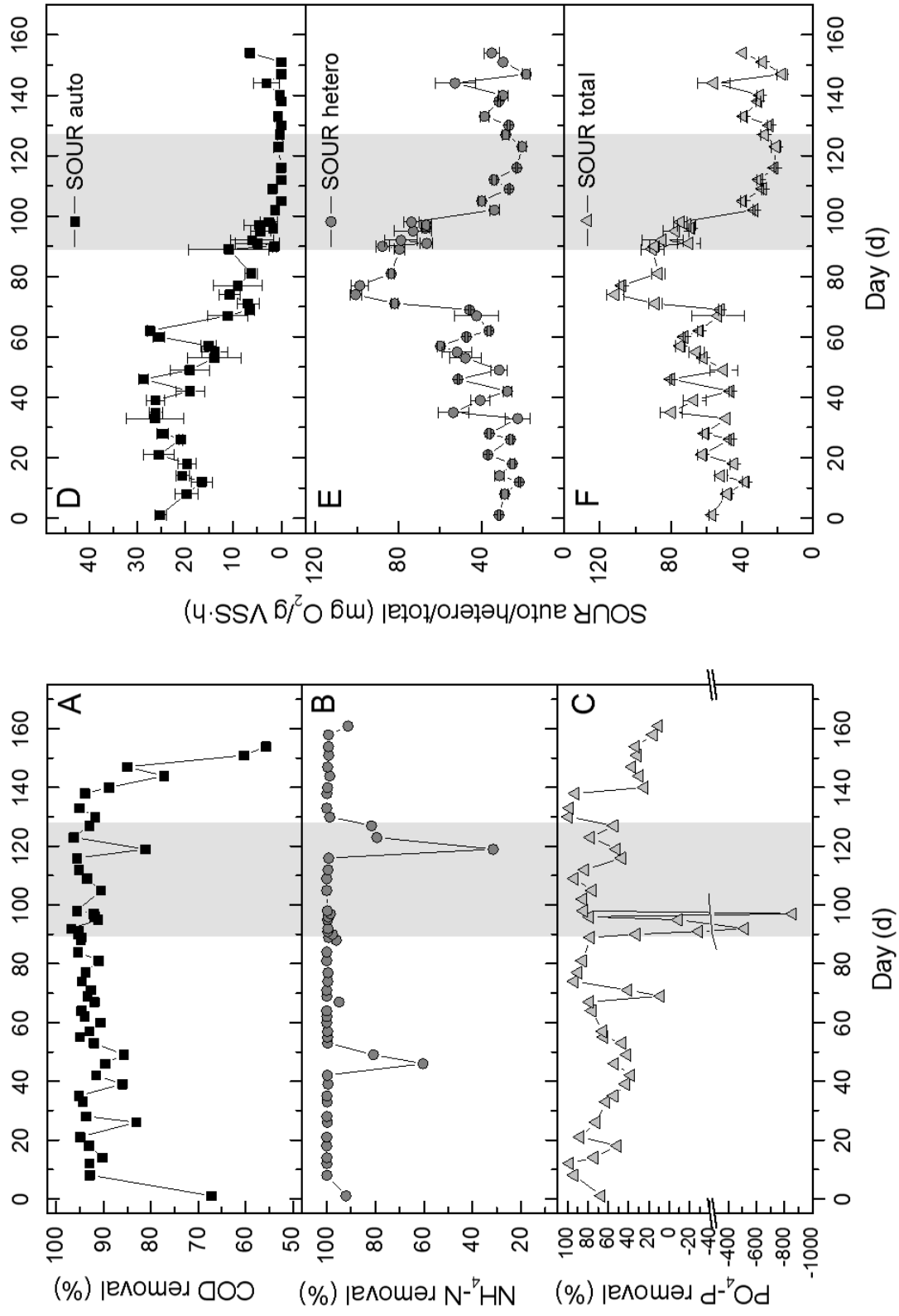

Figure 5-24: Removal performances (A-C) and respirometric activity (D=F) of P3. Grey area marks the period of phosphorous limitation

Even after the influent was changed back to normal wastewater, sludge settleability did not improve and the plant continued to lose sludge through the effluent. This was probably caused by the influent rate that was kept constant throughout the entire operation, which might have caused biomass washout when the SS concentration was very low (<1g/L). The phosphorous loading also spiked toward the end of the phase as sampling was done only every 3 days and the loading could not be adjusted optimally to the actual biomass concentration as the plant continued to lose biomass at a high rate in the days between the measurements.

A foam layer was seen in the anoxic reactor about a week after P-limitation was started. The brown foam became darker, denser (scum) and putrefied with time. It reappeared when removed. Foaming was also seen in the aerobic reactor but no accumulation of scum was observed, most probably due to turbulence of the aeration, which did not allow the scum to accumulate. Figure 5-25 shows the foam/scum formation on day 118 (A), 123 (B) and day 130 (C), which corresponded respectively to day 29 and 34 of P-limitation and 3 days after the limitation was lifted. The foaming stopped on 140, 13 days after phosphorous was resupplied.

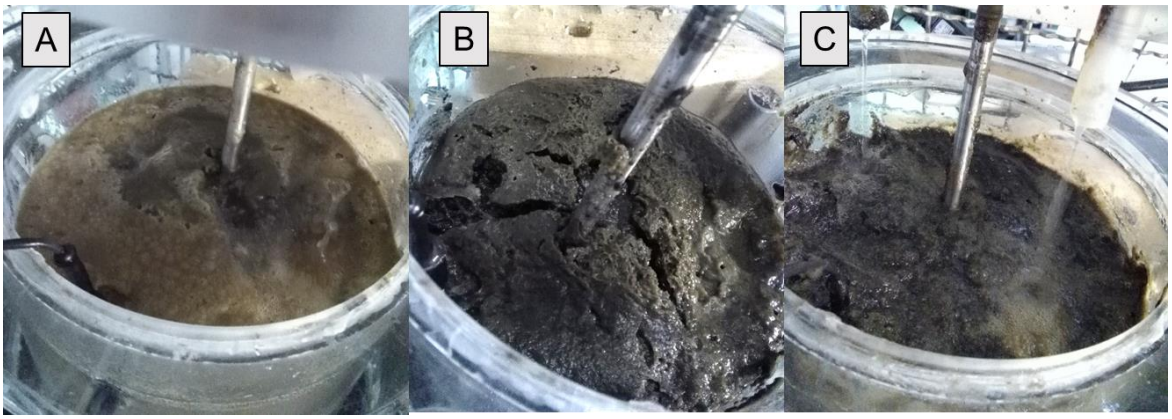

Figure 5-25: Scum/foam formation in the anoxic tank on day 118 (A), 123 (B) and 130 (C)

It seemed that after a certain period of being at low phosphorous loading when KH_2PO_4 was removed on day 53, the production of EPS started to decrease, shown by the lower protein and carbohydrate contents of the EPS (Figure 5-26). When the loading was further decreased to an almost zero value when the peptone was changed, more EPS were produced on average by the flocs. Nevertheless, it is only speculative that phosphorous removal increased the EPS production as the values fluctuated, where Lowry protein showed very higher fluctuations. The production of EPS, however, clearly decreased again when phosphate was resupplied.

The formation of foam and scum was expected during phosphorous deficiency. It has been reported in many literature that phosphorous limitation in activated sludge is associated with increased EPS production [119] [13]. It is possible that when the phosphorous concentration was lowered by the omission of KH_2PO_4, EPS was used as the nutrient supply to counter the deficiency, thus the observed lower EPS content. However, when the wastewater was totally devoid of

phosphorous, some cells might have not survived the starvation period. Lysed cells released the cellular contents to the bulk fluid which contributed to more EPS and increased protein and polysaccharide concentration in the bulk fluid. Jorand et al. [120] reported that a significant amount of the EPS was hydrophobic. The hydrophobicity was contributed primarily by the proteins whereas carbohydrates were mainly hydrophilic. The increase in hydrophobicity as a result of the release of a high amount of proteins during the P-limiting period might have caused the foam and scum formation.

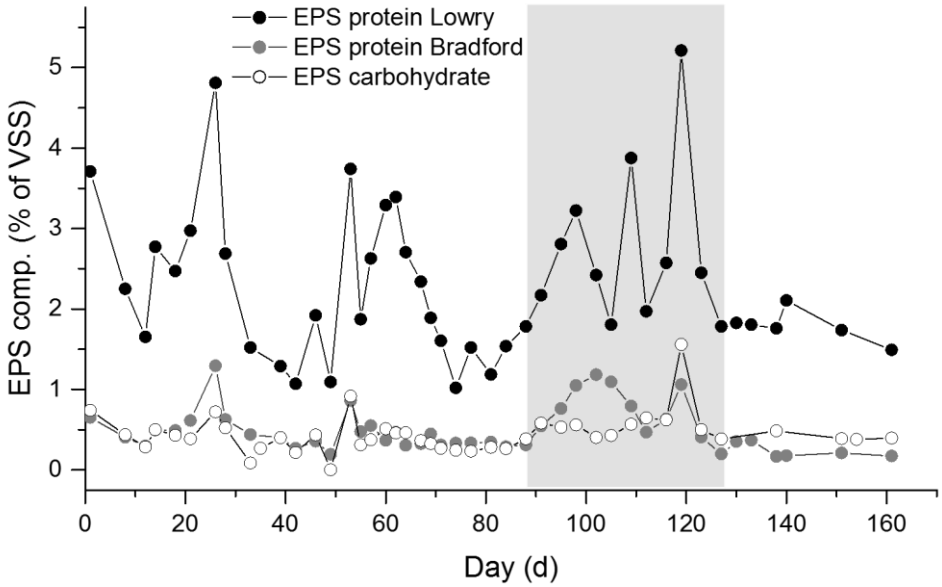

Figure 5-26: EPS protein and carbohydrate contents of P3. Grey area marks the period of phosphorous limitation

5.2.5 Phase 4: Phosphorous Limiting Condition II

Phosphorous limiting condition was repeated in phase 4 (P4) as the low biomass concentration at the end P3 did not allow enough EPS to be extracted for proteomics analysis. Peptone from meat was used from the beginning of the phase and phosphorous limitation was introduced by excluding KH_2PO_4 from the synthetic wastewater. P4 was operated for 50 days, 21 days of which was phosphorous limited.

Figure 5-27 (A) shows the profiles of the PO_4-P and total phosphorous (TP) concentrations as well as the PO_4-P loading of P4. The phosphorous limiting wastewater was supplied from day 15 until day 40 (values shown in the graph on day 15 are the values measured before the influent was changed). As observed in P3, the SVI values increased under phosphorous limitation, when the C:P ratio higher than 100:0.1 (C/P >1,000; Figure 5-27 (B)). The C:P ratio, in this case, was calculated from the ratio of COD to TP instead of PO_4-P, as the PO_4-P concentrations of the influent during the limitation period were below the detection limit of 0.05 mg/L. The SVI values increased

from < 250 mL/g to values >500 mL/g. The highest value measured was almost 1,400 mL/g, a clear case of sludge bulking. Recurrent sludge bulking events during this period contributed to sludge washout, causing the SS concentration to drop (Figure 5-27 (C)). When the phosphorous limitation was lifted, SVI decreased gradually to the normal value < 250 mL/g and SS concentration also increased again.

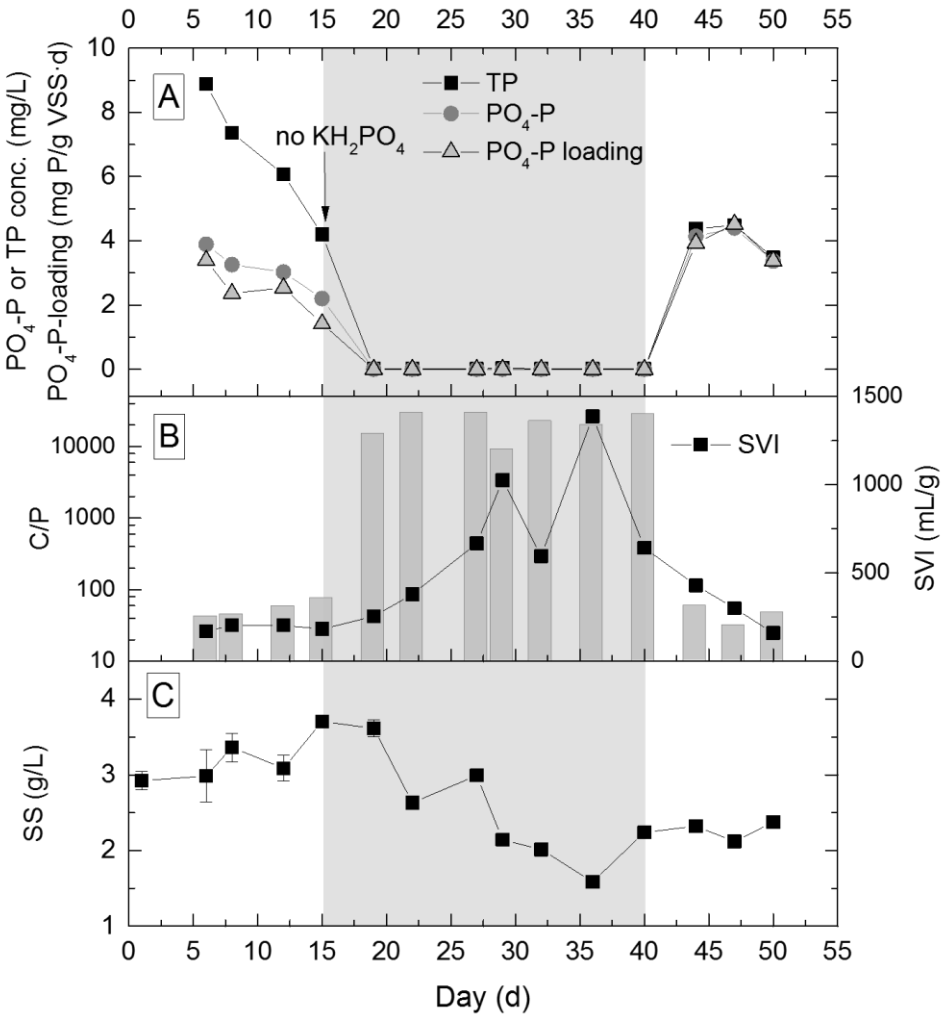

Figure 5-27: Profiles of influent PO_4-P concentration, TP concentration and PO_4-P loading (A), SVI and C/P ratio (B) and SS concentration (C) of P4. Grey area marks the period of phosphorous limitation, after which synthetic wastewater with complete composition was supplied.

COD and ammonium removal were not affected by the phosphorous limiting condition as the removal performance stayed beyond 85 and 95 % respectively throughout the entire phase (Figure 5-28 (A and B)). As observed in P3, phosphorous concentration was higher in the effluent than in the influent during the limitation period, as indicated by the negative phosphorous removal (Figure 5-28 (C)). The biomass also showed a continuous reduction in respirometric activity during this period, as illustrated by heterotrophic, autotrophic, and thus also the total SOUR (Figure 5-28 (D-F)). All affected parameters showed recovery once the influent was changed back to the complete composition with phosphorous.

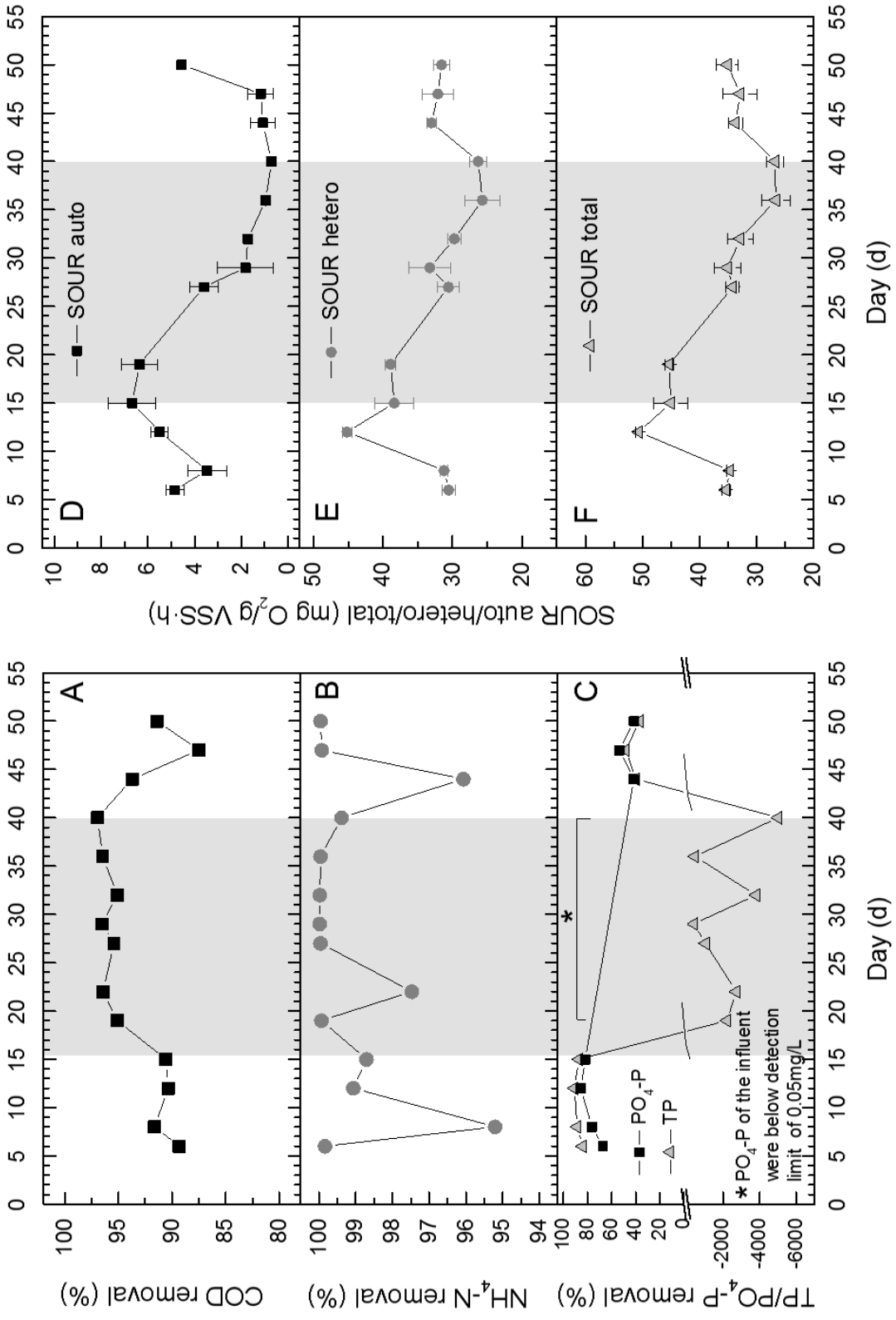

Figure 5-28: Removal performances (left) and respirometric activity (right) of P4. Grey area marks the period of phosphorous limitation

Foaming was seen in the anoxic reactor about a week after the phosphorous limitation was started. As opposed to the observation during P3, the foam did not accumulate to form a thick scum layer on top of the water surface. Instead, it got washed out pretty quickly. Another interesting observation was that this time, a thick biofilm layer was formed on the wall of the aerobic reactor. The biofilm layer had an uneven surface with hollow areas that had a bubble-like feature. It is common to find biofilms with a heterogeneous surface. Instead of having a uniform monolayer, most biofilms contain voids and channels to allow the permeation of nutrients and oxygen, and the exchange of metabolic products with the bulk fluid [121,122]. The biofilm layer started to fall off directly after influent with phosphorous was supplied again at day 44 and within a day, the wall of the aerobic reactor was free from the biofilm. No new biofilm growth was observed until the end of phase on day 50.

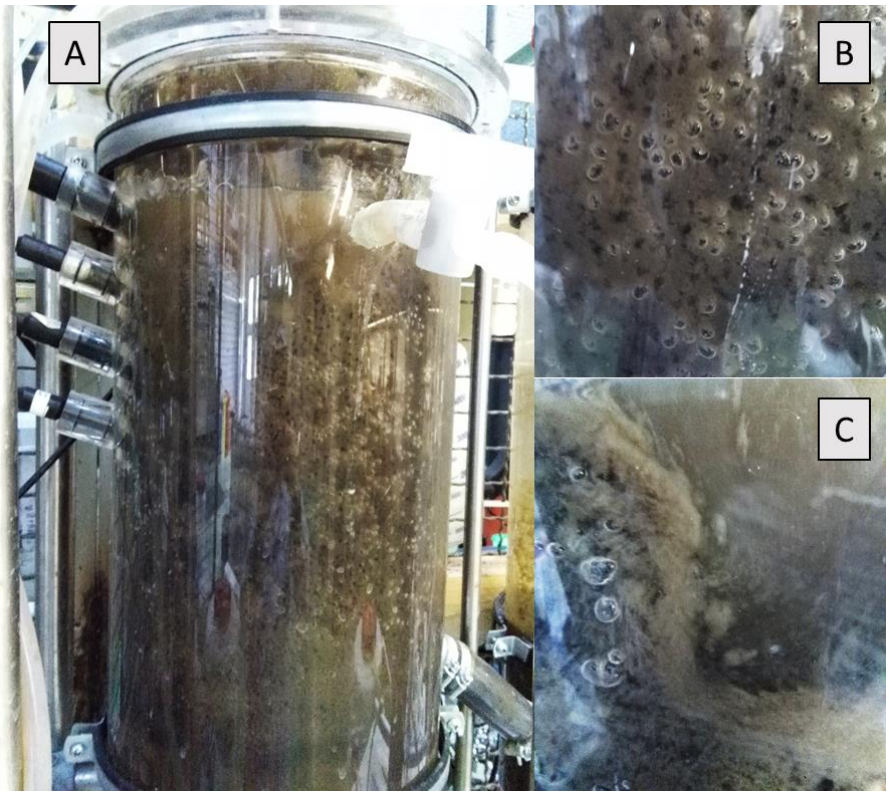

Figure 5-29: Picture of the aerobic reactor on day 44. (A)Thick biofilm formation on the reactor wall. (B) Close-up picture of the 'bubbles' on the biofilm (C) Biofilm started to fall off once influent containing phosphorous was supplied

Different than in P3, the EPS protein content of the sludge in P4 showed a clear decrease in amount during phosphorous limitation. The protein content rose again under P-replete condition (Figure 5-30). The hypothesis is that the biomass was able to adopt different strategies during P-starvation. The high concentration of EPS during P-limiting period of P3 was probably due to the combined effects of increased EPS production and cell lysis, which released the cellular contents to the bulk fluid, causing the formation of a significant amount of foam/scum. In that case, the nutrients from the EPS and lysed cells would be available to other cells to maintain their

viability. In P4, the EPS was probably primarily used to create a biofilm layer to protect the cells from starvation, as the bacteria in the biofilm were surrounded by a nutrient-rich EPS layer. Thus, a low amount of EPS was measured in the sludge outside the biofilm.

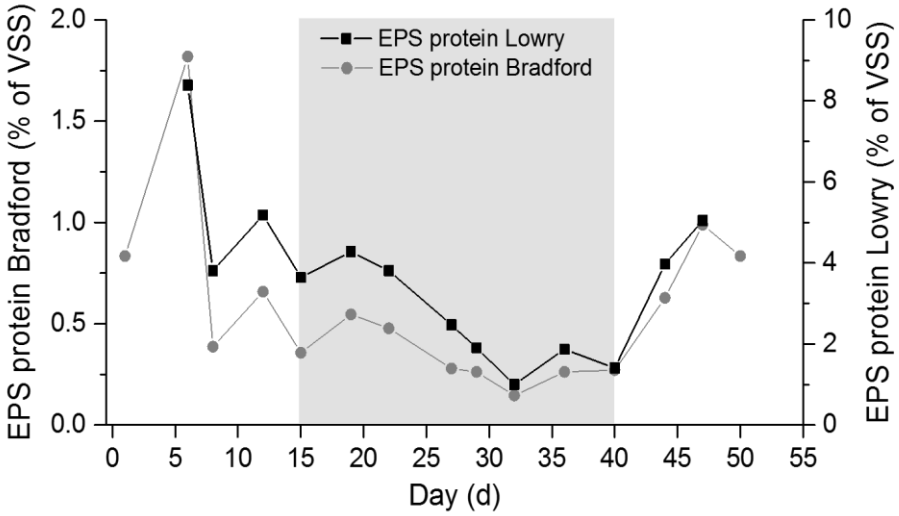

Figure 5-30: EPS protein content of P4. Grey area marks the period of phosphorous limitation

5.2.6 Proteomics of Phase 4

To understand the changes in the activated sludge system in response to P-limitation at the molecular level, protein expression in total protein (TP) and EPS samples of P4 were analysed using quantitative (LFQ) proteomics.

5.2.6.1 Protein Identification

As the proteomics results of P1, the number of proteins groups belonging to the genus *Candidatus* Accumulibacter was also found in the highest amount in all samples of P4 (discussed previously in Section 5.2.3.4). This was followed by proteins related to the genera *Dechloromonas*, *Nitrosomonas*, *Nitrosospira,* and *Azospira* for both total protein and EPS samples, the order of which varied slightly according to samples (Figure 5-31 and Figure 5-32). *Nitrosomonas* and *Nitrosospira* are nitrifiers, whereas *Candidatus* Accumulibacter, *Dechloromonas* and *Azospira* are denitrifiers that are commonly found in WWTPs [96,123,124]. Foam/scum samples showed proteins from the same genera as TP samples, albeit in different amounts.

A total of 1,100 protein groups were found in the samples of P4. The number of protein groups identified in the EPS samples was higher than in the TP samples. Between 24−171 protein groups were identified in TP samples whereas the number of protein groups identified in EPS samples ranged between 110−346 protein groups, averaging 3.7 times more identification than TP samples.

Considering the significant role of EPS in the floc and biofilm formation, the high number of proteins found in EPS further illustrates its importance in the activated sludge process.

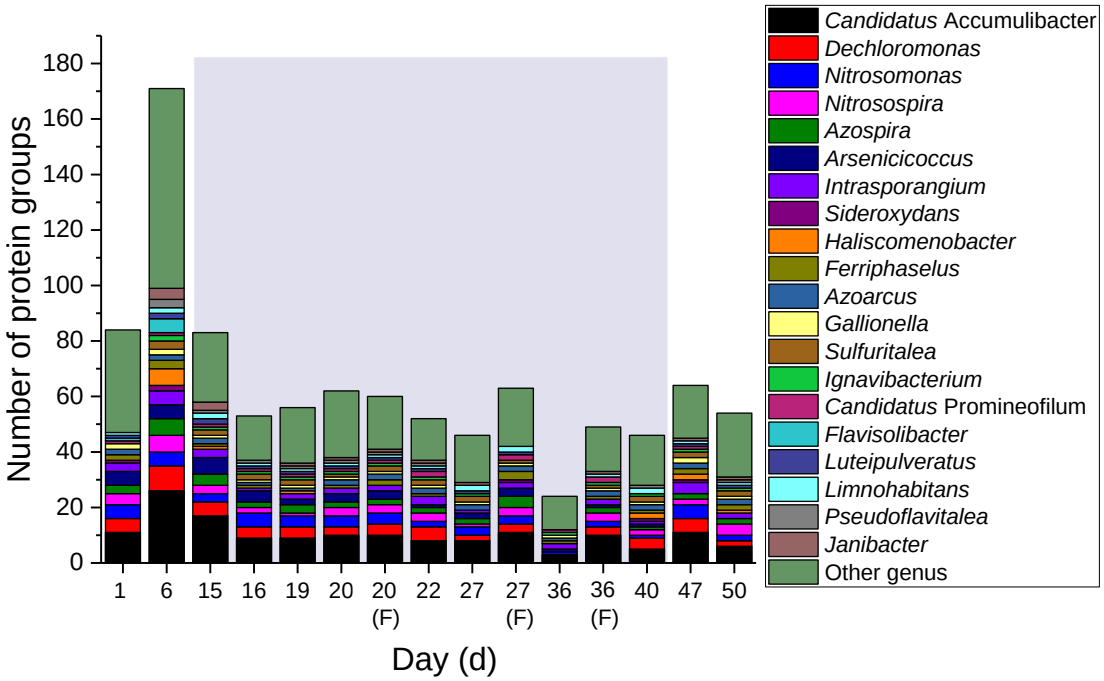

Figure 5-31: Number of protein groups in total protein and foam/scum (F) samples of P4, classified according to the genera. Only the 20 genera with the highest protein groups are differentially coloured. Blue-shaded area marks the period of phosphorous limitation

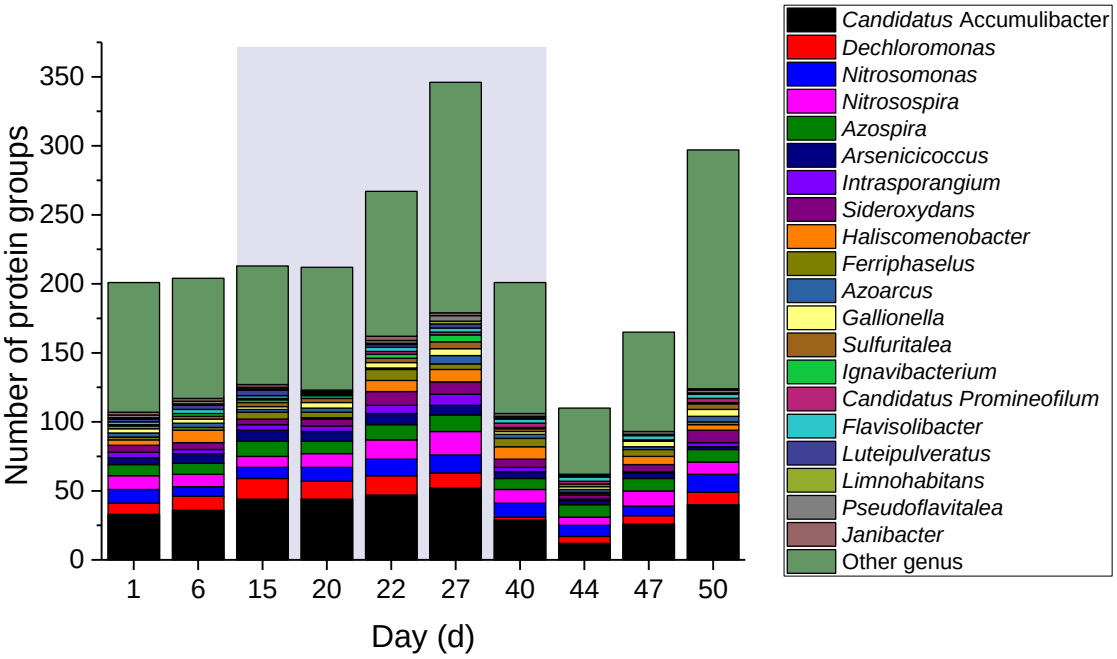

Figure 5-32: Number of protein groups in EPS samples of P4, classified according to the genera. Only the 20 genera with the highest protein groups are differentially coloured. Blue-shaded area marks the period of phosphorous limitation

The number of protein groups found in the EPS samples was higher than previously reported in the literature [69,125,126], signifying a successful extraction method. The identifications in TP samples were low despite high protein concentration of crude extract and significant protein profiles visualised using SDS-PAGE, showing that further optimisation is probably necessary for the post-extraction steps of total protein prior to LC-MS/MS to increase the peptide yield. One of the steps that could be further investigated is the protein purification prior to proteomics, which is the applied method of methanol/chloroform (M/C) extraction. M/C extraction method is reportedly utilised to extract hydrophobic proteins [127], although the original literature stated that this method is applicable for both soluble and hydrophobic proteins [91]. Whole-cell lysates contain a combination of hydrophilic (non-membrane) and hydrophobic (membrane) proteins, whereby the hydrophilic proteins are more abundant. It is possible that the difference in hydrophobicity between intracellular and extracellular proteins brought different results in protein yield during M/C extraction of TP and EPS, and subsequently lower peptide yield in the TP samples.

Figure 5-33 shows the number of protein groups belonging to TP and EPS samples according to the functional categories. Proteins responsible for carbohydrate metabolism made the highest amount of all proteins in the EPS samples, followed by those attributed to the genetic information processing, energy metabolism and amino acid metabolism. In contrast, proteins responsible for carbohydrate metabolism and genetic information processing were found in an almost similar amount in TP samples. These were followed by protein groups associated with environmental information processing, amino acid metabolism and cellular processes.

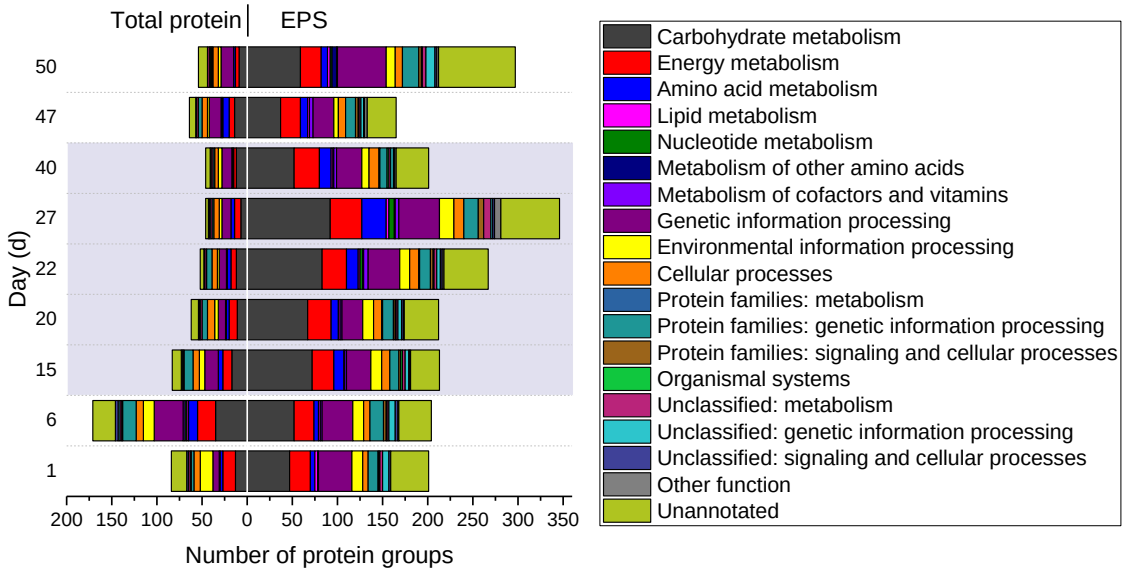

Figure 5-33: Number of protein groups in total protein and EPS samples of P4, classified according to functional categories. Blue-shaded area marks the period of phosphorous limitation

It is important to note that the number of proteins belonging to each category indicates their diversity and not the quantitative abundance of individual proteins, which will be the subject of the following section. It can be seen that the period of phosphorous limitation (shaded in blue) caused the rise in the number of proteins expressed across all functional categories in the EPS samples. The increase in the number of proteins in the EPS sample signifies possible microbial strategies of using different pathways to continue the metabolism. The number of proteins dropped again towards the end of P-starvation period, indicating probable adaptation. The opposite was true for TP samples where either fewer proteins were expressed (e.g. proteins associated with carbohydrate, energy and amino acid metabolism) or there were no significant changes in the protein expression (e.g. proteins for cellular processes). It is possible that as the cells were significantly affected by P-deficiency, the strategies for survival were directed towards the EPS. Most extracellular proteins originate from the cells themselves. During P-starvation, cell lysis occurred. The extracellular enzymes from lysed cells possibly served as an 'external digestive system' to catalyse the metabolism of biopolymers, generating products that could be taken up as carbon and energy sources by the cells [125]. The formation of the biofilm layer further supported the idea that the cells defended themselves from the adverse effects of nutrient deficiency by utilising the EPS.

5.2.6.2 Protein Quantification

Figure 5-34 and Figure 5-35 show the 10 most abundantly expressed proteins in TP or foam/scum and EPS samples respectively. The abundance in LFQ intensity is log2-transformed to decrease the effect of outliers. In all samples, chaperonin GroEL was the most abundant protein, consistent with the literature which stated that this member of heat-shock proteins was essential for bacterial growth in all conditions and not only under (heat) stress condition [128]. Other protein groups that were also highly expressed were various ATP binding cassettes (ABC transporters), F-type ATPases, enzymes responsible for carbohydrate metabolism (acetyl-CoA and propionyl-CoA synthetase), elongation factor Tu and antioxidant enzymes (alkyl hydroperoxide reductase in TP and isocitrate dehydrogenase in EPS). In EPS samples, cold-shock protein (CspA family) was also highly expressed. The high abundance of these proteins suggests that the most active cell functions were perhaps ensuring proper protein folding, transmembrane transport, energy metabolism and protection of cells from damage caused by reactive oxygen species.

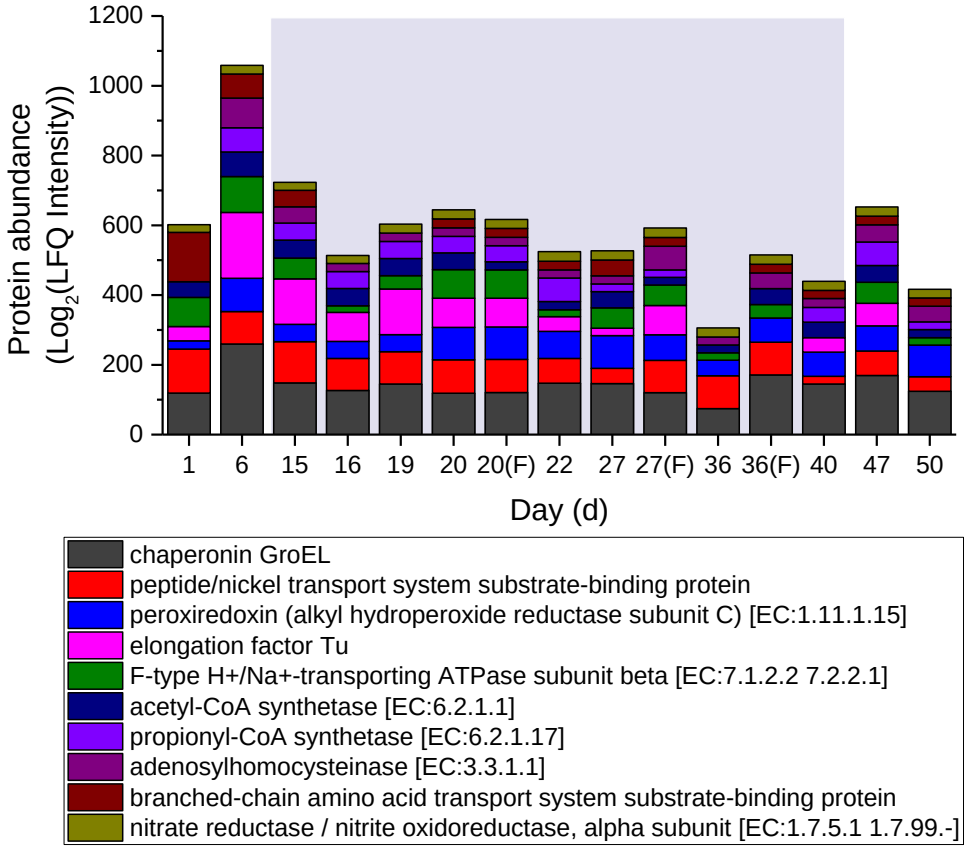

Figure 5-34: Log2-LFQ intensity of the 10 most abundant proteins in total protein and foam/scum (F) samples of P4. Blue-shaded area marks the period of phosphorous limitation

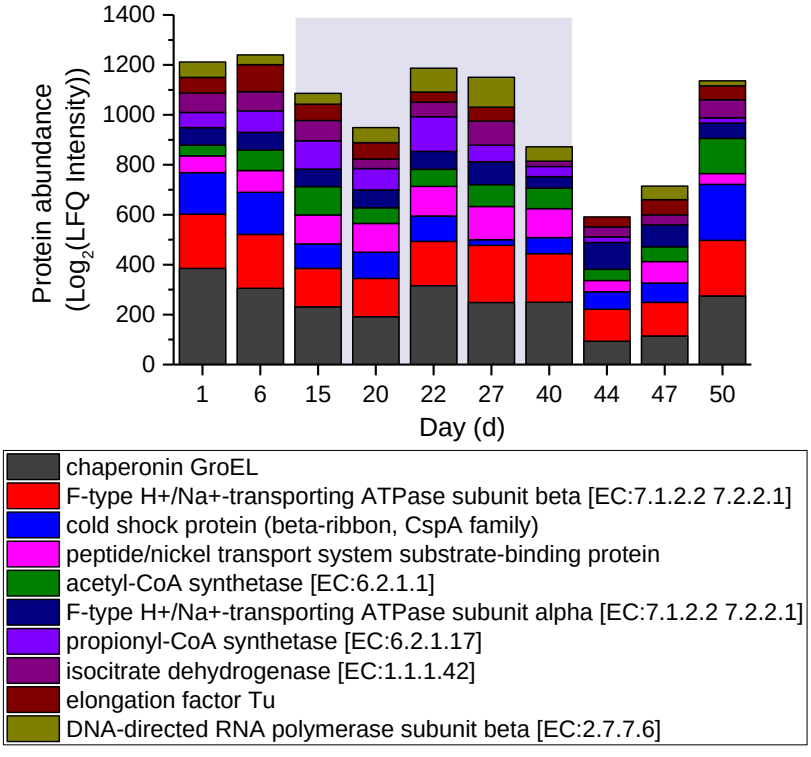

Figure 5-35: Log2-LFQ intensity of the 10 most abundant proteins in EPS samples of P4. Blue-shaded area marks the period of phosphorous limitation

5.2.6.3 Protein-level Response to P-limitation

The protein-level response towards P-limitation was investigated by analysing the changes in the intensity of various proteins, focussing on the stress-related proteins (heat shock proteins and antioxidant enzymes) and proteins associated with phosphorous utilisation. Due to an extensive amount of data, the intensity values shown for each type of protein are the cumulative LFQ intensity of all organisms containing these proteins.

1. Stress-related Proteins

Heat Shock Proteins

Figure 5-36 shows the changes in the log2-LFQ intensity of the heat shock proteins (HSPs) GroEL, GroES, DnaK and HtpG in TP (left) and EPS samples (right). No changes in the abundance of the GroEL and GroES could be specifically attributed to the P-starved condition in the TP samples (Figure 5-36 (left)) and DnaK and HtpG were not detected in these samples. In the EPS samples (Figure 5-36 (right)), the abundance of GroEL showed an increase of 125-fold while GroES and DnaK increased 34 and 38-fold respectively at the beginning of the P-limited period. Their intensity values decreased again at the end of the limitation period. In contrast, HtpG decreased under P-limitation.

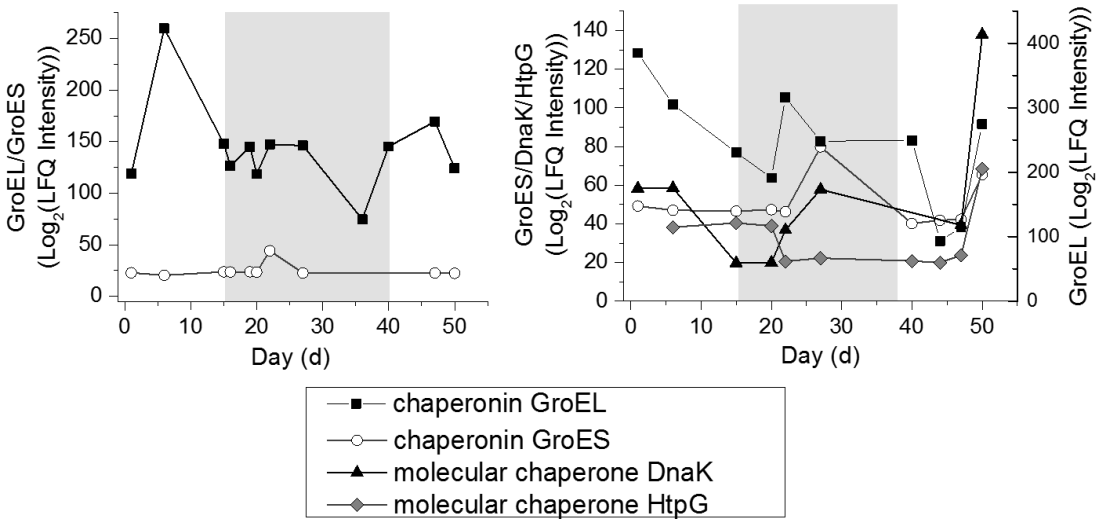

Figure 5-36: Changes in the abundance of heat shock proteins in TP (left) and EPS samples (right) of P4. Grey area marks the period of phosphorous limitation

HSPs are essential in ensuring that proteins reach their native conformation and are functional. Their expression is increased under stressed conditions. GroEL in combination with GroES is necessary for bacterial growth [128] and required at the early stage of substrate folding. HSP90, on the other hand, assists folding at a later stage [129], but bacterial HSP90 (HtpG) was found not

necessarily essential for cell viability [130]. This may explain the difference in response shown by HtpG compared to the other chaperones to P-limitation. The increase of GroEL, GroES and DnaK in the EPS sample at the end of phase was probably due to stress caused by overloading. This supports the statement that major molecular chaperones and their co-chaperones are induced by a variety of stress conditions and unlike other proteins, operate with little substrate specificity [129].

Antioxidant Enzymes

Partial reduction of molecular oxygen during aerobic metabolism causes oxidative stress by forming reactive oxygen intermediates (ROI) such as superoxide, hydrogen peroxide (H_2O_2) and hydroxyl peroxide (Eq. (5-1)) [25,131]. ROIs are highly toxic and may chemically damage DNA, proteins and membranes [132]. Cells under P-limitation may sustain further oxidative stress [133]. Accordingly, the expression of antioxidant enzymes is anticipated to be elevated in response to P-deficiency to defend the cells against the ROIs.

$$\underset{\text{Oxygen}}{O_2} \xrightarrow{e^-} \underset{\text{Superoxide}}{O_2^-\cdot} \xrightarrow{e^-} \underset{\text{Hydrogen peroxide}}{H_2O_2} \xrightarrow{e^-} \underset{\text{Hydroxyl radical}}{OH^-\cdot} \xrightarrow{e^-} \underset{\text{Water}}{H_2O} \qquad (5\text{-}1)$$

Figure 5-37 (right) shows the relative abundance of the antioxidant enzymes superoxide dismutase, alkyl hydroperoxide reductase subunit C (AhpC) and catalase in the EPS samples of P4. Superoxide dismutase detoxifies by converting two molecules of superoxide into H_2O_2 and oxygen, while alkyl hydroperoxide reductase (Ahp) defends the cell from H_2O_2 and organic peroxides by converting the H_2O_2 into water and the hydroperoxides into their corresponding alcohols [132]. Catalase, also known as hydroperoxidase, acts by catalysing the breakdown of H_2O_2 into water and oxygen [134]. Out of the three enzymes, only the expression of catalase showed a clear elevation in the P-limiting period in the EPS samples, amounting up to 40-fold of the intensity prior to P-limitation. The study of *E. coli* revealed that catalase was the predominant scavenger of H_2O_2 at high concentration, while H_2O_2 was primarily degraded by Ahp at low concentration [135]. It is therefore understandable that catalase is overexpressed during P-starved condition as the concentration of H_2O_2 is expected to be high at this condition. In contrast to the EPS samples, the abundance of AhpC in the TP samples increased in response to P-limitation (Figure 5-37 (left)). Superoxide dismutase was not detected and catalase was only measured in only 1 sample of TP (not shown in the diagram). It was also demonstrated in *E. coli* that Ahp was essential for the viability of P-starved cells [136], which is probably the reason why Ahp was able to be quantified consistently in TP samples but not other antioxidant enzymes.

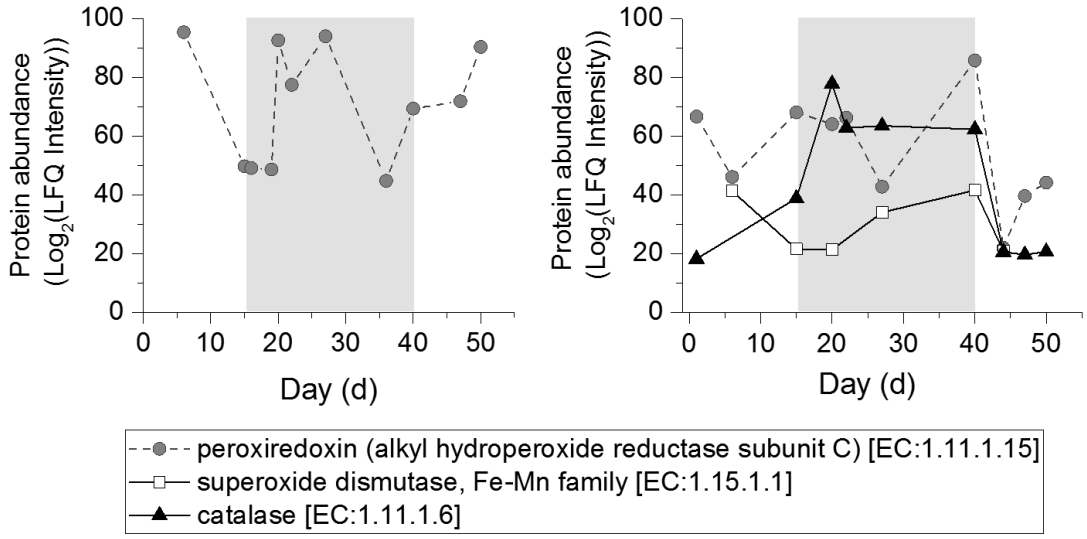

Figure 5-37: Changes in the abundance of antioxidant enzymes in TP samples (left) and EPS samples (right) of P4. Grey area marks the period of phosphorous limitation

2. Enzymes Related to Nitrification Activity

Ammonium monooxygenases (AMO) subunit A (AmoA) was not able to be quantified in the TP sample and was quantified only in one EPS sample, while AMO subunit B (AmoB) was quantified only in one TP sample and none of the EPS samples. AMO was reported to present both in soluble and in membrane-bound fractions of the cell [137,138]. Its activity dropped considerably upon cell rupture [137]. This phenomenon was previously discussed by Ensign et al. [29] and hypothesized to be caused by the loss of copper from AMO in the lysed cell. Therefore, aside from the possibility that the discovery of these enzymes by LFQ method is limited because AMO is produced in small amount by the AOBs, some of the enzymes might instead have been deactivated (underwent post-translational modification) upon lysis, thus could no longer be identified by mass spectrometry.

The enzyme hydroxylamine dehydrogenase (or hydroxylamine oxidoreductase HAO, EC:1.7.2.6) was given closer investigation as in the proteomics of P1, the nitrification activity was found to be related to the intensity of HAO instead of AMO. The abundance of HAO in the TP samples was contributed by *Nitrosomonas* sp. strain Is79A3 and in the EPS samples, its intensity was contributed by two different organisms, uncultured *Nitrosomonas* sp. and *Nitrosomonas* sp. strain Is79A3 (Figure 5-38). It was observed that HAO-expression was not particularly affected by P-starvation. Therefore the decrease in nitrification activity as soon as KH_2PO_4 was removed from the wastewater may have been due to other reasons, such as possible cellular damage as a result of starvation.

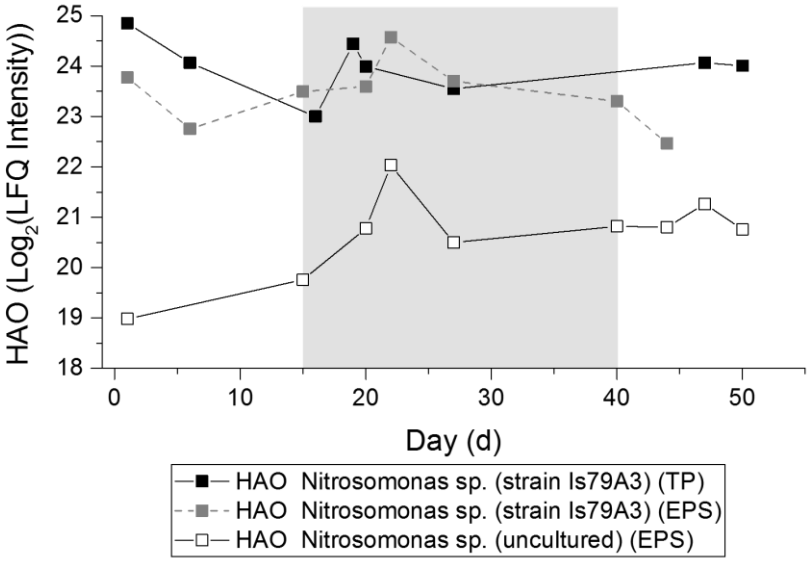

Figure 5-38: Intensity of HAO in TP and EPS samples of P4. Grey area marks the period of phosphorous limitation

3. Enzyme Related to Bacterial Adhesion and Bioflocculation

The annotation results were analysed for proteins related to bacterial adhesion and flocculation, such as flagellin and type IV pili [139,140], to examine how they affected sludge settling property. As expected, these proteins were not found in TP sample as they belong to the extracellular organelles of the bacteria. Flagellin was able to be quantified consistently in the EPS samples, as shown in Figure 5-39, while type IV pili protein was only found in one sample (not shown in the diagram). Flagellin is the structural protein that is a part of the filament of the flagellum. Bacterial flagellum was previously thought to have the sole function of providing motility to the cell. Recently, it has been demonstrated that flagella also play a role in bacterial adhesion as well as the invasion to a host cell with the help of flagellin [141]. Comparison between the expression of flagellin and the SVI, however, failed to find a relationship between the two parameters.

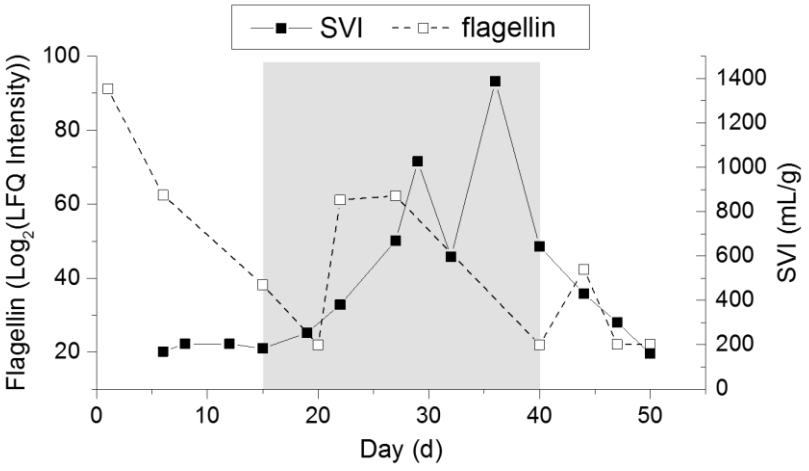

Figure 5-39: LFQ intensity of flagellin in EPS sample of P4. Grey area marks the period of phosphorous limitation

4. Enzyme Related to P-Starvation

The overexpression of alkaline phosphatase enzyme is anticipated during the P-limiting period and it has been described in many organisms as a response to P-starvation [133,142,143]. However, the enzyme was not detected in this study. Alkaline phosphatase functions by cleaving the phosphate moiety of organic molecules so that the phosphate becomes available to the cell. It is formed only when the concentration of inorganic phosphate (P_i) becomes limiting and inhibited when P_i is in excess. That way, P_i is preferably used than the organic phosphate at high P_i concentration. In *E. coli*, complete inhibition of alkaline phosphatase was seen at 100 mM P_i/L [142]. Alkaline phosphatases are believed to be located at the cell surface, although the exact location is unclear. They are said to be either membrane-bound by occupying the periplasmic space between the inner and the outer membrane layers or extracellularly secreted to the cell surface or into the medium [144]. Periplasmic alkaline phosphatase should be able to be harvested through sonication, as so the tightly-bound extracellular alkaline phosphatase through EPS extraction. It is only when the enzyme is fully soluble in the solution that it would be lost through the washing step prior to TP or EPS extraction.

Several hypotheses can be made as to why alkaline phosphatase was not found in this study despite alkaline phosphatase enzyme (EC: 3.1.3.1) was found in 132 distinct organisms in the database used. As activated sludge contains a variety of organisms hence most probably differently located alkaline phosphatases, some enzymes should be able to be extracted using either TP or EPS extraction method. It is therefore suspected that the enzyme was lost as a result of extraction conditions which were probably suboptimal for the activity of such enzyme. As mentioned above, alkaline phosphatase is inhibited in the excess of P_i. The content of inorganic phosphate P_i in the PBS solution (6 mM/L) used for TP and EPS extraction may have been enough to inhibit the enzyme. Another possible explanation is that the enzyme was inactivated by the low pH of TCA solution used for protein concentration step, although the TCA solution was washed out with acetone and the protein was neutralised with Na_2CO_3 solution afterwards, and the acid inactivation of the enzyme is said to be reversible [145]. If the enzymes were inactivated post-translationally, it cannot be identified by LC-MS/MS, as identification is only possible for amino acid or protein sequences that are already contained in the database.

5.2.7 Phase 5: Nitrogen Limiting Condition

The nitrogen limiting condition in phase 5 (P5) was introduced in three stages. The nitrogen loading was gradually reduced by the removal of ammonium chloride followed by peptone from the synthetic wastewater in the first and the second stage, and lastly the removal of EDTA from the trace metal solution in the third stage (Figure 5-40 (A)).

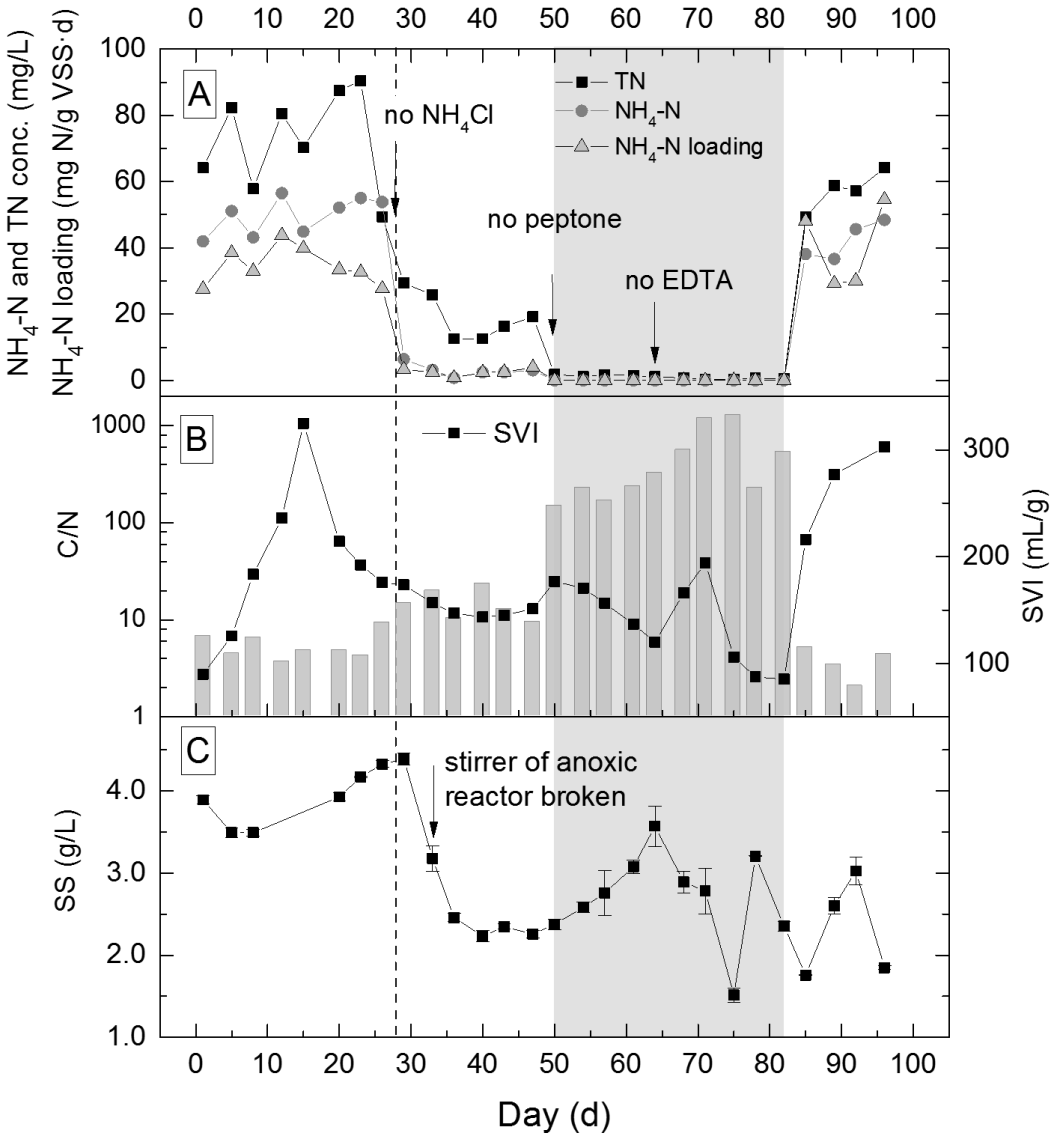

Figure 5-40: (A)Profiles of influent ammonium loading, TN and NH_4-N concentration, (B) C/N ratio and SVI, and (C) SS concentration of P5. Dashed line indicates values measured after NH_4Cl removal. Grey area marks the period of nitrogen limitation, after which synthetic wastewater with complete composition was provided

P5 was operated for a total of 96 days. Under normal condition, the wastewater had a COD:TN (total nitrogen) ratio of about 100:18 (C/N = 5.5). This ratio, although higher than the 100:5 ratio (C/N = 20) recommended by the literature, was in the normal range of WWTP Kaßlerfeld, where the seed sludge originated. The nitrogen limiting condition was introduced by removing ammonium

chloride from the synthetic wastewater from day 27. At this condition, the wastewater had a C/N of 14 (Figure 5-40 (B)). Therefore the system was considered nitrogen limited only after peptone was removed from the influent on day 50, where the average the C/N value was higher than 20. In this case, the C/N values were >100. As some bacteria are able to use EDTA as nitrogen source [146], EDTA was excluded from the trace metal solution from day 64 until day 82 to investigate the response of the system when it was completely devoid of nitrogen source.

On day 33, due to broken stirrer in the anoxic reactor, the sludge at the bottom of the reactor had to be removed as it showed no respiration activity as a result of prolonged anoxic condition. This caused the decrease of SS concentration from 4.4 to 3.2 g/L shown in Figure 5-40 (C). The SVI value was unaffected by this event and stayed <200 mg/L showing that the settleability was not affected by the sudden changes in SS concentration (Figure 5-40 (B)). As the wastewater loading was adjusted to the new SS concentration so that it resembled the value before the sludge loss, any following changes in the measured parameters in this period are hereby assumed to be caused only by NH_4Cl removal.

The steady SVI value after NH_4Cl removal showed that the sludge settling property was unaffected by the decrease in nitrogen loading (Figure 5-40 (B)). The biomass did not show a significant reduction in growth when peptone was removed from the influent composition, as the SS concentration continued to increase (Figure 5-40 (C)). The increase of SS concentration positively affected sludge settleability, as shown by the reduction in SVI values. However, the sludge properties might still have been negatively affected by the nitrogen limitation as the effluent was turbid and contained a high amount of small sludge flocs despite good settling. After EDTA was excluded from the wastewater composition, SS concentration started to decrease, thereby increasing the SVI values. After day 71, 7 days after the removal of EDTA, SS concentrations fluctuated. This was not caused by sludge loss to the effluent as no sludge was seen in the effluent tank. Wild denitrification could also be ruled out be since the NO_3-N values of the effluent were constantly below 0.1 g/L. Instead, after the removal of EDTA, recurrent sludge bulking events were observed in the clarifier, although the SVI showing improvement during measurement. As the sludge could not be efficiently recirculated, highly concentrated mixed liquor could be seen in the clarifier. This caused the fluctuation in the SS value of the anoxic and the aerobic reactor, where the sludge sample for SS measurement was taken. SVI values increased after normal effluent was supplied to the plant, probably caused by the sudden increase in nitrogen loading. Sludge bulking continued to be observed until the end of P5.

Regarding the removal performance, the sludge showed a slight decrease in COD and NH_4-N removal performances after NH_4Cl was removed from the wastewater, although both values were still higher than 90% (Figure 5-41 (A and B)). Total nitrogen removal was also affected, showing a decrease from 55 to 31% removal. All three removal values recovered after one or two

measurements. TP removal was severely affected and exhibited a continuous decrease in removal performance from 84 to 41% (Figure 5-41 (C)). COD and TN removal did not show significant changes when peptone was removed in addition to the NH_4Cl. TP removal, on the other hand, dropped to values <10%. When EDTA was eliminated from the influent, TN removal plunged to negative values, indicating that cell lysis might have taken place (Figure 5-41 (C)). The removal performance however recovered within two measurements (after about a week). Interestingly, COD removal was not significantly affected by this further elimination of nitrogen while TP removal was unchanged from before, staying below 10%. When the nitrogen limitation was lifted, COD and TN removal values were negatively affected by the sudden increase in nitrogen loading. These values, however, recovered afterwards. As opposed to COD and TN, TP removal showed an increase in value after the influent was back to the normal composition. The phosphorous removal, however, decreased again. Unexpectedly, ammonium removal seemed to not be affected by the changes in loading before and after the nitrogen limiting period.

The steady ammonium removal values were not reflected by the autotrophic SOUR. The autotrophic SOUR value already started to decrease before NH_4Cl was removed and its value continued to drop afterwards (Figure 5-41 (D)). The percentage of autotrophic activity was reduced from between 24−37% to merely 4−15 % of the total activity after NH_4Cl removal. Hence the development of total SOUR reflected that of heterotrophic SOUR (Figure 5-41 (E)). Heterotrophic SOUR value fluctuated prior to NH_4Cl removal and did not show any significant changes after the initial reduction in ammonium loading (Figure 5-41 (E)). Both autotrophic and heterotrophic bacteria exhibited a significant decrease in activity after peptone was removed from the influent composition and this downward trend continued after EDTA removal. After nitrogen was resupplied, heterotrophic activity recovered but the autotrophic activity remained low.

It is possible that the discrepancy between the ammonium removal and the autotrophic activity, especially after the nitrogen source was replenished, was due to increased uptake of nitrogen by the microbes to compensate for the nitrogen starvation period. As a result, ammonium continued to be consumed and removed from the wastewater. On the other hand, ammonium oxidising bacteria (AOB) are known to take longer to recover from any disturbances due to their slower growth rate [114], hence the observed low autotrophic activity even after the change from nitrogen-limited to nitrogen-replete condition.

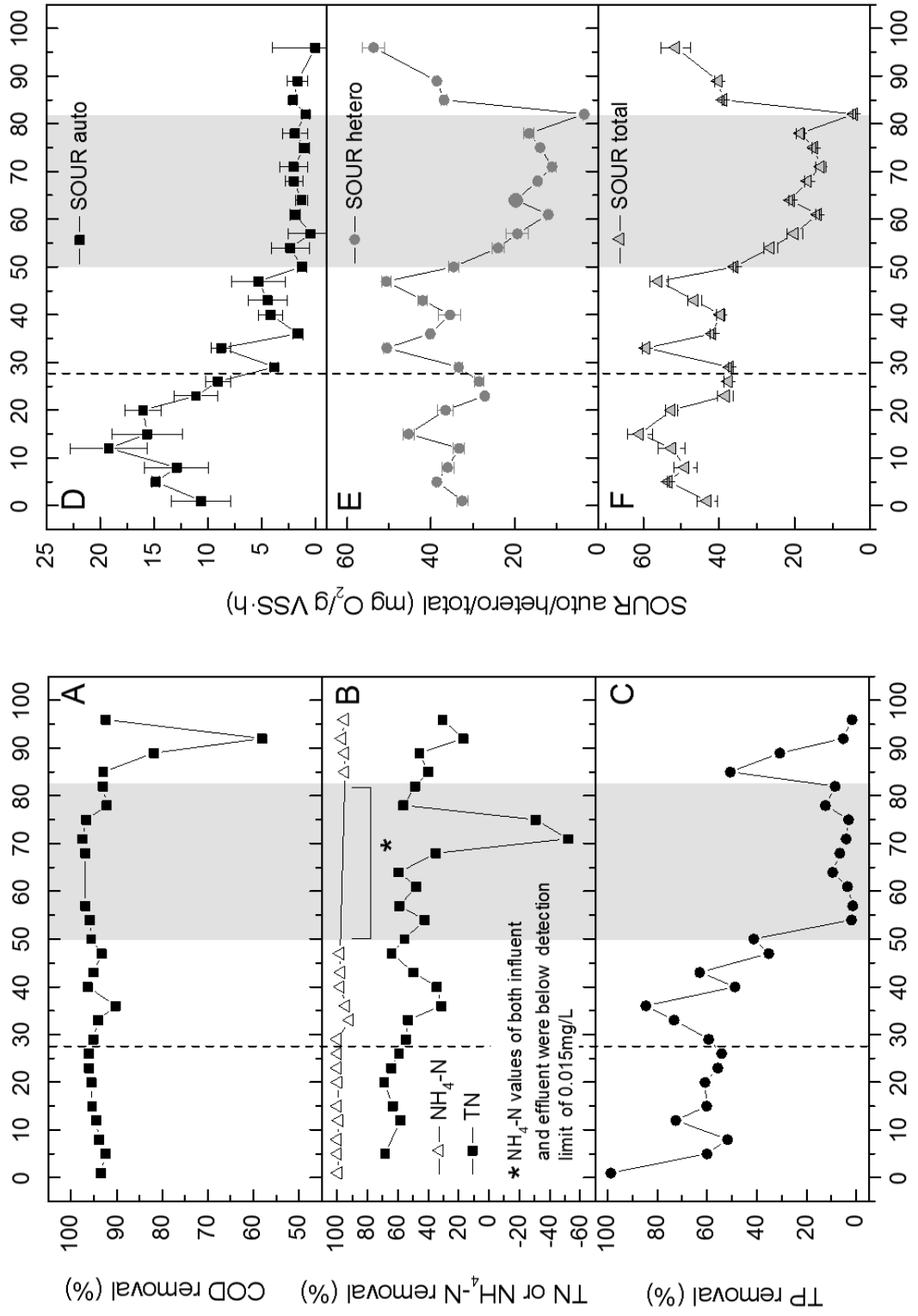

Figure 5-41: Removal performances (left) and respirometric activity (right) of P5. Dashed line indicates values measured after NH_4Cl removal. Grey area marks the period of nitrogen limitation

Other than the sludge bulking problem in the clarifier, neither foaming nor biofilm formation was observed during the operation of P5. As for the EPS content, the value of EPS protein content showed similar changes to P4 under nutrient limitation. EPS protein content, measured by both Lowry and Bradford, dropped with decreasing nitrogen loading. A significant drop in value was seen during nitrogen limiting period. The protein content increased again once the nitrogen limiting period ended.

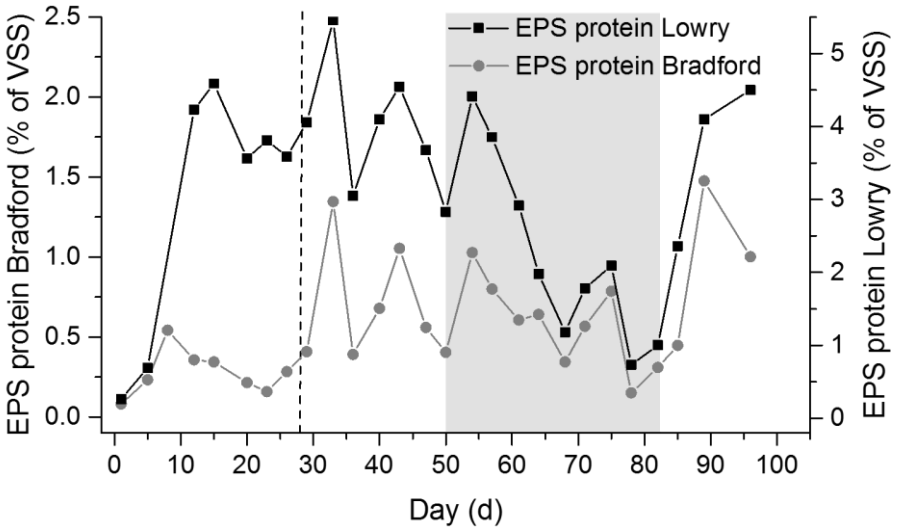

Figure 5-42: EPS protein content of P5. Dashed line indicates values measured after NH_4Cl removal. Grey area marks the period of nitrogen limitation

5.2.8 Proteomics of Phase 5

To gain insight into the bacterial response towards N-limitation, protein expression in total protein (TP) and EPS samples of P5 were analysed using quantitative (LFQ) proteomics.

5.2.8.1 Protein Identification

Figure 5-43 and Figure 5-44 show the number of protein groups found in TP and EPS samples of P5 respectively. A total of 1,320 protein groups were identified in these samples. They were assigned taxonomically and 77.4% of them (1022 protein groups) could be annotated for their function using KEGG annotation tool, GhostKOALA [98]. In terms of the genera of the organisms, the annotation results of P5 were similar to those of P4. Proteins groups related to the genus *Candidatus* Accumulibacter were found in the highest amount followed by the genera *Nitrosospira*, *Dechloromonas*, *Nitrosomonas,* and *Azospira* (the order of which varied slightly according to samples) in both TP and EPS samples.

Also similar to the results of P4, protein groups responsible for carbohydrate metabolism were found in the highest amount in all EPS samples and most TP samples, followed by protein groups responsible for genetic information processing, energy metabolism and amino acid metabolism (Figure 5-45).

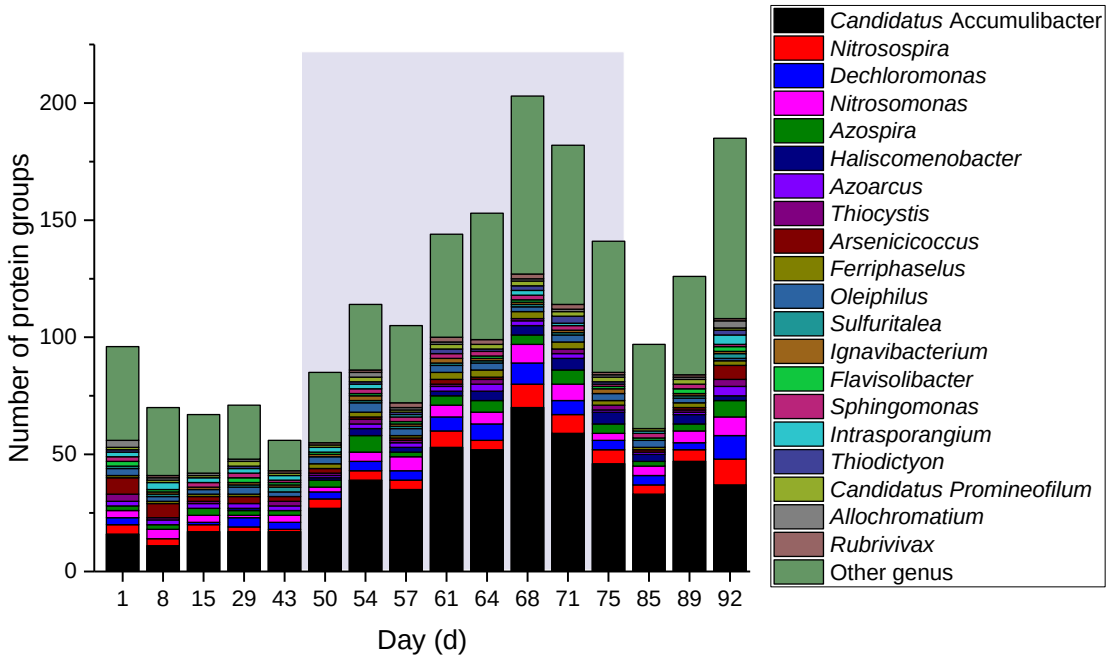

Figure 5-43: Number of protein groups in total protein samples of P5, classified according to the genera. Only the 20 genera with the highest protein groups are differentially coloured. Blue-shaded area marks the period of nitrogen limitation

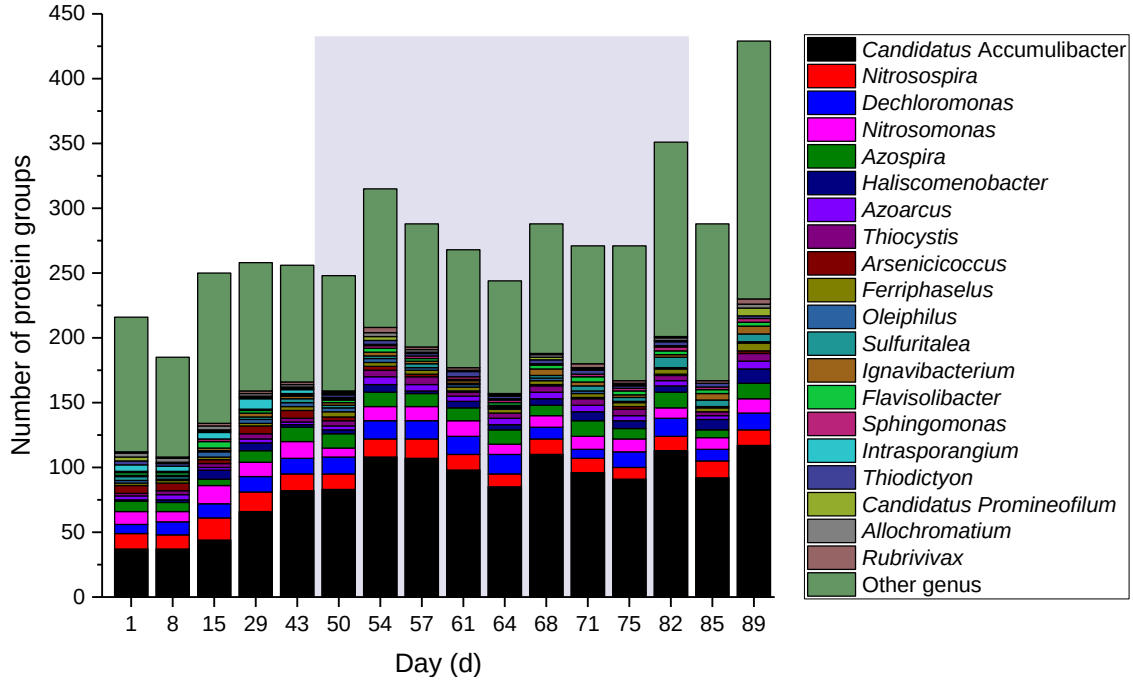

Figure 5-44: Number of protein groups in EPS samples of P5, classified according to the genera. Only the 20 genera with the highest protein groups are differentially coloured. Blue-shaded area marks the period of nitrogen limitation

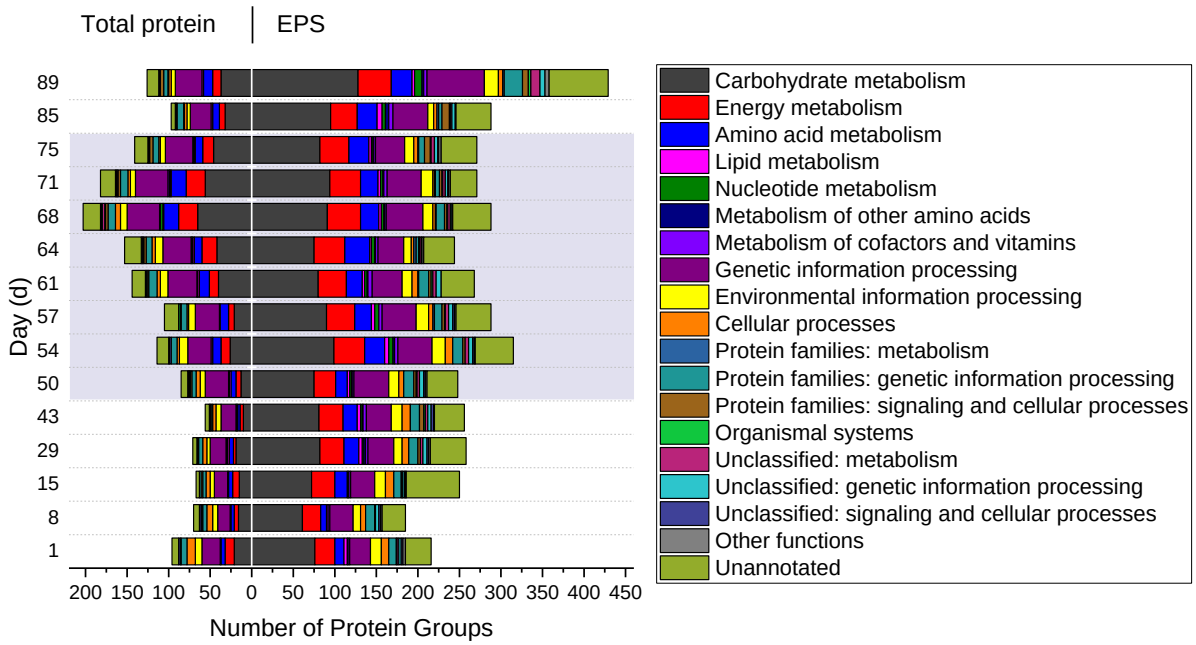

Figure 5-45: Number of protein groups in total protein and EPS samples of P5, classified according to functional categories. Blue-shaded area marks the period of nitrogen limitation

The number of protein groups found in TP samples was less than the EPS samples. This was discussed in previously Section 5.2.6.1. Between 56−203 protein groups were identified in TP samples and the number of protein groups identified in the EPS samples was between 185−429 distinct groups. TP samples showed a gradual increase in the number protein groups in all functional categories during N-limiting period until day 68, after which the numbers decreased again, probably due to adaptation (Figure 5-45). This result is in contrast to the observation seen during P-limiting period, during which the number of protein groups identified decreased, showing that the activated sludge system was differently affected by N-limitation. The total number of protein groups in the EPS samples were on average slightly higher during N-limiting period than before the limitation but the values remained almost constant throughout this period, unlike the clear increase in the number of protein groups observed in the TP samples. The functional categories that had seen an increase in the number of proteins mostly belonged to the categories of carbohydrate metabolism, energy metabolism, genetic information processing, and amino acid metabolism. Other functions such as lipid metabolism did not seem to be much affected by N-starvation while proteins responsible for cellular processes were found in lower number during this period. The high number of proteins assigned to the carbohydrate metabolism especially in the EPS samples illustrates the importance of carbohydrate metabolism in EPS, as carbohydrate is one of its major components.

5.2.8.2 Protein Quantification

Figure 5-46 and Figure 5-47 show the 10 most abundantly expressed enzymes in TP and EPS samples of P5 respectively. Consistent with the result of P4, GroEL was also the most abundant protein in most of the TP and EPS samples of P5. When investigating the role of GroEL in *E. coli* proteome, Kerner et al. [147] found that GroEL promoted the folding of about 250 different proteins. 85 proteins were obligate GroEL-dependant to achieve native state under normal growth conditions, including 13 essential proteins, proving that GroEL is essential for cell viability. Other proteins that were highly expressed were also similar to P4, which included F-type ATPases, enzymes related to carbohydrate metabolism (acetyl-CoA and propionyl-CoA synthetase, Enolase), elongation factor Tu, and antioxidant enzymes (alkyl hydroperoxide reductase in TP and isocitrate dehydrogenase in EPS). What differed this time was that the samples also showed high expression of glutamine synthetase (GS), an important enzyme in nitrogen metabolism for the synthesis of glutamine [148], which will be discussed in the following section.

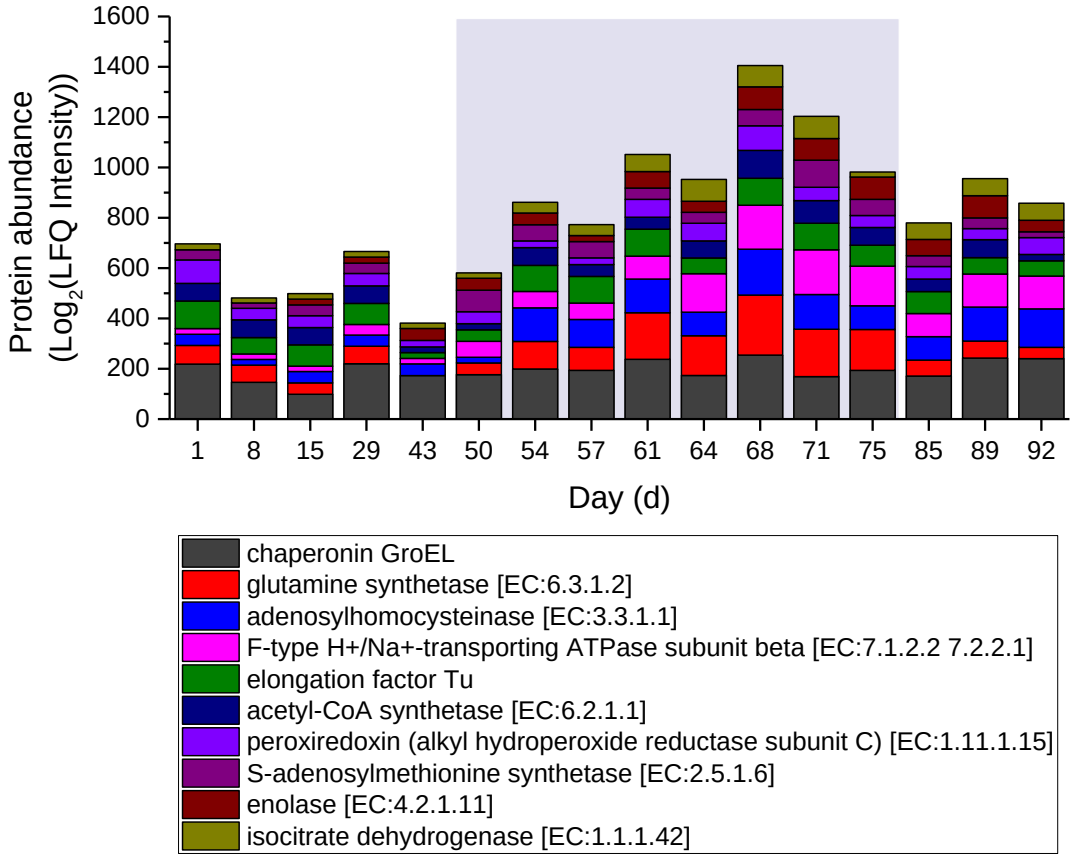

Figure 5-46: Log2-LFQ intensity of the 10 most abundant proteins in total protein samples of P5. Blue-shaded area marks the period of nitrogen limitation

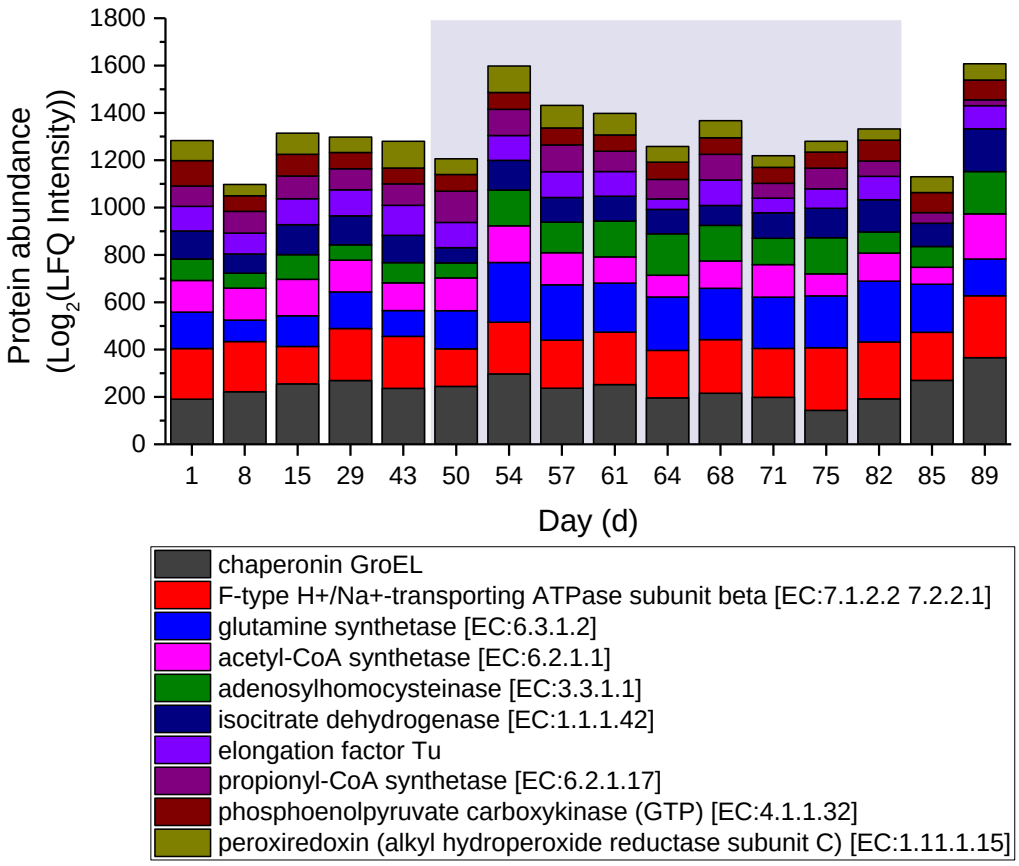

Figure 5-47: Log2-LFQ intensity of the 10 most abundant enzymes in EPS samples of P5. Blue-shaded area marks the period of nitrogen limitation

1. Stress-related Proteins

Antioxidant Enzymes

The differential expressions of four antioxidant enzymes isocitrate dehydrogenase 2 (IDH2), catalase, alkyl hydroperoxide reductase (Ahp) and superoxide dismutase (SOD) are shown in Figure 5-48. It can be seen that these enzymes were overexpressed during the period of N-limitation in the TP samples (Figure 5-48 (A) and (C)). The expressions of isocitrate dehydrogenase 2 and Ahp were increased considerably, while catalase and SOD were almost exclusively expressed during N-deficiency. Isocitrate dehydrogenases (IDH1 and IDH2) catalyse the decarboxylation of isocitrate into alpha-ketoglutarate. IDH1 is NAD+-dependent while IDH2 is NADP+-dependent [149]. The antioxidant role of the latter has been described in the literature [150,151]. It defends the cell by producing NADPH for the reduction of oxidised glutathione, a reaction that is catalysed by glutathione reductase [150]. The product, reduced glutathione, is then utilised by glutathione oxidase to break down H_2O_2 [25]. As opposed to the TP samples, the changes in expression of the different antioxidant enzymes in the EPS samples did not seem to be related to the N-deficiency.

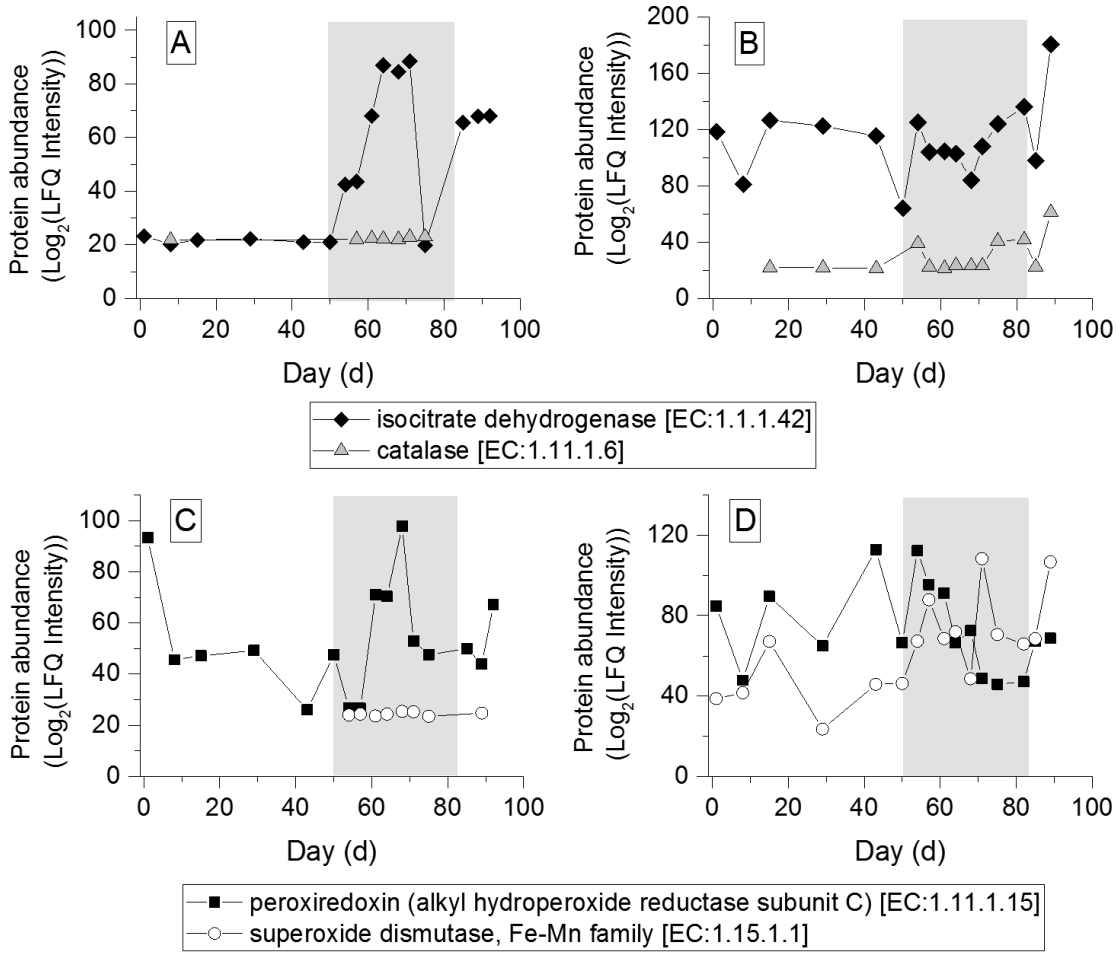

Figure 5-48: Upper diagram: Log2-LFQ intensity of isocitrate dehydrogenase and catalase enzymes in TP (A) and EPS samples (B) of P5. Lower diagram: Log2-LFQ intensity of Ahp and superoxide dismutase of TP (C) and EPS samples (D) of P5.

DNA-binding Protein from Starved Cells

DNA-binding protein from starved cells (Dps) was identified in 4 samples of the EPS at the beginning of the N-starvation period, showing that the cells activated protective mechanism against potential damage caused by N-deficiency. Although Dps is primarily a cytoplasmic protein, its presence in the outer membrane has also been reported [152]. This enzyme protects the cell from multiple stressors such as oxidative stress and starvation in two ways: (1) Dps binds to the DNA thus producing Dps-DNA crystals whose function is to shield the DNA from physical damage and (2) through its ferrooxidase activity, where it utilises H_2O_2 to oxidise Fe(II) into Fe(III), thereby significantly reducing the formation of highly reactive hydroxyl radicals, which would be produced if H_2O_2 reacts with Fe(II) in a strictly chemical manner (Fenton reaction) without enzyme catalysis [153,154]. Bacteria deficient in the Dps was proven to have a significantly lower survival rate when subjected to different kinds of stressors [153].

2. Enzymes Related to Nitrification Activity

Consistent with the proteomics finding of P1, the lowest autotrophic respirometric activity was measured when the enzyme hydroxylamine dehydrogenase (HAO) was of lowest abundance (Figure 5-49 (right)). The trend in the changes of autotrophic SOUR was seen more similar to the combined intensity of both TP and EPS (Figure 5-49 (right)) rather than the intensity of just TP or EPS samples (Figure 5-49 (left)). Wilhelm et al. [155] reported more than 70% decrease in hydroxylamine oxidation rate after 28 d of ammonia starvation. In in vitro investigations using SDS-PAGE and Western blot, they demonstrated that the HAO activity and protein-level were stable and not significantly affected by ammonia starvation up to 223 d and concluded that the decrease in hydroxylamine oxidation rate might be attributed to cellular damage rather than the decrease in HAO-protein level or its activity. This study provided a rather mixed result. Upon closer investigation, the abundance of HAO in the EPS samples was contributed by two different organisms, uncultured *Nitrosomonas* sp. and *Nitrosomonas* sp. strain Is79A3. The abundance of HAO of the *Nitrosomonas* sp. strain Is79A3 indicated that HAO was stable during a prolonged period of N-starvation up to 32 d, as HAO was continuously measured during this period, while the HAO of uncultured *Nitrosomonas* sp. could only be quantified prior to starvation period. In any case, the HAO-level was affected by the starvation period. HAO abundance of *Nitrosomonas* sp. strain Is79A3 of the EPS demonstrated a continuous drop in intensity, with a total of 4.8-fold decrease from the beginning to the end of the starvation period. Assuming that quantification of HAO from uncultured *Nitrosomonas* sp. was limited by low protein abundance, this further proves that the HAO level dropped as a result of N-deficiency. From the expression of HAO, it can be concluded that the decrease in nitrification activity during N-starvation was also a result of lower HAO-level and not only due to the damage of cellular structure as proposed by Wilhelm et al. [155]. This result shows the advantage of using quantitative proteomics to analyse differential protein expression. Relative quantification can be done more accurately with the help of LFQ, which is based on peptide ion signal intensity compared to the gel-based methods like SDS-PAGE and Western blot. AmoA and AmoB were not found in TP samples and identified only in one sample each in EPS samples, probably due to low abundance or post-translational modification, as discussed in Section 5.2.6.3.

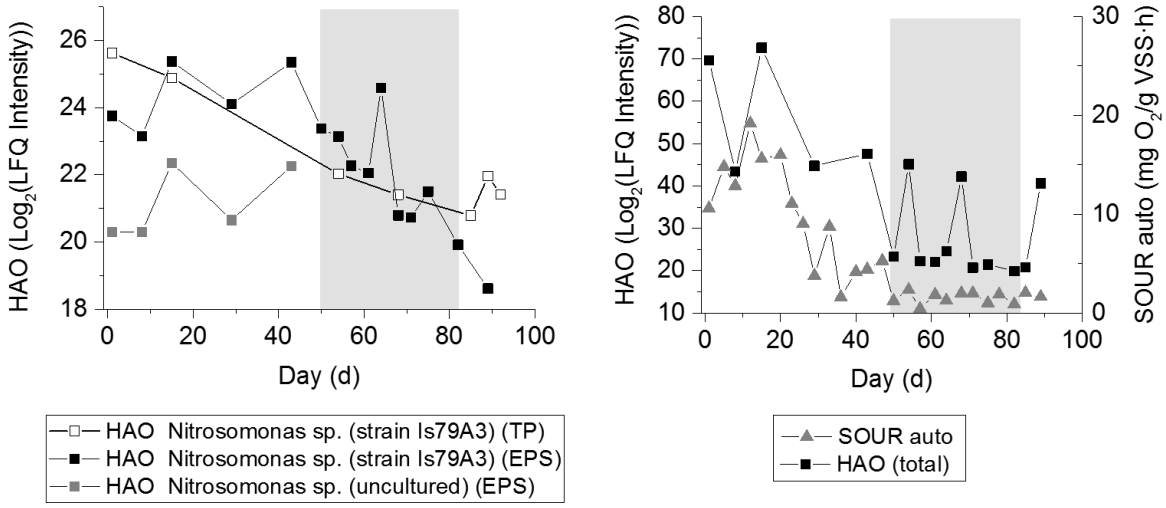

Figure 5-49: Relative abundance of HAO enzyme in TP and EPS samples (left) and total relative abundance compared to autotrophic SOUR (right) of P5

3. Enzymes Associated to Nitrogen Utilisation

The samples were also investigated for enzymes that were typically found during nitrogen starvation. Under N-replete condition, ammonium is assimilated by glutamate dehydrogenase (GDH) to produce glutamate. In N-starved condition, the metabolism is shifted to the glutamine synthetase (GS)/glutamate synthase (GO-GAT) system as the affinity of GDH for ammonium is insufficient to assimilate ammonium under this condition [148]. The assimilation of ammonium through GS/GO-GAT system occurs in two steps. In the first step, GS utilises ammonium and glutamate to produce glutamine. In the following step, GO-GAT synthesizes 2 moles of glutamate via 2-oxoglutarate and the glutamine produced by GS (reviewed in [156]). As can be seen in Figure 5-50, the enzymes GS and GO-GAT were overexpressed during N-limiting period. The changes in intensity were very pronounced in the EPS samples, with an average intensity of 95-fold, 41-fold and 63-fold higher during limitation period than in normal condition for GS, GO-GAT small chain and GO-GAT large chain respectively. The increase in the intensity of GS was in TP sample happened gradually, with the maximum intensity measured after 20 days of nitrogen starvation. GO-GAT large chain was found exclusively during the limiting period in the TP sample at the time when the concentration of GS was the highest, while GO-GAT small chain was found in 6 TP samples, 4 of which in the limiting period. Urease was only found in the EPS samples during the starvation period and only after GS was formed. This observation is in accordance with the theory that the formation of urease is regulated by GS and urease expression is strongly repressed in the presence of ammonium [157], also through the action of GS [158]. The sole function of urease is to supply the cell with ammonia. The expression of urease shows that to counter the ammonia depletion, the system reacted by forming ammonia from urea. Accordingly, urea substrate transport protein was also measured during this period (not shown in the diagram).

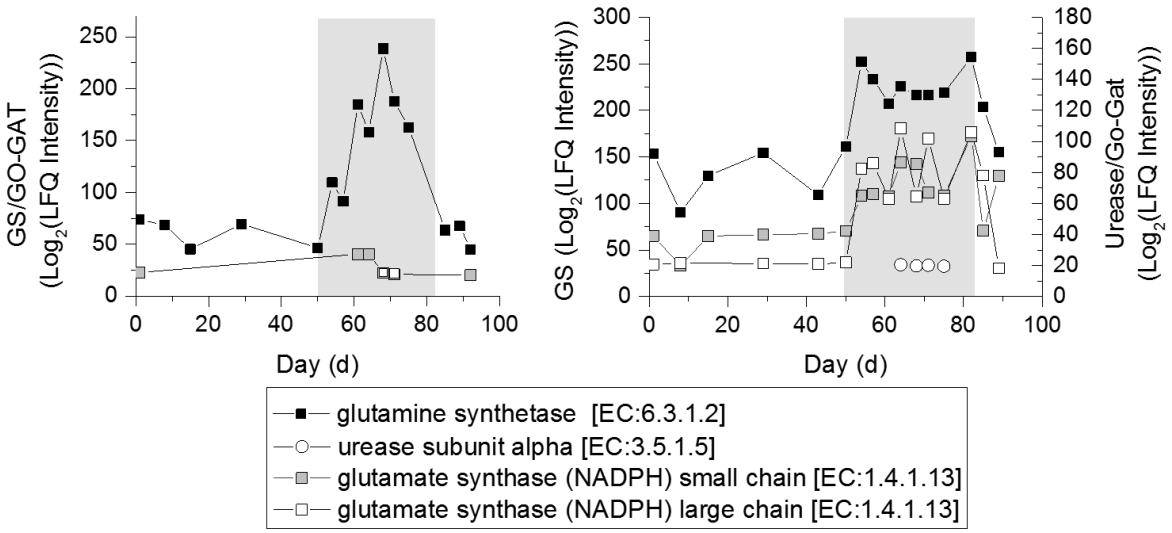

Figure 5-50: Changes in the abundance of GS, GO-GAT and urease in TP (left) and EPS samples (right) of P5. Grey area marks the period of nitrogen limitation

Other than the urease activity, the other survival strategy of the system was through the formation of ammonia from nitrogen gas, as evidenced by the expression of nitrogenase enzymes, namely the nitrogenase molybdenum-iron protein subunit alpha and beta, as well as nitrogenase iron protein, during the N-limiting period in both TP and EPS samples.

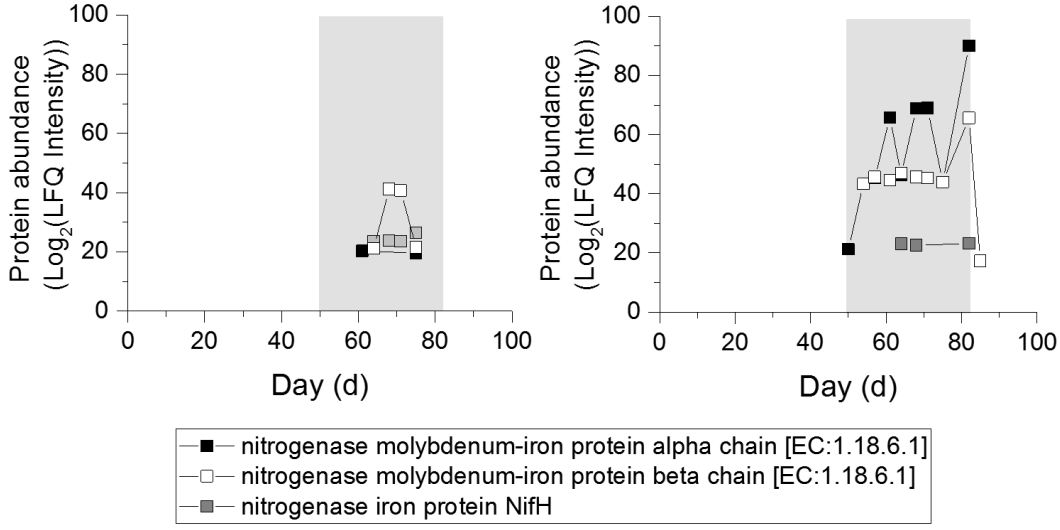

Figure 5-51: Abundance of the enzymes nitrogenases in TP (left) and EPS samples (right) of P5. Grey area marks the period of nitrogen limitation

4. Enzyme Related to Bacterial Adhesion and Bioflocculation

As opposed to the result of P4, the expression of flagellin seemed to have affected sludge settleability in P5 (Figure 5-52). Prior to nitrogen limiting period, the abundance of flagellin was observed to have an inverse relationship with the SVI. Low abundance of flagellin was measured at high SVI and vice versa. The flagella of the bacteria (which contains thousands of flagellin proteins) were demonstrated to promote bacterial adhesion by reaching the gaps and narrow spaces between structures that cannot be accessed by the cells (reviewed in [141]). It is possible that the low abundance of flagellin resulted in weaker or looser flocs with lower settleability. It can be seen that the abundance of flagellin protein experienced a continuous decrease during the N-limiting period, probably affected by the lack of nitrogen. The low flagellin abundance might explain the observation of turbidity and recurrent sludge bulking events during this period, as discussed in Section 5.2.7, despite good settleability displayed by the SVI values. The intensity of flagellin was not quantifiable after N-limiting period, probably due to low even lower abundance than before. During this time, sludge settling surged to from 85 mL/g to around 300 mL/g indicating poorer settleability. From these results, it is speculated that flagellin protein plays a significant role in bacterial adhesion and flocculation thus also sludge settling.

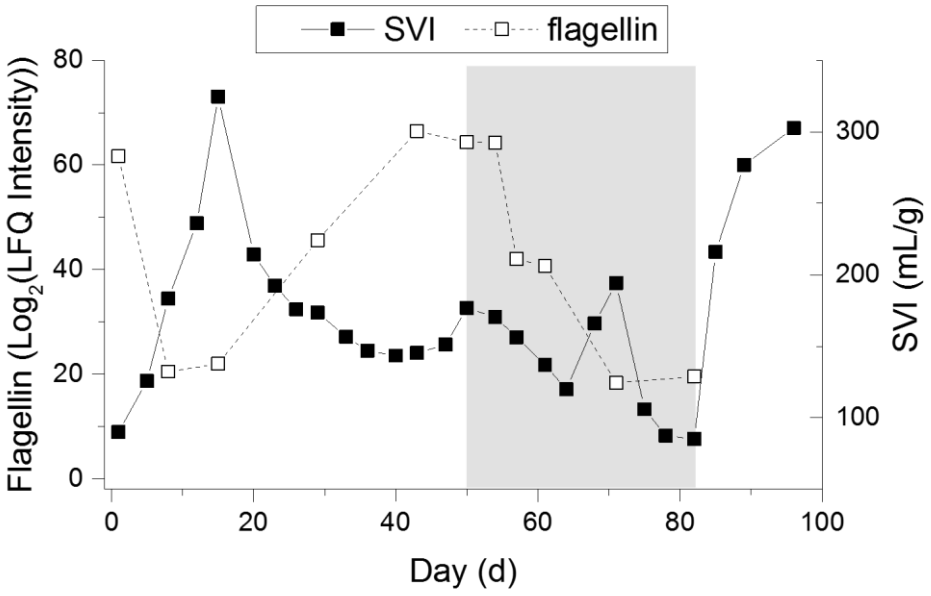

Figure 5-52: LFQ intensity of flagellin in EPS sample of P5. Grey area marks the period of nitrogen limitation

5.3 Overall Discussion

A good biomass parameter should show a strong correlation with the activity regardless of the state of the sludge. The analyses of activated sludge from industrial and lab-scale plants in this study point to the conclusion that VSS is more reliable than total protein concentration in estimating active biomass. One of the main functions of proteins that contributes to the activity of bacteria is their enzymatic role which catalyses biochemical reactions. The attributes of an enzyme are its specificity and selectivity [159]. Furthermore, enzyme excretion is highly regulated depending on the type of biochemical reactions. A high concentration of enzymes does not necessarily mean high activity. In some cases, an enzyme is upregulated during low activity to induce a biochemical reaction or restore it to a normal level and repressed during high activity so a correlation between enzymes and activity is not always possible. The probable explanation as to why total protein quantification failed to reliably quantify active biomass, at least when the activity is represented by the OUR, would be that the total protein quantification does not only measure a cocktail of different enzymes, including those unrelated to the aerobic respiration but also non-enzyme proteins. This has been proven by the proteomics analyses. However, there are a few specific cases that would probably benefit from using total protein concentration as biomass quantification method, for example plants treating wastewater containing a high concentration of organic substances such as pulp mill wastewater or wastewater from the food industry with a high concentration of lipid and other organics as these substances will result in overestimation of the VSS. In normal cases, VSS was proven to be satisfactory in estimating active biomass, which is a relief for the plant operators as compared to protein extraction and quantification, VSS measurement is a standardized method that is cheap, quick and can be quantified relatively easily without complicated instruments.

The reports on the influence of EPS on sludge settleability and dewaterability have been contradictory. This was also the conclusion of the EPS investigation of this study. A good review of this matter is provided by Liu and Fang [7]. Most studies have tried to relate sludge properties to the protein and carbohydrate contents of the EPS. Some studies compared sludge settling and/or dewatering properties directly to the total EPS, which is the sum of its protein and carbohydrate contents [4]. In some others [4,160] and also in this study, the sludge characteristics were compared to the protein and carbohydrate contents separately. There are also studies that resort to utilising carbohydrate to protein ratio [161]. Several publications differentiated not only between protein and carbohydrate contents but also sub-specify the EPS between soluble EPS, loosely-bound and tightly-bound EPS [104]. The various ways to estimate the roles of EPS on sludge properties based on the concentration of its components and the conflicting results published by the researchers proved that this method is lacking and the EPS properties as well as its roles cannot be generalised.

The results of this study proved that quantitative proteomics using LFQ-MS is beneficial in gaining further understanding of the activated sludge process under different conditions. Looking at the functions of the proteins identified in the EPS samples, it is evident that EPS has the same importance as the whole-cell protein, if not more in regard to maintaining the stability of activated sludge process. EPS was found to contain chaperones, transport proteins, antioxidant enzymes, and other proteins that are essential for cell integrity under normal conditions, as well as under environmental stress. It is no wonder that in the last years, a lot of metaproteomics researches of activated sludge have been focussing on the proteins of the EPS rather than the whole-cell proteins [125,140]. The response of the activated sludge system towards nitrogen limitation was clearer than its response towards phosphorous starvation. Various antioxidant enzymes and DNA-binding protein from starved cells (Dps) were upregulated during N-limiting period signifying that nitrogen depletion might potentially cause oxidative stress and DNA-damage and the system reacted to prevent them from happening. The system also showed clear strategies towards mitigating the effects the N-deficiency by increasing nitrogen uptake through GS/GO-GAT enzymes and the expressions of urease and nitrogenases. The response of the system towards P-limitation was less obvious. The expression of stress-related enzymes such as several heat shock proteins and antioxidant enzymes were elevated during this period but how the system regulated phosphorous uptake and metabolism was unclear.

It is important to also discuss the challenges encountered in using proteomics in activated sludge samples. The main challenge in proteomics analysis of environmental samples like activated sludge compared to pure culture samples is the limited availability of sequence information for protein identification. The microorganisms living in the activated sludge differ from plant to plant and therefore the sludge proteomes are highly variable. In order to increase the identification rates for protein groups, it is essential to define prior to the label-free MS a suitable sludge proteomics database. The use of general databases like NCBI without taxonomic restriction is not productive, as the sheer number of unrelated sequences will elevate the score thresholds for a particular protein group and at the same time will massively increase the computational time. Creating a dedicated database is time-consuming and highly costly, which is not always possible, particularly when measuring only a low amount of samples. In such a case, the choice is limited to using a database published from another plant, which sometimes does not necessarily represent the studied system, or to handpick the sequences belonging to the microorganisms of interest from public databases and pool them together to create a new database for identification, with the risk of missing the organisms or proteins which could be significant to the treatment system. The database of WWTP Aalborg [96] was used as a compromise in this study. It contains a reasonable amount of amino acid sequences (297317 entries) including sequences from most organisms involved in conventional wastewater treatment. The identification is considered successful as the amount of proteins identified, especially in the EPS sample were mostly higher than reported in the literature. Still, it is suspected that identification was biased towards proteins from the EBPR

microbial community as proteins related to *Candidatus* Accumulibacter were found in the highest abundance in all samples analysed.

The various organisms and proteins in the samples also complicated the analysis and interpretation of the results. Firstly, there is no extraction method that works with all types of proteins in the activated sludge. In the case of this study, some of the proteins such as AMO and alkaline phosphatase are suspected to be more sensitive towards the extraction procedure used and were probably deactivated or modified in the process so that they could no longer be identified, or could only be identified in a few samples. Secondly, the different organisms in the system resulted in a huge amount of data. Due to this reason, protein abundance in this study was grouped into the types of proteins and not differentiated between organisms. By describing the protein changes as cumulative LFQ intensity of all organisms containing these proteins, the resulted differential expression may have been less accurate as different organisms deal with phosphorous and nitrogen limitation differently due to different tolerance and the variations between enzyme expressions and regulations.

6 Conclusions and Outlook

This present study analysed the total protein and the EPS in continuous flow activated sludge systems and it involved three main investigations: (1) the applicability of total protein quantification for estimation of active biomass, (2) determination of the roles of the EPS components in sludge settleability and dewaterability and (3) proteomics analysis of total protein and EPS to understand the changes in activated sludge under various conditions at the molecular level, taking examples of systems under nitrogen and phosphorous limitation. Activated sludge samples from three industrial WWTPs were analysed for 7−9 weeks and a lab-scale plant was operated for a total of 474 days for these purposes.

The major results of this study are as follows:

1. The comparison between the biomass parameters of total protein, SS and VSS with the respirometric activity points to the conclusion that VSS was the only reliable parameter in estimating active biomass. From the proteomics analyses, it was found that total protein contains a variety of proteins and enzymes, also those that was unrelated to the aerobic respiration, which is probably the reason why its concentration failed to correlate with the respirometric activity.

2. The results on the roles of protein and carbohydrate contents of the EPS on sludge settleability and dewaterability were contradictory between the industrial and lab-scale plant samples and the correlations, if any, were weak. The EPS properties were found to differ from plant to plant. Defining the roles of the EPS basing solely on the concentration of its components was concluded to be insufficient.

3. Quantitative proteomics using LFQ-MS was proven useful in retrieving information on the changes in activated sludge system under different conditions for further understanding of the treatment process. Comparison with the literature pointed out the advantage of relative quantification using this method compared to the gel-based methods of SDS-PAGE and western blot as its quantification was more accurate.

4. With the help of quantitative proteomics, there is now more appreciation towards the roles of the EPS on sludge stability and integrity. EPS was found to contain chaperones, transport proteins, antioxidant enzymes, and other important proteins.

5. Quantitative proteomics also allowed an insight into how the nitrification process was affected by different stress conditions such as pH fluctuations, and also nitrogen and phosphorous limitation. The enzyme HAO was observed to be affected by extreme pH

fluctuations and nitrogen starvation but not by phosphorous limitation. The lower autotrophic activity during P-limiting period was probably due to the damage of cellular structure instead of the underexpression of nitrification-related enzymes.

6. Ferritin is speculated to play a significant role in sludge adhesion and thus flocculation and settling. This is based on the comparison of the relative abundance of this protein with the SVI in the last phase of the study. High abundance of ferritin was measured at low SVI values and vice versa. Therefore, the result suggested that this protein promoted sludge settling.

7. Proteomics measurement using LFQ-MS was also able to provide an insight into the strategies adopted by the sludge under nitrogen and phosphorous limitation. While the response of the sludge towards phosphorous limitation was more in terms of general stress response i.e. overexpression of certain heat shock proteins and antioxidant enzymes, its response towards nitrogen limitation was more obvious. Other than the upregulation of various antioxidant enzymes and DNA-binding protein from starved cells (Dps), the system also showed clear strategies towards increasing nitrogen uptake through GS/GO-GAT system and the expressions of urease and nitrogenases.

It is believed that this is the first time that LFQ-MS is used to follow long-term changes in the expressions of various enzymes under nitrogen and phosphorous limitations in an activated sludge system or perhaps even in an environmental system. This study has allowed further understanding of the activated sludge process under these conditions based on the differential protein expression. It has also provided the procedure and strategies for applying proteomics without having a dedicated database. This study has also contributed to a successful extraction and purification procedure of EPS for LFQ-MS.

For future research, the extraction and purification method of total protein needs to be further optimised as only a relatively small amount of proteins were able to be identified and quantified in this study compared to the EPS samples. Optimisation also needs to be done to ensure the proteins of interest e.g. alkaline phosphatase are not modified during extraction and the following steps prior to LC-MS so that they can be identified. Based on the results of this study, protein identification was highly dependent on the database used. The use of the database from another treatment system may create identification bias to the organisms contained in the database. Recent progress in the field of metagenomics, especially the sequencing of DNA from non-culturable organisms may alleviate the current problem of database availability. Otherwise, future metaproteomics researchers are highly suggested to assemble a dedicated metagenomics/metaproteomics database to increase protein identification rate. Future researches should also contemplate combining database-driven identification with de novo sequencing as the

latter does not require a reference database and is able to measure also post-translationally modified proteins.

In conclusion, quantitative proteomics is a valuable method for an insight into the changes in activated sludge process. Considering the various information that can be retrieved using this method and parallel with the progress of metagenomics, the use of quantitative metaproteomics is expected to expand in activated sludge study and other fields of environmental study as well.

7 References

[1] Owusu-Apenten, R. K. (2002). *Food protein analysis. Quantitative effects on processing*. *Food science and technology series, volume 118*, Dekker, New York. ISBN 0824706846.

[2] Bitton, G. (2011). *Wastewater microbiology*. *4th edition*, John Wiley & Sons, Hoboken, N.J. ISBN 0470630337.

[3] Frølund, B., Palmgren, R., Keiding, K., and Nielsen, P. H. (1996). Extraction of extracellular polymers from activated sludge using a cation exchange resin, *Water Research*, *30* (8), pp. 1749–1758. DOI 10.1016/0043-1354(95)00323-1.

[4] Hoa, P. T., Nair, L., and Visvanathan, C. (2003). The effect of nutrients on extracellular polymeric substance production and its influence on sludge properties, *WATER SA -PRETORIA-*, *29* (4), pp. 437–442.

[5] Urbain, V., Block, J. C., and Manem, J. (1993). Bioflocculation in activated sludge: an analytic approach, *Water Research*, *27* (5), pp. 829–838. DOI 10.1016/0043-1354(93)90147-A.

[6] Yücesoy, E., Lüdemann, N., Lucas, H., Tan, J., and Denecke, M. (2012). Protein analysis as a measure of active biomass in activated sludge, *Water Science & Technology*, *65* (8), pp. 1483–1489.

[7] Liu, Y. and Fang, H. H. P. (2003). Influences of Extracellular Polymeric Substances (EPS) on Flocculation, Settling, and Dewatering of Activated Sludge, *Critical Reviews in Environmental Science and Technology*, *33* (3), pp. 237–273. DOI 10.1080/10643380390814479.

[8] Bugg, T. (2004). *Introduction to enzyme and coenzyme chemistry.* 2nd ed., Blackwell, Oxford. ISBN 1-4051-1452-5.

[9] Twyman, R. M. (2014). *Principles of proteomics.* 2nd ed., Garland Science, New York. ISBN 978-0-8153-4472-8.

[10] Wilmes, P. and Bond, P. L. (2004). The application of two-dimensional polyacrylamide gel electrophoresis and downstream analyses to a mixed community of prokaryotic microorganisms, *Environmental Microbiology*, *6* (9), pp. 911–920. DOI 10.1111/j.1462-2920.2004.00687.x.

[11] Denecke, M. (2006). Protein extraction from activated sludge, *Water Science & Technology*, *54* (1), pp. 175–182. DOI 10.2166/wst.2006.385.

[12] Gray, N. F. (2004). *Biology of wastewater treatment.* 2nd ed. *Series on enviromental science and management, volume 4*, Imperial College Press, London. ISBN 1860943284.

[13] Jenkins, D., Richard, M. G., and Daigger, G. T. (2004). *Manual on the causes and control of activated sludge bulking, foaming, and other solids separation problems.* 3rd ed., Lewis Publishers, Boca Raton. ISBN 1-84339-046-9.

[14] Nielsen, P. H., Saunders, A. M., Hansen, A. A., Larsen, P., and Nielsen, J. L. (2012). Microbial communities involved in enhanced biological phosphorus removal from wastewater—a model system in environmental biotechnology, *Current opinion in biotechnology*, *23* (3), pp. 452–459. DOI 10.1016/j.copbio.2011.11.027.

[15] von Sperling, M. (2007). *Activated sludge and aerobic biofilm reactors*. *Biological wastewater treatment series, volume 5*, IWA Publishing, London. ISBN 9781780402123.

[16] Mann, T., Berger, M., Kern, G., Lemke, J., and Klockner, D. et al. (2011). *Wastewater, 2. Aerobic Biological Treatment*. *Ullmann's Encyclopedia of Industrial Chemistry*, Wiley-VCH. ISBN 1435-6007.

[17] Gerardi, M. H. (2006). *Wastewater bacteria*. *Wastewater microbiology series*, Wiley-Interscience, Hoboken, N.J. ISBN 0471206911.

[18] Levinson, W. (2004). *Medical microbiology & immunology*. *Examination & board review.* 8th ed. *A Lange Medical Book*, McGraw-Hill, New York. ISBN 0-07-143199-3.

[19] Liu, S. (2013). *Bioprocess Engineering*, Elsevier, Amsterdam. ISBN 9780444595256.

[20] Seviour, R. J. and Nielsen, P. H. (2010). *Microbial ecology of activated sludge.* 2nd ed., IWA, London. ISBN 1843390329.

[21] Buetow, D. E. and Levedahl, B. H. (1962). Decline in the cellular content of RNA, protein and dry weight during the logarithmic growth of Euglena gracilis, *Journal of General Microbiology*, *28*, pp. 579–584. DOI 10.1099/00221287-28-4-579.

[22] Schlegel, H. G. and Zaborosch, C. (1992). *Allgemeine Mikrobiologie.* 7th ed. *Flexibles Taschenbuch Bio*, Thieme, Stuttgart. ISBN 3134446073.

[23] Wiesmann, U., Choi, I. S., and Dombrowski, E.-M. (2007). *Fundamentals of biological wastewater treatment*, Wiley-VCH, Weinheim. ISBN 9783527312191.

[24] Kuypers, M. M. M., Marchant, H. K., and Kartal, B. (2018). The microbial nitrogen-cycling network, *Nature Reviews Microbiology*, *16* (5), p. 263. DOI 10.1038/nrmicro.2018.9.

[25] Champe, P. C. and Harvey, R. A. (1994). *Biochemistry.* 2nd ed., J.B. Lippincott, Philadelphia. ISBN 0-397-51091-8.

[26] Foster, M.H., Klopping, P.H., Dailey, R.C., and Kirkpatrick, S.B. (2003). *Using respirometry to evaluate the impact of macronutrients application in pulp and paper aerated stabilization basins.* Proceedings 2003 Tappi Environmetal Conference.

[27] Henze, M., van Loosdrecht, M., Ekama, G., and Brdjanovic, D. (2008). *Biological wastewater treatment*. *Principles, modelling and design*, IWA, London. ISBN 9781843391883.

[28] Mara, D. and Horan, N. (2003). *Handbook of Water and Wastewater Microbiology*, Academic Press, London. ISBN 978-0-12-470100-7.

[29] Ensign, S. A., Hyman, M. R., and Arp, D. J. (1993). In vitro activation of ammonia monooxygenase from Nitrosomonas europaea by copper, *Journal of Bacteriology*, *175* (7), pp. 1971–1980.

[30] Dworkin, M., Falkow, S., Rosenberg, E., Schleifer, K.-H., and Stackebrandt, E. (2006). *Ecophysiology and Biochemistry*. *The Prokaryotes, Volume 2*, Springer, New York, NY. ISBN 978-0-387-30742-8.

[31] Caranto, J. D. and Lancaster, K. M. (2017). Nitric oxide is an obligate bacterial nitrification intermediate produced by hydroxylamine oxidoreductase, *Proceedings of the National Academy of Sciences*, *114* (31), pp. 8217–8222. DOI 10.1073/pnas.1704504114.

[32] Daims, H., Lebedeva, E. V., Pjevac, P., Han, P., and Herbold, C. et al. (2015). Complete nitrification by *Nitrospira* bacteria, *Nature*, *528* (7583), p. 504. DOI 10.1038/nature16461.

[33] von Sperling, M. (2007). *Basic principles of wastewater treatment*. *Biological wastewater treatment series, volume 2*, IWA Publishing, London. ISBN 1-68015-585-7.

[34] Wang, L. K. (2010). *Environmental biotechnology*. *Handbook of environmental engineering, volume 10*, Humana Press, New York. ISBN 978-1-58829-166-0.

[35] Liu, S. (2017). Chapter 11 - How Cells Grow in *Bioprocess engineering*, pp. 629–697. ISBN 978-0-444-63783-3.

[36] Monod, J. (1949). The Growth of Bacterial Cultures, *Annual Review of Microbiology*, *3* (1), pp. 371–394. DOI 10.1146/annurev.mi.03.100149.002103.

[37] Pal, P. (2017). *Industrial water treatment process technology*, Elsevier, Cambridge MA. ISBN 978-0-12-810391-3.

[38] Pal, P. (2017). Chapter 3 - Biological Treatment Technology in *Industrial water treatment process technology*, pp. 65–144. ISBN 978-0-12-810391-3.

[39] Doble, M. and Kruthiventi, A. K. (2005). *Biotreatment of industrial effluents*, Elsevier Butterworth-Heinemann, Amsterdam, Boston. ISBN 0-7506-7838-0.

[40] Ndon, U. J. (2007). Analysis and Kinetics of the Sequencing Batch Reactors, *Environmental Engineering Science*, *24* (4), pp. 505–514. DOI 10.1089/ees.2006.0096.

[41] Jørgensen, P. E., Eriksen, T., and Jensen, B. K. (1992). Estimation of viable biomass in wastewater and activated sludge by determination of ATP, oxygen utilization rate and FDA hydrolysis, *Water Research*, *26* (11), pp. 1495–1501. DOI 10.1016/0043-1354(92)90069-G.

[42] Lebaron, P., Servais, P., Agogue, H., Courties, C., and Joux, F. (2001). Does the high nucleic acid content of individual bacterial cells allow us to discriminate between active cells and inactive cells in aquatic systems?, *Applied and Environmental Microbiology*, *67* (4), pp. 1775–1782.

[43] Hagman, M. and La Cour Jansen, J. (2007). Oxygen uptake rate measurements for application at wastewater treatment plants, *VATTEN*, *63* (2), pp. 131–138.

[44] Spanjers, H. and Vanrolleghem, P. A. (1995). Respirometry as a tool for rapid characterization of wastewater and activated sludge, *Water Science & Technology*, *311995* (2), pp. 105–114.

[45] Möller, J. (2018). *Entwicklung eines Messsystems zur Ermittlung der Nitrifikationsaktivität*. *Forum Siedlungswasser-, Wasser- und Abfallwirtschaft*, Shaker Verlag, Aachen. ISBN 978-3-8440-5813-0.

[46] Inui, T., Tanaka, Y., Okayasu, Y., and Tanaka, H. (2002). Application of toxicity monitor using nitrifying bacteria biosensor to sewerage systems, *Water Science & Technology*, *45* (4-5), pp. 271–278.

[47] Walsh, G. (2014). *Proteins*. *Biochemistry and biotechnology.* 2nd. ed, Wiley-Blackwell, Chichester. ISBN 9780470669853.

[48] Liu, S. (2017). *Bioprocess engineering*. *Kinetics, sustainability, and reactor design*, Elsevier, Amsterdam, Boston. ISBN 978-0-444-63783-3.

[49] National Human Genome Research Institute. *Protein,* can be found under https://www.genome.gov/genetics-glossary/Protein. Accessed on 22/6/2019.

[50] Bitton, G. (2002). *Encyclopedia of environmental microbiology*, John Wiley & Sons, New York. ISBN 0471263397.

[51] MacGregor, B. J. (2002). Phylogenetically Based Methods in Microbial Ecology in *Encyclopedia of environmental microbiology*, . John Wiley & Sons, New York. ISBN 0471263397.

[52] Nannipieri, P. (2006). *Nucleic acids and proteins in soil*. *Soil biology, volume 8*, Springer, Berlin. ISBN 9783540294498.

[53] Sridhar, M. K. C. and Pillai, S. C. (1973). Proteins in Wastewater and Wastewater Sludges, *Water Pollution Control Federation*, *45* (7), pp. 1595–1600.

[54] Okafor, N. (2007). *Modern industrial microbiology and biotechnology*, Science Publishers, Enfield, NH. ISBN 978-1-57808-434-0.

[55] Wingender, J., Neu, T. R., and Flemming, H.-C. (1999). *Microbial extracellular polymeric substances*. *Characterization, structure, and function*, Springer, New York. ISBN 3540657207.

[56] Nielsen, P. H. (2002). Activated Sludge - The Floc in *Encyclopedia of environmental microbiology.* ISBN 0471263397.

[57] Sheng, G.-P., Yu, H.-Q., and Li, X.-Y. (2010). Extracellular polymeric substances (EPS) of microbial aggregates in biological wastewater treatment systems: A review, *Biotechnology Advances*, *28* (6), pp. 882–894.

[58] Frølund, B., Griebe, T., and Nielsen, P. H. (1995). Enzymatic activity in the activated-sludge floc matrix, *Applied Microbiology and Biotechnology*, *43* (4), pp. 755–761. DOI 10.1007/BF00164784.

[59] Lowry, O. H., Rosebrough, N. J., Farr, A. L., and Randall, R. J. (1951). Protein Measurement with the Folin Phenol Reagent, *Journal of Biochemical Chemistry*, *193* (1), pp. 265–275.

[60] Moore, J. C., DeVries, J. W., Lipp, M., Griffiths, J. C., and Abernethy, D. R. (2010). Total Protein Methods and Their Potential Utility to Reduce the Risk of Food Protein Adulteration, *Comprehensive Reviews in Food Science and Food Safety*, *9* (4), pp. 330–357. DOI 10.1111/j.1541-4337.2010.00114.x.

[61] Peterson, G. L. (1979). Review of the folin phenol protein quantitation method of Lowry, Rosebrough, Farr and Randall, *Analytical Biochemistry*, *100* (2), pp. 201–220. DOI 10.1016/0003-2697(79)90222-7.

[62] Avella, A. C., Görner, T., Yvon, J., Chappe, P., and Guinot-Thomas, P. et al. (2011). A combined approach for a better understanding of wastewater treatment plants operation: Statistical analysis of monitoring database and sludge physico-chemical characterization, *Water Research*, *45* (3), pp. 981–992. DOI 10.1016/j.watres.2010.09.028.

[63] Bradford, M. M. (1976). A rapid and sensitive method for the quantitation of microgram quantities of protein utilizing the principle of protein-dye binding, *Analytical Biochemistry*, *72* (1-2), pp. 248–254.

[64] Berges, J. A., Fisher, A. E., and Harrison, P. J. (1993). A comparison of Lowry, Bradford and Smith protein assays using different protein standards and protein isolated from the marine diatom Thalassiosira pseudonana, *Marine Biology*, *115* (2), pp. 187–193. DOI 10.1007/BF00346334.

[65] Starcher, B. (2001). A Ninhydrin-Based Assay to Quantitate the Total Protein Content of Tissue Samples, *Analytical Biochemistry*, *292* (1), pp. 125–129. DOI 10.1006/abio.2001.5050.

[66] Friedman, M. (2004). Applications of the Ninhydrin Reaction for Analysis of Amino Acids, Peptides, and Proteins to Agricultural and Biomedical Sciences, *Journal of Agricultural and Food Chemistry*, *52* (3), pp. 385–406. DOI 10.1021/jf030490p.

[67] Bradshaw, R. A. and Burlingame, A. L. (2005). From proteins to proteomics, *IUBMB LIFE*, *57* (4-5), pp. 267–272. DOI 10.1080/15216540500091536.

[68] Maron, P.-A., Ranjard, L., Mougel, C., and Lemanceau, P. (2007). Metaproteomics: A New Approach for Studying Functional Microbial Ecology, *Microbial Ecology*, *53* (3), pp. 486–493. DOI 10.1007/s00248-006-9196-8.

[69] Albertsen, M., Stensballe, A., Nielsen, K. L., and Nielsen, P. H. (2013). Digging into the extracellular matrix of a complex microbial community using a combined metagenomic and metaproteomic approach, *Water Science & Technology*, *67* (7), pp. 1650–1656. DOI 10.2166/wst.2013.030.

[70] Steiner, C., Nolte, H., Azizan, A., Krüger, M., and Denecke, M. et al. (2019). Quantitative proteomics for monitoring microbial dynamics in activated sludge from landfill leachate treatment, *Environ. Sci.: Water Res. Technol.* (6). DOI 10.1039/C8EW00892B.

[71] Wang, M., You, J., Bemis, K. G., Tegeler, T. J., and Brown, D. P. G. (2008). Label-free mass spectrometry-based protein quantification technologies in proteomic analysis, *Briefings in functional genomics & proteomics*, *7* (5), pp. 329–339. DOI 10.1093/bfgp/eln031.

[72] Silva, J. C., Gorenstein, M. V., Li, G.-Z., Vissers, J. P. C., and Geromanos Scott J. (2006). Absolute Quantification of Proteins by LCMSE, *Molecular & Cellular Proteomics*, *5* (1), pp. 144–156. DOI 10.1074/mcp.M500230-MCP200.

[73] Bantscheff, M., Lemeer, S., Savitski, M. M., and Kuster, B. (2012). Quantitative mass spectrometry in proteomics: critical review update from 2007 to the present, *Analytical and Bioanalytical Chemistry*, *404* (4), pp. 939–965. DOI 10.1007/s00216-012-6203-4.

[74] Cox, J., Hein, M. Y., Luber, C. A., Paron, I., and Nagaraj, N. et al. (2014). Accurate proteome-wide label-free quantification by delayed normalization and maximal peptide ratio extraction, termed MaxLFQ, *Molecular & Cellular Proteomics*, *13* (9), pp. 2513–2526. DOI 10.1074/mcp.M113.031591.

[75] Bantscheff, M., Schirle, M., Sweetman, G., Rick, J., and Kuster, B. (2007). Quantitative mass spectrometry in proteomics: a critical review, *Analytical and Bioanalytical Chemistry*, *389* (4), pp. 1017–1031. DOI 10.1007/s00216-007-1486-6.

[76] Sidoli, S., Kulej, K., and Garcia, B. A. (2017). Why proteomics is not the new genomics and the future of mass spectrometry in cell biology, *The Journal of cell biology*, *216* (1), pp. 21–24. DOI 10.1083/jcb.201612010.

[77] Al Shweiki, M. R., Mönchgesang, S., Majovsky, P., Thieme, D., and Trutschel, D. et al. (2017). Assessment of Label-Free Quantification in Discovery Proteomics and Impact of Technological Factors and Natural Variability of Protein Abundance, *Journal of Proteome Research*, *16* (4), pp. 1410–1424. DOI 10.1021/acs.jproteome.6b00645.

[78] DIN EN 872:2005 (2005). *Water quality - Determination of suspended solids - Method by filtration through glass fibre filters*.

[79] DIN 38409-1 (1987). *Determination of the total solid residue, the filtrate solids residue and the residue on ignition*.

[80] DIN EN 14702-1 (2006). *Characterisation of sludges – Settling properties – Part 1: Determination of settleability (Determination of the proportion of sludge volume and sludge volume index)*.

[81] Yücesoy, E. (2009). *Estimation of Microbial Biomass in Sequencing Batch Reactor by Determination of Protein Content of Activated Sludge*. *Forum Siedlungswasser-, Wasser- und Abfallwirtschaft*, Shaker Verlag, Aachen. ISBN 3832291105.

[82] Gerhardt, P. (1994). *Methods for general and molecular bacteriology*, American Soc. for Microbiology, Washington, DC. ISBN 1-55581-048-9.

[83] Dreywood, R. (1946). Qualitative Test for Carbohydrate Material, *Industrial & Engineering Chemistry Analytical Edition*, *18* (8), p. 499. DOI 10.1021/i560156a015.

[84] DIN EN 14701-1 (2006). *Characterisation of sludges - Filtration properties - Part 1: Capillary suction time (CST)*.

[85] HeGo Biotec . *CST-Messung,* can be found under https://www.hego-biotec.de/cst-messung/. Accessed on 5/12/2018.

[86] Rosner, B. (2011). *Fundamentals of biostatistics.* 7th ed., Brooks/Cole Cengage Learning, Boston. ISBN 978-0-538-73349-6.

[87] Zhang, Y., Zhang, H., Chu, H., Zhou, X., and Zhao, Y. (2013). Characterization of dissolved organic matter in a dynamic membrane bioreactor for wastewater treatment, *Chinese Science Bulletin*, *58* (15), pp. 1717–1724. DOI 10.1007/s11434-013-5710-9.

[88] Giesy, J. P. and Briese, L. A. (1978). Particulate formation due to freezing humic waters, *Water Resources Research*, *14* (3), pp. 542–544. DOI 10.1029/WR014i003p00542.

[89] Abernathy, D. G., Spedding, G., and Starcher, B. (2009). Analysis of Protein and Total Usable Nitrogen in Beer and Wine Using a Microwell Ninhydrin Assay, *Journal of the Institute of Brewing*, *115* (2), pp. 122–127. DOI 10.1002/j.2050-0416.2009.tb00356.x.

[90] Mok, Y. K., Arantes, V., and Saddler, J. N. (2015). A NaBH4 Coupled Ninhydrin-Based Assay for the Quantification of Protein/Enzymes During the Enzymatic Hydrolysis of Pretreated Lignocellulosic Biomass, *Applied Biochemistry and Biotechnology*, *176* (6), pp. 1564–1580. DOI 10.1007/s12010-015-1662-7.

[91] Wessel, D. and Flügge, U. I. (1984). A method for the quantitative recovery of protein in dilute solution in the presence of detergents and lipids, *Analytical Biochemistry*, *138* (1), pp. 141–143. DOI 10.1016/0003-2697(84)90782-6.

[92] Rappsilber, J., Mann, M., and Ishihama, Y. (2007). Protocol for micro-purification, enrichment, pre-fractionation and storage of peptides for proteomics using StageTips, *Nature protocols*, *2* (8), pp. 1896–1906. DOI 10.1038/nprot.2007.261.

[93] Weiss-Sadan, T., Itzhak, G., Kaschani, F., Yu, Z., and Mahameed, M. et al. (2019). Cathepsin L Regulates Metabolic Networks Controlling Rapid Cell Growth and Proliferation, *Molecular & Cellular Proteomics*, *18* (7). DOI 10.1074/mcp.RA119.001392.

[94] Cox, J., Neuhauser, N., Michalski, A., Scheltema, R. A., and Olsen, J. V. et al. (2011). Andromeda: a peptide search engine integrated into the MaxQuant environment, *Journal of Proteome Research*, *10* (4), pp. 1794–1805. DOI 10.1021/pr101065j.

[95] Cox, J. and Mann, M. (2008). MaxQuant enables high peptide identification rates, individualized p.p.b.-range mass accuracies and proteome-wide protein quantification, *Nature Biotechnology*, *26* (12), pp. 1367–1372. DOI 10.1038/nbt.1511.

[96] Albertsen, M., Hansen, L. B. S., Saunders, A. M., Nielsen, P. H., and Nielsen, K. L. (2012). A metagenome of a full-scale microbial community carrying out enhanced biological phosphorus removal, *International Society for Microbial Ecology Journal*, *6* (6), pp. 1094–1106. DOI 10.1038/ismej.2011.176.

[97] Meyer, B., Papasotiriou, D. G., and Karas, M. (2011). 100% protein sequence coverage: a modern form of surrealism in proteomics, *Amino Acids*, *41* (2), pp. 291–310. DOI 10.1007/s00726-010-0680-6.

[98] Kanehisa, M., Sato, Y., and Morishima, K. (2016). BlastKOALA and GhostKOALA: KEGG Tools for Functional Characterization of Genome and Metagenome Sequences, *Journal of Molecular Biology*, *428* (4), pp. 726–731. DOI 10.1016/j.jmb.2015.11.006.

[99] Nielsen, P. H., Daims, H., and Lemmer, H. (2009). *FISH handbook for biological wastewater treatment*. *Identification and quantification of microorganisms in activated sludge and biofilms by FISH*, IWA Publishing, London. ISBN 9781843392316.

[100] Stephen, J. R., Kowalchuk, G. A., Bruns, M.-A. V., McCaig, A. E., and Phillips, C. J. et al. (1998). Analysis of β-Subgroup Proteobacterial Ammonia Oxidizer Populations in Soil by Denaturing Gradient Gel Electrophoresis Analysis and Hierarchical Phylogenetic Probing, *Applied and Environmental Microbiology*, *64* (8), pp. 2958–2965.

[101] Crocetti, G. R., Hugenholtz, P., Bond, P. L., Schuler, A., and Keller, J. et al. (2000). Identification of polyphosphate-accumulating organisms and design of 16S rRNA-directed probes for their detection and quantitation, *Applied and Environmental Microbiology*, *66* (3), pp. 1175–1182. DOI 10.1128/aem.66.3.1175-1182.2000.

[102] Björnsson, L., Hugenholtz, P., Tyson, G. W., and Blackall, L. L. (2002). Filamentous Chloroflexi (green non-sulfur bacteria) are abundant in wastewater treatment processes with biological nutrient removal, *Microbiology (Reading, England)*, *148* (Pt 8), pp. 2309–2318. DOI 10.1099/00221287-148-8-2309.

[103] Gich, F., Garcia-Gil, J., and Overmann, J. (2001). Previously unknown and phylogenetically diverse members of the green nonsulfur bacteria are indigenous to freshwater lakes, *Archives of Microbiology*, *177* (1), pp. 1–10. DOI 10.1007/s00203-001-0354-6.

[104] Li, X. Y. and Yang, S. F. (2007). Influence of loosely bound extracellular polymeric substances (EPS) on the flocculation, sedimentation and dewaterability of activated sludge, *Water Research*, *41* (5), pp. 1022–1030. DOI 10.1016/j.watres.2006.06.037.

[105] Carles, P.-N., Carlos, D.-F., A., G. M., and Barth, F. S. (2013). Critical assessment of extracellular polymeric substances extraction methods from mixed culture biomass, *Water Research*, *47* (15), pp. 5564–5574. DOI 10.1016/j.watres.2013.06.026.

[106] Flemming, H.-C. and Wingender, J. (2001). Relevance of microbial extracellular polymeric substances (EPSs)- Part I: Structural and ecological aspects, *Water Science & Technology*, *43; Jg. 2001* (6), pp. 1–8.

[107] Duncan, A. J., Bott, C. B., Terlesky, K. C., and Love, N. G. (2000). Detection of GroEL in activated sludge: a model for detection of system stress, *Letters in Applied Microbiology*, *30* (1), pp. 28–32. DOI 10.1046/j.1472-765x.2000.00641.x.

[108] Laemmli, U. K. (1970). Cleavage of structural proteins during the assembly of the head of bacteriophage T4, *Nature*, *227; Jg. 1970* (5259), pp. 680–685.

[109] Benndorf, D., Balcke, G. U., Harms, H., and Bergen, M. von (2007). Functional metaproteome analysis of protein extracts from contaminated soil and groundwater, *International Society for Microbial Ecology Journal*, *1* (3), pp. 224–234.

[110] Perkins, D. N., Pappin, Darryl J. C., Creasy, D. M., and Cottrell, J. S. (1999). Probability-based protein identification by searching sequence databases using mass spectrometry data, *Electrophoresis*, *201999* (18), pp. 3551–3567. DOI 10.1002/(SICI)1522-2683(19991201)20:18<3551::AID-ELPS3551>3.0.CO;2-2.

[111] Acland, A., Agarwala, R., Barrett, T., Beck, J., and Benson, D. A. (2014). Database resources of the National Center for Biotechnology Information, *Nucleic acids research*, *42* (Database Issue), D7-17. DOI 10.1093/nar/gkt1146.

[112] The UniProt Consortium (2017). UniProt: the universal protein knowledgebase, *Nucleic acids research*, *45* (D1), D158-D169. DOI 10.1093/nar/gkw1099.

[113] Rosenberg, E. (2013). *The prokaryotes -prokaryotic physiology and biochemistry*, Springer, New York. ISBN 978-3-642-30141-4.

[114] Bock, E. and Wagner, M. (2013). Oxidation of Inorganic Nitrogen Compounds as an Energy Source in *The prokaryotes -prokaryotic physiology and biochemistry*, pp. 83–118. ISBN 978-3-642-30141-4.

[115] Storz, G. and Hengge, R. (2000). *Bacterial stress responses*, ASM Press, Washington, D.C. ISBN 1555811922.

[116] Bott, C. B., Duncan, A. J., and Love, N. G. (2001). Stress protein expression in domestic activated sludge in response to xenobiotic shock loading, *Water Science & Technology*, *43* (1), pp. 123–130.

[117] Hesselmann, R. P.X., Werlen, C., Hahn, D., van der Meer, Jan Roelof, and Zehnder, A. J.B. (1999). Enrichment, Phylogenetic Analysis and Detection of a Bacterium That Performs Enhanced Biological Phosphate Removal in Activated Sludge, *Systematic and Applied Microbiology*, *22* (3), pp. 454–465. DOI 10.1016/S0723-2020(99)80055-1.

[118] Liu, J. R. and Liss, S. N. (2007). The impact of reduced phosphorus levels on microbial floc properties during biological treatment of pulp and paper wastewaters, *Water Science & Technology*, *55* (6), pp. 73–79. DOI 10.2166/wst.2007.214.

[119] Bhathena, J., Driscoll, B. T., Charles, T. C., and Archibald, F. S. (2006). Effects of Nitrogen and Phosphorus Limitation on the Activated Sludge Biomass in a Kraft Mill Biotreatment System, *Water Environment Research*, *78* (12), pp. 2303–2310.

[120] Jorand, F., Boué-Bigne, F., Block, J. C., and Urbain, V. (1998). Hydrophobic/hydrophilic properties of activated sludge exopolymeric substances, *Water Science & Technology*, *37* (4), pp. 307–315. DOI 10.1016/S0273-1223(98)00123-1.

[121] Costerton, J. W. (1995). Overview of microbial biofilms, *Journal of Industrial Microbiology*, *15* (3), pp. 137–140. DOI 10.1007/BF01569816.

[122] Davey, M. E. and O'toole, G. A. (2000). Microbial Biofilms: from Ecology to Molecular Genetics, *Microbiol. Mol. Biol. Rev.*, *64* (4), pp. 847–867. DOI 10.1128/MMBR.64.4.847-867.2000.

[123] Han, H., Song, B., Song, M. J., and Yoon, S. (2019). Enhanced Nitrous Oxide Production in Denitrifying Dechloromonas aromatica Strain RCB Under Salt or Alkaline Stress Conditions, *Front. Microbiol.*, *10*, p. 1203. DOI 10.3389/fmicb.2019.01203.

[124] Heylen, K., Vanparys, B., Wittebolle, L., Verstraete, W., and Boon, N. et al. (2006). Cultivation of Denitrifying Bacteria: Optimization of Isolation Conditions and Diversity Study, *Appl. Environ. Microbiol.*, *72* (4), pp. 2637–2643. DOI 10.1128/AEM.72.4.2637-2643.2006.

[125] Zhang, P., Shen, Y., Guo, J.-S., Li, C., and Wang, H. et al. (2015). Extracellular protein analysis of activated sludge and their functions in wastewater treatment plant by shotgun proteomics, *SCIENTIFIC REPORTS*, *5*, p. 12041. DOI 10.1038/srep12041.

[126] Silva, A., Carvalho, G., Soares, R., Coelho, A., and Barreto Crespo, M.T. (2012). Step-by-step strategy for protein enrichment and proteome characterisation of extracellular polymeric substances in wastewater treatment systems, *Applied Microbiology and Biotechnology*, *95* (3), pp. 767–776. DOI 10.1007/s00253-012-4157-2.

[127] Vertommen, A., Panis, B., Swennen, R., and Carpentier, S. C. (2010). Evaluation of chloroform/methanol extraction to facilitate the study of membrane proteins of non-model plants, *Planta*, *231* (5), pp. 1113–1125. DOI 10.1007/s00425-010-1121-1.

[128] Fayet, O., Ziegelhoffer, T., and Georgopoulos, C. (1989). The groES and groEL heat shock gene products of Escherichia coli are essential for bacterial growth at all temperatures, *Journal of Bacteriology*, *171* (3), pp. 1379–1385.

[129] Saibil, H. (2013). Chaperone machines for protein folding, unfolding and disaggregation, *Nature reviews. Molecular cell biology*, *14* (10), pp. 630–642. DOI 10.1038/nrm3658.

[130] Honoré, F. A., Méjean, V., and Genest, O. (2017). Hsp90 Is Essential under Heat Stress in the Bacterium Shewanella oneidensis, *Cell Reports*, *19* (4), pp. 680–687. DOI 10.1016/j.celrep.2017.03.082.

[131] Chen, L., Xie, Q.-w., and Nathan, C. (1998). Alkyl Hydroperoxide Reductase Subunit C (AhpC) Protects Bacterial and Human Cells against Reactive Nitrogen Intermediates, *Molecular Cell*, *1* (6), pp. 795–805. DOI 10.1016/S1097-2765(00)80079-9.

[132] Atack, J. M. and Kelly, D. J. (2009). Oxidative stress in Campylobacter jejuni: responses, resistance and regulation, *Future microbiology*, *4* (6), pp. 677–690. DOI 10.2217/fmb.09.44.

[133] Feng, T.-Y., Yang, Z.-K., Zheng, J.-W., Xie, Y., and Li, D.-W. et al. . Examination of metabolic responses to phosphorus limitation via proteomic analyses in the marine diatom *Phaeodactylum tricornutum*, *SCIENTIFIC REPORTS*, *5*, p. 10373. DOI 10.1038/srep10373.

[134] Chelikani, P., Fita, I., and Loewen, P. C. (2004). Diversity of structures and properties among catalases, *Cellular and Molecular Life Sciences*, *61* (2), pp. 192–208. DOI 10.1007/s00018-003-3206-5.

[135] Seaver, L. C. and Imlay, J. A. (2001). Alkyl Hydroperoxide Reductase Is the Primary Scavenger of Endogenous Hydrogen Peroxide in Escherichia coli, *Journal of Bacteriology*, *183* (24), pp. 7173–7181. DOI 10.1128/JB.183.24.7173-7181.2001.

[136] Moreau, P. L., Gérard, F., Lutz, N. W., and Cozzone, P. (2001). Non-growing Escherichia coli cells starved for glucose or phosphate use different mechanisms to survive oxidative stress‡, *Molecular Microbiology*, *39* (4), pp. 1048–1060. DOI 10.1046/j.1365-2958.2001.02303.x.

[137] Gilch, S., Meyer, O., and Schmidt, I. (2009). A soluble form of ammonia monooxygenase in Nitrosomonas europaea, *Biological chemistry*, *390* (9), pp. 863–873. DOI 10.1515/BC.2009.085.

[138] Schmidt, I., Look, C., Bock, E., and Jetten, M. S. M. (2004). Ammonium and hydroxylamine uptake and accumulation in Nitrosomonas, *Microbiology (Reading, England)*, *150* (Pt 5), pp. 1405–1412. DOI 10.1099/mic.0.26719-0.

[139] Dong, J., Zhang, Z., Yu, Z., Dai, X., and Xu, X. et al. (2017). Evolution and functional analysis of extracellular polymeric substances during the granulation of aerobic sludge used to treat p-chloroaniline wastewater, *Chemical Engineering Journal*, *330*, pp. 596–604. DOI 10.1016/j.cej.2017.07.174.

[140] Zhang, P., Zhu, J., Xu, X.-Y., Qing, T.-P., and Dai, Y.-Z. et al. (2019). Identification and function of extracellular protein in wastewater treatment using proteomic approaches: A minireview, *Journal of environmental management*, *233*, pp. 24–29. DOI 10.1016/j.jenvman.2018.12.028.

[141] Haiko, J. and Westerlund-Wikström, B. (2013). The Role of the Bacterial Flagellum in Adhesion and Virulence, *Biology*, *2* (4), pp. 1242–1267. DOI 10.3390/biology2041242.

[142] Torriani, A. (1960). Influence of inorganic phosphate in the formation of phosphatases by Escherichia coli, *Biochimica et Biophysica Acta*, *38*, pp. 460–469. DOI 10.1016/0006-3002(60)91281-6.

[143] Dick, C. F., Dos-Santos, A. L. A., and Meyer-Fernandes, J. R. (2011). Inorganic Phosphate as an Important Regulator of Phosphatases, *Enzyme Research*, *2011*. DOI 10.4061/2011/103980.

[144] Cembella, A. D., Antia, N. J., and Harrison, P. J. (1984). The utilization of inorganic and organic phosphorus compounds as nutrients by eukaryotic microalgae: a multidisciplinary perspective. Part 2, *Critical reviews in microbiology*, *11* (1), pp. 13–81. DOI 10.3109/10408418409105902.

[145] Scutt, P. B. and Moss, D. W. (1968). Reversible inactivation of alkaline phosphatase in acid solution, *Enzymologia*, *35* (3), pp. 157–167.

[146] Witschel, M., Egli, T., Zehnder, A. J., Wehrli, E., and Spycher, M. (1999). Transport of EDTA into cells of the EDTA-degrading bacterial strain DSM 9103, *Microbiology (Reading, England)*, *145 (Pt 4)*, pp. 973–983. DOI 10.1099/13500872-145-4-973.

[147] Kerner, M. J., Naylor, D. J., Ishihama, Y., Maier, T., and Chang, H.-C. et al. (2005). Proteome-wide Analysis of Chaperonin-Dependent Protein Folding in Escherichia coli, *Cell*, *122* (2), pp. 209–220. DOI 10.1016/j.cell.2005.05.028.

[148] Amon, J., Titgemeyer, F., and Burkovski, A. (2010). Common patterns - unique features: nitrogen metabolism and regulation in Gram-positive bacteria, *FEMS microbiology reviews*, *34* (4), pp. 588–605. DOI 10.1111/j.1574-6976.2010.00216.x.

[149] Wang, P., Song, P., Jin, M., and Zhu, G. (2013). Isocitrate dehydrogenase from Streptococcus mutans: biochemical properties and evaluation of a putative phosphorylation site at Ser102, *PloS one*, *8* (3), e58918. DOI 10.1371/journal.pone.0058918.

[150] Jo, S.-H., Son, M.-K., Koh, H.-J., Lee, S.-M., and Song, I.-H. et al. (2001). Control of Mitochondrial Redox Balance and Cellular Defense against Oxidative Damage by Mitochondrial NADP+-dependent Isocitrate Dehydrogenase, *J. Biol. Chem.*, *276* (19), pp. 16168–16176. DOI 10.1074/jbc.M010120200.

[151] Lee, S. M., Huh, T.-L., and Park, J.-W. (2001). Inactivation of NADP+-dependent isocitrate dehydrogenase by reactive oxygen species, *Biochimie*, *83* (11), pp. 1057–1065. DOI 10.1016/S0300-9084(01)01351-7.

[152] Calhoun, L. N. and Kwon, Y. M. (2011). Structure, function and regulation of the DNA-binding protein Dps and its role in acid and oxidative stress resistance in Escherichia coli: a review, *Journal of applied microbiology*, *110* (2), pp. 375–386. DOI 10.1111/j.1365-2672.2010.04890.x.

[153] Karas, V. O., Westerlaken, I., and Meyer, A. S. (2015). The DNA-Binding Protein from Starved Cells (Dps) Utilizes Dual Functions To Defend Cells against Multiple Stresses, *Journal of Bacteriology*, *197* (19), pp. 3206–3215. DOI 10.1128/JB.00475-15.

[154] Chiancone, E. and Ceci, P. (2010). The multifaceted capacity of Dps proteins to combat bacterial stress conditions: Detoxification of iron and hydrogen peroxide and DNA binding, *Biochimica et Biophysica Acta (BBA) - General Subjects*, *1800* (8), pp. 798–805. DOI 10.1016/j.bbagen.2010.01.013.

[155] Wilhelm, R., Abeliovich, A., and Nejidat, A. (1998). Effect of long-term ammonia starvation on the oxidation of ammonia and hydroxylamine by Nitrosomonas europaea, *J Biochem*, *124* (4), pp. 811–815. DOI 10.1093/oxfordjournals.jbchem.a022184.

[156] Margelis, S., D'Souza, C., Small, A. J., Hynes, M. J., and Adams, T. H. et al. (2001). Role of Glutamine Synthetase in Nitrogen Metabolite Repression in Aspergillus nidulans, *Journal of Bacteriology*, *183* (20), pp. 5826–5833. DOI 10.1128/JB.183.20.5826-5833.2001.

[157] Friedrich, B. and Magasanik, B. (1977). Urease of Klebsiella aerogenes: control of its synthesis by glutamine synthetase, *Journal of Bacteriology*, *131* (2), pp. 446–452.

[158] McCarty, G. W. (1995). The role of glutamine synthetase in regulation of nitrogen metabolism within the soil microbial community, *Plant and Soil*, *170* (1), pp. 141–147. DOI 10.1007/BF02183062.

[159] Bugg, T. D. H. (2012). *Introduction to Enzyme and Coenzyme Chemistry*, John Wiley & Sons, Ltd, Chichester, UK. ISBN 9781118348970.

[160] Cetin, S. and Erdincler, A. (2004). The role of carbohydrate and protein parts of extracellular polymeric substances on the dewaterability of biological sludges, *Water Science & Technology*, *50; Jg. 2004* (9), pp. 49–56.

[161] Shin, H.-S., Kang, S.-T., and Nam, S.-Y. (2000). Effect of carbohydrates to protein in EPS on sludge settling characteristics, *Biotechnology and Bioprocess Engineering*, *5* (6), pp. 460–464. DOI 10.1007/BF02931948.

Appendices

Appendix 1: Standard Curves for Quantification of Protein and Carbohydrate in Activated Sludge from Industrial WWTP

Modified Lowry for total protein: standard curves of BSA and humic acid in lysis buffer

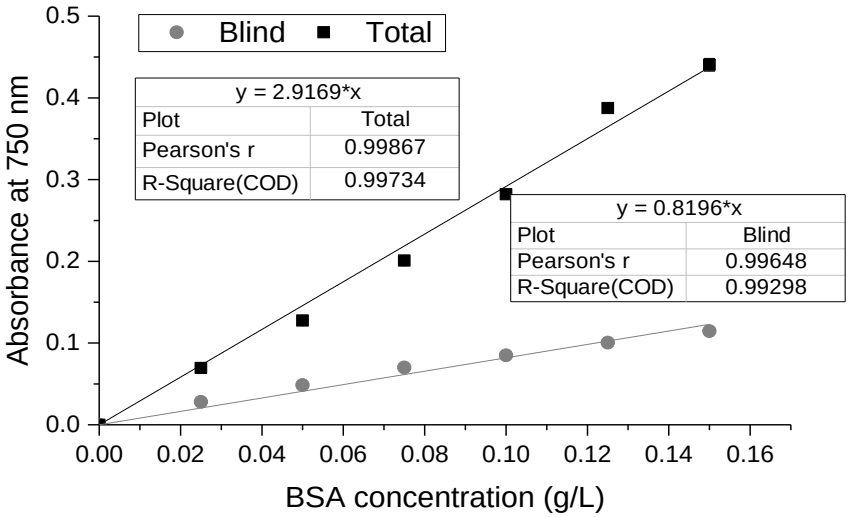

Figure A1: Standard curves of BSA in lysis buffer for modified Lowry assay

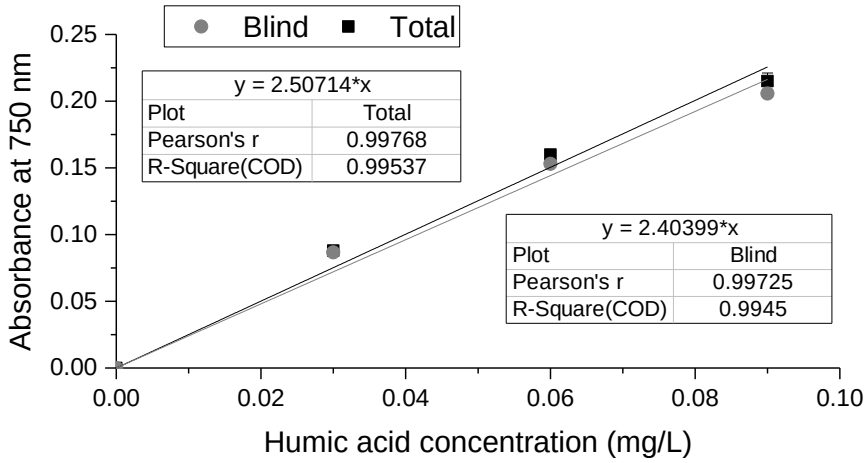

Figure A2: Standard curves of humic acid in lysis buffer for modified Lowry assay

Table A1: Difference in gradients due to elimination of $CuSO_4$

	BSA	**Humic Acid**
Total	2.9169	2.5071
Blind	0.8196	2.4040
Difference	$\Delta BSA = \frac{\lvert 2.9169 - 0.8196 \rvert}{2.9169} = 71.9\%$	$\Delta HA = \frac{\lvert 2.5071 - 2.4040 \rvert}{2.5071} = 4.1\%$

Modified Lowry for total protein: standard curves of BSA and humic acid in PBS

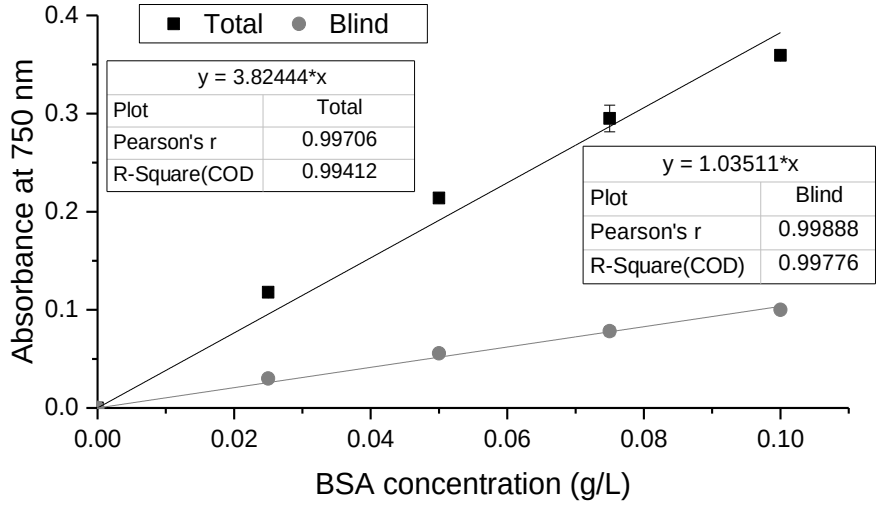

Figure A3: Standard curves of BSA in PBS for modified Lowry assay

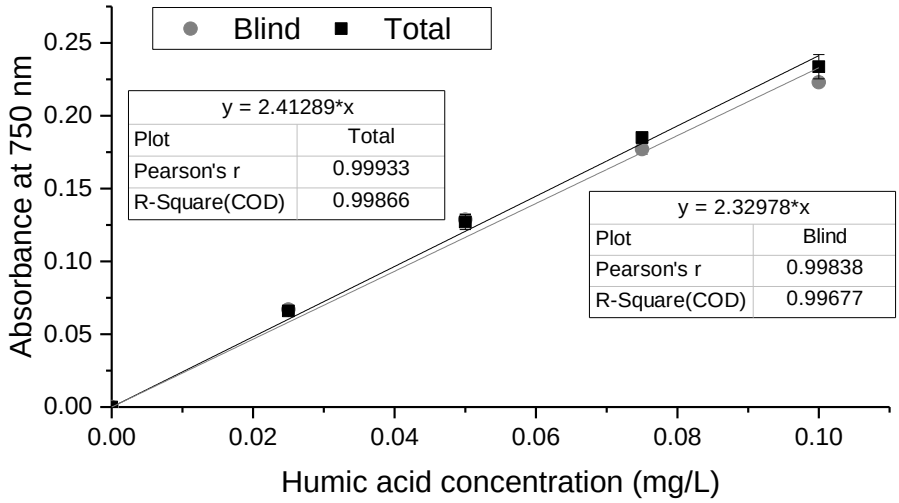

Figure A4: Standard curves of humic acid in PBS for modified Lowry assay

Table A2: Difference in gradients due to elimination of $CuSO_4$

	BSA	**Humic Acid**
Total	3.8244	2.4129
Blind	1.0351	2.3298
Difference	$\Delta BSA = \frac{\lvert 3.8244 - 1.0351 \rvert}{3.8244} = 72.9\%$	$\Delta HA = \frac{\lvert 2.3453 - 2.3298 \rvert}{2.3453} = 3.4\%$

Anthrone assay for EPS: standard curve of glucose in PBS

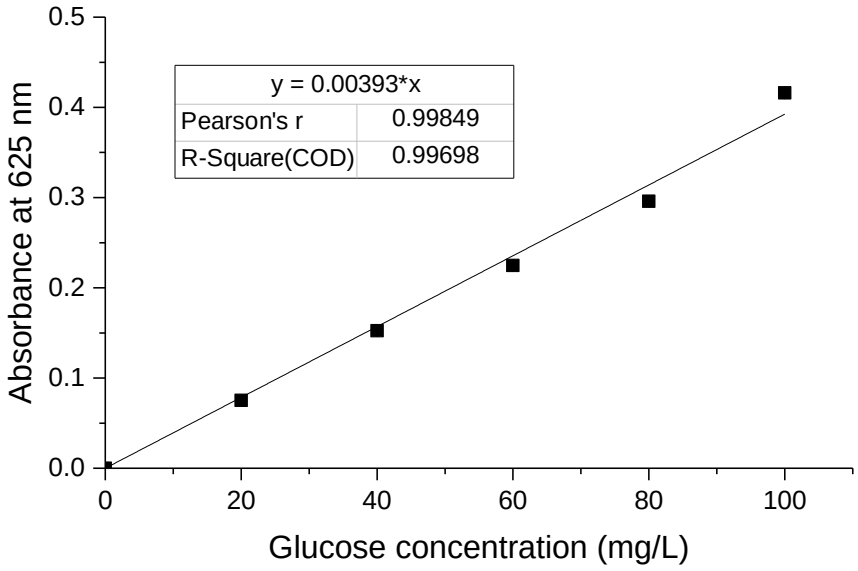

Figure A5: Standard curve of glucose in PBS for anthrone assay

Appendix 2: Standard Curves for Quantification of Protein in Activated sludge from Lab-scale Plant WWTP

Lowry assay (Bio-RAD DC protein assay): standard curve of BSA in PBS

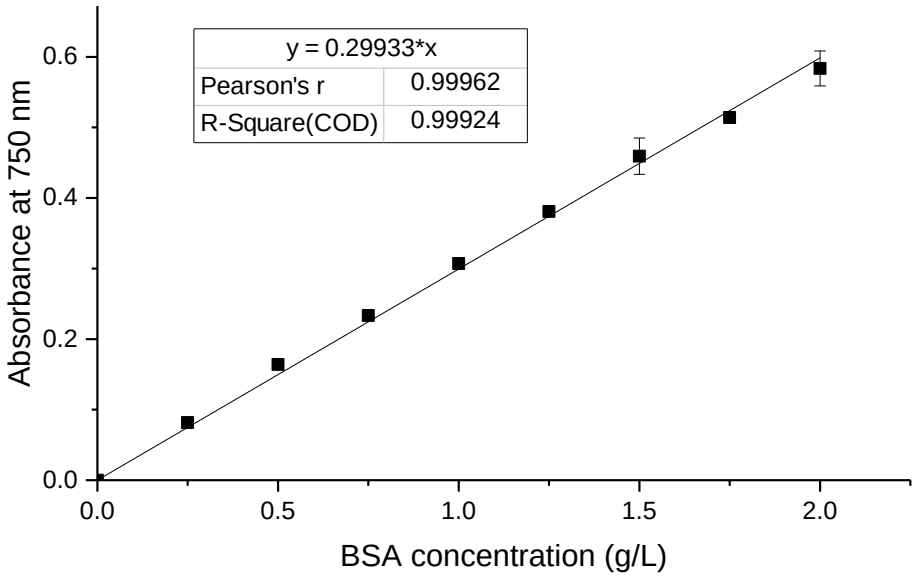

Figure A6: Standard curve of BSA in PBS for Lowry assay

Bradford assay (Bio-RAD Protein Assay): standard curve of BSA in PBS

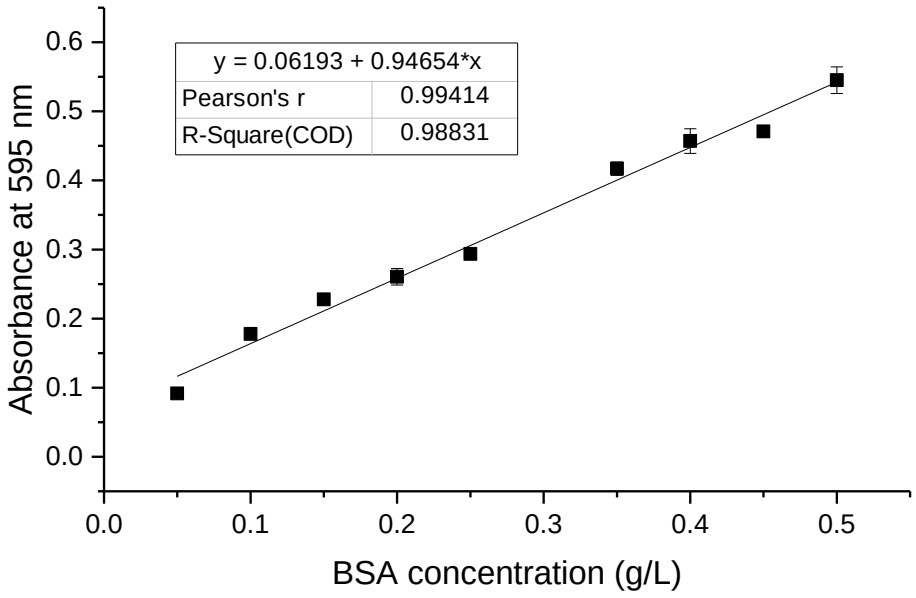

Figure A7: Standard curve of BSA in PBS for Bradford assay

Bradford assay (Bio-RAD Protein Assay): standard curve of BSA in PBS for low protein concentration

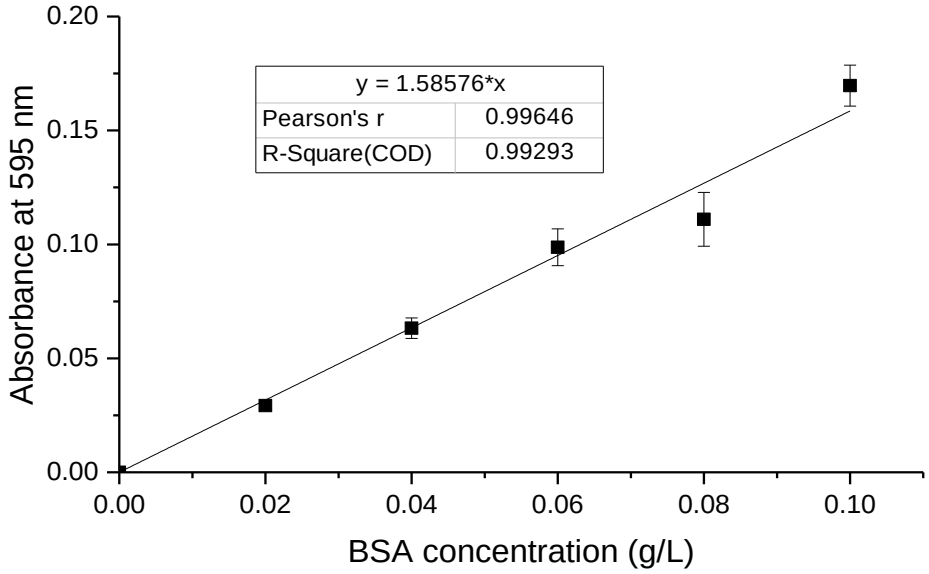

Figure A8: Standard curve of BSA (low concentration) in PBS for Bradford assay

Ninhydrin assay: standard curve of BSA in PBS

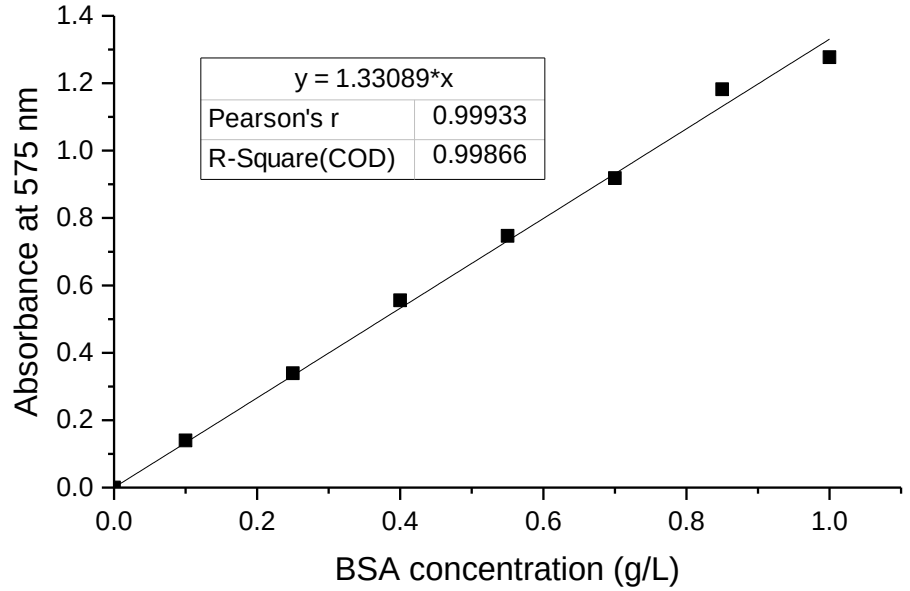

Figure A9: Standard curve of BSA in PBS for ninhydrin assay

Appendix 3: Correlation of Biomass Parameters to total OUR in phase 1 (P1) and phase 2 (P2)

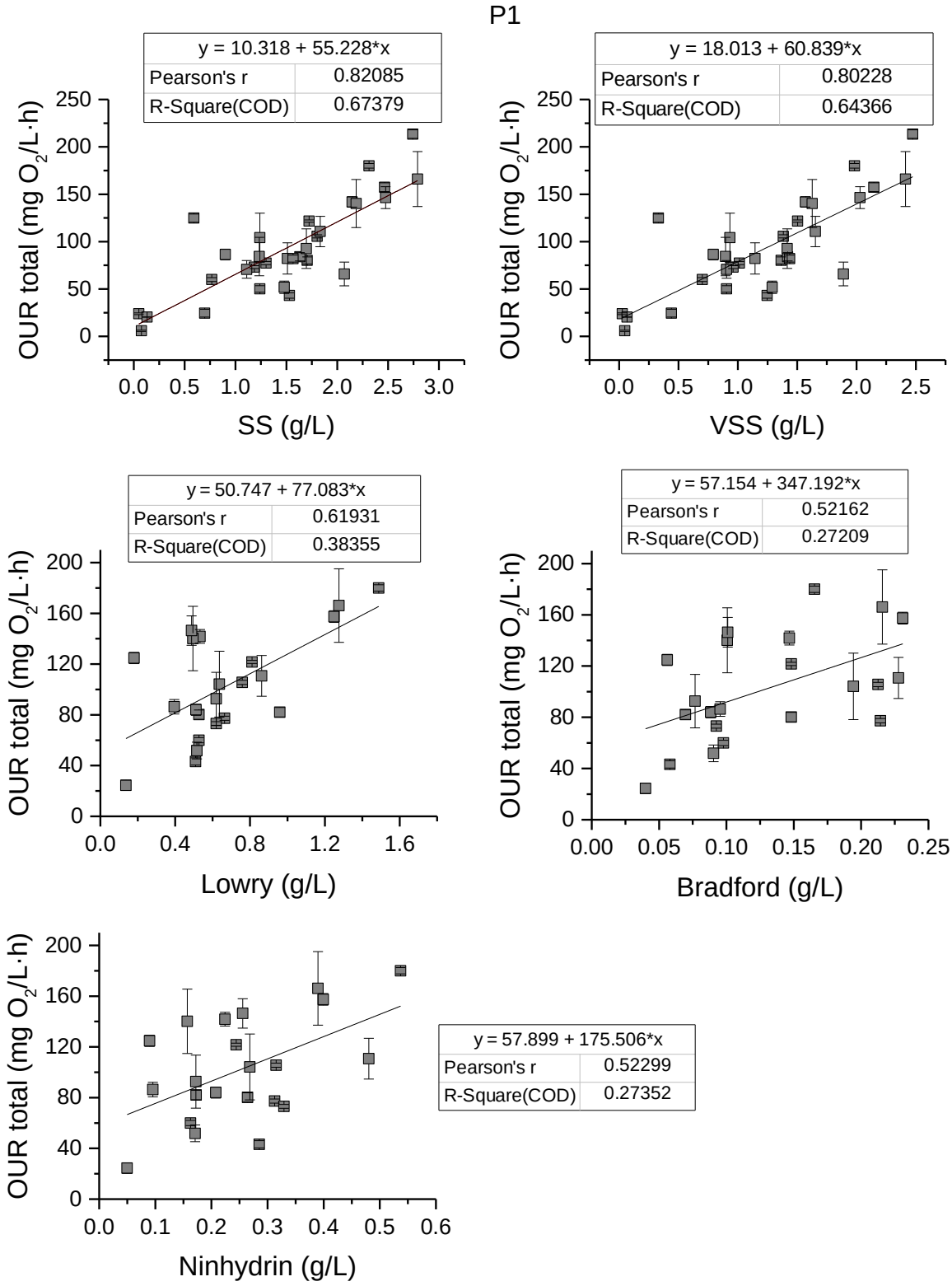

Figure A10: Correlation between total OUR and SS, VSS and protein concentration according to the Lowry, Bradford and ninhydrin methods of P1

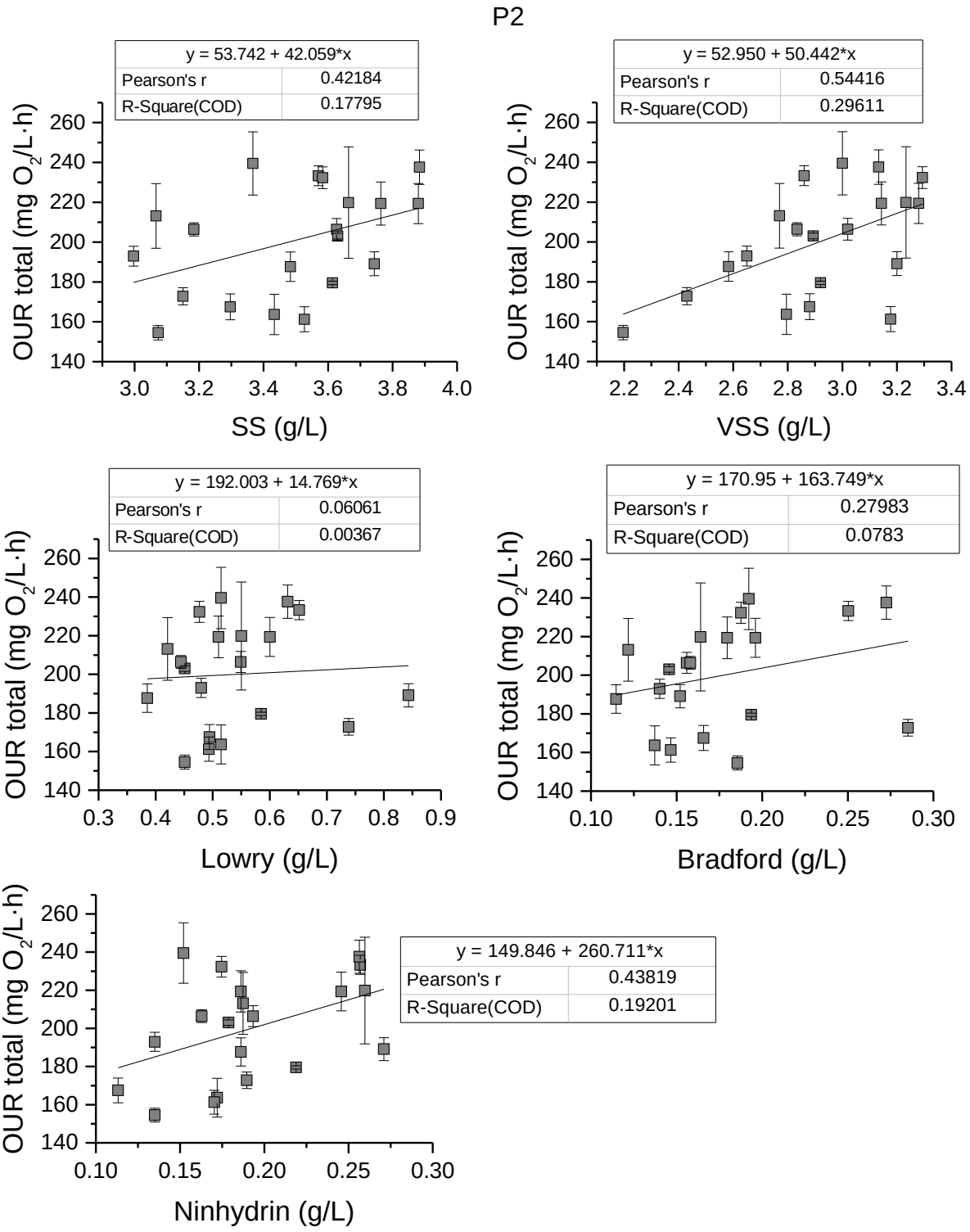

Figure A11: Correlation between total OUR and SS, VSS and protein concentration according to the Lowry, Bradford and ninhydrin methods of P2

Appendix 4: Critical Values for Pearson's r

Table A3: Table of critical values for Pearson's r

	Level of Significance for a Two-tailed Test					
df	**0.2**	**0.1**	**0.05**	**0.02**	**0.01**	**0.001**
1	0.951	0.988	0.997	1.000	1.000	1.000
2	0.800	0.900	0.950	0.980	0.990	0.999
3	0.687	0.805	0.878	0.934	0.959	0.991
4	0.608	0.729	0.811	0.882	0.917	0.974
5	0.551	0.669	0.755	0.833	0.875	0.951
6	0.507	0.621	0.707	0.789	0.834	0.925
7	0.472	0.582	0.666	0.750	0.798	0.898
8	0.443	0.549	0.632	0.715	0.765	0.872
9	0.419	0.521	0.602	0.685	0.735	0.847
10	0.398	0.497	0.576	0.658	0.708	0.823
11	0.380	0.476	0.553	0.634	0.684	0.801
12	0.365	0.457	0.532	0.612	0.661	0.780
13	0.351	0.441	0.514	0.592	0.641	0.760
14	0.338	0.426	0.497	0.574	0.623	0.742
15	0.327	0.412	0.482	0.558	0.606	0.725
16	0.317	0.400	0.468	0.542	0.590	0.708
17	0.308	0.389	0.456	0.529	0.575	0.693
18	0.299	0.378	0.444	0.515	0.561	0.679
19	0.291	0.369	0.433	0.503	0.549	0.665
20	0.284	0.360	0.423	0.492	0.537	0.652
21	0.277	0.352	0.413	0.482	0.526	0.640
22	0.271	0.344	0.404	0.472	0.515	0.629
23	0.265	0.337	0.396	0.462	0.505	0.618
24	0.260	0.330	0.388	0.453	0.496	0.607
25	0.255	0.323	0.381	0.445	0.487	0.597
26	0.250	0.317	0.374	0.437	0.479	0.588
27	0.245	0.311	0.367	0.430	0.471	0.579
28	0.241	0.306	0.361	0.423	0.463	0.570
29	0.237	0.301	0.355	0.416	0.456	0.562
30	0.233	0.296	0.349	0.409	0.449	0.554
40	0.202	0.257	0.304	0.358	0.393	0.490
60	0.165	0.211	0.250	0.295	0.325	0.408
120	0.117	0.150	0.178	0.210	0.232	0.294
∞	0.057	0.073	0.087	0.103	0.114	0.146

Reference:
https://www.radford.edu/~jaspelme/statsbook/Chapter%20files/Table_of_Critical_Values_for_r.pdf. Accessed on 6/5/2019

Appendix 5: 16S rRNA Sequencing Result Kaßlerfeld sludge

Table A4: 16S rRNA sequencing result of Kaßlerfeld sludge in decreasing abundance. The percentage is calculated omitting the abundance of eukaryotes

Phylum	Class	Order	Family	Genus	%
Bacteroidetes	Sphingobacteriia	Sphingobacteriales	Saprospiraceae	uncultured	9.0
Proteobacteria	Betaproteobacteria	Burkholderiales	Comamonadaceae	uncultured	8.1
Proteobacteria	Deltaproteobacteria	Myxococcales	Haliangiaceae	Haliangium	4.1
Bacteroidetes	Sphingobacteriia	Sphingobacteriales	uncultured	uncultured bacterium	2.9
Actinobacteria	Acidimicrobiia	Acidimicrobiales	Acidimicrobiales Incertae Sedis	Candidatus Microthrix	2.8
Proteobacteria	Gammaproteobacteria	Xanthomonadales	Xanthomonadales Incertae Sedis	Candidatus Competibacter	2.4
Proteobacteria	Betaproteobacteria	Rhodocyclales	Rhodocyclaceae	uncultured	2.4
Bacteroidetes	Sphingobacteriia	Sphingobacteriales	Chitinophagaceae	Terrimonas	2.3
Chloroflexi	Anaerolineae	Anaerolineales	Anaerolineaceae	uncultured	2.2
Proteobacteria	Betaproteobacteria	Burkholderiales	Comamonadaceae	Other	2.2
Proteobacteria	Betaproteobacteria	Rhodocyclales	Rhodocyclaceae	Sulfuritalea	2.1
Bacteroidetes	Bacteroidia	Bacteroidia Incertae Sedis	Draconibacteriaceae	uncultured	1.8
Acidobacteria	Holophagae	Holophagales	Holophagaceae	Geothrix	1.7
Saccharibacteria	uncultured bacterium	uncultured bacterium	uncultured bacterium	uncultured bacterium	1.6
Proteobacteria	Betaproteobacteria	Rhodocyclales	Rhodocyclaceae	Other	1.5
Proteobacteria	Deltaproteobacteria	Myxococcales	Polyangiaceae	uncultured	1.5
Chloroflexi	Caldilineae	Caldilineales	Caldilineaceae	uncultured	1.4
Chloroflexi	Chloroflexia	Chloroflexales	Roseiflexaceae	Roseiflexus	1.4
Proteobacteria	Epsilonproteobacteria	Campylobacterales	Campylobacteraceae	Arcobacter	1.3
Proteobacteria	Gammaproteobacteria	Run-SP154	uncultured bacterium	uncultured bacterium	1.3
Bacteroidetes	Sphingobacteriia	Sphingobacteriales	AKYH767	uncultured bacterium	1.2
Actinobacteria	Actinobacteria	Micrococcales	Intrasporangiaceae	Tetrasphaera	1.1
Proteobacteria	Gammaproteobacteria	Xanthomonadales	Xanthomonadaceae	uncultured	1.0
Bacteroidetes	Flavobacteriia	Flavobacteriales	Flavobacteriaceae	Flavobacterium	1.0
Gemmatimonadetes	Gemmatimonadetes	Gemmatimonadales	Gemmatimonadaceae	uncultured	0.9
Proteobacteria	Deltaproteobacteria	Myxococcales	Nannocystaceae	Nannocystis	0.9
Proteobacteria	Deltaproteobacteria	Bdellovibrionales	Bdellovibrionaceae	Bdellovibrio	0.8
Proteobacteria	Deltaproteobacteria	Myxococcales	mle1-27	uncultured bacterium	0.8
Proteobacteria	Betaproteobacteria	Nitrosomonadales	Nitrosomonadaceae	uncultured	0.7
Proteobacteria	Betaproteobacteria	Burkholderiales	Comamonadaceae	Acidovorax	0.7
Bacteroidetes	Cytophagia	Cytophagales	Cytophagaceae	uncultured	0.6
Acidobacteria	Subgroup 6	uncultured bacterium	uncultured bacterium	uncultured bacterium	0.6
Bacteroidetes	Sphingobacteriia	Sphingobacteriales	env.OPS 17	uncultured bacterium	0.6
Actinobacteria	Actinobacteria	PeM15	uncultured bacterium	uncultured bacterium	0.6
Chloroflexi	1-20	uncultured Chloroflexia bacterium	uncultured Chloroflexia bacterium	uncultured Chloroflexia bacterium	0.6

-Table A4 continued-

Phylum	Class	Order	Family	Genus	%
Proteobacteria	Alphaproteobacteria	Caulobacterales	Hyphomonadaceae	Hirschia	0.6
Proteobacteria	Alphaproteobacteria	Rhodospirillales	Acetobacteraceae	Stella	0.6
Proteobacteria	Betaproteobacteria	Burkholderiales	Comamonadaceae	Piscinibacter	0.6
Proteobacteria	Betaproteobacteria	Rhodocyclales	Rhodocyclaceae	Dechloromonas	0.6
Proteobacteria	Betaproteobacteria	Rhodocyclales	Rhodocyclaceae	Zoogloea	0.6
Proteobacteria	Deltaproteobacteria	Myxococcales	Polyangiaceae	Sorangium	0.6
Saccharibacteria	Other	Other	Other	Other	0.6
Bacteroidetes	Flavobacteriia	Flavobacteriales	NS9 marine group	uncultured bacterium	0.5
Bacteroidetes	Sphingobacteriia	Sphingobacteriales	PHOS-HE51	uncultured bacterium	0.5
Bacteroidetes	Sphingobacteriia	Sphingobacteriales	Chitinophagaceae	uncultured	0.5
Bacteroidetes	Sphingobacteriia	Sphingobacteriales	Chitinophagaceae	Ferruginibacter	0.5
Gemmatimonadetes	Gemmatimonadetes	Gemmatimonadales	Gemmatimonadaceae	Gemmatimonas	0.5
Verrucomicrobia	OPB35 soil group	uncultured bacterium	uncultured bacterium	uncultured bacterium	0.4
Proteobacteria	Alphaproteobacteria	Rhodospirillales	Rhodospirillaceae	uncultured	0.4
Bacteroidetes	Sphingobacteriia	Sphingobacteriales	Lentimicrobiaceae	uncultured bacterium	0.4
Proteobacteria	Betaproteobacteria	Rhodocyclales	Rhodocyclaceae	Candidatus Accumulibacter	0.4
Proteobacteria	Deltaproteobacteria	Oligoflexales	0319-6G20	uncultured bacterium	0.4
Proteobacteria	Gammaproteobacteria	Aeromonadales	Aeromonadaceae	Aeromonas	0.4
Proteobacteria	Gammaproteobacteria	Xanthomonadales	uncultured	uncultured bacterium	0.3
Chlorobi	Chlorobia	Chlorobiales	SJA-28	uncultured bacterium	0.3
Nitrospirae	Nitrospira	Nitrospirales	Nitrospiraceae	Nitrospira	0.3
Proteobacteria	Gammaproteobacteria	Cellvibrionales	Spongiibacteraceae	BD1-7 clade	0.3
Actinobacteria	Acidimicrobiia	Acidimicrobiales	Acidimicrobiaceae	CL500-29 marine group	0.3
Bacteroidetes	Sphingobacteriia	Sphingobacteriales	Saprospiraceae	Haliscomenobacter	0.3
Proteobacteria	Alphaproteobacteria	Alphaproteobacteria Incertae Sedis	uncultured	uncultured bacterium	0.3
Spirochaetae	Spirochaetes	Spirochaetales	Leptospiraceae	Turneriella	0.3
Ignavibacteriae	Ignavibacteria	Ignavibacteriales	Ignavibacteriaceae	Ignavibacterium	0.2
Chloroflexi	TK10	uncultured bacterium	uncultured bacterium	uncultured bacterium	0.2
Bacteroidetes	Sphingobacteriia	Sphingobacteriales	NS11-12 marine group	uncultured bacterium	0.2
Acidobacteria	Solibacteres	Solibacterales	Solibacteraceae (Subgroup 3)	Other	0.2
Proteobacteria	Alphaproteobacteria	Sphingomonadales	Sphingomonadaceae	Novosphingobium	0.2
Acidobacteria	Holophagae	Subgroup 7	uncultured bacterium	uncultured bacterium	0.2
Bacteroidetes	Sphingobacteriia	Sphingobacteriales	Chitinophagaceae	Filimonas	0.2
Gracilibacteria	uncultured bacterium	uncultured bacterium	uncultured bacterium	uncultured bacterium	0.2
Proteobacteria	Alphaproteobacteria	Rhodobacterales	Rhodobacteraceae	Rhodobacter	0.2
Proteobacteria	Alphaproteobacteria	Sphingomonadales	Sphingomonadaceae	Other	0.2
Proteobacteria	Betaproteobacteria	Burkholderiales	Burkholderiaceae	Lautropia	0.2
Proteobacteria	Deltaproteobacteria	Myxococcales	Phaselicystidaceae	Phaselicystis	0.2

-Table A4 continued-

Phylum	Class	Order	Family	Genus	%
Proteobacteria	Deltaproteobacteria	SAR324 clade (Marine group B)	uncultured bacterium	uncultured bacterium	0.2
Verrucomicrobia	Opitutae	Opitutales	Opitutaceae	Opitutus	0.2
Proteobacteria	Betaproteobacteria	Nitrosomonadales	Nitrosomonadaceae	Nitrosomonas	0.1
Proteobacteria	Betaproteobacteria	Rhodocyclales	Rhodocyclaceae	Denitratisoma	0.1
Proteobacteria	Betaproteobacteria	Rhodocyclales	Rhodocyclaceae	Thauera	0.1
Proteobacteria	Betaproteobacteria	Burkholderiales	Comamonadaceae	Comamonas	0.1
Proteobacteria	Alphaproteobacteria	Rhizobiales	Hyphomicrobiaceae	Hyphomicrobium	0.1
Proteobacteria	Alphaproteobacteria	Caulobacterales	Hyphomonadaceae	Woodsholea	0.1
Chlorobi	Chlorobia	Chlorobiales	OPB56	uncultured bacterium	0.1
Actinobacteria	Acidimicrobiia	Acidimicrobiales	uncultured	uncultured bacterium	0.1
Proteobacteria	Alphaproteobacteria	Sphingomonadales	Sphingomonadaceae	Sphingobium	0.1
Proteobacteria	Gammaproteobacteria	Xanthomonadales	Xanthomonadales Incertae Sedis	uncultured	0.1
Acidobacteria	Holophagae	Subgroup 10	ABS-19	Other	0.1
Bacteroidetes	Sphingobacteriia	Sphingobacteriales	Saprospiraceae	Phaeodactylibacter	0.1
Firmicutes	Clostridia	Halanaerobiales	ODP1230B8.23	uncultured bacterium	0.1
Latescibacteria	uncultured bacterium	uncultured bacterium	uncultured bacterium	uncultured bacterium	0.1
Proteobacteria	Alphaproteobacteria	Rhizobiales	Phyllobacteriaceae	Mesorhizobium	0.1
Proteobacteria	Alphaproteobacteria	Rhodobacterales	Rhodobacteraceae	Rhodovulum	0.1
Proteobacteria	Betaproteobacteria	SC-I-84	uncultured bacterium	uncultured bacterium	0.1
Proteobacteria	Deltaproteobacteria	Myxococcales	P3OB-42	Other	0.1
Proteobacteria	SPOTSOCT00m83	uncultured bacterium	uncultured bacterium	uncultured bacterium	0.1
Acidobacteria	Subgroup 6	Other	Other	Other	0.1
Cyanobacteria	Melainabacteria	Obscuribacterales	uncultured bacterium	uncultured bacterium	0.1
Gracilibacteria	Other	Other	Other	Other	0.1
Ignavibacteriae	Ignavibacteria	Ignavibacteriales	BSV26	Other	0.1
Proteobacteria	Alphaproteobacteria	Caulobacterales	Caulobacteraceae	Phenylobacterium	0.1
Proteobacteria	Alphaproteobacteria	Rhizobiales	Bradyrhizobiaceae	Other	0.1
Proteobacteria	Alphaproteobacteria	Rhizobiales	Hyphomicrobiaceae	Devosia	0.1
Proteobacteria	Alphaproteobacteria	Rhizobiales	Hyphomicrobiaceae	Pedomicrobium	0.1
Proteobacteria	Alphaproteobacteria	Rickettsiales	SM2D12	uncultured bacterium	0.1
Proteobacteria	Alphaproteobacteria	Sphingomonadales	Sphingomonadaceae	Sphingopyxis	0.1
Proteobacteria	Betaproteobacteria	Burkholderiales	Alcaligenaceae	uncultured	0.1
Proteobacteria	Betaproteobacteria	Burkholderiales	Comamonadaceae	Hydrogenophaga	0.1
Proteobacteria	Deltaproteobacteria	Bradymonadales	Other	Other	0.1
Proteobacteria	Gammaproteobacteria	Pseudomonadales	Pseudomonadaceae	Pseudomonas	0.1
TM6 (Dependentiae)	uncultured bacterium	uncultured bacterium	uncultured bacterium	uncultured bacterium	0.1
Other	Other	Other	Other	Other	1.4

Erklärung

Hiermit erkläre ich, dass ich die vorliegende Arbeit mit dem Titel **“Protein-based Assessment of Activated Sludge”** selbst verfasst und keine außer den angegebenen Hilfsmitteln und Quellen benutzt habe.

Außerdem versichere ich, diese Arbeit in dieser oder einer ähnlichen Form nicht bei einer anderen Universität eingereicht zu haben.

_____ _____

Ort, Datum Asma Sumayyah Azizan